FORMING EVALUATION METRICS AND METHODS

FOR COMPLEX STRETCH BROKEN AND CONTINUOUS CARBON FIBER PARTS

by

Madison Eve Dube

A thesis submitted in partial fulfillment
of the requirements for the degree

of

Master of Science

in

Mechanical Engineering

MONTANA STATE UNIVERSITY
Bozeman, Montana

May 2023

©COPYRIGHT

by

Madison Eve Dube

2023

All Rights Reserved

ACKNOWLEDGEMENTS

I would first like to acknowledge my family: Dr. Michael Dube, Adrienne Dube, and Allyson Dube, for without them I would not have had the financial support for my undergraduate degree, the perseverance to pursue my masters degree, or the support to complete it. A special thanks is extended to Venkat Krisshna and Dr. Mark Owkes for their support and guidance through the assembly of this document. My sincerest gratitude is given to Dalton Nold, Ted Beebe, and Lena Fitzsimmons for their procurement of various imagery used within this document to represent aircraft structures and carbon fiber. I would also like to thank Dan Samborsky, Alexey Dynkin, Rachel Neal, Brock Himmerite, and Brock Rugg for sharing their knowledge on carbon fiber manufacturing and 3D printing as well as their acquisition of data and reviews of this document. Additionally, I have extreme appreciation for my thesis committee members Dr. Cecily Ryan, Dr. Douglas Cairns, Dr. Michael Edens, and Christopher Ridgard for the knowledge they have bestowed upon me pertaining to carbon fiber research and aircraft structures. I would also like to thank them for advising me throughout this process and agreeing to participate in my thesis defense. Finally, I would like to thank the entire students, staff, and faculty on the Stretch Broken Carbon Fiber Project. Without their dedication to developing stretch broken carbon fiber as well as their willingness to assist others, my evaluation method could not be completed.

This work was funded by US ARMY Combat Capabilities Development Command Aviation & Missile Center Technology Development Directorate (Contract number: W911W6-18-0050).

TABLE OF CONTENTS

1. INTRODUCTION 1

2. BACKGROUND 8

Corner Thinning and Thickening 9
Resin Pooling 11
Wrinkling 12
Thickness Variation 13
Forming Depth 14
Void Content 14
Bridging 16
Strain 17
Springback 17

3. METHODOLOGY 19

Testing Procedure 19
Test Preparation Procedure 19
Cross-Sectioning and Scanning Procedure 21
Analysis Procedure 24
Metric Definition, Measurement, Analysis, and Scoring Procedures 25
Bridging 25
Definition: 25
Measurement Procedure: 26
Analysis Procedure: 27
Scoring Procedure: 27
Wrinkling 28
Definition: 28
Measurement Procedure: 30
Analysis Procedure: 32
Scoring Procedure: 32
Thickness Variation 35
Definition: 35
Measurement Procedure: 35
Analysis Procedure: 37
Scoring Procedure: 38
Forming Depth 39
Definition: 39
Measurement Procedure: 39
Analysis Procedure: 41

TABLE OF CONTENTS – CONTINUED

Scoring Procedure: 41
Corner Thinning 43
Definition: 43
Measurement Procedure: 43
Analysis Procedure: 45
Scoring Procedure: 46
Corner Thickening 47
Definition: 47
Measurement Procedure: 48
Analysis Procedure: 49
Scoring Procedure: 50
Resin Pooling 52
Definition: 52
Measurement Procedure: 52
Analysis Procedure: 54
Scoring Procedure: 54
Texture Defects 56
Definition: 56
Measurement Procedure: 60
Analysis Procedure: 60
Scoring Procedure: 62
Additional Measurements and Analyses not Used for Scoring 63
Splitting 64
Definition: 64
Measurement Procedure 64
Analysis Procedure 65
Stretch versus Slip 65
Definition: 65
Measurement Procedure 67
Analysis Procedure 68
Forming Score Procedure 70
Performed Trials 72
Curved C-channel Trials 72
Rounded Hat channel Trials 72
Sinusoidal C-channel Trials 73

4. RESULTS AND DISCUSSION 74

Curved C-channel Results and Discussion 74
Continuous Carbon Fiber Results 74

TABLE OF CONTENTS – CONTINUED

Lowest Forming Score:.....74
Highest Forming Score:.....77
Stretch Broken Carbon Fiber Results.....83
Lowest Forming Score:.....83
Highest Forming Score:.....88
Curved C-channel Discussion.....93
Rounded Hat channel Results and Discussion.....103
Continuous Carbon Fiber Results.....103
Stretch Broken Carbon Fiber Results.....107
Rounded Hat channel Discussion.....111
Sinusoidal C-channel Results and Discussion.....113
Continuous Carbon Fiber Results.....113
Sinusoidal C-channel Discussion.....119

5. METHOD PERFORMANCE DISCUSSION.....122

6. CONCLUSIONS.....125

7. FUTURE WORK RECOMMENDATIONS.....127

REFERENCES CITED.....132

APPENDICES.....136

APPENDIX A : Appendix A: Material Data Sheets.....137
MSU SBCF Prepreg Batches.....138
Hexcel IM7 Fibers.....139
Hexcel 8552 Resin.....141
APPENDIX B : Appendix B: Additional Complex Part Trial Results.....145
Additional Curved C Channel Results.....146
Part MD005.....147
Part MD006.....153
Part MD007.....158
Part MD008.....163
Part MD009.....168
Part MD011.....173
Part MD012.....178
Part MD017.....183
Part MD020.....189
Unscored Curved C Channel Trial.....194

TABLE OF CONTENTS – CONTINUED

Part MD002....194
Additional Sinusoidal C Channel Results....195
Part MD023....196
APPENDIX C : Appendix C: MatLab Code....201
Curved C Channel Code....202
Main Curved C Channel Script....202
Curved C Channel Data Extraction Function....204
Rounded Hat Channel Code....208
Main Rounded Hat Channel Script....208
Rounded Hat Channel Data Extraction Function....211
Sinusoidal C Channel Code....215
Main Sinusoidal C Channel Script....215
Sinusoidal C Channel Data Extraction Function....217
Sinusoidal C Thickness Analysis Function....221
Cartesian Coordinate Designed Functions....222
Stretching vs Slipping Function....222
Thickness Variation Function....224
Forming Depth Function....226
Polar Coordinate Designed Functions....229
Stretching vs Slipping Function....229
Thickness Variation Function....231
Forming Depth Function....234
Additional Functions....236
Wrinkling Function....236
Resin Pooling Function....238
Corner Thinning Function....239
Corner Thickening Function....241
Bridging and Resin Pooling Comparison Function....243
Bridging Function....244

LIST OF TABLES

Table Page

3.1 Bridging Metric Rankings 28
3.2 Wrinkling Metric Rankings 34
3.3 Thickness Metric Rankings 38
3.4 Forming Depth Metric Rankings 42
3.5 Corner Thinning Metric Rankings 46
3.6 Corner Thickening Metric Rankings 51
3.7 Resin Pooling Metric Rankings 55
3.8 Texture Metric Rankings 61
3.9 Texture Scoring Matrix Example 63
3.10 Example of the Final Forming Scoring Matrix 72
4.1 Continuous Carbon Fiber MD019: Texture Results 78
4.2 Continuous Carbon Fiber MD019: Final Forming Score 78
4.3 Continuous Carbon Fiber MD010: Texture Results 82
4.4 Continuous Carbon Fiber MD010 Final Forming Score 83
4.5 Stretch Broken Carbon Fiber MD004: Texture Results 87
4.6 Stretch Broken Carbon Fiber MD004 Forming Score 88
4.7 Stretch Broken Carbon Fiber MD016: Texture Results 92
4.8 Stretch Broken Carbon Fiber MD016: Final Forming Score 93
4.9 Summary of Curved C-channel Results 94
4.10 Continuous Carbon Fiber MD018: Texture Results 106
4.11 Continuous Carbon Fiber MD018: Final Forming Score 106
4.12 Stretch Broken Carbon Fiber MD021: Texture Results 111
4.13 Stretch Broken Carbon Fiber MD021: Final Forming Score 111
4.14 Summary of Rounded Hat channel Results 112

LIST OF TABLES – CONTINUED

Table Page

4.15 Continuous Carbon Fiber MD022: Texture Results 118
4.16 Continuous Carbon Fiber MD022: Final Forming Score....118
A.1 Summary of MSU SBCF Prepreg Batches....138
B.1 Summary of Curved C Channel Results....146
B.2 Continuous Carbon Fiber MD005: Texture Results 148
B.3 Continuous Carbon Fiber MD005: Final Forming Score....148
B.4 Stretch Broken Carbon Fiber MD006: Texture Results....154
B.5 Stretch Broken Carbon Fiber MD006: Final Forming Score 154
B.6 Continuous Carbon Fiber MD007: Texture Results 159
B.7 Continuous Carbon Fiber MD007: Final Forming Score....159
B.8 Continuous Carbon Fiber MD008: Texture Results 164
B.9 Continuous Carbon Fiber MD008: Final Forming Score....164
B.10 Continuous Carbon Fiber MD009: Texture Results 169
B.11 Continuous Carbon Fiber MD009: Final Forming Score....169
B.12 Stretch Broken Carbon Fiber MD011: Texture Results....173
B.13 Stretch Broken Carbon Fiber MD011: Final Forming Score 174
B.14 Stretch Broken Carbon Fiber MD012: Texture Results....179
B.15 Stretch Broken Carbon Fiber MD012: Final Forming Score 179
B.16 Stretch Broken Carbon Fiber MD017: Texture Results....184
B.17 Stretch Broken Carbon Fiber MD017: Final Forming Score 184
B.18 Continuous Carbon Fiber MD020: Texture Results 192
B.19 Continuous Carbon Fiber MD020: Final Forming Score....193
B.20 Summary of Sinusoidal C Channel Results....195
B.21 Continuous Carbon Fiber MD023: Texture Results 196

LIST OF TABLES – CONTINUED

Table Page

B.22Continuous Carbon Fiber MD023: Final Forming Score.....197

LIST OF FIGURES

Figure Page

1.1 Stretch Breaking Process 2
1.2 Curved C-Channel Analogues, Model, and Tooling 3
1.3 Rounded Hat channel Analogues, Model, and Tooling 4
1.4 Sinusoidal C-channel Analogues, Model, and Tooling 6
2.1 Corner Thinning Micrographs from Grankall *et al.* (2021) 10
2.2 Microscopic Example of Corner Thinning and Thickening Defects 11
2.3 Profiles of Carbon Fiber Reinforced Plastic Sheets After Bead Forming 15
2.4 MSU SBCF Panel with Voided Regions 15
2.5 Bridging Example for Hat Cross-Section using Continuous Fiber Woven Preforms: 16
2.6 Springback Angle (theta) Measurement Schematic 18
3.1 Sectioning Examples for the Uncured Layups 19
3.2 Vacuum Bagging Process for Testing 20
3.3 Curved C-channel Cross-Sectioning Example 22
3.4 Curved C-channel Radius Designations 23
3.5 Defect Locations 24
3.6 Bridging Defect Example 25
3.7 Bridging Measurement Schematic 26
3.8 Bridging Measurement on Part Cross-Section 26
3.9 Bridging Data Representation 27
3.10 Bridging Score Examples 29
3.11 Wrinkling Defect Example 29
3.12 Critical Regions for Various Part Types 30
3.13 Wrinkle Measurement Schematic 31

LIST OF FIGURES – CONTINUED

Figure Page

3.14 Wrinkle Data Representation Example 33
3.15 Wrinkle Scoring Examples 34
3.16 Thickness Variation Defect Example 35
3.17 Thickness Measurement Locations Schematic 36
3.18 Thickness Measurement on Part Cross-Section 36
3.19 Thickness Contour Plot Representation 38
3.20 Poor Forming Depth Example 39
3.21 Forming Depth Measurement Schematic 40
3.22 Forming Depth Measurement on Part Cross-Section 40
3.23 Forming Depth Data Representation 41
3.24 Forming Depth Scoring Examples 42
3.25 Corner Thinning Defect Example 43
3.26 Corner Thinning Measurement Locations 44
3.27 Corner Thinning Measurement on Part Cross-Section 44
3.28 Corner Thinning Data Representation 45
3.29 Corner Thinning Scoring Examples 47
3.30 Corner Thickening Defect example 48
3.31 Corner Thickening Measurement Locations 49
3.32 Corner Thickening Measurement on Part Cross-Section 49
3.33 Corner Thickening Data Representation 50
3.34 Corner Thickening Scoring examples 51
3.35 Resin Pooling Defect example 52
3.36 Resin Pooling Measurement Locations 53
3.37 Resin Pooling Measurement on Part Cross-Section 53

LIST OF FIGURES – CONTINUED

Figure Page

3.38 Resin Pooling Data Representation 54
3.39 Resin Pooling Scoring examples 55
3.40 Texture Defect Summary 56
3.41 Hairiness Texture Defect example 57
3.42 Additional Resin Pooling Texture Defect example 57
3.43 Spaghettification Texture Defect Example 58
3.44 Fractures/Shearing Texture Defect Example 58
3.45 Pinholes Texture Defect Example 59
3.46 Waves Texture Defect Example 59
3.47 Splitting Defect Example 64
3.48 Stretching Schematic 65
3.49 Stretching Example 66
3.50 Ply Ply Slippage Schematic 66
3.51 Ply-ply Slippage Visualization 67
3.52 Tool Ply Slippage Schematic 67
3.53 Stretch versus Slip Measurement Schematic 68
3.54 Stretch versus Slip Example 69
4.1 Continuous Carbon Fiber Curved C-channel Part MD019 74
4.2 Continuous Carbon Fiber MD019 Results: Corner Thinning and Thickening 75
4.3 Continuous Carbon Fiber MD019 Results: Bridging and Resin Pooling 76
4.4 Continuous Carbon Fiber MD019 Results: Thickness Variation 76
4.5 Continuous Carbon Fiber MD019 Results: Forming Depth 77
4.6 Continuous Carbon Fiber Curved C-channel Part MD010 79

LIST OF FIGURES – CONTINUED

Figure Page

4.7 Continuous Carbon Fiber MD010 Results: Corner Thinning and Thickening 80
4.8 Continuous Carbon Fiber MD010 Results: Bridging and Resin Pooling 81
4.9 Continuous Carbon Fiber MD010 Results: Thickness Variation 81
4.10 Continuous Carbon Fiber MD010 Results: Forming Depth 82
4.11 Stretch Broken Carbon Fiber Curved C-channel Part MD004 83
4.12 Stretch Broken Carbon Fiber MD004 Results: Corner Thinning and Thickening 84
4.13 Stretch Broken Carbon Fiber MD004 Results: Bridging and Resin Pooling 85
4.14 Stretch Broken Carbon Fiber MD004 Results: Thickness Variation 86
4.15 Stretch Broken Carbon Fiber MD004 Results: Forming Depth 86
4.16 Stretch Broken Carbon Fiber MD004 Results: Wrinkling 87
4.17 Stretch Broken Carbon Fiber Curved C-channel Part MD016 89
4.18 Stretch Broken Carbon Fiber MD016 Results: Corner Thinning and Thickening 90
4.19 Stretch Broken Carbon Fiber MD016 Results: Bridging and Resin Pooling 90
4.20 Stretch Broken Carbon Fiber MD016 Results: Thickness Variation 91
4.21 Stretch Broken Carbon Fiber MD016 Results: Forming Depth 91
4.22 Stretch Broken Carbon Fiber MD016 Results: Wrinkling 92
4.23 Continuous Carbon Fiber MD010 Results: Stretch vs Slip 96
4.24 Continuous Carbon Fiber MD019 Results: Stretch vs Slip 97
4.25 Stretch Broken Carbon Fiber MD004 Results: Stretch vs Slip 98
4.26 Stretch Broken Carbon Fiber MD016 Results: Stretch vs Slip 99

LIST OF FIGURES – CONTINUED

Figure Page

4.27 Final Forming Scores for all Curved C-channel Trials 100
4.28 Metric Forming Scores for all Curved C-channel Trials: Part 1.....101
4.29 Metric Forming Scores for all Curved C-channel Trials: Part 2.....102
4.30 Continuous Carbon Fiber Rounded Hat channel Part MD018 103
4.31 Continuous Carbon Fiber MD018 Results: Corner Thinning and Thickening.....104
4.32 Continuous Carbon Fiber MD018 Results: Bridging and Resin Pooling.....104
4.33 Continuous Carbon Fiber MD018 Results: Thickness Variation.....105
4.34 Continuous Carbon Fiber MD018 Results: Forming Depth 107
4.35 Stretch Broken Carbon Fiber Rounded Hat channel Part MD021 107
4.36 Stretch Broken Carbon Fiber MD021 Results: Corner Thinning and Thickening.....108
4.37 Stretch Broken Carbon Fiber MD021 Results: Bridging and Resin Pooling.....109
4.38 Stretch Broken Carbon Fiber MD021 Results: Thickness Variation 110
4.39 Stretch Broken Carbon Fiber MD021 Results: Forming Depth.....110
4.40 Continuous Carbon Fiber MD018 Results: Stretch vs Slip 114
4.41 Stretch Broken Carbon Fiber MD021 Results: Stretch vs Slip.....115
4.42 Continuous Carbon Fiber Sinusoidal C-channel Part MD022.....115
4.43 Continuous Carbon Fiber MD022 Results: Corner Thinning and Thickening.....116
4.44 Continuous Carbon Fiber MD022 Results: Thickness Variation.....117
4.45 Continuous Carbon Fiber MD022 Results: Wrinkling 119
4.46 Continuous Carbon Fiber MD022 Results: Stretch vs Slip 120
7.1 Void on Cross-Sectional Scan 128

LIST OF FIGURES – CONTINUED

Figure Page

7.2 Springback Measurement Schematic 129
7.3 Other Cross-Sections for Consideration....131
A.1 Hexcel IM7 Fiber Data Sheet Page 1....139
A.2 Hexcel IM7 Fiber Data Sheet Page 2....140
A.3 Hexcel 8552 Resin Data Sheet Page 1....141
A.4 Hexcel 8552 Resin Data Sheet Page 2....142
A.5 Hexcel 8552 Resin Data Sheet Page 3....143
A.6 Hexcel 8552 Resin Data Sheet Page 4....144
B.1 Continuous Carbon Fiber Curved C Channel Part MD005....147
B.2 Continuous Carbon Fiber MD005 Results: Corners 147
B.3 Continuous Carbon Fiber MD005 Results: Bridging and Resin Pooling....149
B.4 Continuous Carbon Fiber MD005 Results: Thickness Variation....149
B.5 Continuous Carbon Fiber MD005 Results: Forming Depth 150
B.6 Continuous Carbon Fiber MD005 Results: Wrinkling 151
B.7 Continuous Carbon Fiber MD005 Results: Stretching versus Slipping 152
B.8 Stretch Broken Carbon Fiber Part MD006....153
B.9 Stretch Broken Carbon Fiber MD006 Results: Corners....153
B.10Stretch Broken Carbon Fiber MD006 Results: Bridging and Resin Pooling....155
B.11Stretch Broken Carbon Fiber MD006 Results: Thickness Variation 155
B.12Stretch Broken Carbon Fiber MD006 Results: Forming Depth....156
B.13Stretch Broken Carbon Fiber MD006 Results: Wrinkling....156
B.14Stretch Broken Carbon Fiber MD006 Results: Stretching versus Slipping....157

LIST OF FIGURES – CONTINUED

Figure Page

B.15Continuous Carbon Fiber Curved C Channel Part MD007 158
B.16Continuous Carbon Fiber MD007 Results: Corners 158
B.17Continuous Carbon Fiber MD007 Results: Bridging and Resin Pooling 160
B.18Continuous Carbon Fiber MD007 Results: Thickness Variation 160
B.19Continuous Carbon Fiber MD007 Results: Forming Depth 161
B.20Continuous Carbon Fiber MD007 Results: Wrinkling 161
B.21Continuous Carbon Fiber MD007 Results: Stretching versus Slipping 162
B.22Continuous Carbon Fiber Curved C Channel Part MD008 163
B.23Continuous Carbon Fiber MD008 Results: Corners 163
B.24Continuous Carbon Fiber MD008 Results: Bridging and Resin Pooling 165
B.25Continuous Carbon Fiber MD008 Results: Thickness Variation 165
B.26Continuous Carbon Fiber MD008 Results: Forming Depth 166
B.27Continuous Carbon Fiber MD008 Results: Wrinkling 166
B.28Continuous Carbon Fiber MD008 Results: Stretching versus Slipping 167
B.29Continuous Carbon Fiber Curved C Channel Part MD009 168
B.30Continuous Carbon Fiber MD009 Results: Corners 168
B.31Continuous Carbon Fiber MD009 Results: Bridging and Resin Pooling 170
B.32Continuous Carbon Fiber MD009 Results: Thickness Variation 170
B.33Continuous Carbon Fiber MD009 Results: Forming Depth 171
B.34Continuous Carbon Fiber MD009 Results: Wrinkling 171

LIST OF FIGURES – CONTINUED

Figure Page

B.35Continuous Carbon Fiber MD009 Results: Stretching versus Slipping 172
B.36Stretch Broken Carbon Fiber Curved C Channel Part MD011 173
B.37Stretch Broken Carbon Fiber MD011 Results: Corners....174
B.38Stretch Broken Carbon Fiber MD011 Results: Bridging and Resin Pooling....175
B.39Stretch Broken Carbon Fiber MD011 Results: Thickness Variation 175
B.40Stretch Broken Carbon Fiber MD011 Results: Forming Depth....176
B.41Stretch Broken Carbon Fiber MD011 Results: Wrinkling....176
B.42Stretch Broken Carbon Fiber MD011 Results: Stretching versus Slipping....177
B.43Stretch Broken Carbon Fiber Curved C Channel Part MD012 178
B.44Stretch Broken Carbon Fiber MD012 Results: Corners....178
B.45Stretch Broken Carbon Fiber MD012 Results: Bridging and Resin Pooling....179
B.46Stretch Broken Carbon Fiber MD012 Results: Thickness Variation 180
B.47Stretch Broken Carbon Fiber MD012 Results: Forming Depth....180
B.48Stretch Broken Carbon Fiber MD012 Results: Wrinkling....181
B.49Stretch Broken Carbon Fiber MD012 Results: Stretching versus Slipping....182
B.50Stretch Broken Carbon Fiber Curved C Channel Part MD017 183
B.51Stretch Broken Carbon Fiber MD017 Results: Corners....183
B.52Stretch Broken Carbon Fiber MD017 Results: Bridging and Resin Pooling....185
B.53Stretch Broken Carbon Fiber MD017 Results: Thickness Variation 185
B.54Stretch Broken Carbon Fiber MD017 Results: Forming Depth....186

LIST OF FIGURES – CONTINUED

Figure Page

B.55Stretch Broken Carbon Fiber MD017 Results: Wrinkling....187
B.56Stretch Broken Carbon Fiber MD017 Results: Stretching versus Slipping....188
B.57Continuous Carbon Fiber Curved C Channel Part MD020....189
B.58Continuous Carbon Fiber MD020 Results: Corners....189
B.59Continuous Carbon Fiber MD020 Results: Bridging and Resin Pooling....190
B.60Continuous Carbon Fiber MD020 Results: Thickness Variation....190
B.61Continuous Carbon Fiber MD020 Results: Forming Depth....191
B.62Continuous Carbon Fiber MD020 Results: Wrinkling....191
B.63Continuous Carbon Fiber MD020 Results: Stretching versus Slipping....192
B.64Stretch Broken Carbon Fiber Curved C Channel Part MD020....194
B.65Continuous Carbon Fiber Curved C Channel Part MD023....196
B.66Continuous Carbon Fiber MD023 Results: Corners....197
B.67Continuous Carbon Fiber MD023 Results: Thickness Variation....198
B.68Continuous Carbon Fiber MD023 Results: Wrinkling....199
B.69Continuous Carbon Fiber MD023 Results: Stretching versus Slipping....200

NOMENCLATURE

$\bar{x}$	Average Thickness
n	Number of Measurements
x_i	Thickness Measurements
t	Material Thickness
R_n	Radius of the Neutral Plane
ρ	Curvature of the Neutral Plane
ϵ_{max}	Bending Strain
n	Number of Measurements
$\frac{d\epsilon_b}{dy}$	Bending Strain Gradient
C_{var}	Coefficient of Variation
$t_{\%}$	Percent of average thickness
t_f	Measured Thickness
t_i	Initial Layup Thickness
L_c	Length of the Cured Laminate
L_u	Length of the Uncured Layup

ABSTRACT

Carbon fiber composites are an ideal material for aircraft structures due to their light weight and high strength and stiffness. Traditional continuous carbon fiber composites are limited by their ability to form into complex geometric features as they have minimal abilities to stretch into a mold. Stretch broken carbon fiber is discontinuous which allows for the different tows of carbon fiber to slip relative to each other allowing for laminate displacements unattainable to continuous carbon fiber.

In order to develop and improve stretch broken carbon fiber manufacturing processes, a method is developed herein to analyze the forming quality of a complex carbon fiber part. This method quantifies common qualitative forming metrics by measuring, evaluating, and scoring carbon fiber defects including: bridging, wrinkling, variation in thickness, forming depth, corner thinning and thickening, resin pooling, and additional texture defects. The scores produced from evaluating the various forming metrics on formed carbon fiber parts are assembled in a weighted matrix to produce an overall forming score. This forming evaluation method is demonstrated on three different geometric mold designs to assess that it is quantitative, repeatable, accounts for many carbon fiber defects, and accounts for discrepancies between the formed part and the designed part.

This method was also tested on different carbon fiber prepreg materials: MSU SBCF/Cycom 977-3 resin from Solvay, MSU SBCF/Hexcel 8552, and Hexcel IM7/8552. Through testing, the method is found to have achieved the method design goals as well as ascertaining areas of improvement for MSU SBCF prepreg which is still under development. Results show that stretch broken carbon fiber and traditional continuous carbon fiber achieve similar overarching forming scores, but outperform one another in different category metrics. MSU SBCF has higher scores in corner thickening and resin pooling; continuous carbon fiber has higher scores in wrinkling and bridging.

The method forms the foundation to evaluate layup practices and autoclave cure cycles when systematically applied in a process development setting. This method is also extendable to dissimilar geometric part types with modifications in suitable metrics.

1

INTRODUCTION

Carbon fiber composites have become increasingly utilized in a broad number of industries over the years. One area that has greatly benefited from the use of composite materials is the aerospace industry. Great strides have been made since the Wright brothers' first powered flight on the *Wright Flyer I* in 1903 (1). Compared to modern aircraft, this first airplane seemed rudimentary as it was constructed with "timber [beams] covered in fabric" (2). Nowadays, aircraft such as the Boeing 787 widely incorporate composite materials and in some cases composites even "account for about 50% of the aircraft" (3). Carbon fiber composites are lightweight while retaining similar strength and stiffness to steel, making it an ideal material for improving aircraft efficiency (4). While traditional carbon fiber composites are ideal for their strength-to-weight properties, forming these materials into the complex geometries required for aircraft structures has proven difficult. Conventional metals can be formed using a wide variety of methods such as bending, stretching, roll forming, or stamping out with a press (5). Unfortunately, most of these methods do not easily apply to carbon fiber laminates as the in-extensible nature of the fibers does not allow for it to stretch or stamp simply into a mold (6). Hand layup is still commonly used for creating complex geometries out of carbon fiber which has "processing times spanning hours and even days" (7). It is from this necessity for carbon fiber with increased forming capabilities that birthed the creation of stretch broken carbon fiber (SBCF). Stretch broken carbon fiber takes traditional carbon fiber tows and breaks them at their natural occurring flaws by the use of cylindrical rollers driven at varying speeds as outlined in Figure 1.1 (8). The discontinuity and unidirectionality of the fibers now permits the SBCF to elongate in the direction of the fiber, allowing the material to take shape while minimizing the adverse effects of ply-ply

shearing (9). This ability for the carbon fiber to now form or "stretch" into a mold enables complex geometries otherwise difficult to achieve with continuous fiber plies.

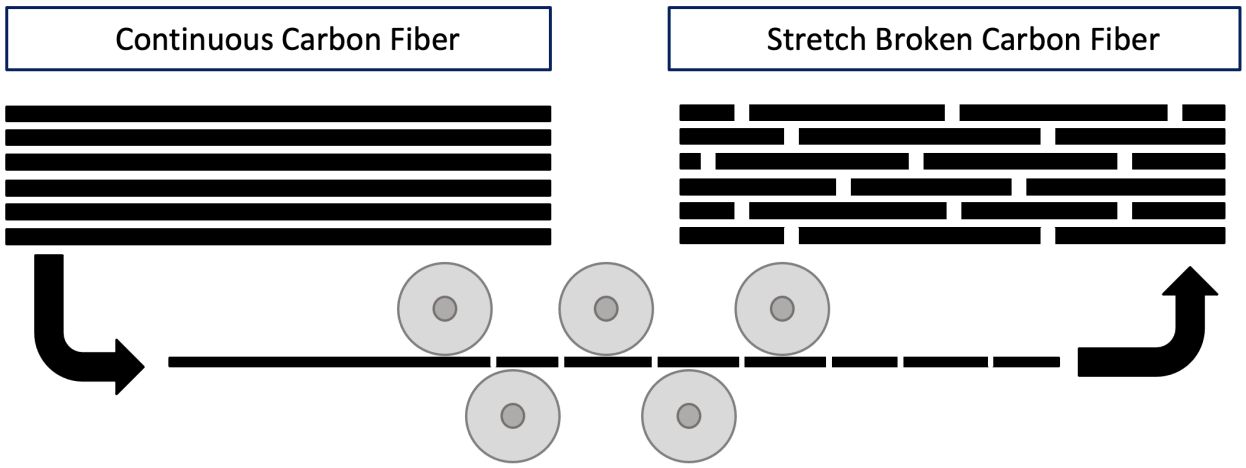


Figure 1.1: Stretch Breaking Process: Continuous Carbon Fiber tows passed through rollers running at differential speeds to stretch break at natural flaws producing Stretch Broken Carbon Fiber tows

Traditional continuous carbon fiber, when subjected to the deep draw method of forming (using vacuum, heat, and pressure to draw a layup into a mold), has two predominate forming mechanisms: ply-ply slippage, where the individual carbon fiber plies slip relative to each other (intralaminar shearing), and tool-ply slippage, where the entire laminate slips relative to the tool surface (10). While these mechanisms of forming are fundamental for part quality, exploiting stretching for stretch broken carbon fiber could greatly increase the forming potential of the material as it has another forming mechanism present apart from the other frictional mechanisms of tool-ply slippage and ply-ply slippage (11). Studying the forming mechanisms present in a complex part could allow for a deeper understanding of the material behavior during the forming and curing process. This additional information could provide insight to the presence of carbon fiber defects.

To test the forming capabilities of SBCF when applied to complex aircraft geometries, a set of parts needs to be designed that is representative of aircraft structures, for example,

internal aircraft fuselage and wing structures. After review of images from the frames of many different aircraft and structural component cross-sections outlined in Peery's (2011) *Aircraft Structures* textbook, three main part designs have been selected for this study with several other saved for future experimentation (12). The part selections include "Curved C" channels, "Rounded Hat" channels, and "Sinusoidal C" channels. This study uses smaller molds (less than $6\,in$ [$15.24\,cm$] by $12\,in$ [$30.48\,cm$] by $4\,in$ [$10.16\,cm$]) to keep material usage down and remain within tool manufacturing dimensional constraints. Larger molds are also designed for future complex geometry testing.

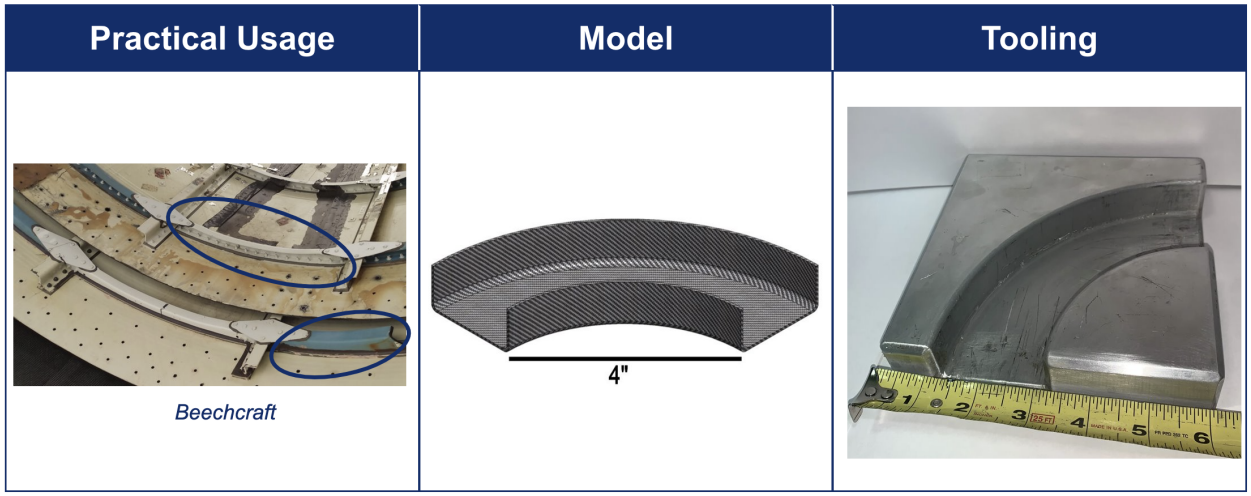


Figure 1.2: Curved C-Channel: LEFT - Beechcraft aircraft fuselage frame analogue, CENTER - designed model, RIGHT - aluminum tooling utilized

The Curved C-Channel design is chosen to be representative of the internal fuselage framework of aircraft. In Figure 1.2, the practical usage, model, and tooling design for the Curved C-Channel is represented. Practical usage of the Curved C-Channel can be seen in the fuselage frame of a standard Beechcraft aircraft (photo taken by SBCF members at NIAR). Based on this structural feature, the model is designed to incorporate a 90° curvature with a simple C-channel cross-section. From the model design, a negative channel molding is designed to use a deep drawing forming method complete with a vacuum bag and autoclave

temperatures and pressures. This preliminary mold is designed with 0.125 *in* [0.32 *cm*] radii corners for both the convex and concave features. The radii of curvature for the "walls" of the C-channel are 3 *in* [7.62 *cm*] and 5 *in* [12.70 *cm*], while the span of the C-channel is 2 *in* [5.08 *cm*] and the depth is 1 *in* [2.54 *cm*] seen in Figure 3.4. The mold for the Curved C-Channel tests was manufactured out of 6061 aluminum, which was chosen for availability and low stock metal costs (13).

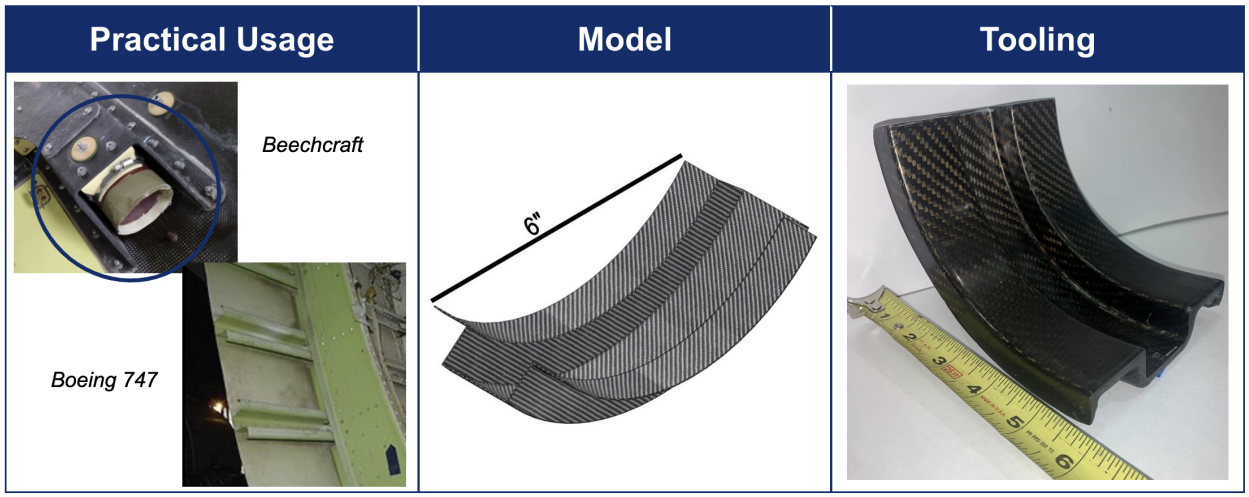


Figure 1.3: Rounded Hat channel: LEFT - Beechcraft aircraft fuselage frame and Boeing 747 fuselage frame analogues (14), CENTER - designed model, RIGHT - carbon fiber tooling utilized

Like the Curved C-Channel, the Rounded Hat channel is also chosen because it is representative aircraft fuselage frames. Figure 1.3 illustrates the practical usage, design model, and tooling design for the Rounded Hat channel. For the practical usage, two separate images are included, one from a standard Beechcraft fuselage (mentioned previously) and the other from a Boeing 747 fuselage (14). The model varies slightly from the practical usage as it incorporates a curvature in addition to the curvatures of the hat shaped cross-section. This model has a hat shaped cross-section designed in such a way that there are no closed geometries when mounted to an aircraft fuselage. The tooling mold is designed to include

a negative geometry feature for the carbon fiber to draw into during the forming process. This mold also features 0.125 in [0.32 cm] radii on the convex and concave curvatures. This finished mold is approximately 4.5 in [11.43 cm] (width) by 5.0 in [12.70 cm] (height) by 5.0 in [12.70Ccm] (depth). Unlike the Curved C-Channel mold, the Hat mold was made from Solvay LTM®16B Tooling Prepreg (15). This Rounded hat mold is curated first by 3D printing a male master mold on a INTAMSYS FUNMAT 3D Printer using 3DTex's high temperature nylon filaments which are designed to withstand temperatures of up to 250°F [121°C] and pressures of up to 90 psi [620 KPa] (16; 17). Once the master mold is printed, it is sanded, coated with TC-1614 epoxy penetrating sealing and coating resin system, and cured in an oven at 170°F [76°C] to set the epoxy following standard practices (18; 19). The tooling prepreg is then laid up around the master mold following manufacturer's instructions. After the addition of each ply, the master mold and tooling prepreg partial layup is vacuum bagged to consolidate each layer in the laminate. Once the entire mold is laid up, the entire part is vacuum bagged and completes a precure at 176°F [80°C] and 90psi [620KPa] for 180 minutes. Following the precure, the carbon fiber is demolded from the 3D print filament and cured again, this time at 375°F [190°C] and atmospheric pressure for 470 minutes (15).

The Sinusoidal C-channel is chosen as a representation of internal aircraft wing structures, specifically the spars. Typically, I–beams are used in the spars of aircraft, but they lack torsional stiffness (12). The incorporation of a sinusoidal pattern into the web of an I–beam seeks to improve the stiffness capabilities of a traditional I–beam. The practical usage for a Sinusoidal I–beam as well as the model and tooling for a Sinusoidal C-channel are illustrated in Figure 1.4. The practical application of sinusoidal I–beams in the metalworking industry are very common and the practical usage imagery presents an example of this (20). The model closely represents this geometry, but instead modifies the I-beam cross-section to a C-channel cross-section. For tooling purposes, it is beneficial to work towards this Sinusoidal I–beam in increments. Before a full Sinusoidal I–beam can be manufactured, it is

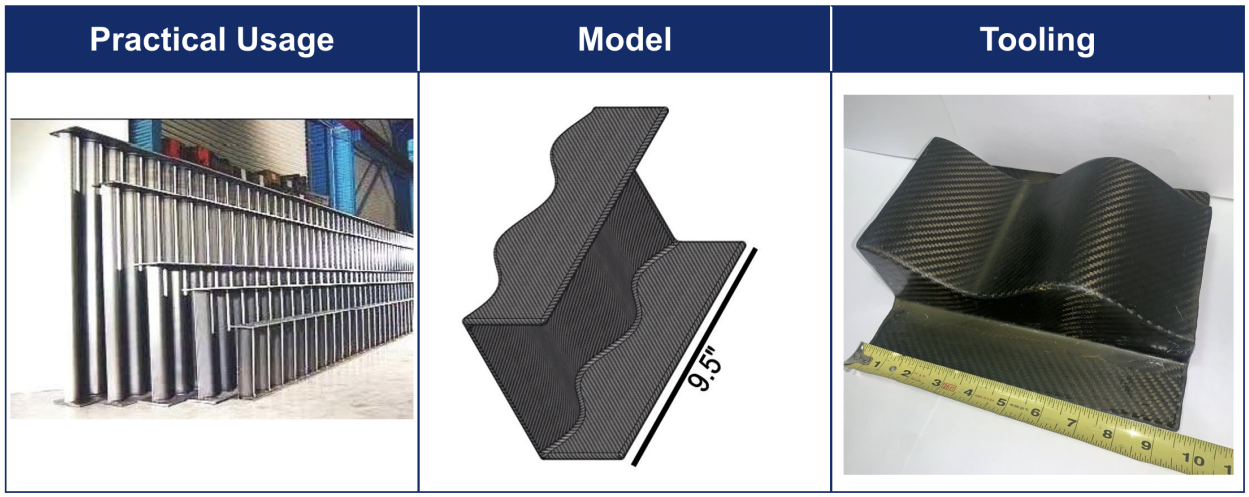


Figure 1.4: Sinusoidal C-channel: LEFT - metal I-beam analogue (20), CENTER - designed model, RIGHT - carbon fiber tooling utilized

first simpler to construct half of it resulting in a Sinusoidal C-channel. This mold is designed within the dimensions of $9\,in$ [$22.86\,cm$] (width) by $9.5\,in$ [$24.13\,cm$] (depth) by $3\,in$ [$7.62\,cm$] (height). Similar to the Rounded Hat channel, this Sinusoidal C-channel mold is constructed with the same tooling prepreg material and manufacturing techniques described above.

There are a number of different carbon fiber materials used in this study. For the continuous carbon fiber, Hexcel IM7/8552 prepreg is used and detailed material info is listed in Appendix A (21; 22). For the stretch broken carbon fiber, two separate materials are used, spanning four different material batches. The fiber used in the stretch broken carbon fiber prepreg is manufactured by the Montana State University (MSU). MSU SBCF is created by stretch breaking Hexcel IM7 fiber tows within a stretch breaking machine provided by Hexcel Corporation (21). Two different resin systems are used between the different prepreg batches. Hexcel 8552 is used in batches P0030 and P0031 (22). Solvay 977-3 is used in batches P0025 and P0029 (23). All stretch broken material data info is presented in Appendix A. It is important to note that MSU SBCF prepreg is still under development as the manufacturing process is still being optimized. This results in differences in material data for the different

batches.

Once all molds are manufactured and the carbon fiber parts are cured, it is necessary that there is a method in place to evaluate the parts produced for their forming quality. The requirements for this method of evaluating the forming quality are as follows:

- Primarily quantitative
- Repeatable
  - Well documented
  - Timely
  - Easily applied to multiple part geometries
- Account for most carbon fiber forming defects
- Account for geometry discrepancies between the design and the formed part
- Represented as an overall "forming score"

For this study, the development of a forming quality evaluation method is the primary goal. This detailed documentation will outline the process of defect metric definitions, measurements, analysis, and forming scoring, as well as how the method applies to the various part geometries presented. To develop this method, various carbon fiber defects must be researched and analyzed for common measurement practices and defect selections.

BACKGROUND

While carbon fiber may be the optimal choice for aircraft materials, the manufacturing and forming of carbon fiber composites poses unique challenges that traditional metals do not have. Metals are an isotropic material that have the same properties in every direction, making them simpler to model and predict their behaviors. Carbon fiber composites can be modeled as a transversely isotropic material that has different material properties in each direction due to the heterogeneous nature of the material (3). The structures within an airframe are geometrically complex as they can involve curvatures on multiple axes as well as small radii that the material must form into and bend along. When attempting to form these geometries using carbon fiber, a method for evaluating the overall forming quality of the part needs to be established. Engineers and researchers from the referenced materials have quantified forming by evaluating common material defects and overall part geometry defects. These defects include:

- Corner thinning and thickening
- Resin pooling
- Wrinkling
- Thickness variation
- Forming depth
- Void content
- Bridging
- Expected versus measured strain
- Springback effect

Corner Thinning and Thickening

Corner thinning is a geometric phenomenon where a noticeable decrease in the thickness of the material is present after it is formed over a positive mold radius or convex curvature (24). Thinning of the material at these locations, for example on an aircraft structure, could decrease the overall strength of the part leading to the risk of catastrophic failure that must be compensated for by over-designed subcomponents. It is therefore important to measure the thinning present and use this defect to evaluate the overarching forming quality of carbon fiber parts by calculating the amount of thinning the material experiences. Yanagimoto *et al.* (2012) performed forming evaluations of single bead, hat, and V shaped geometries when subjected to the shallow drawing and press forming methods (25). Using a microscope and image processing software, they were able to analyze the thinning and ply structure at the corners of interest. Microscopy is a useful tool when studying the fiber behavior at these regions, as it allows the researcher to see the microstructure of the carbon fiber laminate after it has been subjected to the pressures and temperatures of the forming processes (26). Grankall *et al.* (2021) also used microscopy to view the orientation and deformation of the individual carbon fiber plies at the areas where corner thinning is present (27). This method was used to evaluate a channel with an L-shaped cross-section when formed around a positive mold (27). These micrographs of the corner thinning defect are seen in Figure 2.1. While microscopy is a valuable tool in analyzing this defect, Grankall *et al.* (2021) also measured the thickness of the corners by hand via the use of calipers to confirm their measurements (27).

While carbon fiber laminates tend to display corner thinning as they are formed over a positive radius mold, corner thickening is present when they are drawn into a negative radius mold or concave curvature (24). Centea *et al.* (2015), took note that positive shaped molds result in corner thinning while negative shaped molds exhibit corner thickening primarily due to resin pooling (28). Even without resin pooling, the carbon fiber plies also experience an

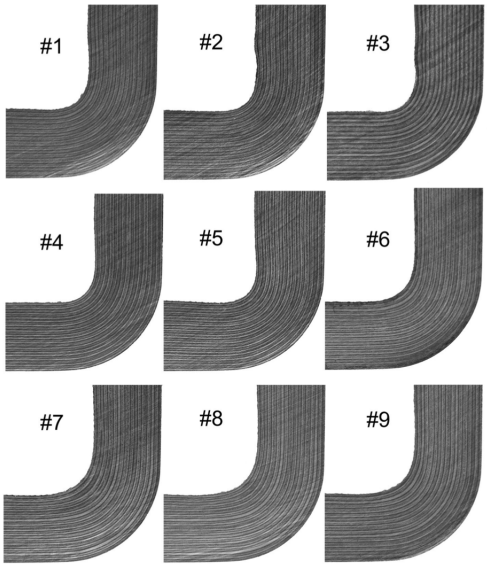


Figure 2.1: Corner Thinning Micrographs from Grankall *et al.* (2021) *Vacuum-Assisten Hot-Forming Using Tailored Laminate Temperature.* Corners 1, 2, 3, and 5 show corner thinning. Corners 6, 7, 8, and 9 show corner thickening. (27)

increase in thickness at these locations. Centea *et al.* (2015) formed a hat shaped part that was complete with both "convex and concave corner geometries" (28). An intensifier, or soft matched mold, was used to help "press" the carbon fiber material into the concave negative radii (28). Using microscopy, the thickness of the corners at both the concave and convex curvatures were measured and evaluated (28). Corner thinning on the concave corners and corner thickening in the convex corners are visually discernible in Figure 2.2 (28).

In summary, two main methods have been used to measure corner thinning and corner thickening. The first is microscopic imaging combined with image analysis software, and the second is using hand measurements of the regions of interest with digital calipers. Microscopy is an ideal measurement method as it is accurate and easily repeatable. However, sample preparation for microscopy is time consuming and difficult. Hand measurements using calipers are simplistic in nature, but do leave additional room for the introduction of human error.

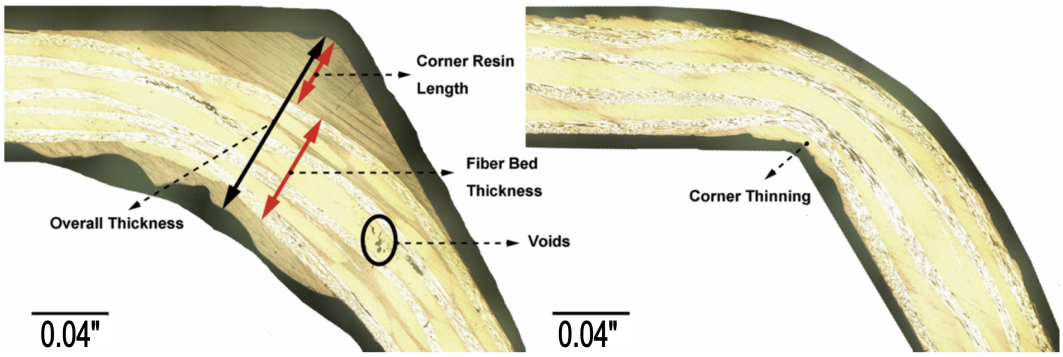


Figure 2.2: Microscopic imaging of corner thinning and thickening defects as adapted from *Defect Reduction Strategies for the Manufacture of Contoured Laminates Using Vacuum BAG-only Prepregs*. The left hand image shows corner thickening due primarily to resin pooling, while the right hand image shows an example of thinning (28).

Resin Pooling

As noted in the previous section, corner thickening is primarily due to a forming defect known as resin pooling into a negative curved mold (28). Due to forming processes that involve external pressure and vacuum pressure within a sealed bag, while elevated temperatures reduce the resin viscosity within the composite matrix, resin is sometimes seen "seeping out" of the composite laminate, creating "resin only regions" in these concave corners. The presence of "resin only regions" means that there are areas within the part that are starved of the resin matrix. Without the matrix to help bond the composite materials, the fibers could then become misaligned, in turn decreasing the strength, quality, and many other performance characteristics of the formed part (3). These resin pooled regions are also incredibly brittle, and lack strength due to there being no fiber within that location. Knowing how much resin is pooling out of the part allows for a metric to determine the forming quality as the quantity and locations of the resin-rich regions negatively impact the strength of the formed part. Centea *et al.* (2015) measured the thickness increase of the corners where these phenomena occurred using microscopy (28). A microscopic image of the corner resin length is presented in Figure 2.2 (28). Along with measuring the thickness of

the corner, the corner length of the resin only regions as well as the angle of the corner were evaluated to understand the volume of "resin accumulation" (28).

Wrinkling

Another defect seen in carbon fiber manufacturing is wrinkling of the plies. Wrinkles appear during the forming process as the carbon fiber laminate folds in on itself to fit into a mold. Wrinkles can result in air pockets within the part and increase thickness variation along the material, as well as decrease the overall strength of the part through ply misorientation within the wrinkled regions. Previous programs used a variety of forming methods on stretch broken carbon fiber to attain a panel with multiple beaded indentations along the laminate (7). These analyses were based primarily on visual observation, and were concerned with the aesthetic properties of the parts (7). While aesthetics are hard to quantify, they are an important metric as a visually displeasing part can be a qualitative indication of defects that lead to a part with reduced performance. Wrinkling also pre-buckles the material, which is detrimental to the compressive strength of the laminate. Through their experimentation, they observed that the effect of natural clamping, clamping due to friction against the tool surface, was sufficient for suppressing wrinkles (7). While wrinkling was not explicitly measured in these experiments, the presence of wrinkling was noted and used as a metric to determine if the part is satisfactory or not.

Hosseini *et al.* (2018) studied wrinkling on woven carbon fiber preforms (29). They measured the onset and amount of rotation of the carbon fiber yards when subjected to tensile loading (29). The wrinkle angle was then compared to the size of the carbon fiber yarns as well as the normalized shear force applied to the testing samples (29). These tests were primarily used for computer simulation validation of wrinkling behavior (29).

Thickness Variation

Researchers and manufacturers commonly observe that the thickness of carbon fiber parts varies after the composite has been formed and cured. Extreme variations in thickness can result in weaker regions of the part while other areas become stronger than needed. Measuring the thickness at various locations along a laminate is a popular method of forming quality evaluation. In the experiments performed by Centea *et al.* (2015), the thicknesses of the carbon fiber parts were measured using micrographs (28). The overall variation of the thickness along the formed composite was calculated with Equation 2.1, using the thickness at different locations along the part, x_i, the average thickness, $\bar{x}$, and the number of measurements taken, n (28). The coefficient of variation was used to evaluate different tool angles as well as the different locations along the tool per experiment (28).

$$\textit{Coefficient of Variation} = \frac{1}{\bar{x}}\sqrt{\frac{\sum (x-\bar{x})^2}{(n-1)}} \tag{2.1}$$

Mujahid *et al.* (2022) also measured the thickness and analyzed it with the overall coefficient of variation when forming hat shaped cross-sections (30). Like Centea *et al.* (2015), the thickness was measured at many different locations along the cross-sections and used to calculate the coefficient of variation using Equation 2.1 (28; 30). Unlike Centea *et al.* (2015), the thickness was measured using a micrometer as opposed to microscopy, and the coefficient of variation in this case was used to determine the overall consolidation of the carbon fiber plies (28). Mujahid *et al.* (2022) found through their coefficient of variation measurements that their modified vacuum bagging technique was effective in reducing the variation of thickness of a laminate (30). Centea *et al.* (2015) found that as the thickness of the laminates increased, the void content also increased (28). They also found that the arc length of the corner regions affected the coefficient of thickness variation for concave corner regions (28). These measurements were used to adjust the processing variables for

the study (28). Grankall *et al.* (2021) also used a hand based measurement technique using calipers to measure the thickness at regions of interest in order to assess their processing conditions (27). They were able to reduce their coefficient of thickness variation to 0.04 by tailoring their temperatures in the hot-forming cycles used (27). In summary, microscopic imaging and hand measurements via micrometer are the two main methods used to measure thickness variation of complex-formed parts to assess processing parameters.

Forming Depth

Often when forming carbon fiber composite parts, particularly when using the vacuum drawing method, the material does not form all the way down into the mold (25). This forming defect results in a final geometry different from the original design, meaning the desired strength and shape of the formed part does not meet the original requirements. The overall forming depth of the formed part can be measured and compared to the depth of the mold (25). Yanagimoto *et al.* (2021) performed single bead tests where the depth that the carbon fiber beads formed was compared to the as-designed bead dimensions (25). Some of the results from this single bead study are presented in Figure 2.3. It can be seen that certain beads, such as the bottom left bead in Figure 2.3, do not form completely to the bottom of the mold.

Void Content

A known material defect in composite manufacturing is the presence of voids within the material. Voids are regions where there are no fibers or resin present and appear as black in an optical micrograph. A microscope image of a SBCF panel with voids present within the composite boxed in red is displayed in Figure 2.4. These air pockets within the material can decrease the strength and stiffness of the part (particularly in compression and shear). "The flexural strength and modulus [is] significantly reduced" with the presence of voids within the laminate (31). Centea *et al.* (2015) observed void content "concentrated in corner regions"

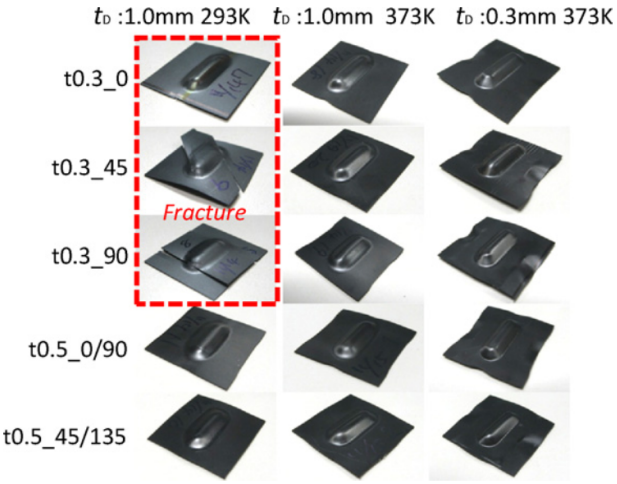


Figure 2.3: Profiles of Carbon Fiber Reinforced Plastic Sheets After Bead Forming. Sheets boxed in red display products with undesirable profiles and surface defects (25)

of their formed hat channels via microscopy (28). The void content percentage was measured and compared to the thickness in specific regions of interest (ROI) (28). These ROI were primarily the convex and concave corners of parts, because the group wanted to explore how the corner thickening and thinning contributed to the percentage of voids (28). These void results allowed them to conclude that voids can be mitigated by improved mold design and processing conditions (28).

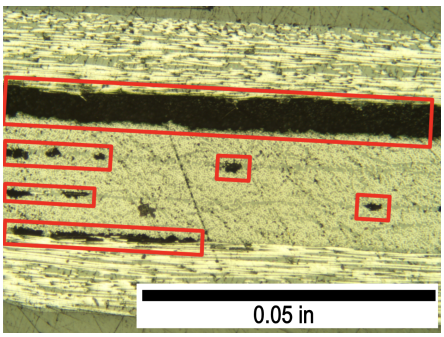


Figure 2.4: MSU SBCF Eight-Ply Panel with Voided Regions highlighted in Red Boxes. Top void spans across the entire figure.

Bridging

Another geometry defect present in the forming of carbon fiber composites is bridging. Bridging occurs when the material spans the gap over a negative molding geometry without fully forming into the corner, resulting in a formed part inconsistent with the designed mold (32).

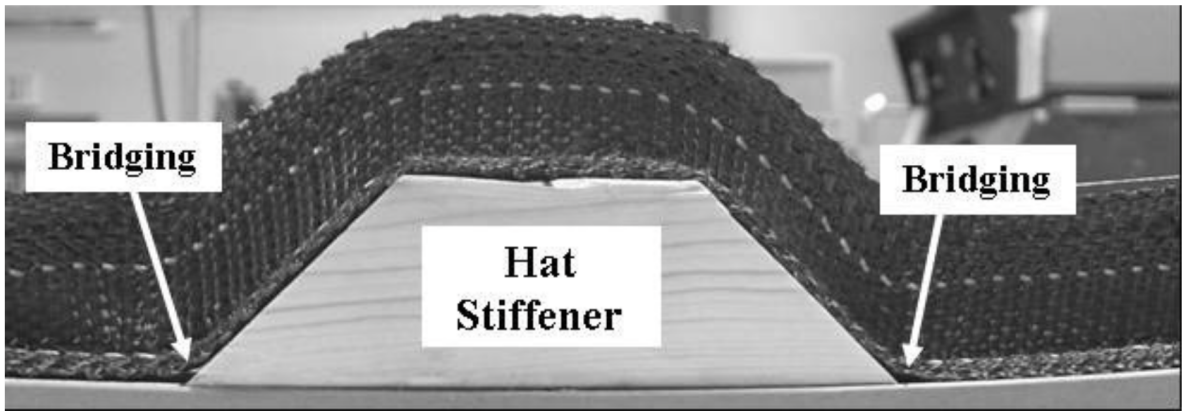


Figure 2.5: Bridging Example for Hat Cross-Section using Continuous Fiber Woven Preforms: bridging observed over the 45°tool angles (32)

Previous experimentation studied bridging behavior when forming carbon fiber woven Pi-preforms over a hat-shaped geometry. An image representing this effect is displayed in Figure 2.5 where bridging is seen in the concave corner regions of the tool (32). Woven pi preforms are made from carbon fibers tows meticulously woven to create a four-pronged piece that can be bent into a T-shaped joint, and later infused with resin during the forming process (32). Bridging was measured at the concave corners of the hat mold by simply measuring the distance of the gap from the formed part to the surface of the mold (32). It was found that "SBCF preforms had greater formability than their continuous counterparts" (32).

Strain

When the material undergoes the forming process, the original carbon fiber prepreg is subject to straining as it slightly stretches to fit the mold (25). The amount of strain the composite is subjected to during the forming process is a complex area of study when evaluating forming as it affects the allowable strain of the cured part. Yanagimoto *et al.* (2012) were concerned with the bending strain at the surface of their single bead parts as well as the gradient of strain in the thickness direction to find the ideal mechanism for formability enhancement (25). Ideally, the "strain gradient in the [the] thickness direction should distribute uniformly in [the] thickness direction" (25). The bending strain was calculated with Equation 2.2 using the thickness of the material, t, as well as the radius of the neutral plane, R_n, and curvature of the neutral plane, ρ (25).

$$\epsilon_{max} = \frac{t}{2R_n} = \frac{\rho t}{2} \tag{2.2}$$

The bending strain gradient is found by taking the derivative of the bending strain with respect to the thickness measurement as seen in Equation 2.3 (25).

$$\frac{d\epsilon_b}{dy} = \frac{2\epsilon_{max}}{t} = \rho \tag{2.3}$$

Through these measurements and calculations, a relationship between the strain and the initiation of necking during forming was determined (25).

Springback

A common defect within any forming process is springback. Springback "is defined as a positive angular difference due to the widening of the angle between the formed composite laminate and the mold geometry" (30). Mujahid *et al.* (2020) sought to decrease the effect of springback by exploring different forming processes for hat-shaped molds (30). While no

noticeable springback was noted, the overall shape of the hat cross-section was measured and the coefficient of determination was calculated to evaluate the possibility of spring back (30). Mujahid *et al.* (2020) concluded that the potential for springback decreases after the curing process (30). Beglinger (1998) also explored the springback effect in his thesis *Forming of Advanced Composite Material* (33). The deformation mode occurring in springback is simple for pure bending (33). In the springback experiments, a carbon fiber sheet was formed in an L shape over a positive aluminum mold with various forming temperatures and durations used (33). Once the material was formed, it was then allowed to cool and measurements of the angle between the material and the tool were taken at 5 minute intervals 30 minutes after forming (33). A schematic of the measurements taken is presented in Figure 2.6. It is noted that the composites used in the spring back test were not allowed to cure, further supporting the conclusions of Mujahid *et al.* (2020) stating that the effect of springback decreases during the curing process (30).

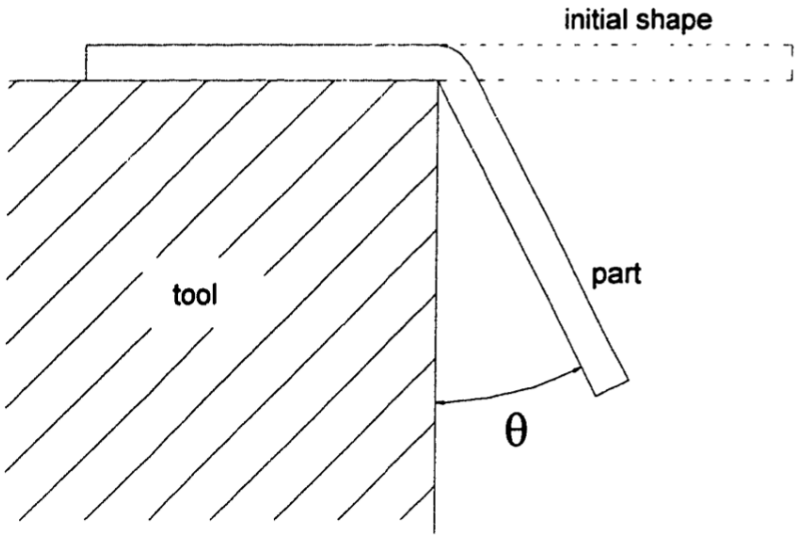


Figure 2.6: Springback Angle (theta) Measurement Schematic for Beglinger's *Forming of Advanced Composite Material* Thesis (1998). Image shows the tool surface with the initial shape of the the part, the part shape, and the angle between the tool and the part. (33)

METHODOLOGY

Testing Procedure

Test Preparation Procedure

Each complex shape test requires a flat or uni-axially curved layup of carbon fiber prepreg plies. The layup orientation is varied for the different shape types based on common layup practices (3). For the Curved C-channel mold, a quasi-isotropic layup of [45/0/-45/90]s is chosen in order to achieve zero degree plies and ninety degree plies at most locations around the curvature of the part. For the preliminary Rounded Hat channel and Sinusoidal C-channel tests, a layup of [0/90]s is selected to simplify the layup process for the curved molds. This layup is then marked via a silver metallic Sharpie on the top and bottom surfaces to divide the part into measurement sections. The sections are on a polar grid system for the Curved C-channel and a Cartesian grid system for the other tooling types. Examples for the section layouts of the Curved C-channel and Rounded Hat channel can be seen in Figure 3.1.

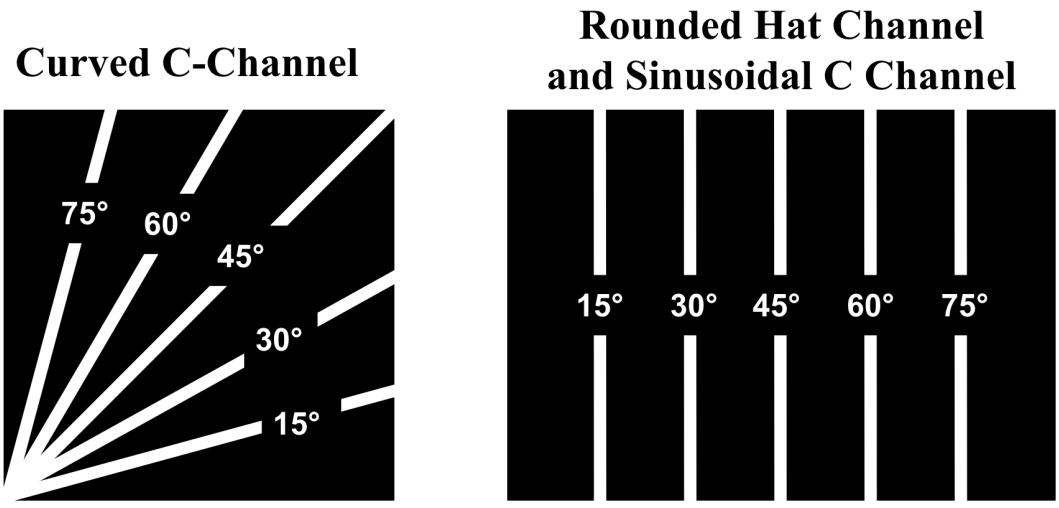


Figure 3.1: Sectioning Examples for the Uncured Layups: LEFT - Curved C-channel Section Diagram, RIGHT - Rounded Hat channel and Sinusoidal C-channel Section Diagram

Note that there are six sections for each, resulting in five cross-sections between the six measurement regions. These cross-section selections are designed to span across the initial cross-section the part is designed with. For example, the Curved C-channel sections are designed so that every cross-sectional scan includes the base C-Channel shape. The Sinusoidal C-channel sections are divided identically to the Rounded Hat channel model from a top down view point, but are spaced to incorporate the major peaks, valleys, and average amplitude points of a sinusoidal function. For future geometries, the sections should be designed to incorporate all of the major features, corners, and cross-sections of a part model. A minimum of five cross-sections is recommended for future geometries.

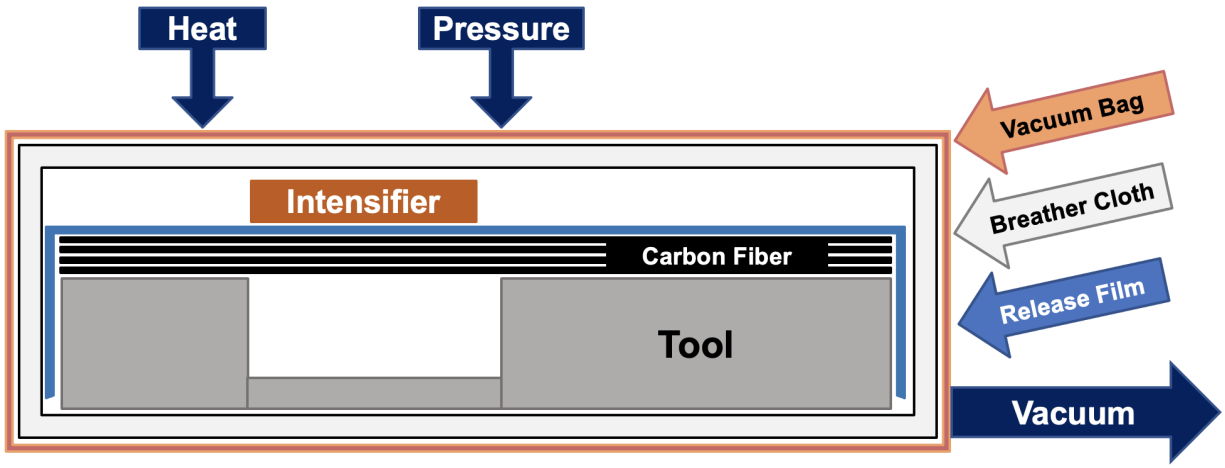


Figure 3.2: Vacuum Bagging Process for Testing: Carbon fiber layup applied atop the tool, layer of release film, intensifier (if choosing to use), breather cloth to evacuate air, and vacuum bag to apply vacuum

Prior to vacuum bagging, the tool mold is coated with ten layers of Frekote 770NC release agent to aid in the removal of the cured part from the tool surface (34). Fiberglass breather strings are sometimes taped using temperature-resistant "flash breaker" tape to the tooling across closed geometry areas to evacuate air underneath the layup (35). The use of breather strings adapts as ideal layup practices are developing. The layup is then applied on top of the tool as desired. The layup shape, orientation, and curvatures are varied between

tests to study their impact on formability. High Elongation FEP Release Film is cut to the curvatures of the tooling and placed on top of the layup in such a way that it allows the carbon fiber to slip and stretch into the tooling without restraint (36). For some tests, a silicone intensifier is applied atop the layup and pressed slightly into the negative portion of the tooling to study the impact of intensifiers on forming quality. This intensifier is a positive matched soft mold purposely sized to fit the laminate between itself and the tool. In some of the tests, the intensifier is pressed down to the bottom of the tool and in other cases, just rests atop the laminate with slight pressure. Several layers of breather cloth are wrapped around the tool and layup to assist in air evacuation through a vacuum bag port (37; 38). The vacuum bag is intentionally cut larger than the tooling so pleats can be added. These pleats allow the bag to fill the tooling during the forming process instead of pulling taught and inhibiting forming. A schematic of the vacuum bagging process is presented in Figure 3.2. The vacuum bag and all of its contents are placed in the autoclave where it will experience vacuum inside of the bag, pressures of up to 90 psi [620.53 KPa] outside of the bag, and high temperatures (80°F [26°C] - 350°F [176°C]) for varying amounts of time depending on the resin type used. In this study, the cure cycle used is based on the manufacturer's recommendation for the particular resin system. Some of the cure cycles used are designed to increase formability by adding in intermediate temperature dwells at lower temperatures before rising to the curing temperature. After cure, the part is demolded, labeled, and prepared for cross-sectioning and scanning by checking that the previous section lines are still intact.

Cross-Sectioning and Scanning Procedure

Some measurements within the forming evaluation criteria require cross-sectioning procedures. To create cross-sections, the sections, as previously drawn on a grid, are cut on the marked lines using a water-cooled tile saw with an eight inch DDM Concut diamond

coated tile blade. Each part is cut into six sections, which allows for five cross-sections, selected to keep within limitations of the part sizes. Once the part is cut, each section is polished on a grinding block with Struers P800 grit sandpaper to remove any stray fibers that cross-sectional cutting resulted in. Once the sections are polished, they are scanning individually on a Mustek Systems flatbed scanner (A3 2400S). An example from Curved C-channel Part MD009 (Hexcel IM7/8552) at the 15 degree cross-section can be seen in Figure 3.3.

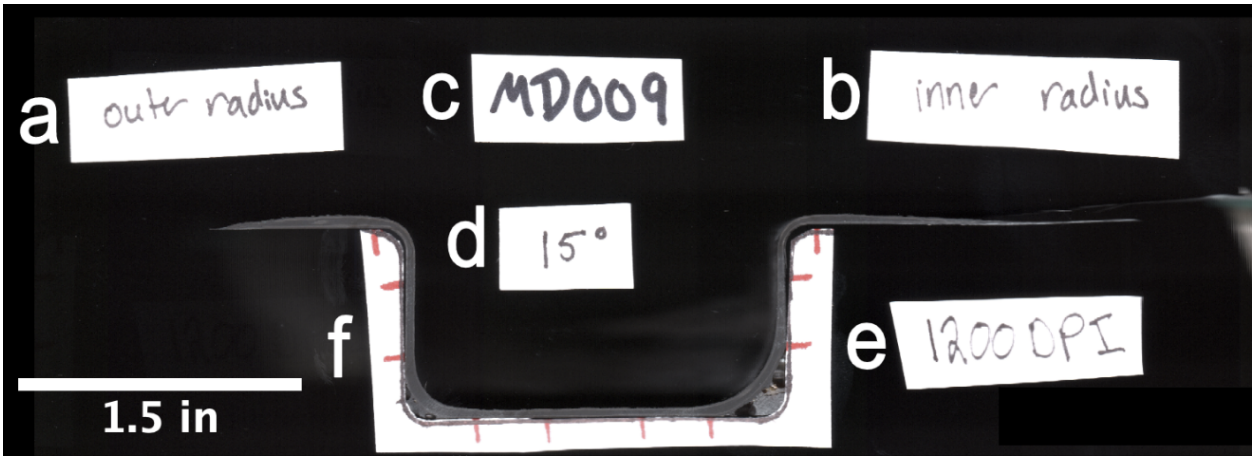


Figure 3.3: Curved C-channel Cross-Sectioning Example: Continuous Carbon Fiber Part (Hexcel IM7/8552). a and b - radius designation labels, c - part name label, d - section designation label, e - scanning quality label, f - measurement locations template

Each section is scanned with a label of the section number (d), a template of the measurement locations (f), a label of the part name (c), labels for the radii designations (a and b), and a label with the scanning quality (e). The scanned images are then processed in Adobe Photoshop to adjust the contrast and brightness so the outer-plies of the laminate are distinct against the scanning backdrop as well as exporting the correct file type for later image analysis.

The radius designations, "radius #1" and "radius #2", are arbitrarily chosen for the Rounded Hat channel and Sinusoidal C-channel parts in order to keep measurements

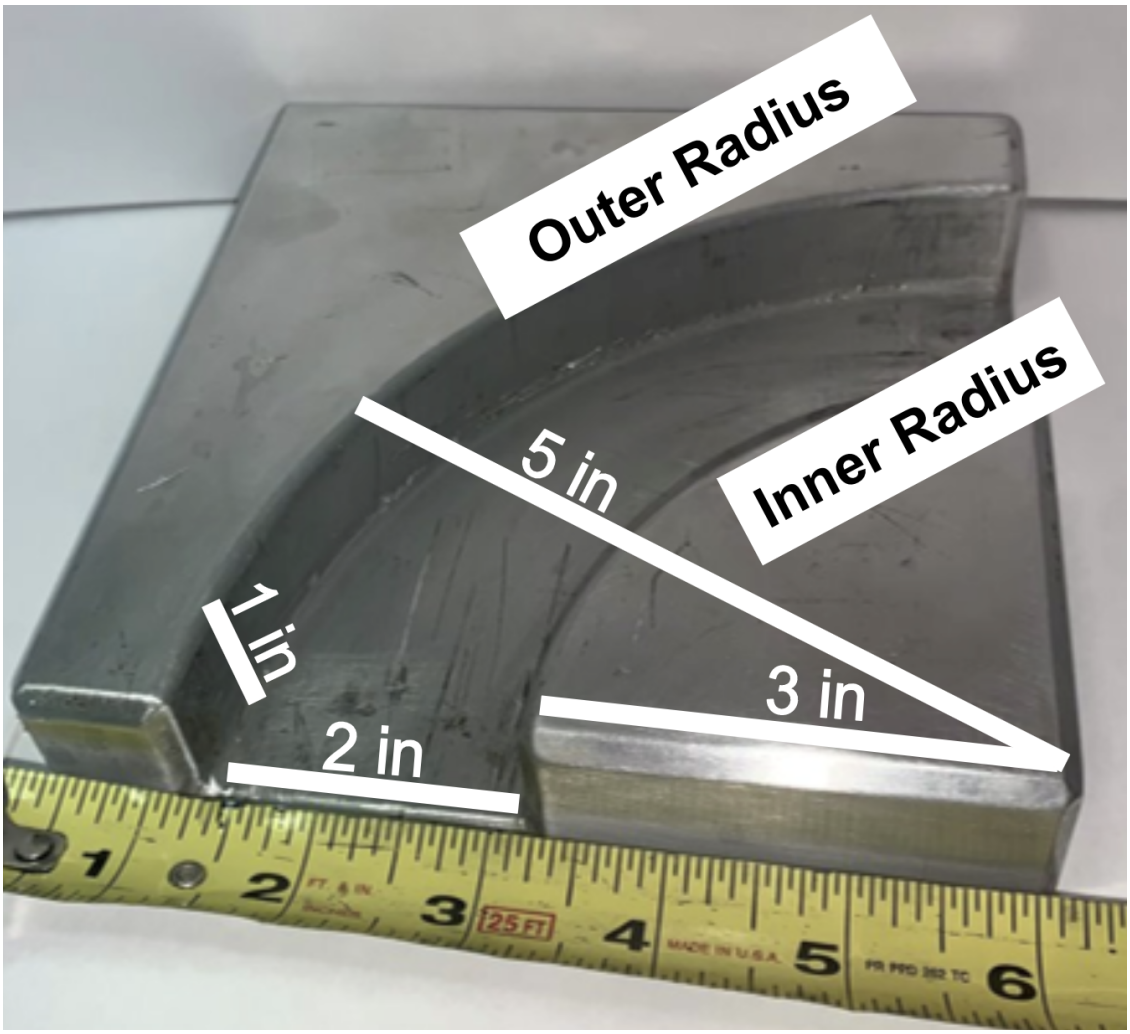


Figure 3.4: Curved C-channel Radius Designations and Dimensions: "Radius #1" = Inner Radius, "Radius #2" = Outer Radius

consistent. The Curved C-channel has specific radius designations with "radius #1" corresponding to the "inner radius" and "radius #2" corresponding to the "outer radius" in Figure 3.4. These radius designations are chosen based on the distance from the origin of curvature on the Curved C-channel parts. The smaller radius of curvature is "radius #1" and the larger radius of curvature is "radius #2". Future geometries possessing more radii could incrementally increase the designations, while maintaining consistency between measurements.

Analysis Procedure

Once the parts are formed and cross-sectioned, a method for evaluating the forming quality is utilized. The goal of the method is to produce a forming score from 0 to 5 for each part made. This score considers many different carbon fiber forming defects and analyzes them in a weighted matrix. Each defect is designated as a "forming metric" with its own unique scoring system and metric weight. The previous studies mentioned in Chapter 2 used many different metrics for evaluating forming quality. Of the metrics listed (as well as some additional ones), the final eight forming metrics are selected (some defect locations presented in Figure 3.5) as bridging (a), wrinkling, thickness variation, forming depth (c), corner thinning (b), corner thickening (a), resin pooling (a), and texture quality. Additionally, metrics of splitting and stretching versus slipping (d) in Figure 3.5) are measured and analyzed to inform the final forming score. These metrics are not included in the 0 to 5 part forming ranking, but are useful in determining the part "usability" and mechanisms of forming present. The details of this final forming score will be explained further in Section 3.

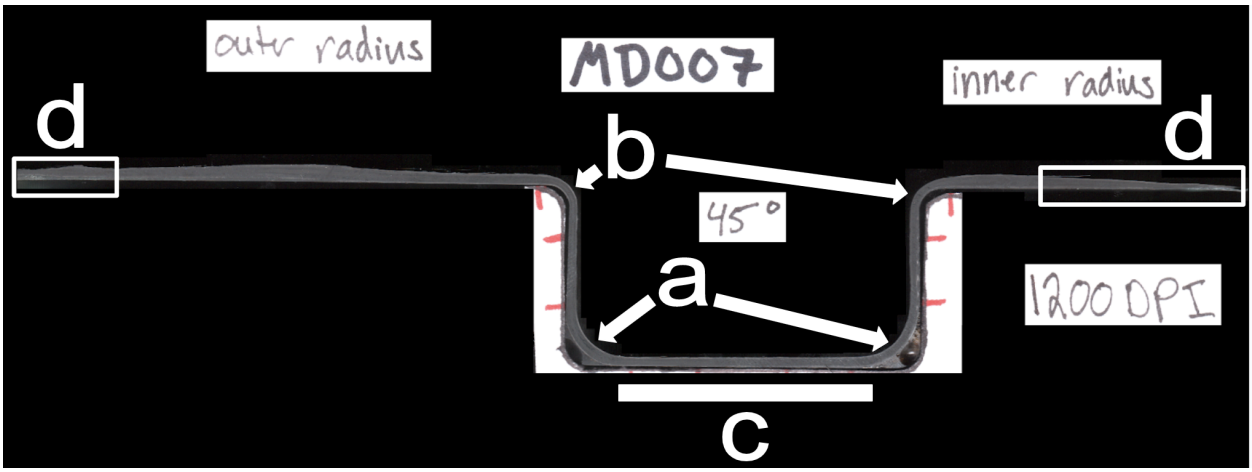


Figure 3.5: Defect Locations: a) bridging, corner thickening, and resin pooling defect locations, b) corner thinning defect location, c) forming depth defect location, d) stretch versus slip partial defect location

Metric Definition, Measurement, Analysis, and Scoring Procedures

This section details the individual metrics chosen for forming evaluation as well as their definitions. The measurement procedures are outlined for each metric to document the forming evaluation process. The analysis sections provide any calculations and data representations. Methods for data visualization were influenced by Doumont's (2014) *Trees, maps, and theorems* textbook (39). Finally, the 0 to 5 scoring rubrics and procedures are presented for each metric.

Bridging

Definition: Bridging for this method of forming analysis is defined as the scenario when the carbon fiber laminate spans the gap across a concave radius mold without meeting the curved tool surface (32). A visual representation of the bridging defect is seen in the red box in Figure 3.6. For the purposes of this method, bridging is evaluated by the distance from the tool surface to the distance of the laminate tool-adjacent ply (Figure 3.7).

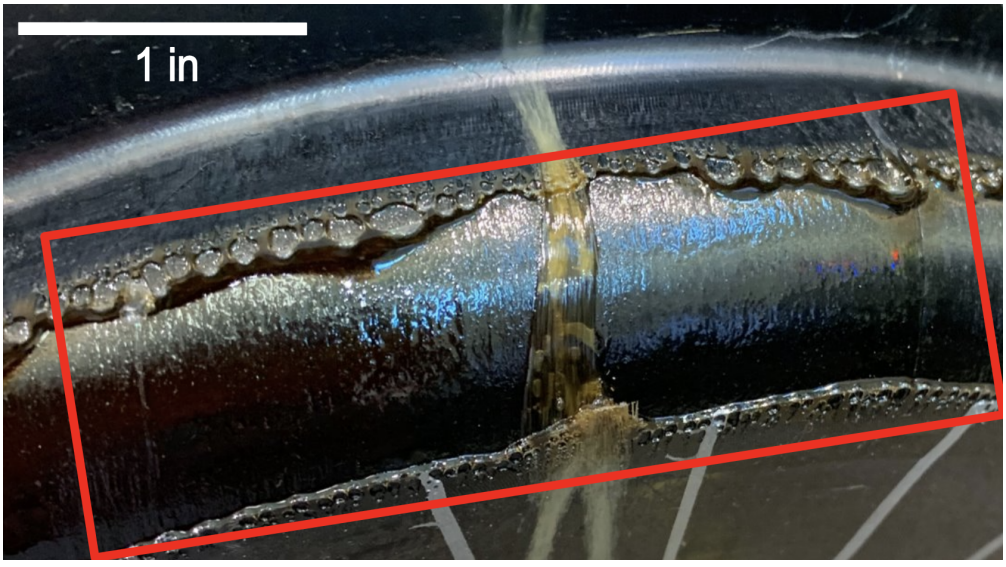


Figure 3.6: Bridging Defect Example: Stretch Broken Carbon Fiber Curved C-channel Part (MSU SBCF/977-3)

Measurement Procedure: Bridging is measured after the cross-sectioning procedure. The bridging measurement is very dependent on correct placement and geometry of the scanned template. The template has the same path line and geometry of the tool surface. From the scanned image, ImageJ can be used to place a line from the tool surface concave curvature to the carbon fiber tool-adjacent ply surface curvature. A schematic of this measurement can be seen in Figures 3.7 and 3.8 where the orange arrows are the bridging gap distance and the "Tool" area coincides with the template shape. It should be noted that the line is placed to contact the bottom ply of the carbon fiber part regardless of whether there is resin pooling or not. The line is analyzed for length in ImageJ and recorded for each concave corner to calculate the bridging gap distance.

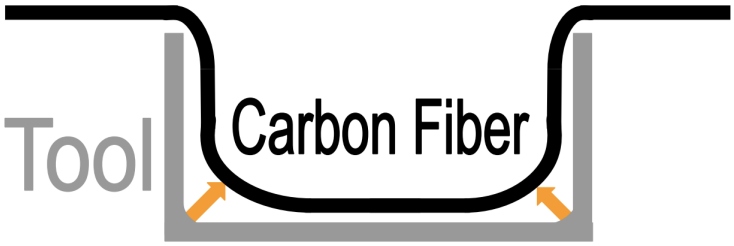


Figure 3.7: Bridging Measurement Schematic: range arrows indicate bridging distance gap between tool and tool-adjacent ply

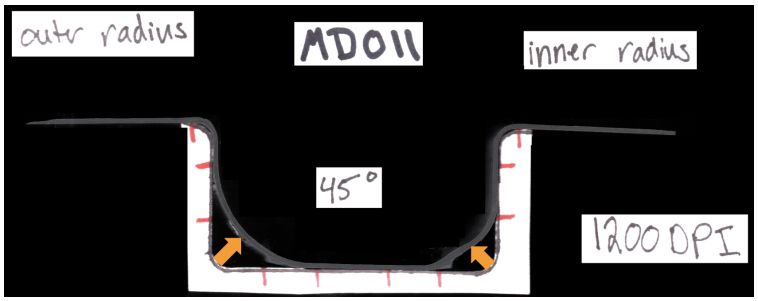


Figure 3.8: Bridging Measurement on Part Cross-Section: orange arrows indicate bridging distance gap between tool and tool-adjacent ply

Analysis Procedure: Bridging gap distance is represented for each concave radius at each cross-section in a bar graph. A representation of these data points can be seen for Curved C-channel part MD019 on a bar chart as the blue data in Figure 3.9. Also on this plot is the resin pooling data. The measured bridging gap lengths are unchanged in this representation. For the later scoring procedure, the bridging gap lengths are also divided by the radius value of the ideal concave corner and multiplied by 100% to achieve a percentage that determines how much larger the gap is than the designed curvature.

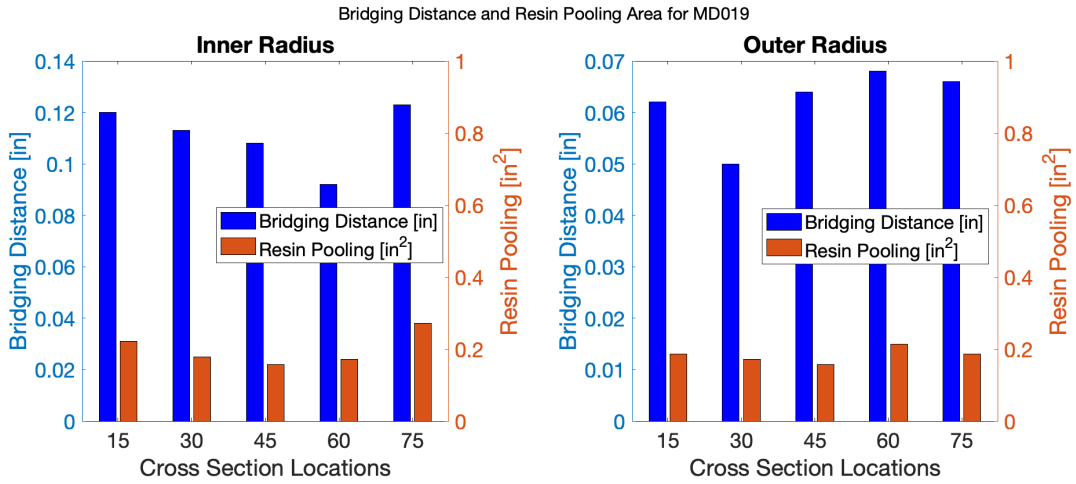


Figure 3.9: Bridging Data Representation: Continuous Carbon Fiber (Hexcel IM7/8552) Curved C-channel Part

Scoring Procedure: The calculation mentioned above for bridging gap distance divided by the ideal part radius percentage and averaging the data by each measurement location is used in Table 3.1. In this table, "Bridging" refers to this calculation, and the ranges are determined based on the collection of tests performed. The scores of 5 to 1 are assigned ranges within an overall range of 0% to 200%. These intermediate ranges are designed to incrementally get larger while the score decreases. For example, the 4 star range is from 0% to 25% bridging which is a 25% gap and the consequent 3 star range is from 25% to 60% bridging which is a 35% range. This system is used to assign all of the ranking values. If the

bridging gap distance is 200% that of the original radius, it receives a bridging score of 0, whereas if the bridging gap distance is 0 units of length, it receives a perfect bridging score of 5.

Table 3.1: Bridging Metric Rankings

Metric	**0**	**1**	**2**	**3**	**4**	**5**
Bridging	Bridging $> 200\%$	$200\% \geq$ Bridging $> 100\%$	$100\% \geq$ Bridging $> 60\%$	$60\% \geq$ Bridging $> 25\%$	$25\% \geq$ Bridging $> 0\%$	No bridging present

Examples of some of these bridging scores on some Curved C-channel carbon fiber parts are presented in Figure 3.10. On the leftmost image in Figure 3.10, an example of the bridging distance on one corner that receives a score of four is presented with the orange arrow indicating the bridging gap measurement. In the scores of 2, 3, and 4 examples, the bridging distance is seen to pass through the region of resin pooling until the arrow reaches the location of the tool adjacent ply per measurement instructions. Any bridging distance gap larger than the score of 1 image would result in the lowest score of 0. None of these scores and rankings presented are used as a method for determining defect acceptability criteria and are instead used to record how much of the defect is present on any given part. This record could allow for tracking of defect improvement or deterioration based on processing parameters.

Wrinkling

Definition: Wrinkling is easily defined as any location containing a wrinkle (7). One of these wrinkles from an earlier complex shape test is analyzed under a microscope to visually understand what the material behavior is in the area with wrinkling. This microscope image is represented in Figure 3.11. From the image, it is seen that wrinkles result in large voided

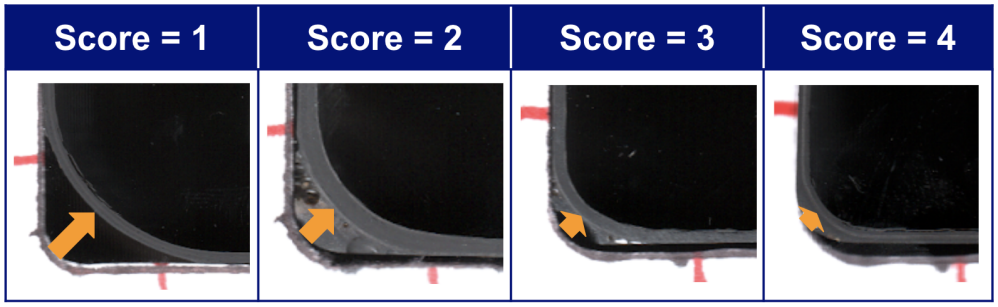


Figure 3.10: Bridging Score Examples as Orange Arrows: LEFT - Bridging score of 1 example , LEFT CENTER - Bridging score of 2 example, RIGHT CENTER - Bridging score of 3 example, RIGHT - Bridging score of 4 example

regions between the plies where there are no resin or fibers present. The plies are also seen to curve across the wrinkle, effectively pre-buckling the material at the wrinkle location. Thus, it is important to understand the area of the wrinkling regions for the part.

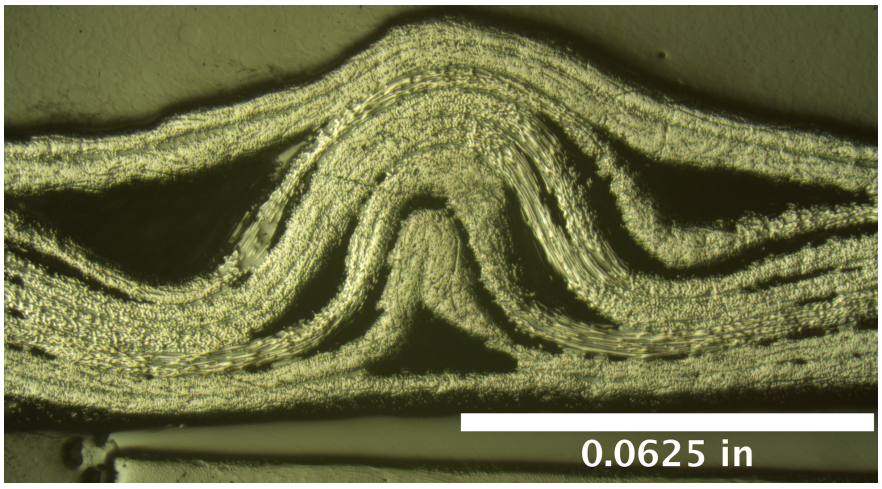


Figure 3.11: Wrinkling Defect Example: Stretch Broken Carbon Fiber Curved C-channel Part

Wrinkling is also defined by whether it occurs in a “critical” or “non-critical” region of the part. In Figure 3.12, the critical regions can be seen for the Curved C-channel, Rounded Hat channel, and Sinusoidal C-channel. The top images are the original model geometry, which is the region of the part deemed critical. The bottom images show complex carbon

fiber part images with the ideal model geometry (critical region) boxed in red. All regions outside of these critical regions are additional material deemed non-critical.

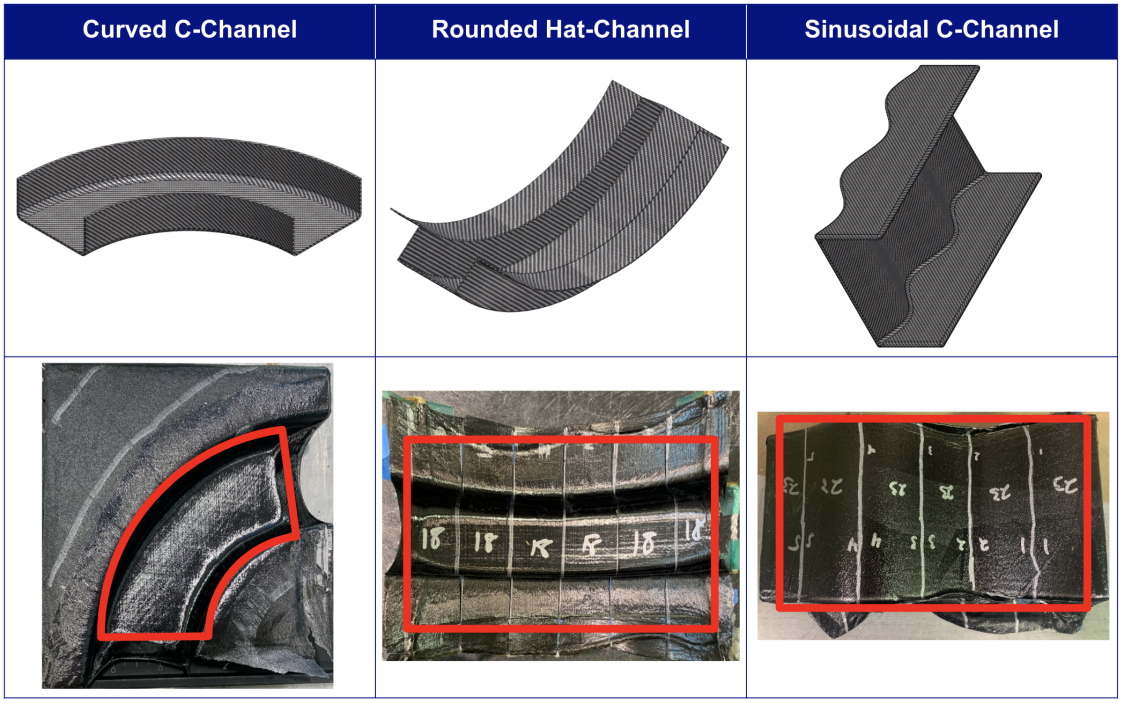


Figure 3.12: Critical Region for Various Part Types: TOP LEFT - Curved C-channel critical region model, BOTTOM LEFT - Curved C-channel critical region on a carbon fiber part boxed in red, TOP CENTER - Rounded Hat channel critical region model, BOTTOM CENTER - Rounded Hat channel critical region on a carbon fiber part boxed in red, TOP RIGHT - Sinusoidal C-channel critical region model, BOTTOM RIGHT - Sinusoidal C-channel critical region on a carbon fiber part boxed in red. The regions shown are the ideal part geometry excluding any overhangs or wraparounds of the completed parts

Measurement Procedure: Wrinkling is measured as the ratio of wrinkle surface area to total surface area as well as the percentage of wrinkling area within the critical region to the critical region surface area defined by part geometry, seen in Figure 3.12. This metric is measured before the cross-sectioning procedure. To measure the wrinkle area, each wrinkle is measured individually. The wrinkle areas are approximated as rectangular in geometry where the width and length of the wrinkles are measured with calipers in inches. In Figure 3.13, a wrinkle area approximation example for Curved C-channel part MD008 can be seen

as the blue rectangular outlines. Note that all of these wrinkles are present in the non-critical region. After a wrinkle is measured, it is traced over with a metallic permanent marker to ensure no duplicate measurements occur. The wrinkle is also denoted with a label of "Critical Region", "Non-Critical", or "Both" to track wrinkle location. If the wrinkle is denoted with the "Critical Region" label, then the entire wrinkle area is included in the critical wrinkle location calculations. If the wrinkle is denoted with the "Non-Critical" label, then the critical wrinkle location calculations are ignored for that wrinkle. If the wrinkle is denoted with the "Both" label, the area of the wrinkle that crosses into the critical region is recorded for the critical wrinkle location calculation.

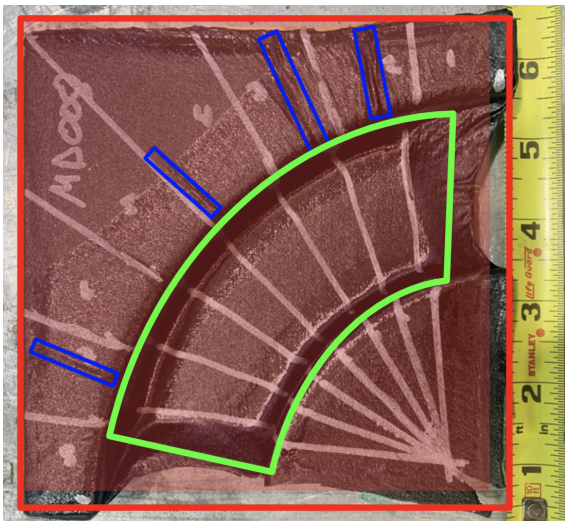


Figure 3.13: Wrinkle Measurement Schematic, Continuous Carbon Fiber Curved C-channel Part: Wrinkle regions highlighted in blue (all wrinkles are within the non-critical region), surface area highlighted in red, critical region highlighted in green

The other half of the wrinkling calculations include the surface area calculations. This surface area is seen as the red highlighted region with the critical region highlighted in green in Figure 3.13. These areas are calculated by measuring the dimensions of the non-critical region surface areas and the critical region surface area and are calculated based on the geometric shape of the regions.

From these measurements, three total values result for each part: 1. the total wrinkle area, 2. the total part area, and 3. the wrinkle area within the critical region.

Analysis Procedure: The wrinkle analysis is calculated two ways: the total wrinkle area as a percentage of the total part area and the wrinkle area within the critical region as a percentage of the total wrinkle area. To represent these data, MatLab is utilized to generate pie charts of these two percentages. An example of the wrinkle data representation can be seen in Figure 3.14 using example values representative of a scenario with 16% wrinkling of the total area and 10% wrinkling in the critical area. The left pie chart in this figure represents the total surface area of the part where the dark blue wedge in this example represents 16% wrinkling of the total surface area and the light blue area is the remaining non-wrinkled area. The pie chart on the right in this figure represents the total wrinkle area where the green region in this example represents 10% of the wrinkles being located within the critical region and the yellow area is the remaining wrinkles outside the critical region.

Scoring Procedure: The wrinkling defect is ranked by a 0 to 5 scoring system defined by the wrinkling within the critical region as well as the total wrinkling. These are defined by the percentages calculated in the analysis section. A score of 5 indicates a "perfect part" which would experience no wrinkling within the critical region as well as the non-critical region. The other rankings fit within certain calculated percentages. The full range of the ranking assignments for the wrinkling metric can be seen in Table 3.2. These ranking assignments are chosen based on the entire set of part data for wrinkling. The primary area of concern for wrinkling is wrinkling within the critical area as that is the region of the part that needs to perform strength wise. The ranges for the scoring where the critical region is concerned are very strict to account for the impact of wrinkling, ranging from 0% wrinkling within the critical region to 3% wrinkling within the critical region. The wrinkling elsewhere category primarily pertains to wasted additional material. If the non-critical region of the

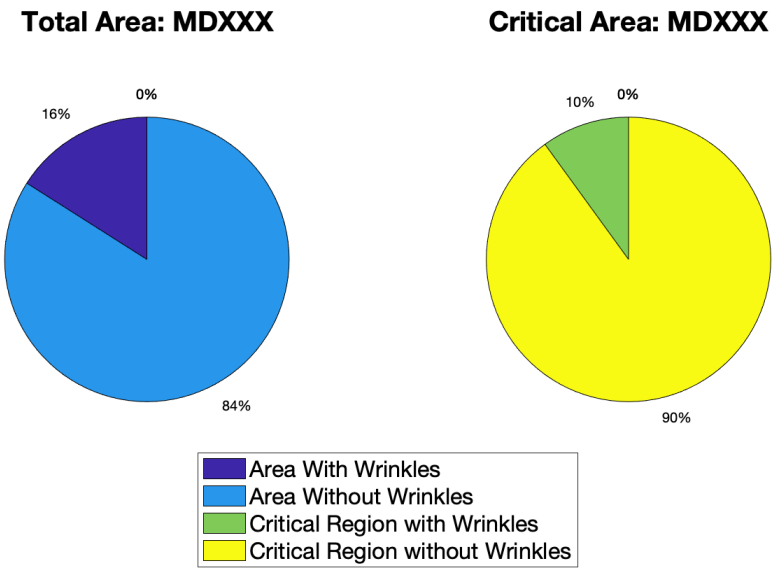


Figure 3.14: Wrinkle Data Representation Example: LEFT - 16% Wrinkling within the total area, RIGHT - 10% Wrinkling within the critical area

part has considerable wrinkling, the material used in that area is effectively wasted. Due to this, the non-critical region wrinkling is still used in the scoring system, but has much wider ranges for each value, ranging from 0% wrinkling elsewhere to 10% wrinkling elsewhere.

In Figure 3.15, are some examples of the scoring for different wrinkling amounts, specifically scores of 1, 3, and 5. The left image in Figure 3.15 is an example of a stretch broken carbon fiber Curved C-channel that earned a score of 1 for wrinkling due to a large wrinkle within the center of the critical region. The center image in Figure 3.15 is a stretch broken carbon fiber Curved C-channel part with no wrinkling within the critical region, but enough wrinkling outside of the critical region to earn a wrinkling score of 3. The right image in Figure 3.15 shows a continuous carbon fiber Curved C-channel part that experienced no wrinkling at any location on the part effectively earning a perfect wrinkling score of 5. This scoring system is not used as a method to determine part acceptance, but instead is used to

Table 3.2: Wrinkling Metric Rankings

Metric	0	1	2	3	4	5
Wrinkling	$>$ 3% wrinkling in critical area	2%-3% wrinkling in critical area or $>$ 10% wrinkling elsewhere	1%-2% wrinkling in critical area or 7%-10% wrinkling elsewhere	0%-1% wrinkling in critical area or 5%-7% wrinkling elsewhere	No wrinkling in critical area and $<$ 5% wrinkling elsewhere	No wrinkling present anywhere on the part

track wrinkle amount and location. These ranges within the wrinkle scores could allow the user to test how certain processing parameters, or input variables, impact the appearance, occurrence, and location of wrinkling within a certain part geometry.

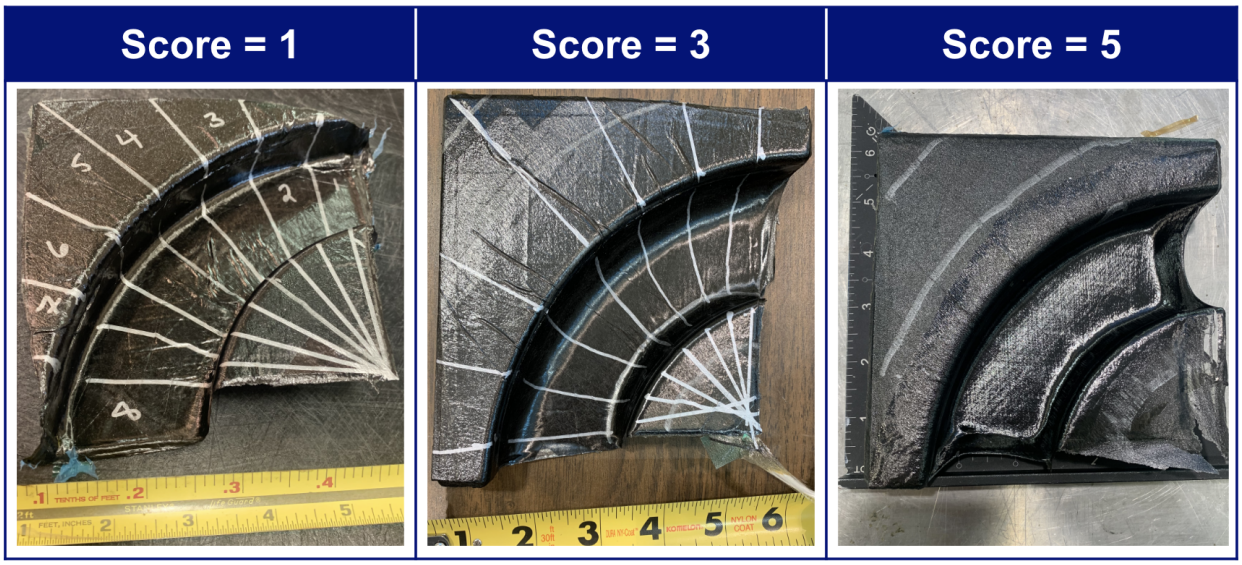


Figure 3.15: Wrinkle Scoring Examples: LEFT - Curved C-channel Wrinkle Score of 1 example, CENTER - Curved C-channel Wrinkle Score of 3 example, RIGHT - Curved C-channel Wrinkles Score of 5 example

Thickness Variation

Definition: Thickness variation is defined as discrepancies in the thickness across the span of the part (27; 28; 30). Certain areas along the fully formed part thicken or thin depending on the geometry, forming mechanisms present, and processing parameters. Severe amounts of thinning can negatively impact the strength performance of the part at these thinned regions where severe amounts of thickening result in variations from the original designed model. A binary image of one of the cross-section scans can be seen in Figure 3.16 to give an example of how thickness changes throughout the part.



Figure 3.16: Thickness Variation Defect Example: Continuous Carbon Fiber Curved C-channel Part (Hexcel IM7/8552)

The example in Figure 3.16 has thinned regions on the walls and bottom of the C-channel where thickening is present on the upper, outer regions. Resin pooling is present in this schematic, contributing to the thickening seen at the concave corner regions.

Measurement Procedure: The thickness variation measurement procedure is a series of thickness measurements across the geometry of the part. These measurements are taken after the cross-sectioning procedure. For each of the five section lines seen in Figure 3.1, ten thickness measurements are taken. These thickness measurements are taken at the red lines on the part template seen in Figure 3.3, and can also be seen as the red circles in Figures 3.17 and 3.18. They include measurements from the flat sections before the convex radii,

measurements on the walls of the critical region defined by part geometry, and measurements of the bottom portion of the critical region defined by part geometry to get a full scope of the part thickness across regions of interest during the forming process. These thickness measurements are taken in ImageJ software by inserting a line from the inner ply to the outer ply at the template locations and analyzing for line length in pixels, converted to length units using appropriate scaling.

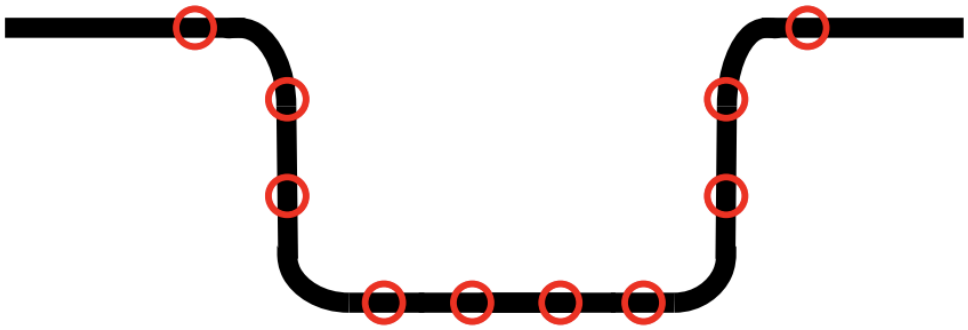


Figure 3.17: Thickness Measurement Locations Schematic: Red circles indicate measurement locations

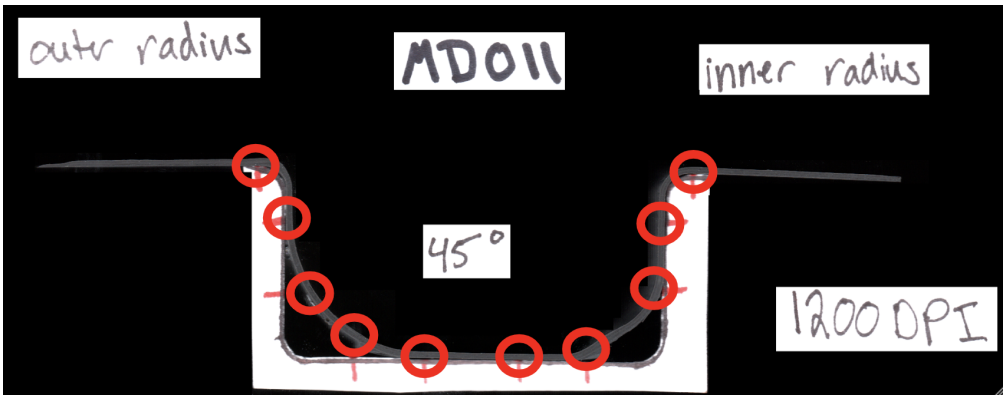


Figure 3.18: Thickness Measurement on Part Cross-Section: Red circles indicate measurement locations based on red template lines

Analysis Procedure: The thickness data are analyzed in two different ways. The first analysis is a calculation for the coefficient of variation, denoted as C_{var}, of the total set of measured thickness data seen in Equation 3.1 (28). In this calculation $\bar{x}$ is the average thickness of the entire data set, x is the thickness location at an individual location, and n is the total number of measurements. The average thickness $\bar{x}$ is saved for other metric calculations (corner thinning and corner thickening). This calculation provides an idea of the variation in thickness for the entire part.

$$C_{var} = \frac{1}{\bar{x}} \sqrt{\frac{\sum (x - \bar{x})^2}{(n-1)}} \tag{3.1}$$

The second analysis is a calculation of percent thinning or percent thickening of the final part when compared to the original layup thickness. This original layup thickness is determined by the material parameters for the carbon fiber type used and the amount of plies in the laminate. Each value is measured as a percent thinning or thickening denoted as $t_{\%}$. The calculation for $t_{\%}$ can be seen in Equation 3.2 where t_f is the measured thickness in ImageJ and t_i is the initial layup thickness.

$$t_{\%} = \frac{t_f - t_i}{t_i} * 100 \tag{3.2}$$

The calculated percent thinning/thickening values are then represented on a contour plot of the entire part. Figure 3.19 illustrates an example of the contour plot for Curved C-channel part MD019. The X,Y, and Z coordinates represent the part geometry where the color-bar indicates the percent thinning and thickening. The yellow regions of the contour plot represent percent thickening of the material after forming whereas the dark blue regions represent percent thinning of the material after forming. Different orientations are displayed to aid in viewing of the entire part surface: one with “radius #1” oriented towards the viewer and the other with “radius #2” oriented towards the viewer.

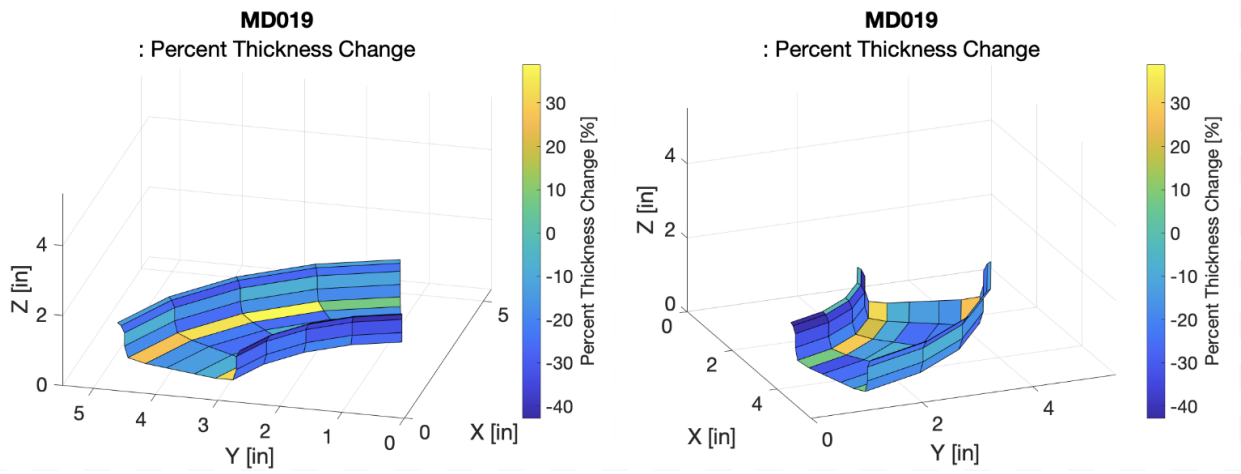


Figure 3.19: Thickness Contour Plot Representation: Continuous Carbon Fiber Curved C-channel Part, LEFT - "Radius #1" orientation, RIGHT - "Radius #2" orientation

Scoring Procedure: The thickness metric scoring is determined by the coefficient of variation calculations. The accepted values for each rank are represented in Table 3.3. The overall range for coefficient of variation is a large range, spanning up to 40% variation in thickness. Based on the previous part data, the range is determined by incrementing in 10% intervals for each score. These ranges are not to determine the part acceptability, but instead are used to record the amount of thickness variation for a given part. These values could allow the user to track how thickness variation improves or decrements when altering input variables such as the layup, cure cycle, material, and bagging procedure.

Table 3.3: Thickness Metric Rankings

Metric	**0**	**1**	**2**	**3**	**4**	**5**
Thickness	$C_{var} >$ 0.4	$0.4 \geq C_{var} \geq$ 0.3	$0.3 \geq C_{var} >$ 0.2	$0.2 \geq C_{var} >$ 0.1	$0.1 \geq C_{var} >$ 0	$C_{var} =$ 0

Forming Depth

Definition: Forming depth for this experimentation is defined as the contact region between the carbon fiber first ply and the flat portion of the negative tool molding (25). Forming depth is measured as the percentage of the material formed to the depth. If the carbon fiber does not form completely into the tool mold, this forming depth metric is easily seen with the naked eye. An example of a part cross-section with poor forming depth is seen in Figure 3.20 for a stretch broken carbon fiber Curved C-channel part.



Figure 3.20: Poor Forming Depth Example: Stretch Broken Carbon Fiber Curved C-channel Part

In Figure 3.20, the flat region of the part bottom is much shorter than the original tool bottom flat region. Forming depth is used to account for the flat regions along the tool to carbon fiber interface that the bridging defect ignores, as bridging is only concerned with the curved, concave radius locations.

Measurement Procedure: Forming depth is also measured after the cross-sectioning and scanning procedure. Forming depth is defined in this case as the contact length of the carbon fiber inner ply to the tool surface in the negative tooling regions for each cross-section. To measure forming depth, ImageJ is used to place a line and analyze for length. The first line measured is the carbon fiber contact length which is found by placing a line from the point of initial contact to the point where it again loses contact with the tool, seen as the pink

rectangle in Figures 3.21 and 3.22. The second line measured is the distance from the tool wall to the start of carbon fiber contact with the tool, shown as the green arrow in Figures 3.21 and 3.22. It is important to measure this distance from what has been designated as "radius #1" for the given complex geometry. The final line is not measured in ImageJ, but directly on the tool with calipers. This line measurement is the distance from the start of the first radius curvature to the second radius curvature, or the distance across the flat bottom of the tool. This measurement is classified as the ideal contact length and is seen as the blue rectangle in Figures 3.21 and 3.22.

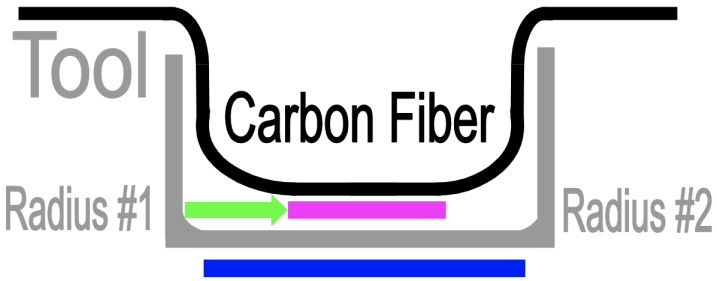


Figure 3.21: Forming Depth Measurement Schematic: Pink line is the carbon fiber forming depth measurement, green arrow is distance over from the tool wall, blue line is the ideal forming depth measurement

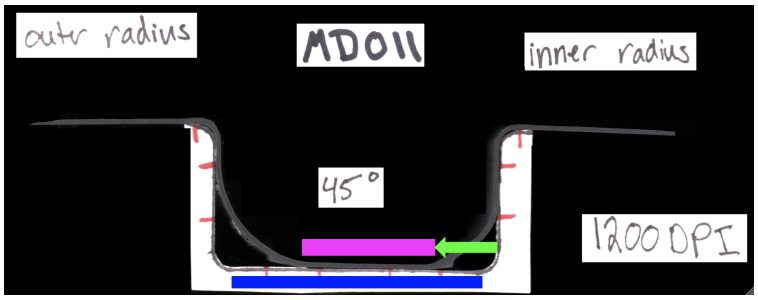


Figure 3.22: Forming Depth Measurement on Part Cross-Section: Pink line is the carbon fiber forming depth measurement, green arrow is the distance over from the tool wall, blue line is the ideal forming depth measurement

Analysis Procedure: The forming depth data are represented in two ways using MatLab. The first way takes the carbon fiber contact length measurements for each cross-section and divides that by the ideal contact length value to determine the "Percent Formed" value for each cross-section. An example of these data points from Curved C-channel part MD019 can be seen as the left bar chart in Figure 3.23.

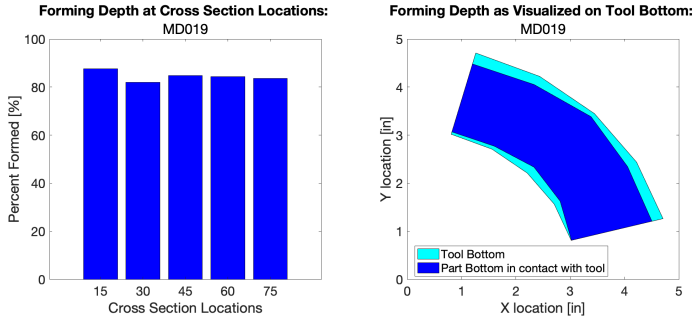


Figure 3.23: Forming Depth Data Representation: Continuous Carbon Fiber Curved C-channel Part, LEFT - Percent Formed Bar Chart, RIGHT - Contact Area Visualization

The second way the forming depth data are represented is a visual area comparison of the actual contact area versus the idea contact area. The idea contact area and geometry are determined by the tool geometry and the ideal contact length measurements. The actual contact area and geometry are determined by the actual contact lengths measurements, the tool geometry (blue rectangle Figure 3.21, and the distance over from the tool wall measurements (green arrow Figure 3.21). The actual contact area, seen in dark blue, is plotted on top of the desired contact area, seen in cyan, for Curved C-channel part MD019 in the right image in Figure 3.23.

Scoring Procedure: Using the percent formed values mentioned above, the forming depth metric can be scored. The values are averaged to obtain an overall percent formed value for the part. This overall percent formed or "Contact" is ranked using Table 3.4. These values in the ranking table are determined based on a range from no contact of the material

to the tool (rank of 0) and the ideal part with complete contact of the material to the tool (rank of 5). The remaining metrics are filled out to increment with larger ranges as the score decreases. For example, a score of 4 has a 10% range where a score of 3 has a 15% range.

Table 3.4: Forming Depth Metric Rankings

Metric	**0**	**1**	**2**	**3**	**4**	**5**
Forming Depth	Does not contact the bottom of the part	$0\% \leq$ Contact $< 55\%$	$55\% \leq$ Contact $< 75\%$	$75\% \leq$ Contact $< 90\%$	$90\% \leq$ Contact $< 100\%$	100% Contact

Examples of what a score of 1, 3, and 5 look like on actual carbon fiber Curved C-channel parts are presented in Figure 3.24. The pink lines in Figure 3.24 represent the contact length of the material to the flat tool bottom. The left image in Figure 3.24 has an example of a stretch broken Curved C-channel part that formed to less than 55% at the 15°cross-section location where the right most image shows a stretch broken Curved C-channel part that formed 100% at the 15°cross-section location. The center image in Figure 3.24 is an example of a continuous carbon fiber Curved C-channel that earned a score of 3 for forming depth at the 45°cross-section location.



Figure 3.24: Forming Depth Scoring Examples (pink lines show contact length): LEFT - Forming Depth Score of 1 example, CENTER - Forming Depth Score of 3 example, RIGHT - Forming Depth Score of 5 example

Corner Thinning

Definition: Corner thinning is a defect that has been commonly observed with traditional continuous carbon fiber. It occurs when carbon fiber is molded over a convex corner mold (24). Fibers that are tangential to the corner path of the tool experience a "log rolling" effect. This log rolling results in the fibers effectively "rolling" over the corner, leaving regions with little to no fibers at these corner locations.

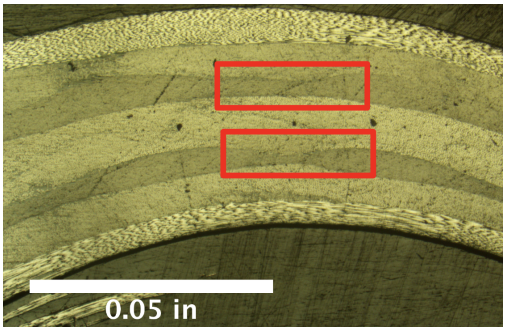


Figure 3.25: Corner Thinning Defect Example: Continuous Carbon Fiber, plies with corner thinning highlighted in red

Figure 3.25 is a microscope image of the corner thinning present for one of the Stretch Broken Carbon Fiber project's single bead tests. In the image, the red boxes highlight where plies three and six rapidly decrease in thickness. This thinning of certain plies mean that the strength provided by the plies at the corner thinning location is decreased significantly.

Measurement Procedure: Corner thinning is also measured after the cross-sectioning procedure. These measurements are taken where the part material forms over the convex radius locations of the tool. All parts presented in this study have only two convex radii locations, but future geometries could have more. For each of the five section lines seen in Figure 3.1, two corner thinning measurements are taken. These measurements are taken approximately at the blue circle denoted in Figures 3.26 and 3.27. Corner thinning is measured in ImageJ at the thinnest location along the convex curvatures. The thinnest

measurement is found with the "Max Inscribed Circles" plugin for the Fiji version of ImageJ (40). To use this plugin, the cross-sectional image scan needs to be converted to a binary image in which the carbon fiber region is white and everything else is black. This plugin is first used by removing the labels from the background. Next, the image is converted to a grey-scale image in Matlab. Once the image is grey-scale, MatLab is used again to convert it to a binary image by adjusting the tolerances in the "imbinarize" MatLab command. The "Max Inscribed Circles" plugin is used to find the smallest circle on the part image, with the diameter of the circle corresponding to the thinnest region on the corner. If corner thinning is not present enough for the "Max Inscribed Circles" plugin to detect, a line is placed at the center of the curvature from inner ply to outer ply and analyzed for length to determine the corner thinning measurement instead.

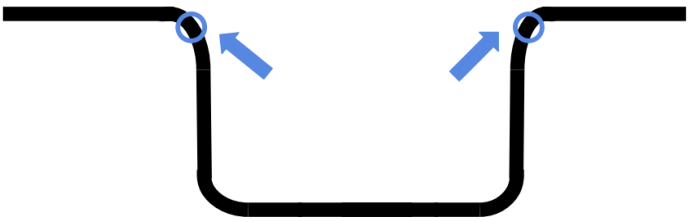


Figure 3.26: Corner Thinning Measurement Locations: Blue circles represent generalized measurement locations

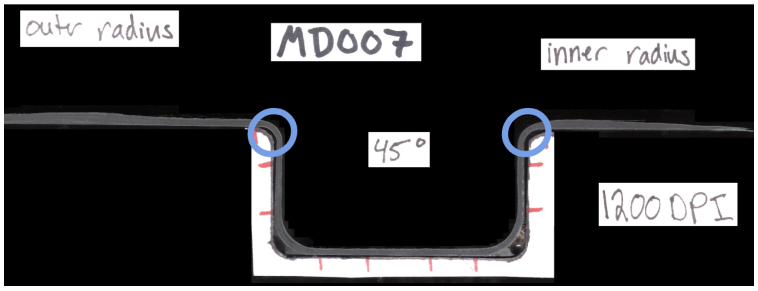


Figure 3.27: Corner Thinning Measurement on Part Cross-Section: Blue circles represent generalized measurement locations

Analysis Procedure: Corner thinning is calculated as a percent of the average thickness, $\bar{x}$, determined using the thickness variation analysis procedure in Subsection 3. Each radius value at each cross-section is represented as a percent of average thickness in a bar graph. A representation of this bar graph for Curved C-channel part MD019 is seen in Figure 3.28. The cross-section location values correspond to the angles at which the cross-sections are cut at on the part. The separate colors for "radius #1" and "radius #2" correlate to the two different convex corners on the tool. The entire corner thinning measurement set is also averaged to obtain an average corner thinning value. Additionally, the corner thinning values are included in the "Percent Thickness Change" contour plots seen in Figure 3.19, but are not included in the thickness data calculations.

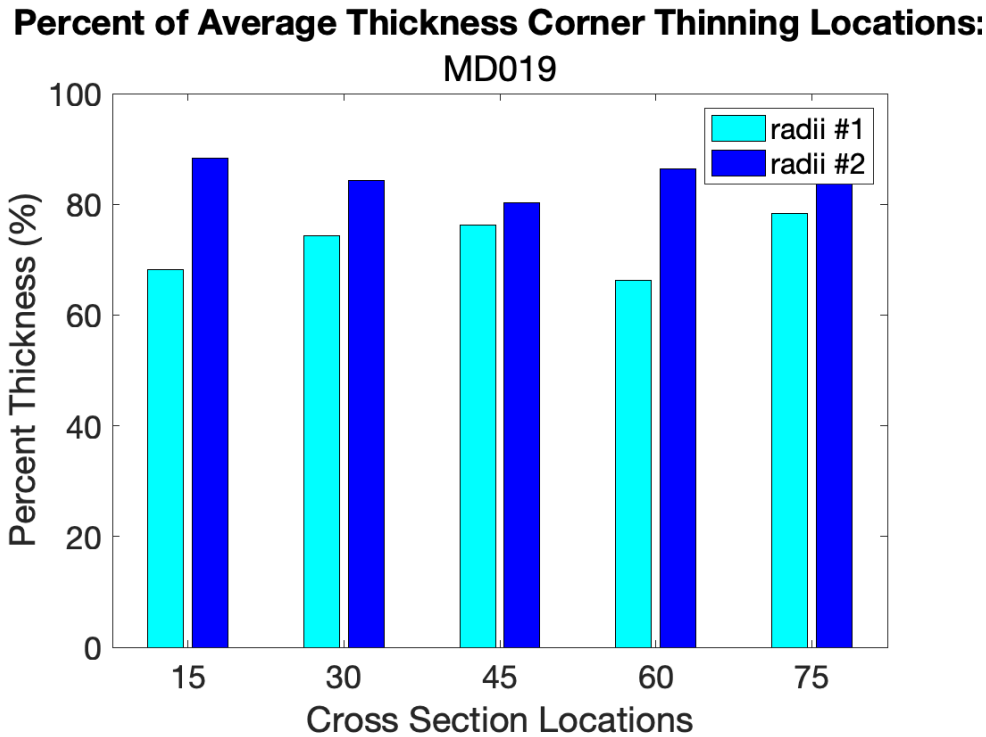


Figure 3.28: Corner Thinning Data Representation: Continuous Carbon Fiber Curved C-channel Part

Scoring Procedure: The corner thinning metric scoring is determined by the average corner thinning value of the measurement set for each part. The breakdown of each ranking score is detailed in Table 3.5. These acceptable value ranges are determined by reviewing the corner thinning data in the complete complex part test set as well as considering unacceptable amounts of thinning. Since thinning weakens a part, very small percentages of thinning are assigned for the 1-5 scores. For example, a score of four has a maximum allowable thinning of 2.5%. This is chosen to account for cases when the material may thicken instead of the expected thinning response, which may skew the average thinning value. A large amount of thinning warranting a score of 0, is set to be greater than or equal to 20% thinning. This score of 0 is chosen based on the part data set largest thinning values. The intermediate scores are chosen to increment between no thinning present (score of 5) and 20% thinning (score of 0). Keep in mind that these scores are not used to determine part acceptability, but instead to record amount and location of a defect. This record of defects could be used to track how different processing variables impact the presence of the corner thinning defect.

Table 3.5: Corner Thinning Metric Rankings

Metric	**0**	**1**	**2**	**3**	**4**	**5**
Corner Thinning	Corner thinning $\geq 20\%$	$20\% >$ Corner thinning $\geq 12.5\%$	$12.5\% >$ Corner thinning $\geq 7.5\%$	$7.5\% >$ Corner thinning $\geq 2.5\%$	$2.5\% >$ Corner thinning $> 0\%$	No corner thinning present

Examples of various thinned corners and the scores assigned to them are presented in Figure 3.29. Greater than 20% thinning is seen in the leftmost image in Figure 3.29 for a continuous carbon fiber Curved C-channel part. A high score of 4 is seen at the rightmost image in Figure 3.29 also for a continuous carbon fiber Curved C-channel part. A corner thinning score of 1 can be seen for a stretch broken carbon fiber Curved C-channel, and a

corner thinning score of 3 is presented for a continuous carbon fiber Curved C-channel in Figure 3.29.

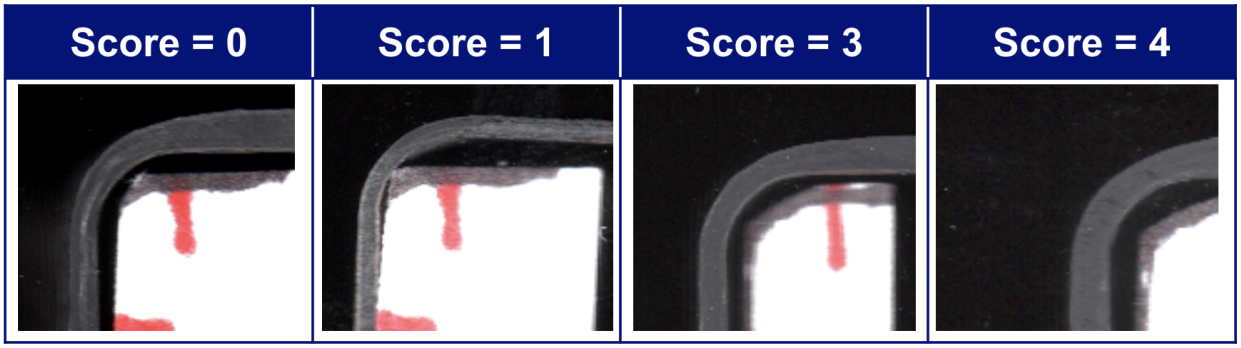


Figure 3.29: Corner Thinning Scoring Examples: LEFT - Corner Thinning Score of 0 example, LEFT CENTER - Corner Thinning Score of 1 example, RIGHT CENTER - Corner Thinning Score of 3 example, RIGHT - Corner Thinning Score of 4 example

Corner thinning percent is calculated by the percent thinning at the corner of the average thickness of the part. The average thickness is measured after the curing process at many location along the part. This means that corner thinning may not directly compare to the regions just adjacent to the corner in Figure 3.29.

Corner Thickening

Definition: Corner thickening is a defect similar to corner thinning as it is dependent on mold geometry. Corner thickening occurs at the concave corners of a mold (24). Current hypotheses suggest that corner thickening is due to the log rolling effect mentioned in the Corner Thinning Section. If the fibers are rolling away from the corner thinning regions, then these fibers must have some place to roll to. In these experiments, the fibers roll into the concave corner regions causing a thickening of the carbon fiber. A binary image of the corner thickening region can be seen in Figure 3.30. Resin pooling is purposely removed from this visualization and analysis as the concern is entirely on the laminate thickening. In this image, a noticeable amount of thickening is present in the corner region.

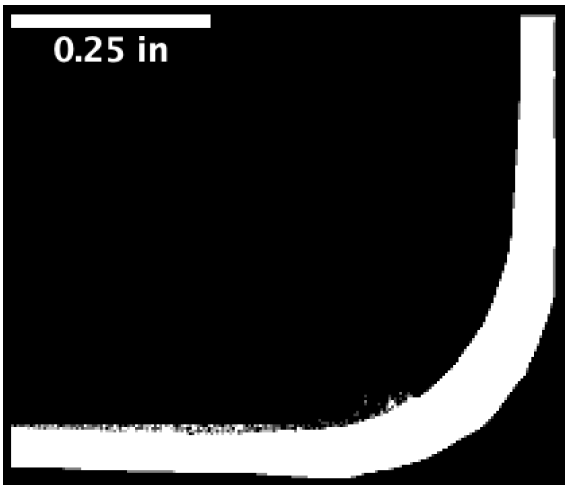


Figure 3.30: Corner Thickening Defect example: Continuous Carbon Fiber (Hexcel IM7/8552) Curved C-channel Part

Measurement Procedure: Corner thickening is measured after the cross-sectioning procedure. These measurements are taken where the part material forms into the concave radius locations of the tool. All parts presented in this study have only two concave radii locations, but future geometries could have more. For each of the five section lines seen in Figure 3.1, two corner thickening measurements are taken. These measurements are taken approximately at the green locations denoted in Figures 3.31 and 3.32. Corner thickening is measured in ImageJ at the thickest location along the concave curvatures. The thickest measurement is found with the "Max Inscribed Circles" plugin for the Fiji version of ImageJ (40). Use and preparation for this plugin is further outlined in the Corner Thinning Measurement Procedure Section 3. The "Max Inscribed Circles" plugin is used to find the largest circle on the part image, with the diameter of the circle corresponding to the thickest region on the corner. If corner thickening is not present enough for the "Max Inscribed Circles" plugin to detect, a line is placed at the center of the curvature from inner ply to outer ply and analyzed for length to instead determine the corner thickening measurement.

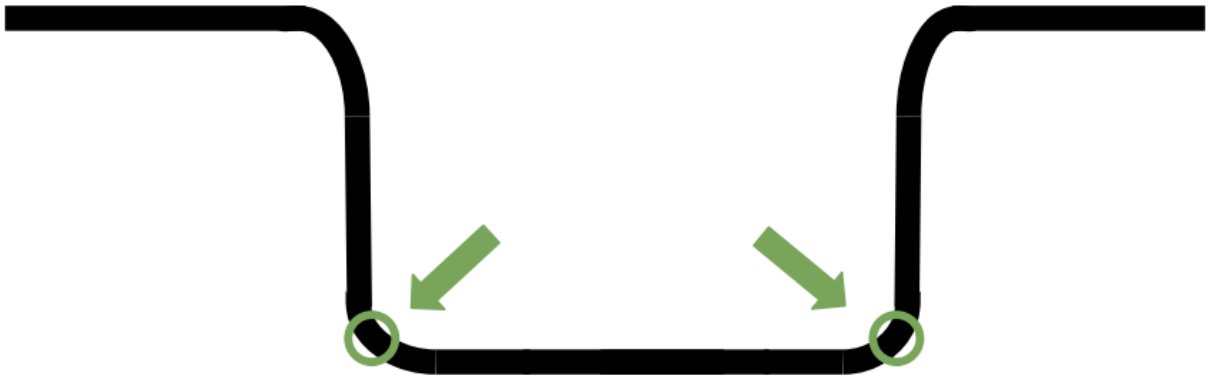


Figure 3.31: Corner Thickening Measurement Locations: Green circles represent generalized measurement locations

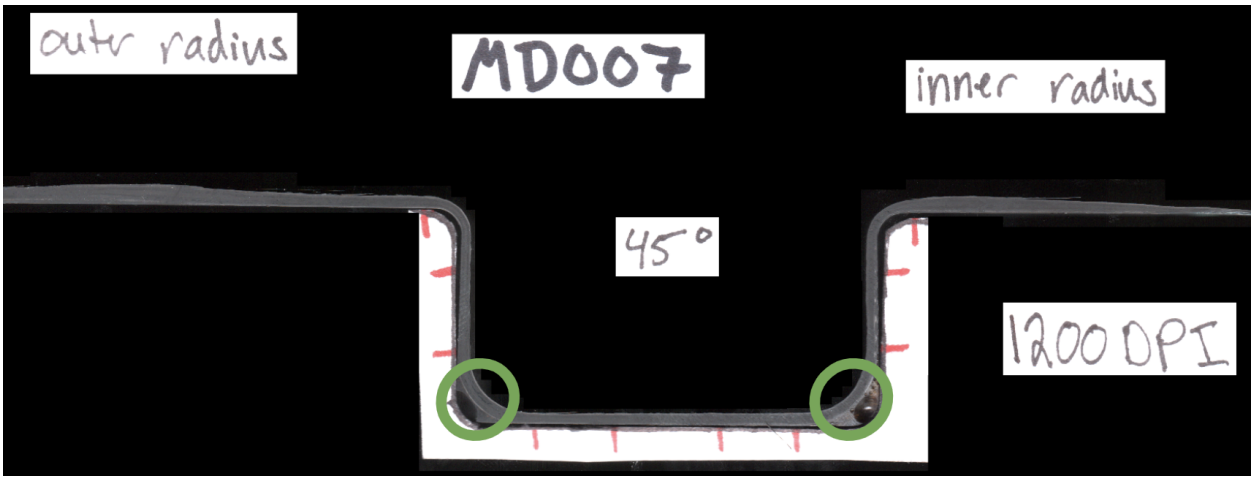


Figure 3.32: Corner Thickening Measurement on Part Cross-Section: Green circles represent generalized measurement locations

Analysis Procedure: Corner thickening is calculated as a percent of the average thickness, $\bar{x}$, determined using the thickness variation analysis procedure. Each radius value at each cross-section is represented as a percent of average thickness in a bar graph. A representation of this bar graph for Curved C-channel part MD019 is seen in Figure 3.33.

In Figure 3.33, the cross-section location values correspond to the angles at which the cross-sections are cut on the part. The separate colors for "radius #1" and "radius #2"

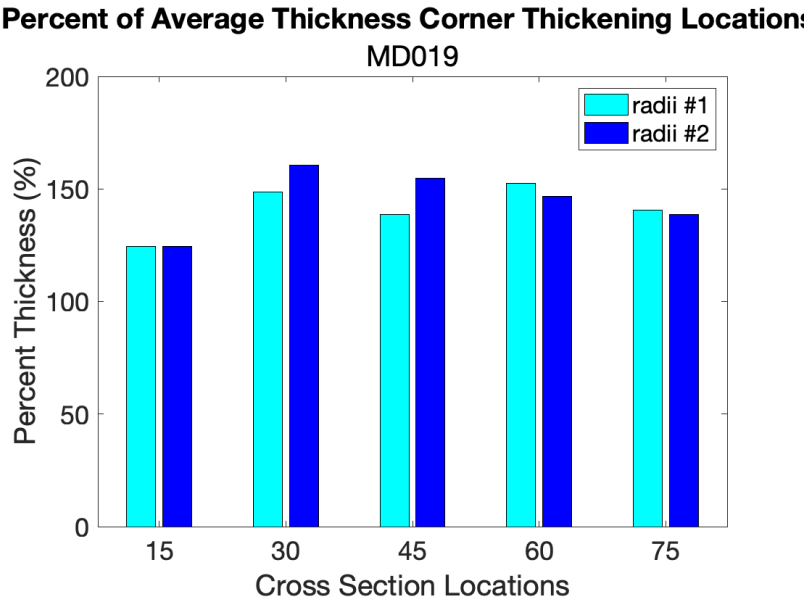


Figure 3.33: Corner Thickening Data Representation: Continuous Carbon Fiber Curved C-channel Part

correlate to the two different concave corners on the tool. The entire corner thickening measurement set is also averaged for the average corner thickening value. Additionally, the corner thickening values are included in the "Percent Thickness Change" contour plots seen in Figure 3.19, but are not included in the thickness data calculations.

Scoring Procedure: The corner thickening metric scoring is determined by the average corner thickening value of the measurement set for each part. The breakdown of each ranking score is detailed in Table 3.6. These corner thickening percentage values are determined by reviewing the corner thickening data present in the complete complex part test set to determine a range of values. A score of 5 correlates to no corner thickening present at every location whereas a score of 0 correlates to an average corner thickening of 25% or greater. This is determined by reviewing the part data with the largest scores while keeping the value similar to that of the corner thinning score of 0. The ranges for the intermediate scores are chosen to divide up the overall range of 0% to 25%. These scores are not set to determine if

a part has acceptable levels of corner thickening, but are instead used to track the amount of the defect present.

Table 3.6: Corner Thickening Metric Rankings

Metric	**0**	**1**	**2**	**3**	**4**	**5**
Corner Thickening	Corner thickening ≥ 25%	25% >Corner thickening≥ 15%	15% >Corner thickening≥ 10%	10% >Corner thickening≥ 5%	5% >Corner thickening> 0%	No corner thickening present

Figure 3.34 presents corner thickening examples with scores of 0, 3, and 4. The leftmost image shows a continuous carbon fiber Curved C-channel with a corner thickening score of 0 and the thickening taking place across the entire curvature. The center image shows a stretch broken carbon fiber Curved C-channel with a corner thickening score of 3 and the thickening taking place at the top left of the image. The rightmost image shows a stretch broken carbon fiber Curved C-channel with a corner thickening score of 4 having minimal thickening across the corner region shown.

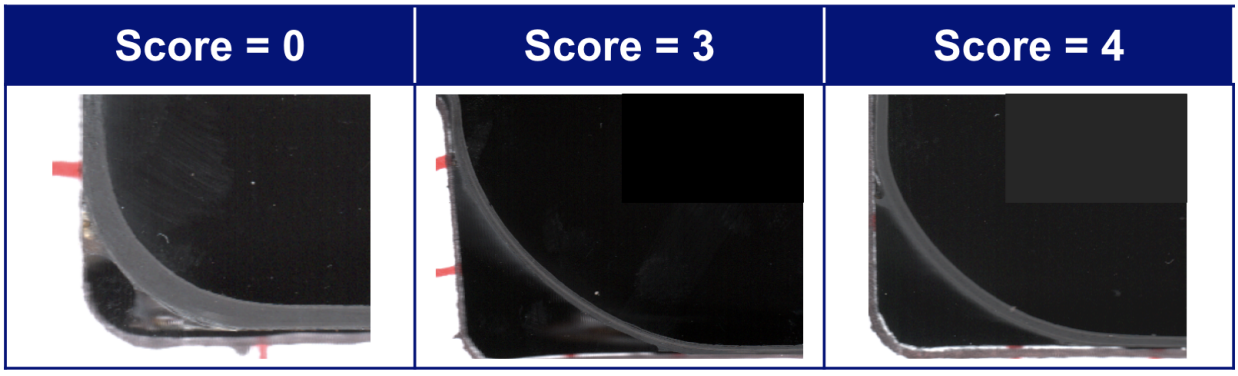


Figure 3.34: Corner Thickening Scoring examples: LEFT - Corner Thickening Score of 0 example, CENTER - Corner Thickening Score of 3 example, RIGHT - Corner Thickening Score of 4 example

Resin Pooling

Definition: Resin pooling for this method is defined as the area of resin pooling present in the concave corners for each cross-section (28). While resin pooling does occur in other areas (which will be discussed later), this specific metric is only concerned with the concave corner regions, because it is where this defect most prominently occurs. During the curing process within the autoclave, the combination of vacuum and temperature causing low resin viscosity sometimes allows for the resin to seep out of the laminate. This resin then fills into the gap between the mold's concave radii and the laminate.

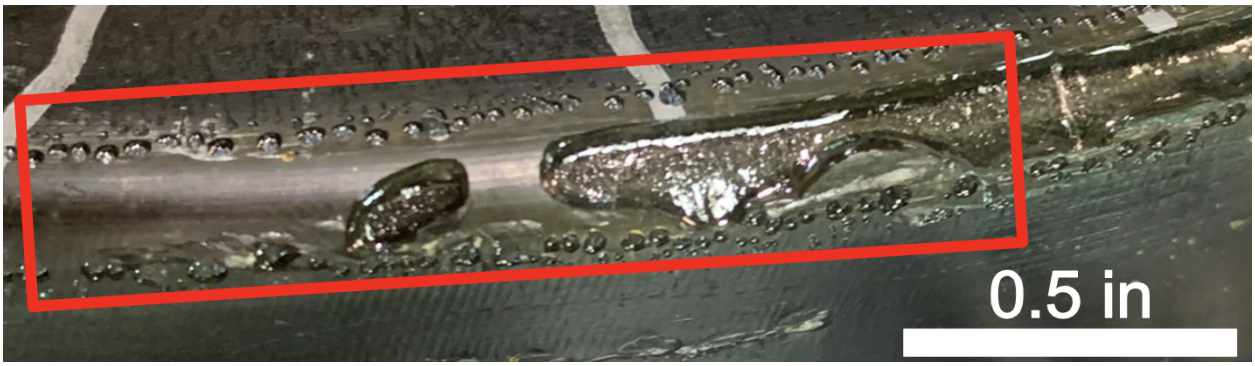


Figure 3.35: Resin Pooling Defect example: Continuous Carbon Fiber Curved C-channel Part

An image of the concave corner region of a part with significant resin pooling can be seen boxed in red in Figure 3.35. This resin pooling region suggests that there are areas of the material that could be resin starved. This resin pooling region is also exceedingly brittle due to the material properties of the resin itself (3).

Measurement Procedure: Resin Pooling is measured after the cross-sectioning procedure. These measurements are taken where the part material forms into the concave radius locations of the tool. All parts presented in this study have only two concave radius locations, but future geometries could have more.



Figure 3.36: Resin Pooling Measurement Locations: Purple circles represent generalized measurement locations, tan regions show resin pooling

For each of the five section lines seen in Figure 3.1, two resin pooling measurements are taken. These measurements are taken at the purple circles denoted in Figure 3.36, also seen as the purple outlined areas in Figure 3.37. Resin pooling is measured in ImageJ using the "Freehand Selections" tool. This tool allows the user to trace around the area of resin pooling and the "Analyze" tool calculates the area of resin pooling at the selection.

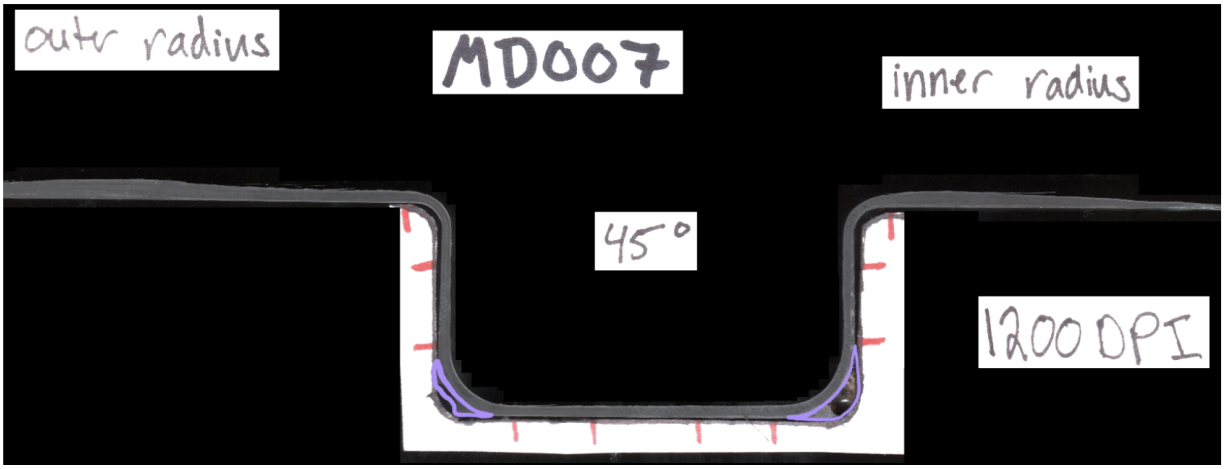


Figure 3.37: Resin Pooling Measurement on Part Cross-Section: Purple lines outline resin pooling area

Analysis Procedure: Resin pooling is analyzed for the total area of resin pooling averaged for all the measurement location resin pooling values for later scoring purposes. The resin pooling area data for each concave radius at each cross-section is also represented in a bar graph with the bridging data.

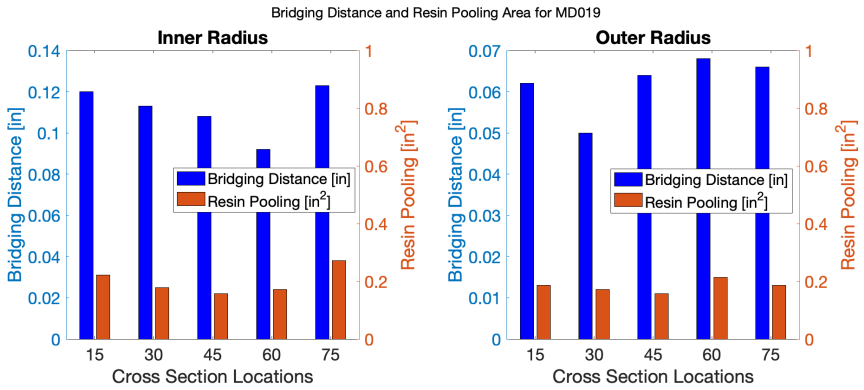


Figure 3.38: Resin Pooling Data Representation: Continuous Carbon Fiber Curved C-channel Part, orange bars show resin pooling data

An example of the resin pooling data for continuous carbon fiber Curved C-channel part MD019 is represented as the orange bars in Figure 3.38. For the Results and Discussion Chapter 4, the resin pooling data are combined with the bridging distance data for comparison.

Scoring Procedure: The resin pooling metric scoring is determined by the total resin pooling area of the measurement set for each part. The breakdown of each ranking score is detailed in Table 3.7. In this table "Resin Pooling" refers to the average resin pooling per measurement location on a part. These resin pooling area values are determined by reviewing the resin pooling data present in the complete complex part test set to determine a range of values. The highest amount of resin pooling from the part set is assigned a score of 1 where any area of resin pooling larger than this would earn a a score of 0. The remaining score ranges are incremented until a perfect score of 5 is assigned with no resin pooling present.

The resin pooling ranges get smaller as the score increases. For example, scores of 3 and 4 have a range of $0.005in^2$ where scores of 1 and 2 have a range of $0.01in^2$. These rankings are to determine the quantity of resin pooling on a certain part and are not to be used as a rule for part acceptability.

Table 3.7: Resin Pooling Metric Rankings

Metric	**0**	**1**	**2**	**3**	**4**	**5**
Resin Pooling	Resin Pooling $> 0.03in^2$	$0.03in^2 \geq$ Resin Pooling $> 0.02in^2$	$0.02in^2 \geq$ Resin Pooling $> 0.01in^2$	$0.01in^2 \geq$ Resin Pooling $> 0.005in^2$	$0.005in^2 \geq$ Resin Pooling $> 0in^2$	No Resin Pooling present

Figure 3.39 presents resin pooling examples with scores of 0, 1, 2, and 4. The three images towards the left of Figure 3.39 display parts with large amounts of resin pooling, earning scores of 0, 1, and 2 based on their areas of resin pooling. The rightmost image in Figure 3.39 shows a stretch broken carbon fiber Curved C-channel with minimal amounts of resin pooling and the top left corner of the image. This amount of resin pooling is very minimal, thus earning a score of 4 for resin pooling at this specific location.

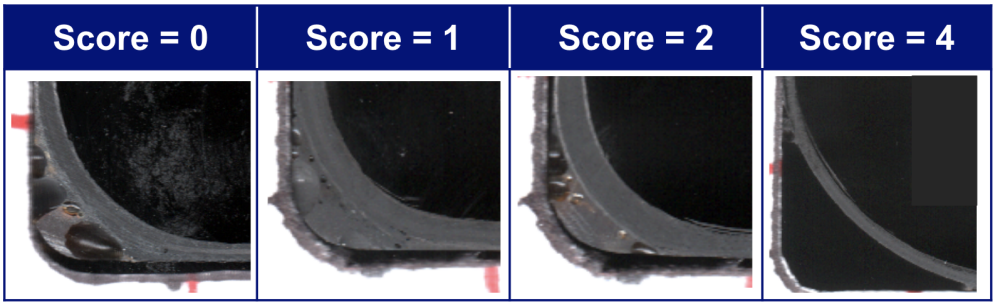


Figure 3.39: Resin Pooling Scoring examples: LEFT - Resin Pooling Score of 0 example, LEFT CENTER - Resin Pooling Score of 1 example, RIGHT CENTER - Resin Pooling Score of 2 example, RIGHT - Resin Pooling Score of 4 example

Texture Defects

Definition: There are many defects that are placed under the metric of texture defects for this complex shape analysis. The texture defects metric considers all the surface defects observed within the MSU SBCF program. These defects are presented in Figure 3.40 denoted as surface "hairiness", additional (non-corner) resin pooling, "spaghettification", fractures/shearing, pinholes, and waves, with the defects highlighted in red circles or boxes where applicable.

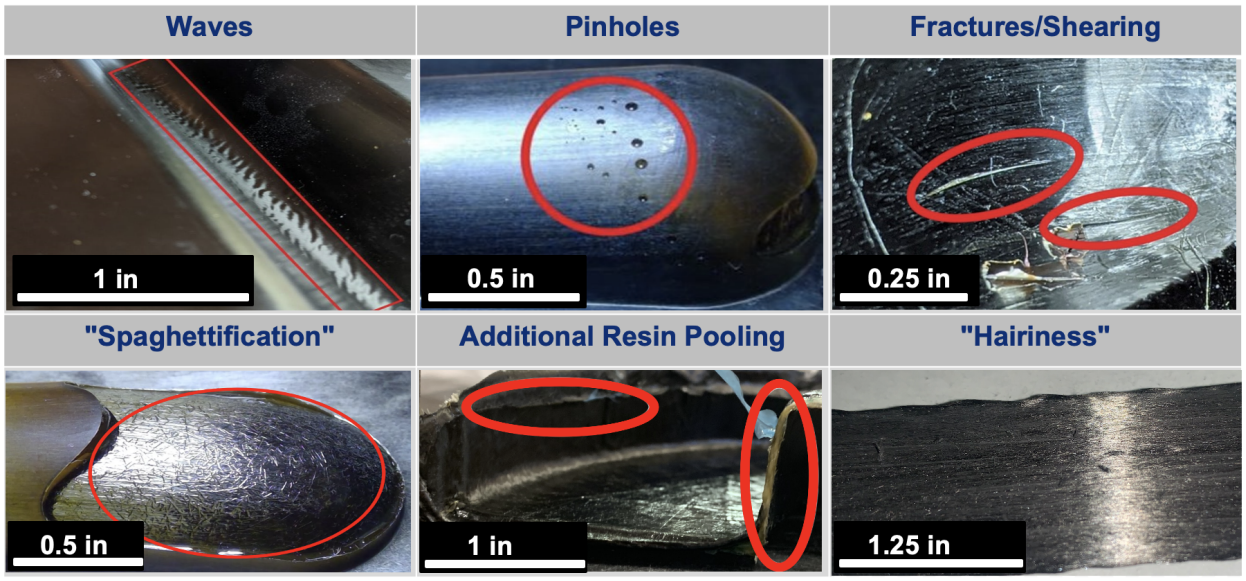


Figure 3.40: Texture Defect Summary: TOP LEFT - Waves Defect example , TOP CENTER - Pinholes Defect example, TOP RIGHT - Fractures/Shearing Defect example, BOTTOM LEFT - Spaghettification Defect example, BOTTOM CENTER - Additional Resin Pooling Defect examples, BOTTOM RIGHT - Hairiness Defect example

Surface "hairiness" pertains to the presence of loose, non-impregnated fibers on the surface of the carbon fiber part. This metric designation is adopted from the textile industry where yarn hairiness is an area of study (41). Sometimes, this hairiness can be observed on the stretch broken carbon fiber prepreg. In Figure 3.41, the hairiness has been exaggerated on a strip of SBCF prepreg for easier visualization of the defect. During the cure cycle, the

hairiness between plies is commonly impregnated with resin, leaving hairiness only detectable on the surface, or outermost plies, of the part.

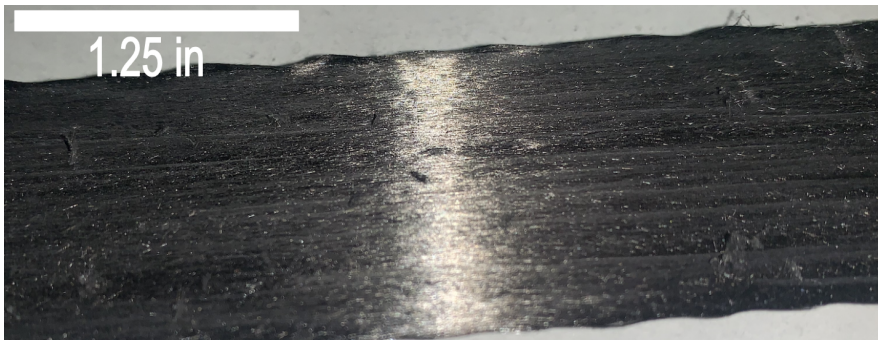


Figure 3.41: Hairiness Texture Defect example: Stretch Broken Carbon Fiber Prepreg Tape

The additional resin pooling texture defect accounts for resin pooling in regions that are not the concave curvature areas. Additional resin pooling can occur in any region on the part, but most commonly appears around the intensifiers or breather strings (if used). In Figure 3.42, additional resin pooling examples can be seen circled in white. The left circles the resin pooling present above the intensifier region. The right circles the resin pooling present around the breather strings.

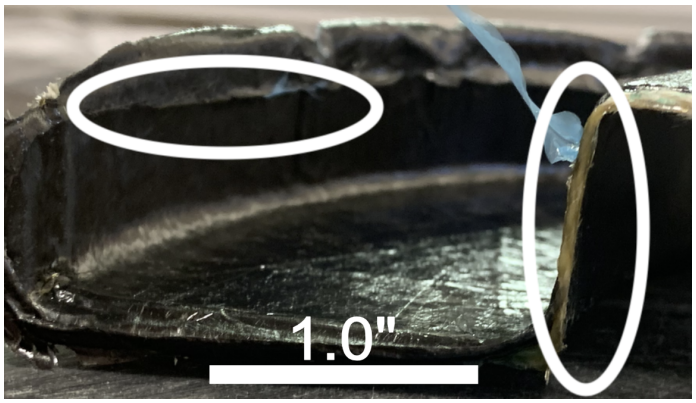


Figure 3.42: Additional Resin Pooling Texture Defect Example: Stretch Broken Carbon Fiber Curved C-channel Part, Left circles additional resin pooling above the intensifier location, Right circles additional resin pooling along the edges of the part

"Spaghettification" is a phenomenon unique to SBCF where fiber direction is random at some region along the surface (42). These fibers are impregnated and cured into the part, thus not exhibiting the loose qualities of the hairiness defect. Current hypotheses are that spaghettification occurs when the hairiness defect is fully impregnated. Prior complex shape testing revealed that spaghettification tends to occur near resin pooling regions. An example of spaghettification can be seen in Figure 3.43.

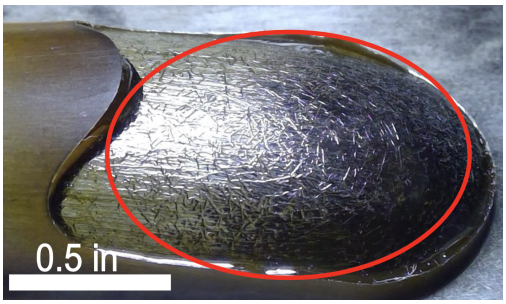


Figure 3.43: Spaghettification Texture Defect Example: Stretch Broken Carbon Fiber, red circle highlights location of spaghettification (42)

Fractures/shearing is a catchall for any separation of adjacent prepreg sections, linear cracks, or surface indentations (42). However, sometimes these defects can be mistaken for markings left either from the tool surface or the demolding process. Circled in red in Figure 3.44, are the regions where fractures/shearing are found on a part made by the MSU SBCF Task 6 team.

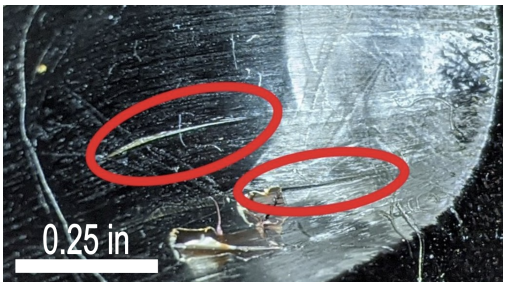


Figure 3.44: Fractures/Shearing Texture Defect Example: Stretch Broken Carbon Fiber, red circles show where fracture/shearing are present (42)

Pinholes are a resin-based defect where there are voids exposed to the surface of the material (42). These pinpricks are due to air bubbles escaping the resin during the curing process. An image of pinholes is seen in Figure 3.45.

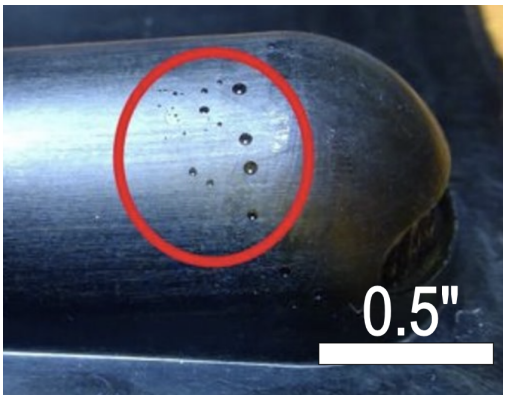


Figure 3.45: Pinholes Texture Defect Example: Continuous Carbon Fiber, red circle highlights location of pinholes (42)

Finally, waves describe any fiber waviness seen on the part. These waves have a sinusoidal-like pattern of fiber direction, making it distinct from the spaghettification defect (42). An example of fiber waviness is boxed in red in Figure 3.46.

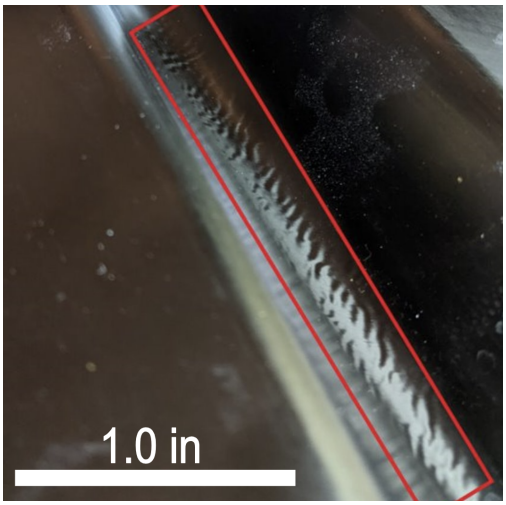


Figure 3.46: Waves Texture Defect Example: Continuous Carbon Fiber, red boxed region displays waviness on a corner feature (42)

Measurement Procedure: The texture based defects are measured via visual analysis. Some of the texture defects are measured with a “is present” or “isn’t present” system while others are counted for quantity. Certain rules are devised to rank and measure each texture defect in a repeatable manner with little room for discrepancies in hopes of avoiding additional human error as described in the Texture Metric Ranking Scheme shown in Table 3.8.

Analysis Procedure: To analyze these texture defects, a ranking system is used to assign each defect a value from zero to five. A score of 5 is associated with an ideal, defect-free part. A score of 0 is associated with a ”worst case scenario” level of defects. Table 3.8 has the ranking criteria for each texture defect. The metric rankings are based on the severity of each metric.

All the metrics have the capability of receiving a score of 5, which signifies no defects present and will not be further discussed. Hairiness has two additional rankings: 3 for some hairiness and 0 for significant hairiness. These rankings are due to the difficulty of quantifying a loose surface texture quality. To assign a quantitative rule for the defect, the ability of loose fibers to be pulled out of the surface of the part is associated with the “very hairy quality”, separating it from the “somewhat hairy quality” surface characteristic.

Additional resin pooling has three additional relevant rankings. A ranking of 3 is used to account for resin pooling seen just above the silicone intensifier as it occurs frequently, but not in significant amounts. A ranking of 1 is used to account for any other minimal resin pooling that cannot be explained by concave corners and intensifiers. Finally, a ranking of 0 is reserved for any resin pooling deemed worse than the other defined rankings.

Like the hairiness metric, spaghettification has two significant rankings. A ranking of 2 denotes if spaghettification seen on the formed part, but in only one location. A ranking of 0 is used for multiple locations of spaghettification.

Fractures/shearing also has two rankings. The severity of fractures/shearing is

Table 3.8: Texture Metric Rankings

Metric	0	1	2	3	4	5
Hairiness	Very hairy quality. Loose fibers can be pulled from the part	N/A	N/A	Somewhat hairy quality. Loose fibers cannot be pulled from the part	N/A	Not hairy. No loose fibers present
Additional Resin Pooling	Significant amounts in many locations	Small amounts in many locations	N/A	Present just above intensifier location	N/A	Not present
Spaghettification	Present in multiple locations	N/A	Present in one location	N/A	N/A	None present
Fractures/ Shearing	Present in critical locations	N/A	N/A	Present in non-critical locations	N/A	None present
Pinholes	More than three present	N/A	Three present	Two present	One present	None present
Waves	Present	N/A	N/A	N/A	N/A	Not present

determined by the critical region of each part, which is defined by the part geometry. If fractures/shearing are noticed in critical locations, it receives a ranking of 0, all other locations result in a ranking of 3.

Unlike the other texture metrics, pinholes have a distinct countable quality. A ranking of 4 is associated with one pinhole present. A ranking of 3 is associated with two counted pinholes. A ranking of 2 denotes three pinholes present. Any more than three pinholes counted on the part earns a score of 0. A ranking of 5 denotes no detectable pinholes. The waves defect is the simplest to rank: 0 if any waves are observed and 5 if no waves are observed.

Scoring Procedure: The rankings assigned to each metric in the analysis procedure are then combined in a weighted calculation to generate a finalized texture score for the formed carbon fiber part. Each texture metric is assigned a weight that correlates to the severity, frequency, and number of significant rankings for the defect. Frequency is determined by the amount of times a defect is observed within the early complex shape trials. Severity is determined by the possible consequences the defect poses. If a defect does not directly or obviously correspond to severe performance detriments, a lower severity is assigned. Chapter 7 outlines how these rankings can be updated based on future testing of the defects. All of these determined weights sum to 100%. Hairiness receives a weight of 30% as it is a common occurrence of the Stretch Broken Carbon Fiber Material during these trials where the resin content and processing is still undergoing optimization, but the severity is moderate to low. Additional resin pooling also receives a weight of 30%, because of the severity it poses to the performance of the cured part and the moderate occurrence. Additional resin pooling present causes areas of low resin impregnation and can result in fiber misalignment. Like additional resin pooling, spaghettification has severe consequences as a result of fiber misalignment, however it does not occur frequently, so it receives a weight of 10%. Fractures/shearing can

weaken the part at the locations of the defect which could result in complications in the performance of the part. For the weaknesses fracture/shearing poses, it receives a ranking of 15% to account for the severity but is slightly lower as the occurrence is low. Pinholes are assigned a weight of 10% as the severity is relatively low due to the size of the defect, however the occurrence is more frequent than some of the other defects. The waves defect can present high severity again due to fiber misalignment. While it does have consequences on part performance, this defect is not commonly observed, and it also has only two significant rankings of a 0 and 5, so currently it receives the lowest weight of 5%.

Table 3.9: Texture Scoring Matrix Example

Metric	Weight	Ranking	Score
Hairiness	30%	5	-
Additional Resin Pooling	30%	4	-
Spaghettification	10%	5	-
Fractures/Shearing	15%	3	-
Pinholes	10%	5	-
Waves	5%	0	-
Total	100%	X	4.15

All of these texture metric weights can be seen in Table 3.9. Additionally, Table 3.9 includes an example of combining the metric weights with the metric rankings. In this example hairiness is ranked 5, additional resin pooling is ranked 4, spaghettification is ranked 5, fractures/shearing is ranked 3, pinholes are ranked 5, and waves are ranked at 0 resulting in an overall texture score of 4.15.

Additional Measurements and Analyses not Used for Scoring

In addition to the other metrics and the scoring method to analyze the defects, there are two other metrics that are measured. These metrics of splitting and stretch versus slip

are metrics that are not included in the forming score nor are scored individually. Instead, the additional measurements are used to give insight to outcome of the final score for each part. Splitting is used as a part "usability" metric whereas stretch versus slip is utilized as a forming mechanism metric that indicates the forming mechanisms present for each part.

Splitting

Definition: Splitting is a potentially catastrophic defect to happen during the forming process of a carbon fiber part. It occurs when the fibers of one or more plies effectively separate from each other leaving at best a gap in one ply layer and at worst leaving a gap throughout the entire thickness (42). An example of splitting on a part in the early stages of development can be seen in Figure 3.47. This defect has severe consequences as an area of zero thickness will impact the strength of a part.



Figure 3.47: Splitting Defect Example: Stretch Broken Carbon Fiber (42)

Measurement Procedure Due to the rarity of occurrence of splitting throughout the experiments as well as the severity it poses to part performance, splitting is measured on a "yes/no" basis by location on the part.

Analysis Procedure If there is no splitting within the part, the analysis of the other metrics determines the final forming score of the complex part. If there is splitting present, the overall forming score is designated as a "Failed Part". This "Failed Part" designation allows for the original forming score to remain for more detailed metric analyses, but still makes it clear that the part is unusable.

Stretch versus Slip

Definition: The stretch versus slip metric is different from the other metrics as it is not a carbon fiber defect, but instead a way to measure the forming mechanisms present. There are three main forming mechanisms that occur when forming SBCF into a mold: stretching, ply-ply slippage, and tool-ply slippage (11).

Stretching is a forming mechanism unique to stretch broken carbon fiber as the discontinuity of the individual fibers allows them to slide past each other, effectively resulting in a "stretched" region (9). A schematic of the stretching forming mechanism is presented in Figure 3.48.



Figure 3.48: Stretching Schematic: LEFT- the stretch broken carbon fiber laminate before stretching, RIGHT - the stretch broken carbon fiber laminate after stretching with an overall increase in laminate length

Graduate researcher Dalton Nold took images of this stretching effect during a heated tensile test of stretch broken carbon fiber, as seen in Figure 3.49 (43). In this image, the silver marker lines drawn on before testing have misaligned from each other during the test allowing for easy visualization of the stretching of SBCF.

Ply-ply slippage, or intralaminar slippage, is when the individual plies slide relative to each other during the forming process. This can result in thin regions towards the edges

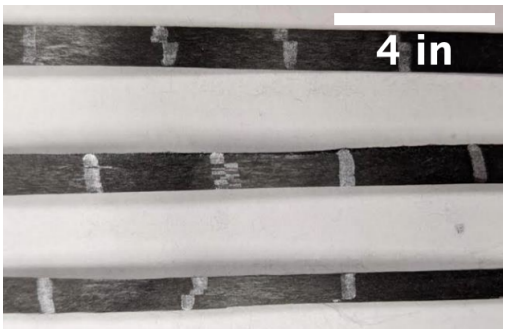


Figure 3.49: Stretching Example: Silver lines drawn on straight before tensile testing and are seen to diplace from one another after tensile testing due to stretching (43)

of the part as well as an overall increased length of the laminate. The regions toward the outer edges of the part resemble "ply drops" which is a layup technique where the technician layers the plies so that less plies are present at the end and build up towards the middle (44). This layup technique is used to control the thickness at regions along a laminate (3). The ply-ply slippage greatly resembles this technique, even though it is an unintentional effect. A schematic of the ply-ply slippage forming mechanism is presented in Figure 3.50. Figure

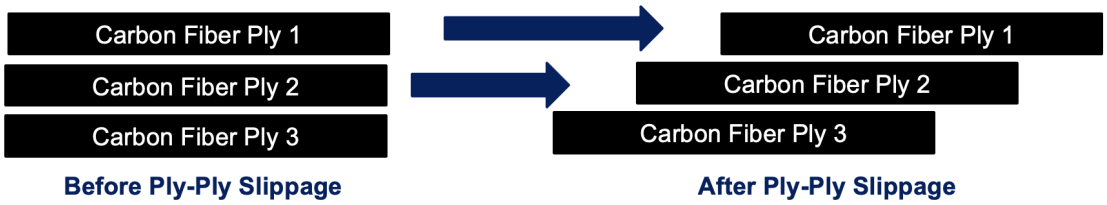


Figure 3.50: Ply Ply Slippage Schematic: LEFT - carbon fiber plies before ply-ply slippage, RIGHT - carbon fiber plies offset from one another after ply-ply slippage resulting in a elongated laminate length

3.51 shows a cross-section region of a part with significant ply-ply slippage. It is seen that the region traveling from left to right gets thicker as the number of plies increase.

Tool-ply slippage is when the entire laminate slides relative to the tool surface (11). Tool-ply slippage is an important mechanism of forming that can be effective in filling a mold. If only tool-ply slippage is present as a forming mechanism, the overall length of

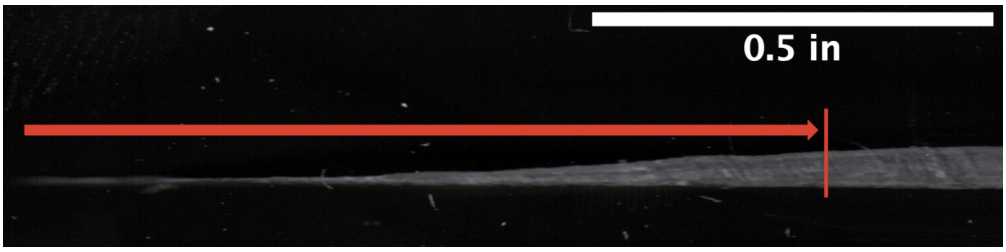


Figure 3.51: Ply-ply Slippage Visualization: Continuous Carbon Fiber (Hexcel IM7/8552). Thickness of the material tapers as it reaches the end, synonymous with ply drops. Red arrow is the ply-ply slip distance

the laminate will not change. Unless the laminate is "perfectly clamped" so it cannot slide relative to the tool surface, it can be assumed that some amount of tool-ply slippage will be present for most experiments. A schematic of tool-ply slippage is presented in Figure 3.52.

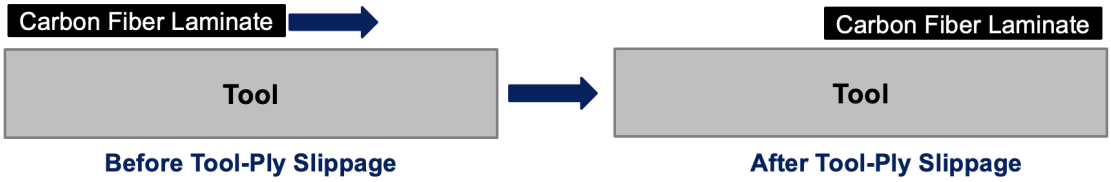


Figure 3.52: Tool Ply Slippage Schematic: LEFT - carbon fiber laminate on the left side of the tool before tool-ply slippage, RIGHT - carbon fiber laminate on the right side of the tool after tool-ply slippage maintaining its original length

Measurement Procedure The stretch versus slip measurement system requires three separate measurements: the first before the vacuum bagging process and the second two after the final cure and cross-sectioning. After the layup is marked with the section lines, Figure 3.1, each line is measured for length. This uncured layup length is designated L_u. After the layup undergoes forming and curing within the autoclave, the section lines are again measured following the path line of the cured part. This is done either with a flexible tape measure or with the segmented line option within the ImageJ program. This cured part length is designated L_c. A schematic of the measurement is represented in Figure 3.53.

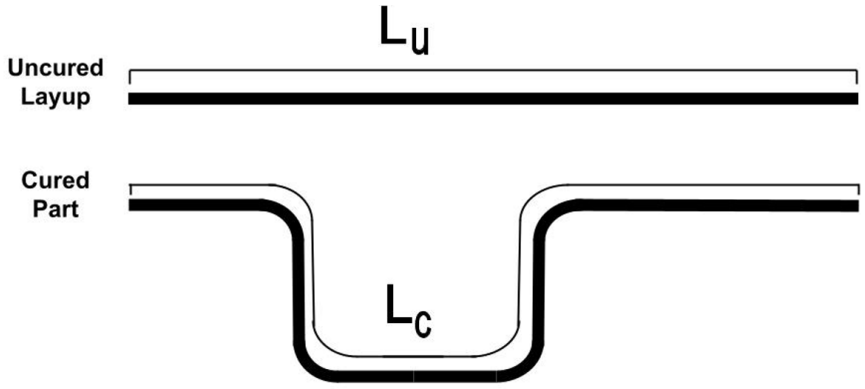


Figure 3.53: Stretch versus Slip Measurement Schematic: TOP - measurement of the length of the uncured layup along the cross-sectioning lines, BOTTOM - measurement of the path length of the cure part along the cross-sectioning lines

To measure ply-ply slippage specifically, ImageJ is used again to measure for length. For example, in Figure 3.51 ply-ply slip length is measured starting on the left from the start of the carbon fiber material to right region where all plies used in the original layup are present denoted as the red arrow. This measurement is repeated on each cross-section on both sides. The lengths on each side for the cross-sections is summed for a total "ply-ply slip length" per cross-section.

Analysis Procedure To analyze the stretch versus slip metric, the initial uncured laminate lengths are compared to the final cured lengths using a formula based on strain calculations. This formula can be seen below in Equation 3.3 using the same variable notation as seen in Figure 3.53. If the "Stretch Ratio" is positive, then stretching and/or ply-ply slippage is present. If the "Stretch Ratio" is equal to zero, then tool-ply slippage is the only mechanism of forming that the layup experienced. If the "Stretch Ratio" is negative, this represents the layup shrinking in on itself during the forming process due to compressive forces on the material, likely resulting in wrinkling.

$$Stretch\ Ratio = \frac{L_c - L_u}{L_u} \tag{3.3}$$

A visual representation of this metric can be seen in Figure 3.54 for stretch broken carbon fiber Curved C-channel part MD016. In this plot, the yellow filled region represents the original shape of the uncured layup, and the cyan filled region show the final "shape" of the cured part based on length measurements. Any region that appears as green, is denotes where the uncured layup and the cured part share dimensions. The dark blue line positioning denotes the measurement locations whereas the length is equivalent to the cured part lengths at each location. The red lines signify how much of the extended blue lines are due to ply-ply slippage. Due to the nature of the cross-sectioning procedure, ply-ply slippage is not measured at the edges of the cured part and is not represented at those locations in the fill plots. In the example presented in Figure 3.54, the entire cross-sectional lengths are seen to increase from the original layup dimensions with some, but not all, of the length increases being due to ply-ply slippage.

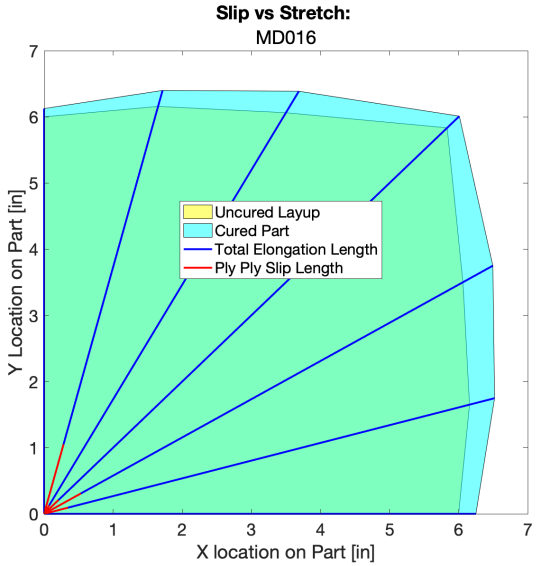


Figure 3.54: Stretch versus Slip Example: Stretch Broken Carbon Fiber Part

Forming Score Procedure

To produce a final score for the final formed quality of the complex carbon fiber parts, a weighted matrix is used to calculate a value on a 0 to 5 scale. An example of how the final matrix is used can be seen in Table 3.10. Each of the metrics in this table have been assigned a "weight" based on severity and occurrence. These preliminary weights were determined by surveying the entire SBCF group by having individuals rank the individual metrics from having the highest to lowest impact on part quality. Chapter 7 outlines methods to refine and expand upon these preliminary weights through strength testing.

Wrinkling has the highest ranking of 17.5% due to the severity and occurrence of the defect. Wrinkling occurs quite frequently due to the nature of the complex geometries the flat layups must form into. Wrinkling, reference Figure 3.11, also introduces the risk of significant intralaminar voids seen in the areas where wrinkling is present. Another consequence of wrinkling is that it pre-buckles the material at the wrinkling location, resulting is decrements to the compressive strength of the laminate at the wrinkling locations. It is for these reasons that wrinkling is currently assigned the highest weight to account for the extreme severity of this defect.

Following wrinkling in order of highest weight applied are the metrics of thickness variation and corner thinning. The weight of 15% for these metrics is due to the severity that significant thinning can pose to the performance and strength of a part (24). A thinner region results in lower tensile and compressive strengths than the original design at the thinned region. Thickness variation also accounts for thickening of the material which results in a geometric result different than the original model design. The higher weight also correlates to the occurrence of these effects, keeping in mind that the corner thinning occurrence tends to be material dependent.

Next, with rankings of 12.5%, are the bridging, forming depth, and resin pooling

metrics. Bridging and forming depth directly relate to the geometry of the final formed part. If the geometry is significantly different from the original design, performance may be significantly impacted. However, small variations are less severe. While the occurrence can be relatively high for these metrics, it is entirely dependent on the material type and the forming methods. Resin pooling receives this weight, because it has a slightly lower severity while occurring more frequently dependent on the material used. Resin pooling itself, is unsightly and adds surface blemishes, but also indicates areas where the carbon fibers are resin starved within the formed part as well as adds a brittle resin region on the surface of the part (3).

Following these metrics is corner thickening with a ranking of 10%. Corner thickening is observed to occur only with certain material types, meaning it has a medium level occurrence. Corner thickening poses some severity, but the thickening of an area of the part does not negatively impact the strength of the part at the location of occurrence. The geometric variances at the corner thickening locations do, however, pose some severity. If the corner region thickens, it does indicate thinning in other regions, but this is already accounted for in the thickness variation metric.

The lowest weighted metric is texture with a weight of 5%. This is due to the medium occurrence and low severity when compared with the other metrics. Texture defects still are an important metric as unseemly parts are undesirable to consumers and manufacturers, yet do not pose the significant strength and performance defects that the other metrics can.

In the example presented in Table 3.10, bridging receives a rank of 2, wrinkling receives a rank of 5, thickness variation and forming depth receive ranks of 3, corner thinning receives a rank of 0, corner thickening and resin pooling receive ranks of 1, and texture receives a rank of 4. Combining all these rankings and weights results in a final forming score of 2.38 out of 5.

Table 3.10: Example of the Final Forming Scoring Matrix

Metric	Weight	Ranking	Score
Bridging	12.5%	2	-
Wrinkling	17.5%	5	-
Thickness Variation	15%	3	-
Forming Depth	12.5%	3	-
Corner Thinning	15%	0	-
Corner Thickening	10%	1	-
Resin Pooling	12.5%	1	-
Texture	5%	4	-
Total	100%	-	2.38

Performed Trials

Curved C-channel Trials

For the Curved C-channel tests, sixteen trials are performed using either stretch broken carbon fiber or continuous carbon fiber. Of these sixteen trials, thirteen are analyzed using the final forming evaluation method while the remaining three are used for defect microscope imagery. Presented in Chapter 4 (Results and Discussion) are two of the continuous carbon fiber results, one with the highest forming score and one with the lowest forming score. Also presented are two of the stretch broken carbon fiber results with the highest forming score and with the lowest forming score. The additional trial results are displayed in Appendix B.

Rounded Hat channel Trials

For the Rounded Hat channel tests, five total trials are performed using either stretch broken carbon fiber or continuous carbon fiber. Of these five trials, two are analyzed using the final forming evaluation method. The remaining three parts are performed on tooling no longer in use to develop a layup method for this part type. These parts receive no

final forming score due to the previous tool's deficits. Presented in Chapter 4 (Results and Discussion) is one trial using continuous carbon fiber and another using stretch broken carbon fiber.

Sinusoidal C-channel Trials

For the Sinusoidal C-channel tests, two trials are performed using continuous carbon fiber, limited by material availability. Both these trials are analyzed using the final forming evaluation method and the results from one of these trials are presented in Chapter 4 (Results and Discussion). The remaining trial results and evaluation are displayed in Appendix B.

RESULTS AND DISCUSSION

Curved C-channel Results and Discussion

Continuous Carbon Fiber Results

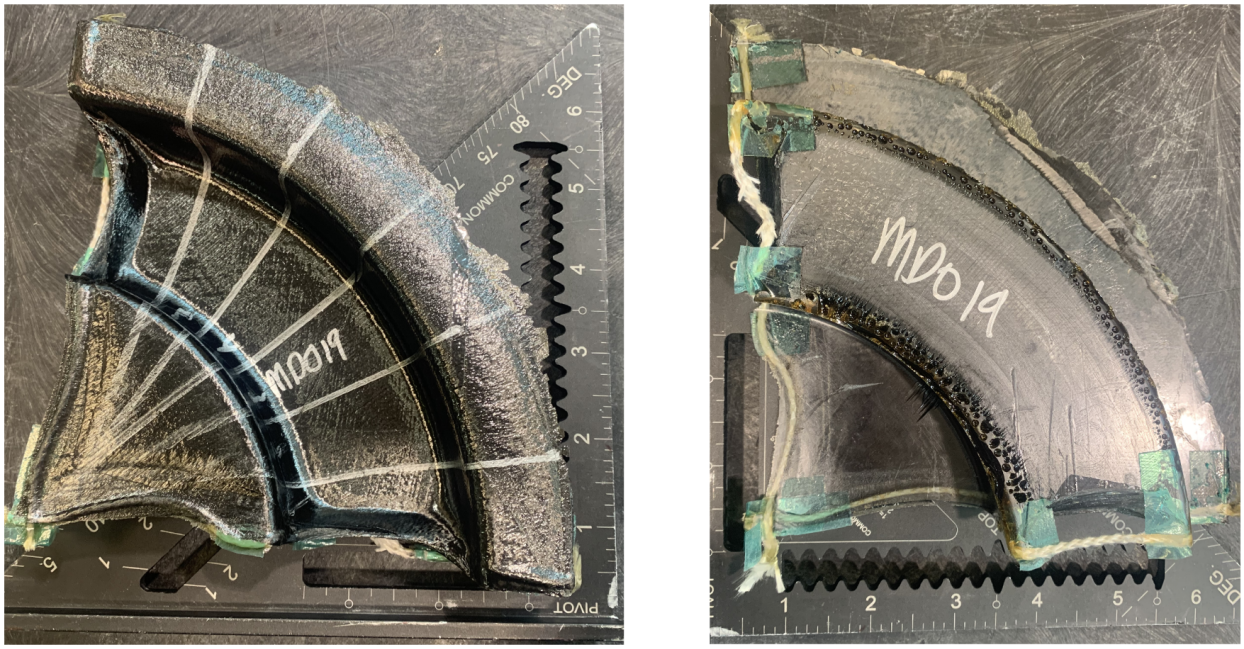


Figure 4.1: Continuous Carbon Fiber Curved C-channel Part MD019: LEFT - Top of Part, RIGHT - Bottom of Part

Lowest Forming Score: The Curved C-channel part made of continuous carbon fiber with the lowest overall forming score is part MD019 with images of the part in Figure 4.1. The part was made with Hexcel IM7/8552 prepreg (21; 22). The part consists of eight plies with a quasi-isotropic layup of [45/0/-45/90]s. This layup was cut in quarter circular shape with a radius of 6 in [15.24 cm]. Breather strings were used on the outer edges of the layup to provide an edge breathing effect. The cure cycle used for the part involved a straight temperature ramp to 250°F [121°C] and holding temperature for 30 minutes. Following this dwell was another straight temperature ramp, this time to 350°F [176°C] and dwelling for 135

minutes. For the entire duration of this cure, a pressure of 85 psi [586 KPa] was used within the autoclave chamber. Seen in Figure 4.2 are the corner thinning and corner thickening results for this test. For all measurement locations and radii, part MD019 has an average corner thinning value of 78.85% of the average thickness earning a corner thinning score of 0. For all measurement locations and radii, part MD019 has an average corner thickening value of 142.86% of the average thickness earning a corner thickening score of 0.

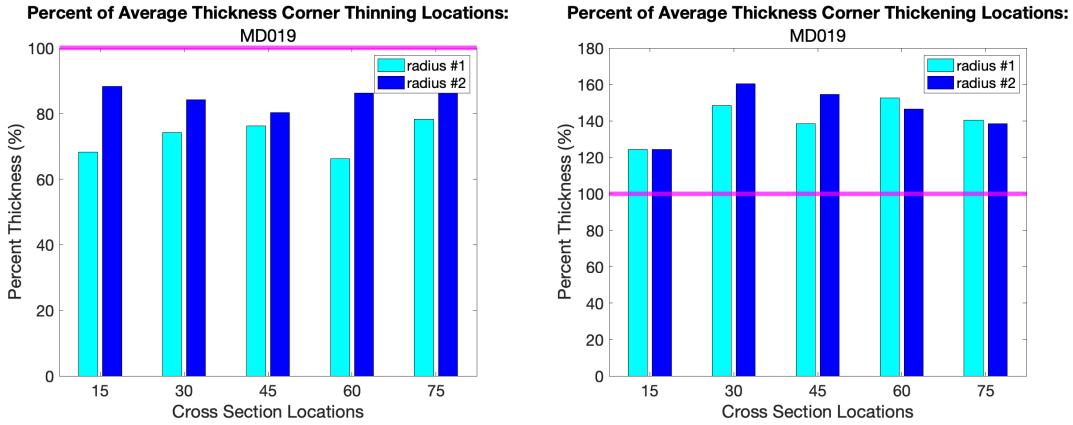


Figure 4.2: Continuous Carbon Fiber MD019 Results: LEFT - Corner Thinning (Average = 78.85%), RIGHT - Corner Thickening (Average = 142.86%)

Figure 4.3 displays the combined resin pooling and bridging results for Curved C-channel part MD019. For all measurement locations, part MD019 has an average bridging distance of 0.0866 in [0.2200 cm] which earns a bridging score of 3, keeping in mind the designed radius of the corner is 0.125 in [0.32 cm]. Part MD019 has a total resin pooling area of 0.0204 in^2 [0.1316 cm^2] when averaging all measurement location data earning a resin pooling score of 1.

The contour plots from two different view angles for part MD019 are seen in Figure4.4. Using Equation 3.1 and the total thickness data set, the coefficient of variation for this part is 0.1566, which earns a thickness variation score of 3.

The forming depth for each cross-section location as well as the forming depth

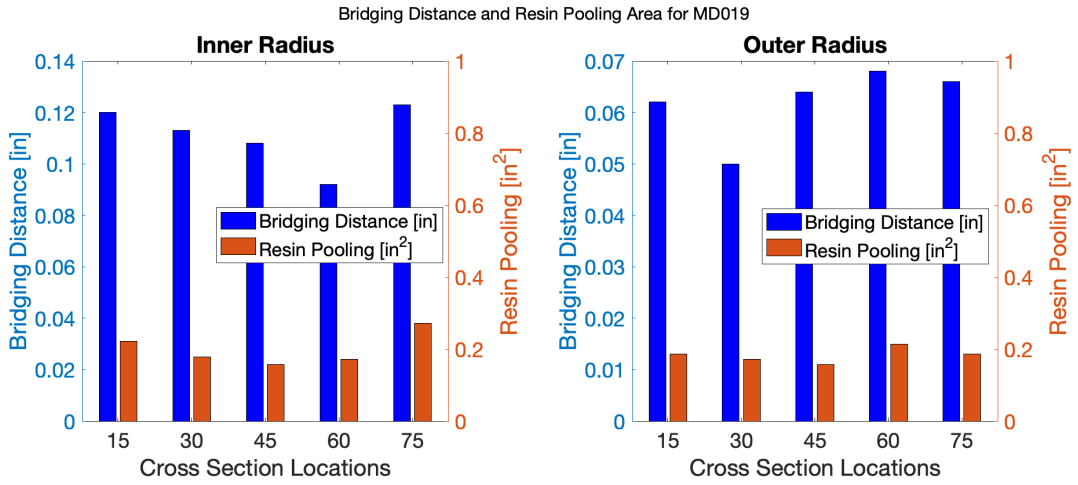


Figure 4.3: Continuous Carbon Fiber MD019 Results: Bridging (Average = 0.125 in) and Resin Pooling (Total = 0.0204 in^2)

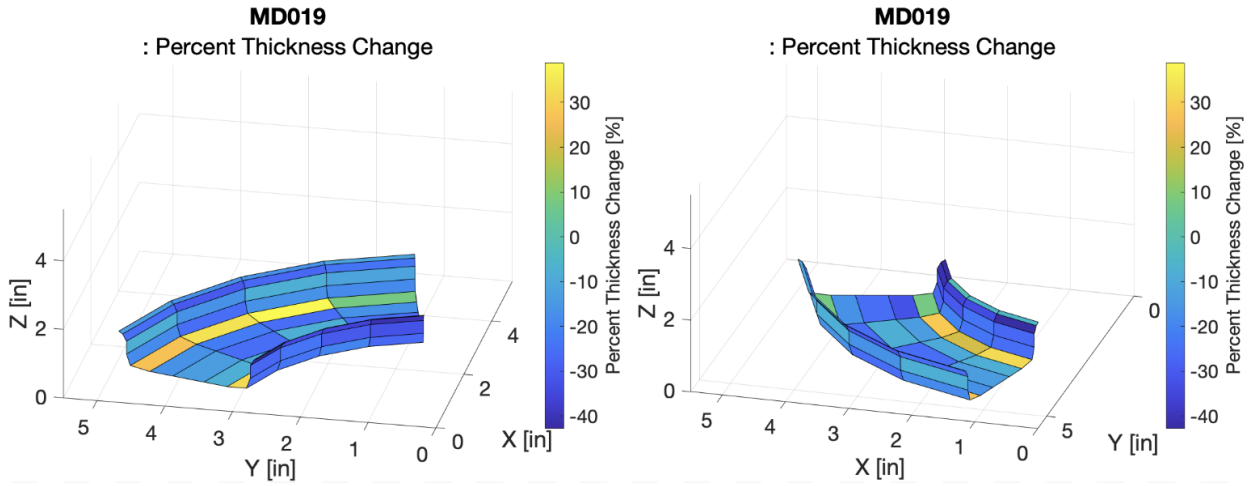


Figure 4.4: Continuous Carbon Fiber MD019 Results: Thickness Variation, LEFT - "Radius #1" Orientation, RIGHT - "Radius #2" Orientation (Coefficient of Variation = 0.1566)

visualization plots are presented in Figure 4.5. For all measurement locations, the average forming depth percent for part MD019 is 84.17%. This value earns a forming depth score of 3.

There is no wrinkling present on the surface of part MD019. The total wrinkling of the part as well as the total wrinkling within the critical region are both 0%, earning part

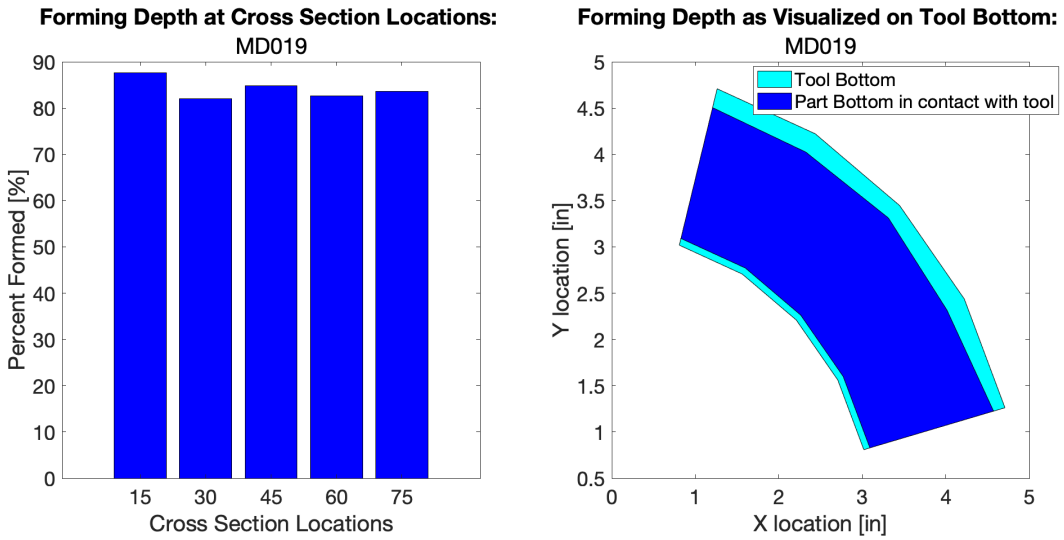


Figure 4.5: Continuous Carbon Fiber MD019 Results: Forming Depth (Average = 84.17%)

MD019 a wrinkling score of 5.

The texture scoring table for Curved C-channel part MD019 is seen in Table 4.1. A Hairiness score of 5 is assigned to the part as it has no loose fibers upon the surface of the part. A score of 4 is assigned to the additional resin pooling defect as the part has very minimal regions of resin pooling at the edges of the part. Part MD019 receives a score of 5 for spaghettification as this defect is not present on the part. Fractures/shearing are detected in the non-critical regions of the part, but are detected in other areas. This earns a score of 3 for fractures/shearing. No pinholes are counted at any location on part MD019 resulting in a score of 5. Waves are present in a few of the convex corner regions on the part effectively earning a score of 0. All of these defects result in a final texture score of 4.15.

Combining the total defect scores for part MD019, a final forming score of 2.28 is achieved. A summary of each defect's score as well as the final forming score is presented in Table 4.2.

Table 4.1: Continuous Carbon Fiber MD019: Texture Results

Metric	Weight	Ranking	Score
Hairiness	30%	5	-
Additional Resin Pooling	30%	4	-
Spaghettification	10%	5	-
Fractures/Shearing	15%	3	-
Pinholes	10%	5	-
Waves	5%	0	-
Total	100%	X	4.15

Table 4.2: Continuous Carbon Fiber MD019: Final Forming Score

Metric	Weight	Ranking	Score
Bridging	12.5%	2	-
Wrinkling	17.5%	5	-
Thickness Variation	15%	3	-
Forming Depth	12.5%	3	-
Corner Thinning	15%	0	-
Corner Thickening	10%	0	-
Resin Pooling	12.5%	1	-
Texture	5%	4.15	-
Total	100%	-	2.28

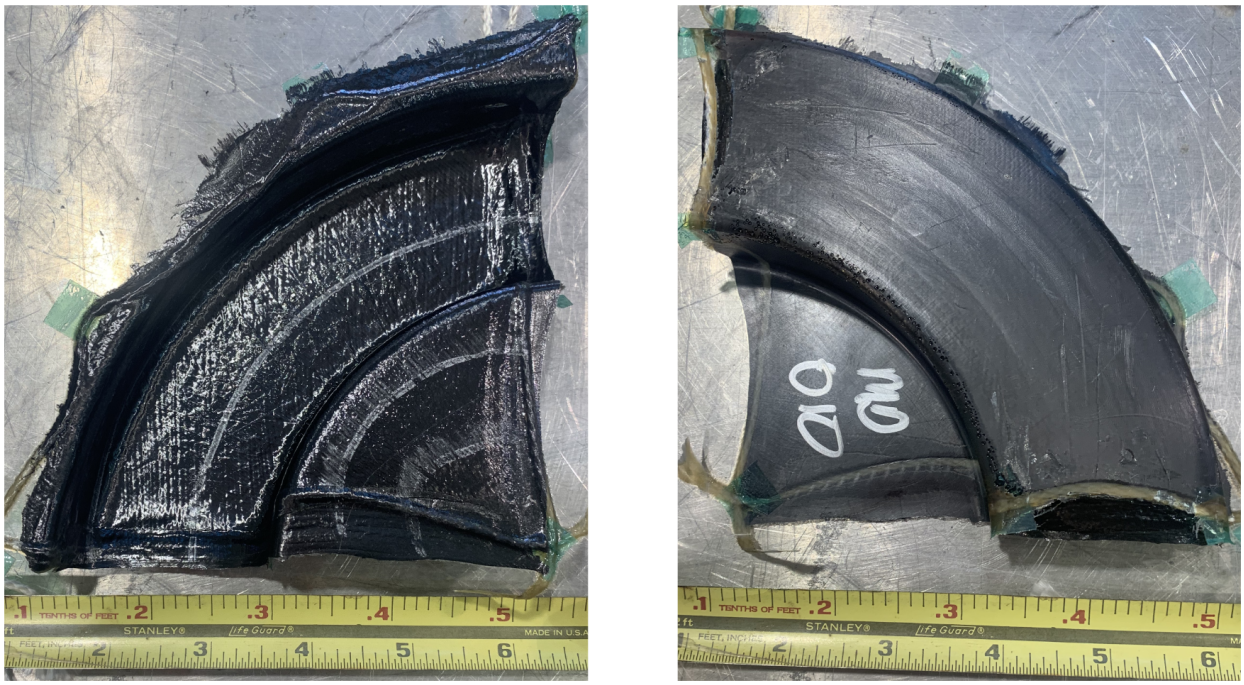


Figure 4.6: Continuous Carbon Fiber Curved C-channel Part MD010: LEFT - Top of Part, RIGHT - Bottom of Part

Highest Forming Score: The Curved C-channel part made of continuous carbon fiber with the highest overall forming score is part MD010, seen in Figure 4.6. The part incorporates Hexcel IM7/8552 prepreg (21; 22). The part has eight plies with a quasi-isotropic layup of [45/0/-45/90]s. The layup was cut in a quarter circular shape with a radius of 6 in [15.24 cm]. Breather strings were used for edge breathing on this part. Once this layup was placed on the tool, a silicone intensifier matched to the tool geometry with space for the laminate was pressed slightly into the negative mold feature of the tool. The cure cycle started with a straight temperature ramp to 350°F [176°C] followed by a dwell of 120 minutes at this temperature. Throughout the duration of the cure, 90 psi [620 KPa] pressure was applied within the autoclave. Figure 4.7 presents the corner thinning and corner thickening results for part MD010. For all measurement locations and radii, part MD010 has an average corner thinning value of 85.81% of the average thickness as well as an average

corner thickening value of 173.13% of the average thickness. This earns part MD010 a corner thinning score of 2 and a corner thickening score of 0.

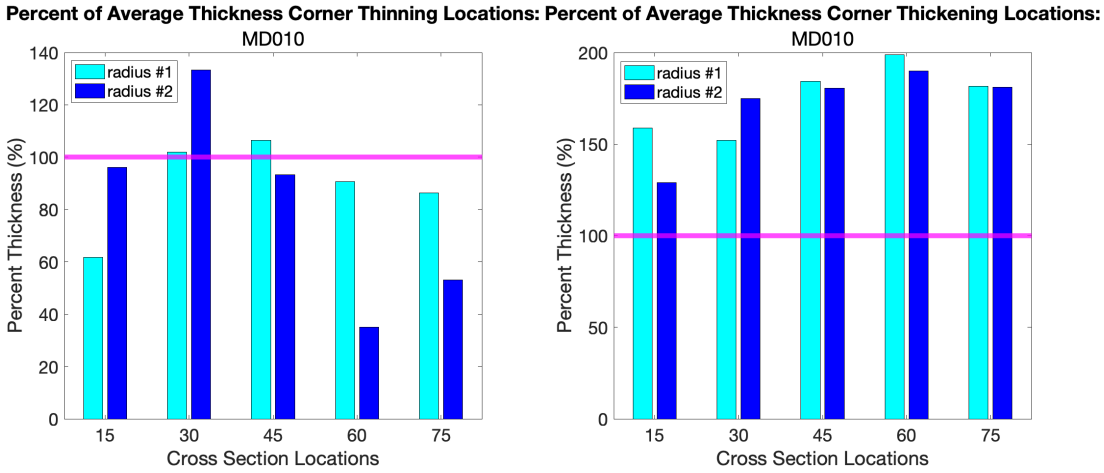


Figure 4.7: Continuous Carbon Fiber MD010 Results: LEFT - Corner Thinning (Average = 85.81%), RIGHT - Corner Thickening (Average = 173.13%)

The combined resin pooling and bridging data for Curved C-channel part MD010 can be seen in Figure 4.8. For all measurement locations and radii, part MD010 has an average bridging distance of $0.0314in$ [$0.0798cm$] and a total resin pooling area $0.0056in^2$ [$0.0361cm^2$]. This earns part MD010 a bridging score of 3 and a resin pooling score of 4.

Figure 4.9 displays the thickness contour plots for part MD010. The coefficient of variation for the entire thickness data set for this part is 0.2021. This earns part MD010 a thickness variation score of 2.

Figure 4.10 displays the forming depth data for part MD010. Averaging the values from all measurement locations earns part MD010 an average forming depth of 94.89%. This results in a forming depth score of 4.

There is no wrinkling present on part MD010. For this part, the total wrinkling, as well as the total wrinkling within the critical area are both 0%. This earns part MD010 a perfect wrinkling score of 5.

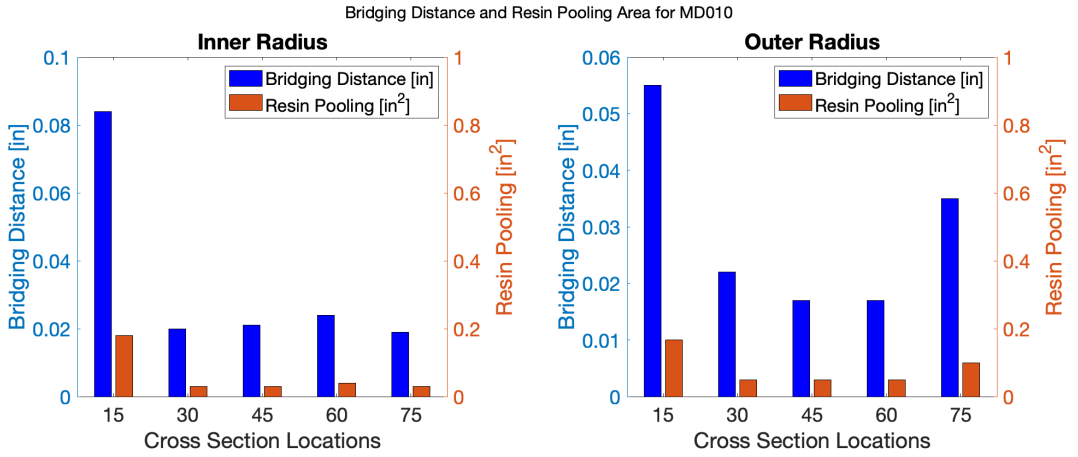


Figure 4.8: Continuous Carbon Fiber MD010 Results: Bridging (Average = 0.0314 in) and Resin Pooling (Total = 0.0056 in^2)

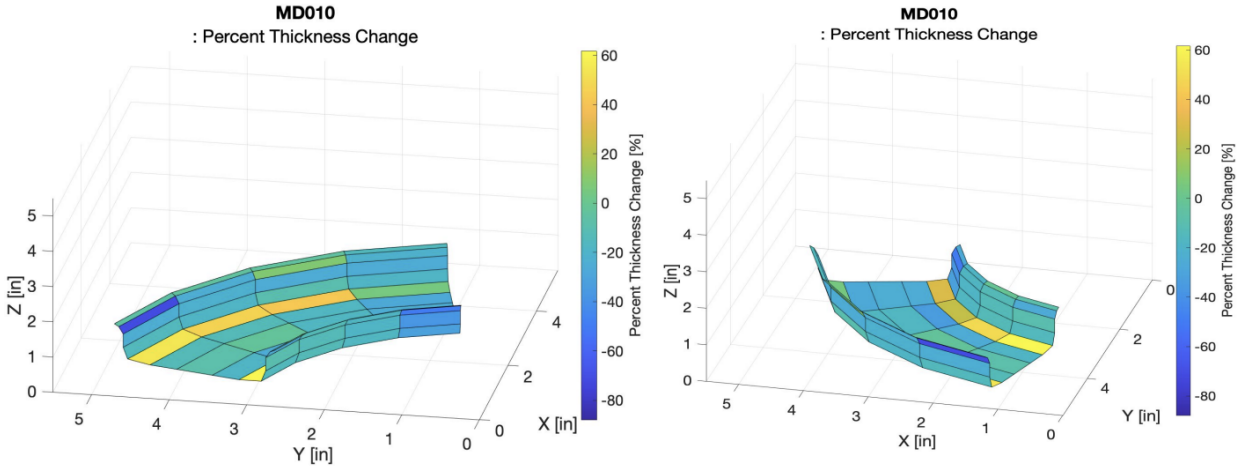


Figure 4.9: Continuous Carbon Fiber MD010 Results: Thickness Variation, LEFT - "Radius #1" Orientation, RIGHT - "Radius #2" Orientation (Coefficient of Variation = 0.2021)

The texture defect scoring results for Curved C-channel part MD010 are presented in Table 4.3. This part displays no loose fibers, earning a hairiness score of 5. Additional resin pooling is noted just above the intensifier location on the part, resulting in a score of 3. This part has one location where spaghettification is present which scores a 2 for this defect. No fractures/shearing, pinholes, or waves are detected on part MD019 earning a score of 5 for

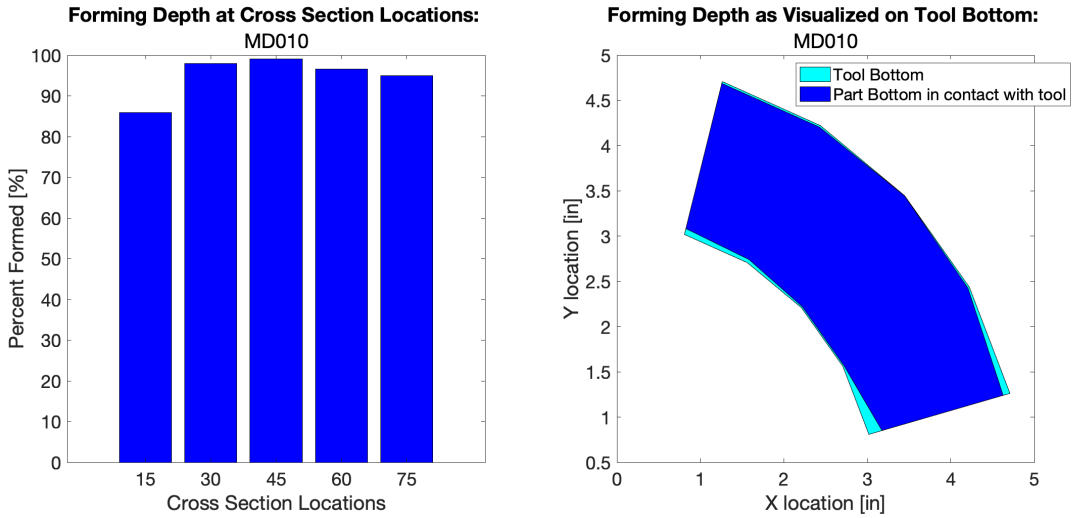


Figure 4.10: Continuous Carbon Fiber MD010 Results: Forming Depth (Average = 94.89%)

each of these defects. The combination of all of the texture defect scores earn continuous Curved C-channel part MD010 a final texture score of 4.1.

Table 4.3: Continuous Carbon Fiber MD010: Texture Results

Metric	Weight	Ranking	Score
Hairiness	30%	5	-
Additional Resin Pooling	30%	3	-
Spaghettification	10%	2	-
Fractures/Shearing	15%	5	-
Pinholes	10%	5	-
Waves	5%	5	-
Total	100%	X	4.1

A final forming score of 3.06 is assigned to part MD010 when combining the individual defect scores. A table outlining the defect scores as well as the final forming score is presented in Table 4.4.

Table 4.4: Continuous Carbon Fiber MD010 Final Forming Score

Metric	Weight	Ranking	Score
Bridging	12.5%	3	-
Wrinkling	17.5%	5	-
Thickness Variation	15%	2	-
Forming Depth	12.5%	4	-
Corner Thinning	15%	2	-
Corner Thickening	10%	0	-
Resin Pooling	12.5%	4	-
Texture	5%	4.1	-
Total	100%	-	3.06

Stretch Broken Carbon Fiber Results



Figure 4.11: Stretch Broken Carbon Fiber Curved C-channel Part MD004: LEFT - Top of Part, RIGHT - Bottom of Part

Lowest Forming Score: The Curved C-channel part made of stretch broken carbon fiber with the lowest overall forming score is part MD004, seen in Figure 4.11. The part was made with MSU SBCF/977-3 prepreg batch P0025, material data in Appendix A (21; 23). Like the others, the part consists of eight plies with a quasi-isotropic layup of [45/0/-45/90]s. The layup was cut in a square shape with dimensions of 6 in [15.24 cm] by 6 in [15.24 cm]. Breather strings were incorporated at a 45°angle across the tool to evacuate air underneath the laminate. The cure cycle for this part started with a straight temperature ramp to 80°F [26°C] and dwelling for 30 minutes. Following this dwell was a straight temperature ramp to 350°F [176°C] and a dwell for 6 hours. 90 psi [620 KPa] pressure was applied in the autoclave for the entire duration of the run. Figure 4.12 displays the corner thinning and corner thickening data for part MD004. For all measurement locations and radii, part MD004 has an average corner thinning value of 89.83% of the average thickness and an average corner thickening value of 102.47% of the average thickness. These values earn part MD004 a corner thinning score of 2 and a corner thickening score of 4.

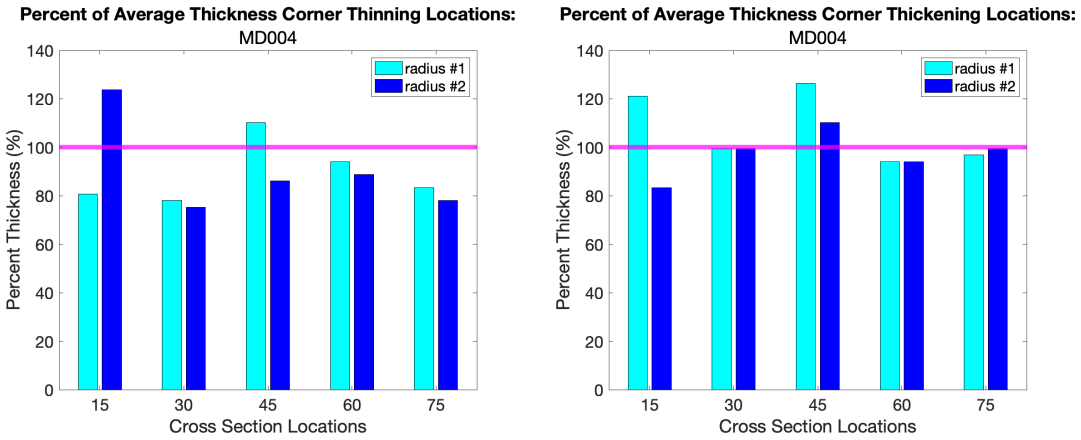


Figure 4.12: Stretch Broken Carbon Fiber MD004 Results: LEFT - Corner Thinning (Average = 89.83%), RIGHT - Corner Thickening (Average = 102.47%)

Figure 4.13 displays the combined resin pooling and bridging data for Curved C-channel part MD004. For all measurement locations, the part has an average bridging distance of

0.1769 in [0.4493 cm] and a total resin pooling area of 0.00129 in^2 [0.00832 cm^2] . This earns part MD004 a bridging score of 1 and a resin pooling score of 4.

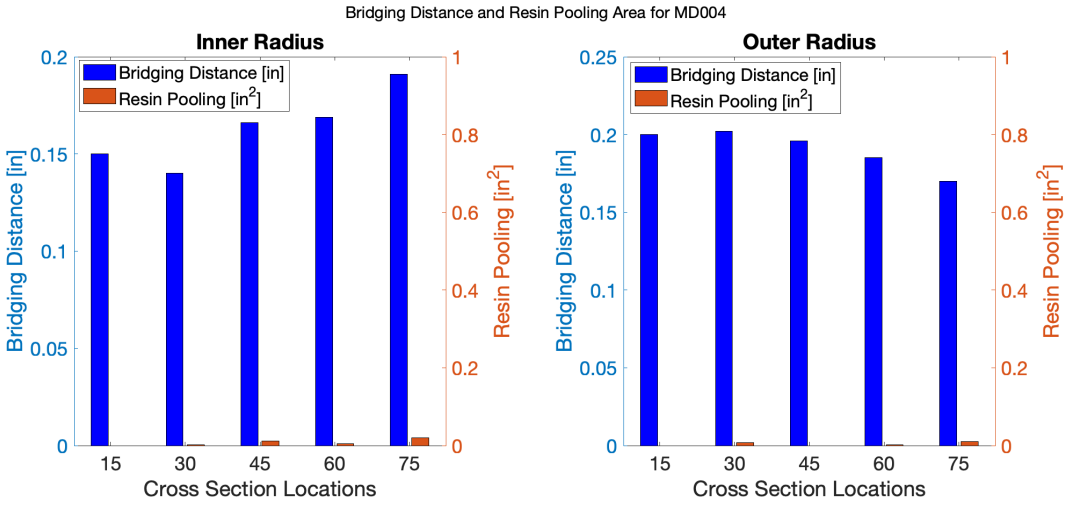


Figure 4.13: Stretch Broken Carbon Fiber MD004 Results: Bridging (Average = 0.1769 in) and Resin Pooling (Average = 0.00129 in^2)

The thickness variation contour plots for part MD004 are displayed in Figure 4.14. For the entire thickness measurement data set, the coefficient of variation is calculated to be 0.1711. This earns part MD004 a thickness variation score of 3.

The forming depth data for part MD004 is seen in Figure 4.15. Averaging the values from all of the measurement locations results in an average forming depth of 64.62%. MD004 then earns a forming depth score of 2.

Figure 4.16 displays the wrinkling data pie charts for part MD004. This part has 2.95% wrinkling within the critical region with additional wrinkling outside of the critical region bringing the total wrinkling up to 3.32%. These values earn part MD004 a wrinkling score of 1.

The texture scoring results for stretch broken Curved C-channel part MD004 are presented in Table 4.5. This part does exhibit some loose parts on the surface, however they are not loose enough to be removed from the part earning a hairiness score of 3. Part

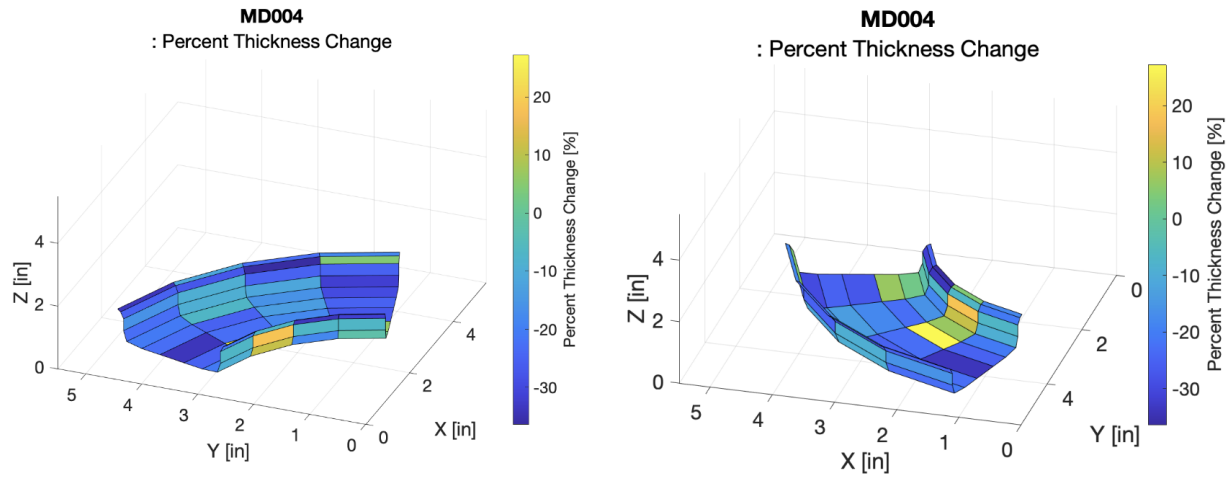


Figure 4.14: Stretch Broken Carbon Fiber MD004 Results: Thickness Variation, LEFT - "Radius #1" Orientation, RIGHT - "Radius #2" Orientation (Coefficient of Variation = 0.1711)

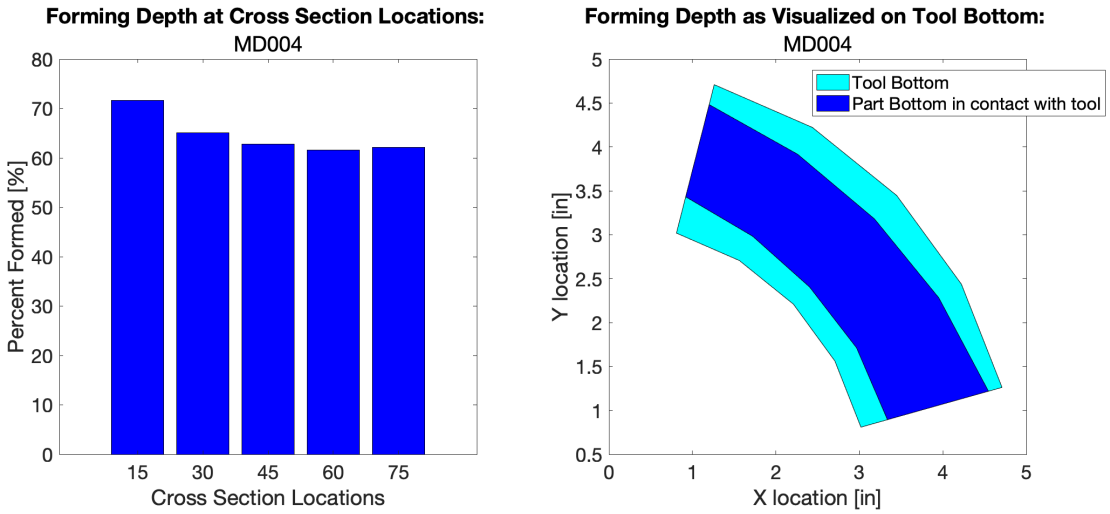


Figure 4.15: Stretch Broken Carbon Fiber MD004 Results: Forming Depth (Average = 64.62%)

MD004 has no regions of additional resin pooling, no regions with spaghettification, and no pinholes counted resulting in a score of 5 for each of these defects. Some fractures/shearing are observed in the non-critical regions of the part, scoring of 3 for this defect. Finally, waves are observed in some areas on the part earning a score of 0. The final texture score

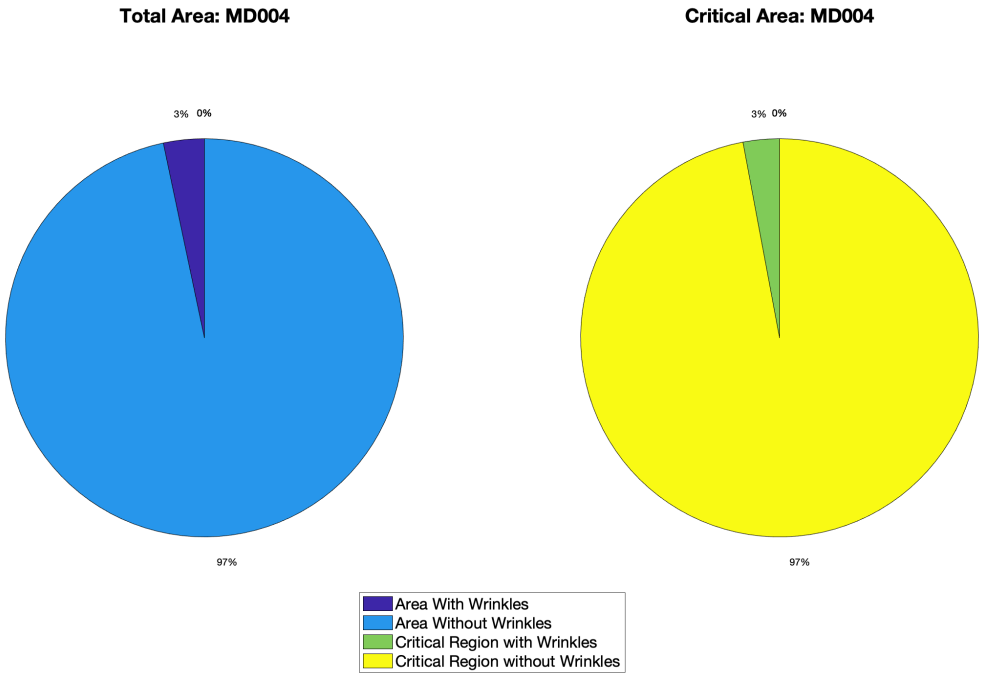


Figure 4.16: Stretch Broken Carbon Fiber MD004 Results: Wrinkling (Total Wrinkling = 3.32%, Critical Region Wrinkling = 2.95%)

for stretch broken Curved C-channel part MD004 is 3.85.

Table 4.5: Stretch Broken Carbon Fiber MD004: Texture Results

Metric	Weight	Ranking	Score
Hairiness	30%	3	-
Additional Resin Pooling	30%	5	-
Spaghettification	10%	5	-
Fractures/Shearing	15%	3	-
Pinholes	10%	5	-
Waves	5%	0	-
Total	100%	X	3.85

Combining all the defect scores within the weighted matrix assigns part MD004 a final

forming score of 2.39. The weighted matrix, defect scores, and the final forming score all are presented in Table 4.6.

Table 4.6: Stretch Broken Carbon Fiber MD004 Forming Score

Metric	Weight	Ranking	Score
Bridging	12.5%	1	-
Wrinkling	17.5%	1	-
Thickness Variation	15%	3	-
Forming Depth	12.5%	2	-
Corner Thinning	15%	2	-
Corner Thickening	10%	4	-
Resin Pooling	12.5%	4	-
Texture	5%	3.85	-
Total	100%	-	2.39

Highest Forming Score: The Curved C-channel part made of stretch broken carbon fiber with the highest overall forming score is part MD016, seen in Figure 4.17. The part was made with MSU SBCF/Solvay 977-3 prepreg batch P0030, material data in Appendix A (21; 23). The part consists of eight plies with a quasi-isotropic layup of [45/0/-45/90]s. The layup was cut in a square shape with dimensions of 6 in [15.24 cm] by 6 in [15.24 cm]. Breather strings were incorporated at the edges of the layup for edge breathing purposes. This layup also used a silicone intensifier matched to the tool design with spacing incorporated to provide room for the laminate. The intensifier was pressed firmly into the mold, using some hand layup to smooth the carbon fiber surface. The cure cycle started with a straight temperature ramp to 80°F [26°C] and dwelling for 30 minutes. Following this dwell was a straight temperature ramp to 350°F [176°C] and a dwell for 6 hours. 90 psi [620 KPa] pressure was applied inside of the autoclave chamber for the entire run duration. The corner thinning and corner

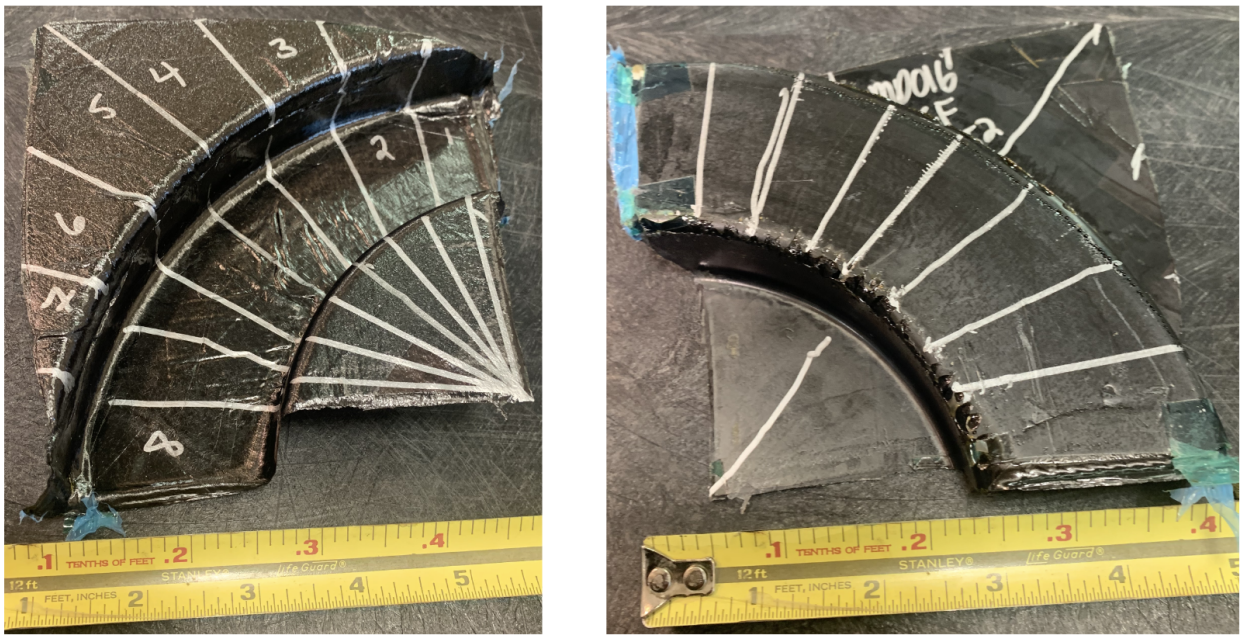


Figure 4.17: Stretch Broken Carbon Fiber Curved C-channel Part MD016: LEFT - Top of Part, RIGHT - Bottom of Part

thickening data can be seen in Figure 4.18 for part MD016. For all measurement locations and radii, this part has an average corner thinning value of 93.80% of the average thickness and an average corner thickening value of 100.81% of the average thickness. This earns part MD016 a corner thinning score of 3 and a corner thickening score of 4.

The combined resin pooling and bridging data for part MD016 is presented in Figure 4.19. For all measurement locations, part MD016 has an average bridging distance of 0.0388 in [0.099 cm] and a total resin pooling area of 0.00490 in^2 [0.03161 cm^2]. These values result in a bridging score of 3 and a resin pooling score of 4 for part MD016.

Figure 4.20 displays the thickness contour plots for part MD016. The coefficient of variation for the entire thickness data set is 0.2169 earning part MD016 a thickness variation score of 2.

The forming depth data is visualized in Figure 4.21 for part MD016. The average forming depth of all the measurement locations is 95.04% earning a forming depth score of

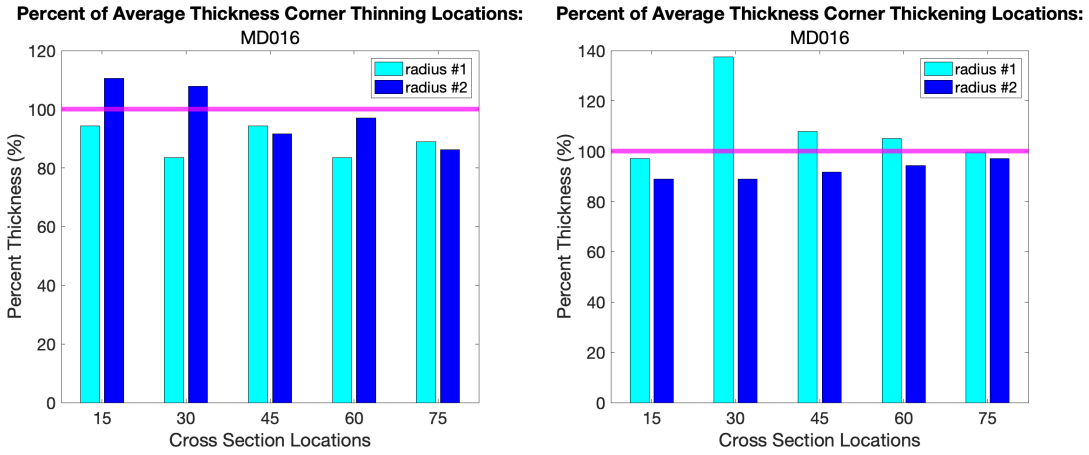


Figure 4.18: Stretch Broken Carbon Fiber MD016 Results: LEFT - Corner Thinning (Average = 93.80%), RIGHT - Corner Thickening (Average = 100.81%)

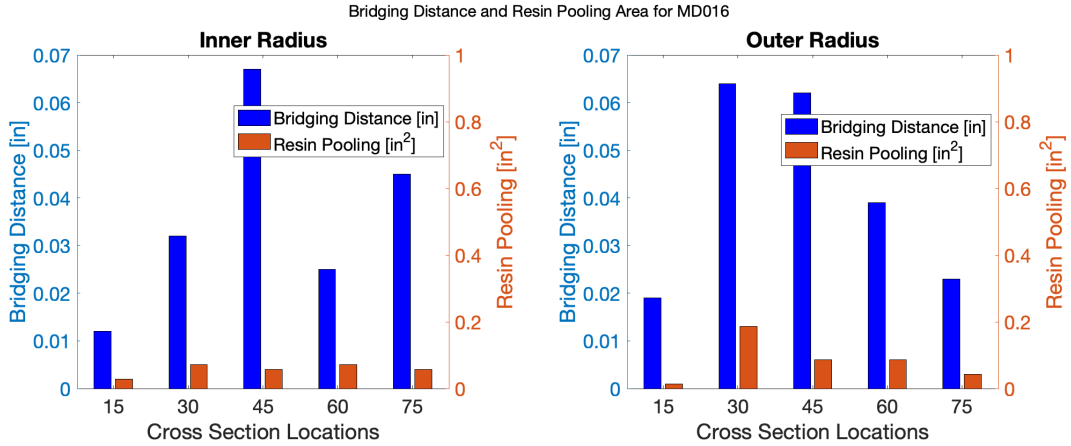


Figure 4.19: Stretch Broken Carbon Fiber MD016 Results: Bridging (Average = 0.0388 in) and Resin Pooling (Total = 0.00490 in^2

4 for part MD016.

The wrinkling data pie charts for part MD016 are displayed in Figure 4.22. The percentage of wrinkles within the critical location for this part is 2.16% while the total percentage of wrinkles is 2.29%. These wrinkling values earn part MD016 a wrinkling score of 1.

The texture ranking results for part MD016 are tabulated in Table 4.7. This part

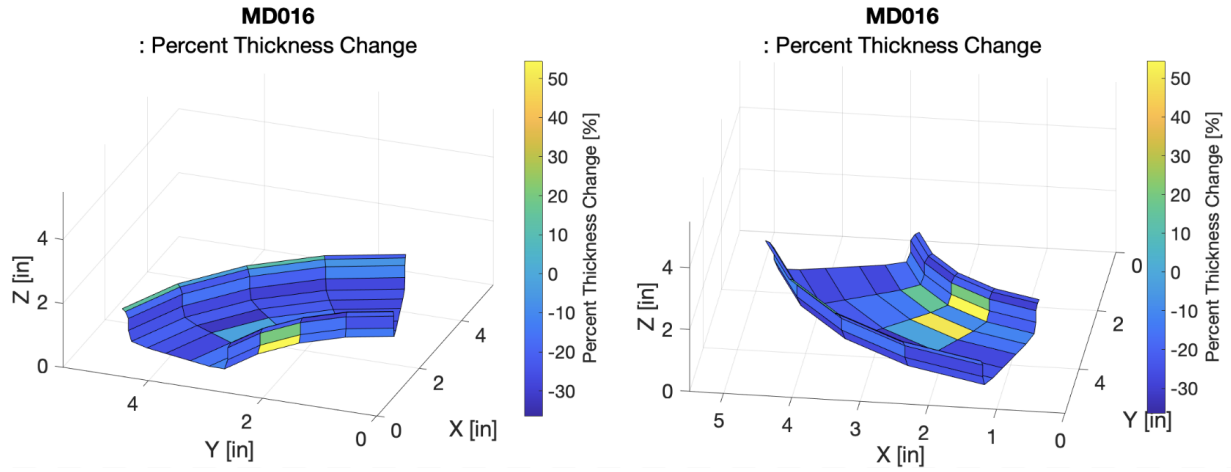


Figure 4.20: Stretch Broken Carbon Fiber MD016 Results: Thickness Variation, LEFT - "Radius #1" Orientation, RIGHT - "Radius #2" Orientation (Coefficient of Variation = 0.2169)

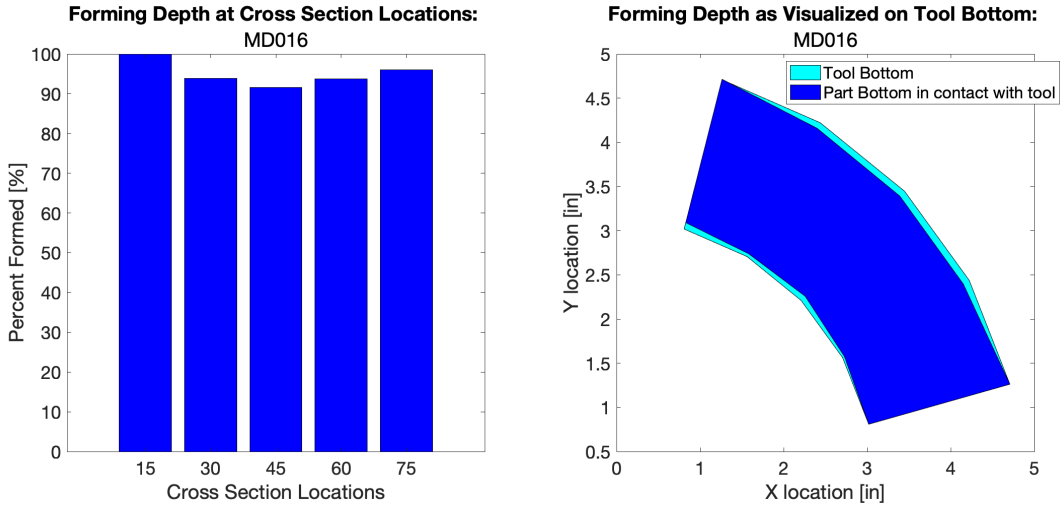


Figure 4.21: Stretch Broken Carbon Fiber MD016 Results: Forming Depth (Average = 95.04%)

receives a perfect score of 5 for the hairiness, spaghettification, and waves texture metrics as it exhibits none of these defects. A score of 3 is assigned for the additional resin pooling defect as this part displays resin pooling just above the intensifier location. For the fractures/shearing defect, part MD016 also receives a 3 as this defect is observed in the

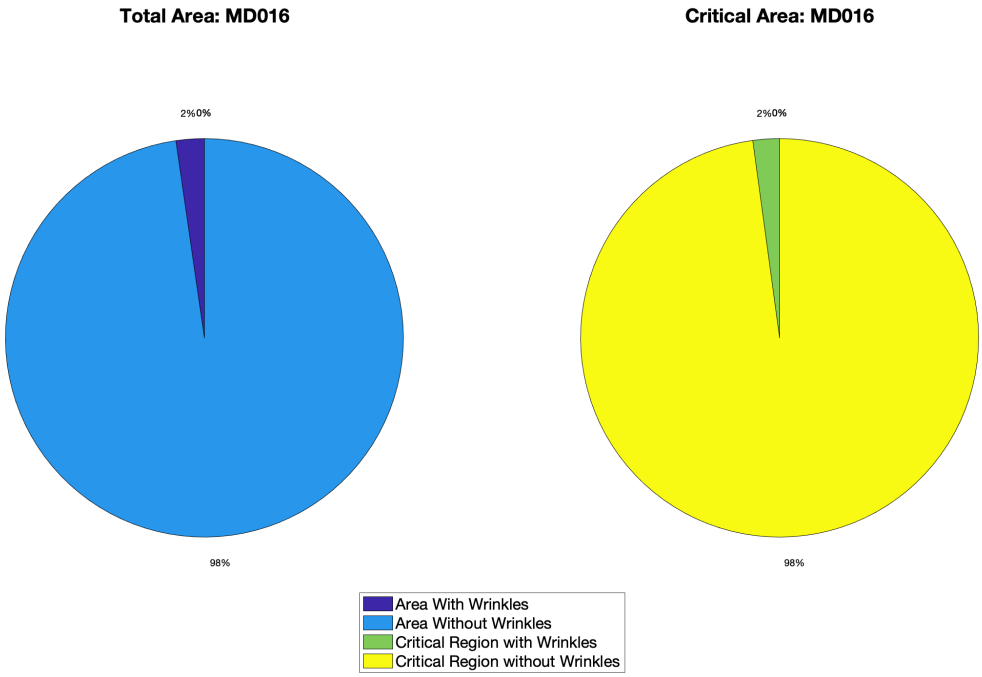


Figure 4.22: Stretch Broken Carbon Fiber MD016 Results: Wrinkling (Total Wrinkling = 2.29%, Critical Region Wrinkling = 2.16%)

non-critical locations. Finally, a score of 3 is assigned to the pinholes defect, because three pinholes are counted on the part. This brings the final texture metric score to 3.9 for part MD016 is.

Table 4.7: Stretch Broken Carbon Fiber MD016: Texture Results

Metric	Weight	Ranking	Score
Hairiness	30%	5	-
Additional Resin Pooling	30%	3	-
Spaghettification	10%	5	-
Fractures/Shearing	15%	3	-
Pinholes	10%	3	-
Waves	5%	5	-
Total	100%	X	3.9

Part MD016 earns a final forming score of 2.895 after combining all the defect scores within the weighted matrix. This final scoring matrix is shown in Table 4.8.

Table 4.8: Stretch Broken Carbon Fiber MD016: Final Forming Score

Metric	Weight	Ranking	Score
Bridging	12.5%	3	-
Wrinkling	17.5%	1	-
Thickness Variation	15%	2	-
Forming Depth	12.5%	4	-
Corner Thinning	15%	3	-
Corner Thickening	10%	4	-
Resin Pooling	12.5%	4	-
Texture	5%	3.9	-
Total	100%	-	2.90

Curved C-channel Discussion

A summary of all the presented Curved C-channel trial results is seen in Table 4.9. The continuous carbon fiber results presented for the Curved C-channel trials (parts MD010 and MD019) indicate a range of performances for some of the metrics. Altogether, the two continuous carbon fiber trials result in no wrinkling, unacceptable levels of corner thickening, and very similar texture scores (MD010 being 4.1 and MD019 being 4.15). For these tests, the presence of an intensifier and an additional dwell at 250°F [121°C] within the cure cycle do not effect these metrics. However, there are variances in the bridging, thickness variation, forming depth, corner thinning, and resin pooling defects. Both continuous carbon fiber parts experience large amounts of corner thickening during the forming process. This gives further support to the log rolling theory that continuous carbon fiber displays when formed over a convex curvature with a concave curvature below it.

Table 4.9: Summary of Curved C-channel Results

	MD010	**MD019**	**MD004**	**MD016**
Material	CF	CF	SBCF	SBCF
Plies	8	8	8	8
Intermediate Dwell	No	Yes	Yes	Yes
Intensifier	Yes	No	No	Yes
Layup Shape	Quarter Circle	Quarter Circle	Square	Square
Scores				
Bridging	3	2	1	3
Wrinkling	5	5	1	1
Thickness Variation	2	3	3	2
Forming Depth	4	3	2	4
Corner Thinning	2	0	2	3
Corner Thickening	0	0	4	4
Resin Pooling	4	1	4	4
Texture	4.1	4.15	3.85	3.9
Final Score	3.06	2.28	2.39	2.9

The large discrepancies in the resin pooling scores is likely due to the presence of an intensifier in one of the cure cycles. Part MD010 uses an intensifier that snugly fits the carbon fiber laminate into the mold, leaving little remaining room for the resin to pool into. This could explain why Part MD010 has a resin pooling score of 4 while part MD019 has a resin pooling score of 1. It is important to note that part MD019 has an intermediate dwell in the cure cycle whereas part MD010 does not, which could also explain the resin pooling variances.

The other metric with a significant difference between the two continuous carbon fiber tests is the corner thinning metric. Both tests do experience corner thinning, with MD010 experiencing an average of 14.19% corner thinning and MD019 experiencing an average of 21.15% corner thinning. While these values place the two parts in rankings of 2 and 0, the overall difference between the two percentages is around 7%. This small change in the different corner thinning results could be due to the effects on resin viscosity that the intermediate dwell provides, or the additional forces applied by the intensifier.

Figures 4.23 and 4.24 show the stretching versus slipping data for parts MD010 and MD019 respectively. Viewing the cyan filled in regions as well as the red line graphs on the figures show that both of the parts experience significant amounts of ply-ply slippage in order to fill into the mold. Part MD010 experiences more consistent ply-ply slippage amounts between the different data sets, which may explain the higher forming score when compared to part MD019.

The stretch broken carbon fiber results presented for the Curved C-channel trials (parts MD004 and MD016) indicate a range of performances for some of the metrics. Altogether, the two stretch broken carbon fiber trials result in small amounts of resin pooling, hardly any corner thickening, and similar scores for the texture metric. Both parts, however, experience large amounts of wrinkling resulting in a score of 1 for each part. Seen in Figures 4.25 and 4.26 are the stretching and slipping plots for stretch broken carbon fiber parts MD004 and

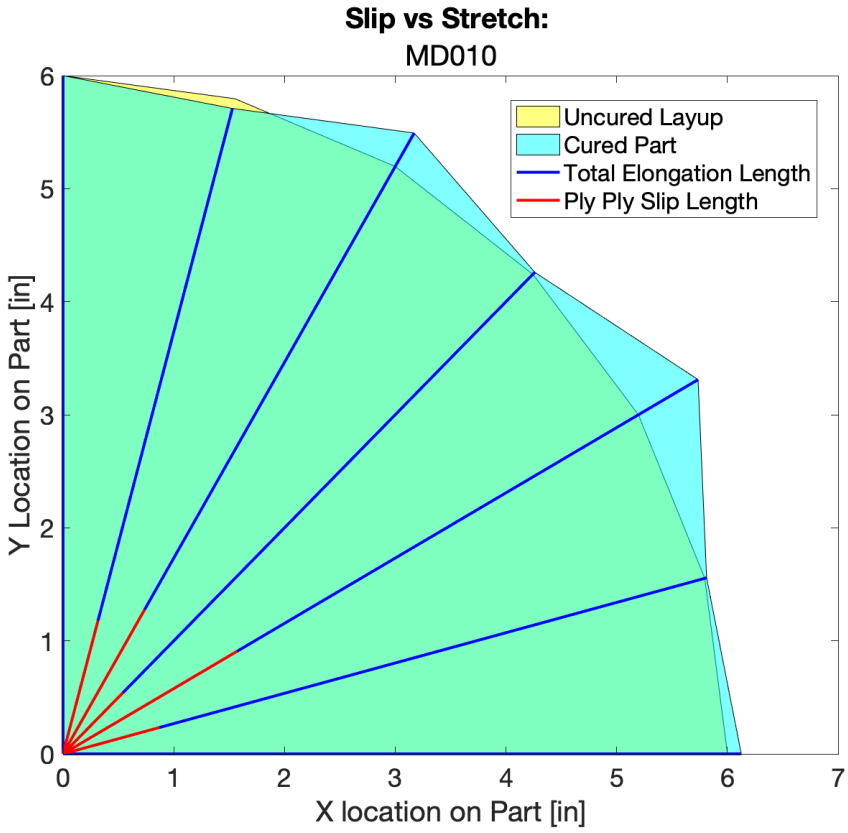


Figure 4.23: Continuous Carbon Fiber MD010 Results: Stretch vs Slip

MD016 respectively. The minuscule amounts of ply-ply slippage for each part provide an explanation for the high wrinkling values. If the individual plies are not slipping relative to each other, or slipping occurs before stretching can, the entire laminate wrinkles under compressive forces during the forming stage of the cure cycle.

The bridging metric score has differences between the two stretch broken carbon fiber test. When observing Table 4.9, the bridging scores seem to be impacted by the presence of an intensifier. Stretch broken part MD004 does not use an intensifier earning a bridging score of 1, whereas part MD016 does use an intensifier earning a higher score of 3. This use of an intensifier also seems to impact the forming depth scores for all tests. For the stretch broken carbon fiber parts in particular, the use of an intensifier increased the forming depth score

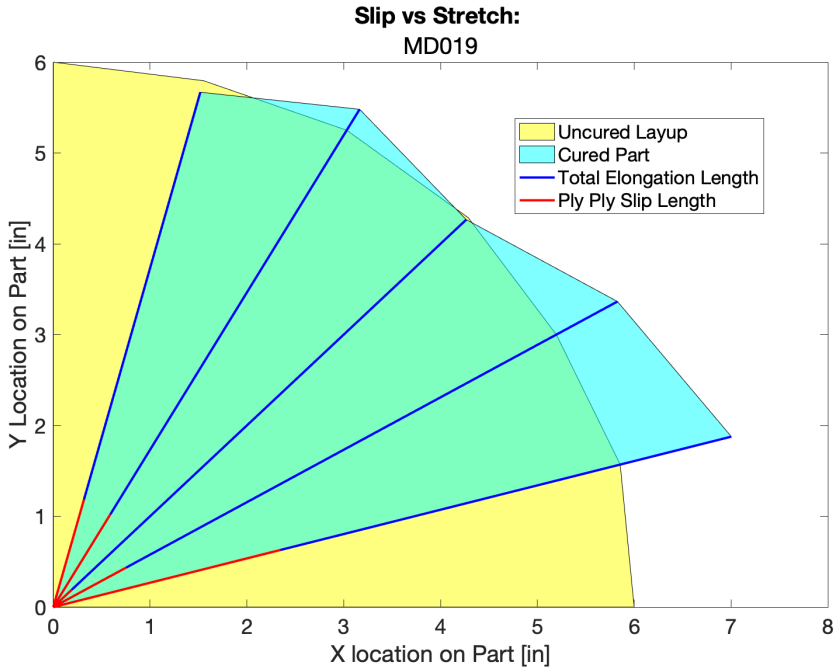


Figure 4.24: Continuous Carbon Fiber MD019 Results: Stretch vs Slip

from 2 (part MD004) to 4 (part MD016). For all of the Curved C-channel tests presented in Table 4.9, the use of an intensifier effectively improves the bridging scores and the forming depth scores for both continuous carbon fiber and stretch broken carbon fiber.

Figure 4.27 displays the final forming scores for all the Curved C-channel trials, including the parts listed in Appendix B. In total, six stretch broken carbon fiber Curved C-channel tests and seven continuous carbon fiber Curved C-channel tests are analyzed with the forming quality metrics. The red plot points show the continuous carbon fiber results, where the blue plot points show the stretch broken carbon fiber results. When viewing the plot, no clear difference between the scores can be seen. All the results have final forming scores between 2.25 and 3.25 with the continuous carbon fiber results having a larger spread between the data points. A breakdown of the individual metric results must be discussed to develop an understanding of the performance for the different fiber types.

Figure 4.28 displays the metric scores for bridging, corner thickening, corner thinning,

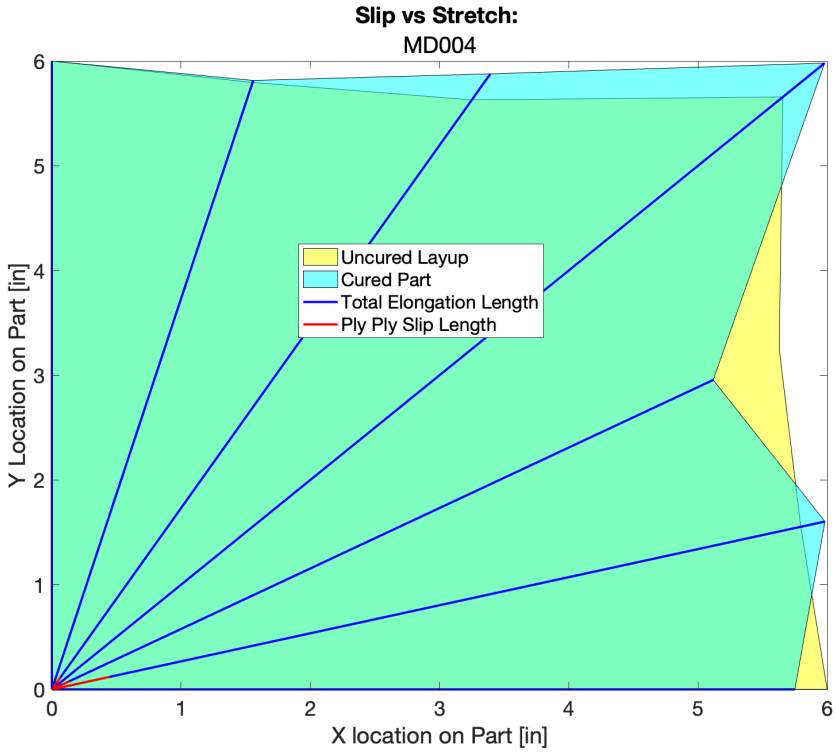


Figure 4.25: Stretch Broken Carbon Fiber MD004 Results: Stretch vs Slip

and forming depth for the Curved C-channel trials. When viewing the bridging scores, on average continuous carbon fiber tends to perform better than stretch broken. Two stretch broken tests, however, performed equivalently or better than the continuous carbon fiber, demonstrating that stretch broken carbon fiber can attain good bridging scores. Both stretch broken tests, part MD016 and part MD017, are from SBCF batch P0030 using 8552 resin and implement the method of preforming with an intensifier. This implies that the method of layup using an intensifier has significant impacts on the bridging data values. Trends like this also are seen in the forming depth score data. Continuous carbon fiber performs better for the forming depth metric than the stretch broken carbon fiber except for parts MD016 and MD017.

The corner thickening score plot in Figure 4.28 shows a metric where stretch broken

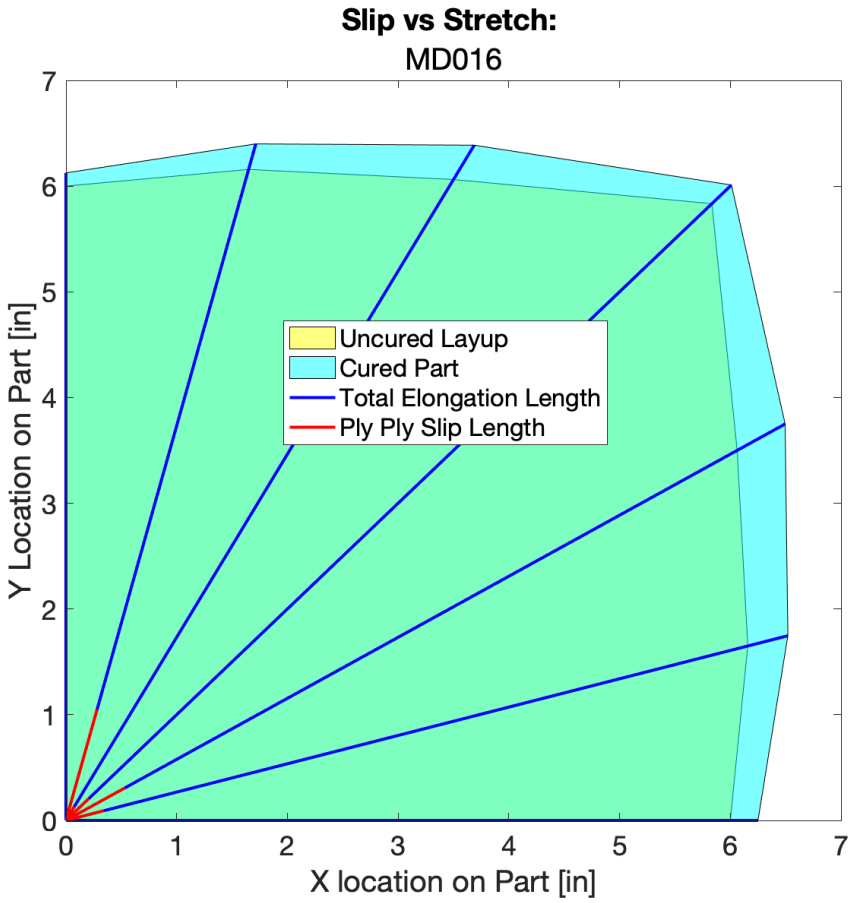


Figure 4.26: Stretch Broken Carbon Fiber MD016 Results: Stretch vs Slip

carbon fiber vastly outperforms the continuous carbon fiber. All the continuous carbon fiber trials score a 0, whereas all the stretch broken carbon fiber trials score either a 3 or a 4. The common corner thickening defect seems to have little impact on stretch broken carbon fiber. Corner thinning scores, however, tell a different story. In total the stretch broken carbon fiber and the continuous carbon fiber have similar results all ranging between scores of 0 and 3. This implies that corner thinning may be impacted by other factors outside of material selection.

Figure 4.29 displays the metric scores for resin pooling, texture, thickness variation, and wrinkling for the Curved C-channel trials. When viewing the resin pooling scores, stretch

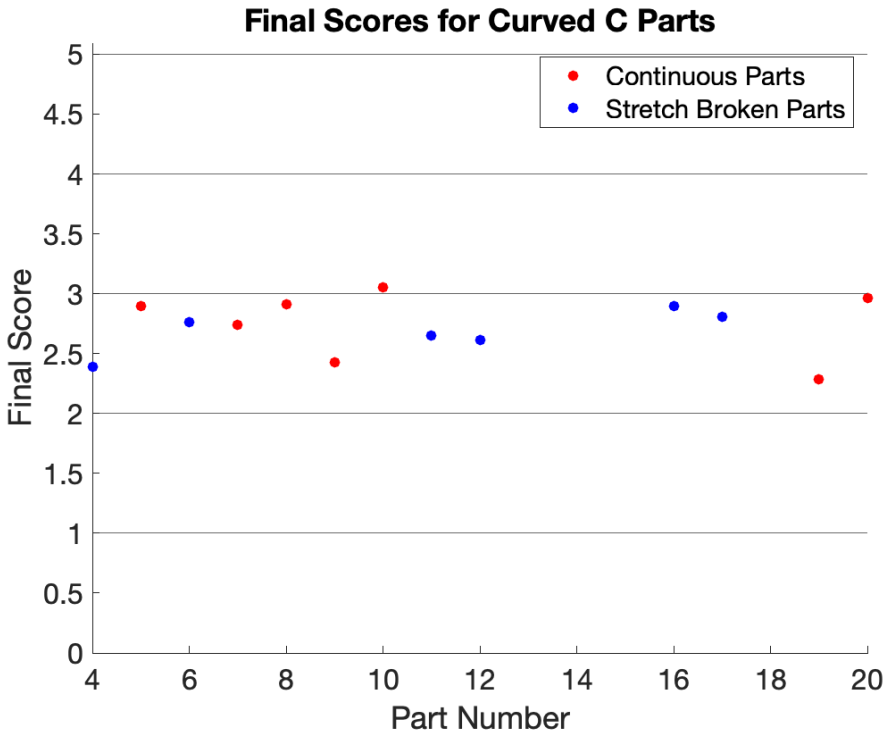


Figure 4.27: Final Forming Scores for all Curved C-channel Trials

broken carbon fiber is seen to outperform continuous carbon fiber for this metric. This is likely due to the manufacturing processes currently in place for prepregging MSU SBCF and the stages the resin goes through prior to the prepregging process.

The texture scores for both stretch broken carbon fiber and continuous carbon fiber are all within the 3.5 to 5 range, meaning that the parts display little texture defects. Continuous carbon fiber does outperform stretch broken carbon fiber for this metric, but not substantially. Stretch broken carbon fiber does tend to score lower on the fractures/shearing category of the texture metric. This is reasonable as the stretch broken carbon fiber prepreg is supplied in one inch tapes that have to be laid adjacent to each other during the layup process. Sometimes the intersection or slight separations between the tape strips are visible, hence causing this defect.

Thickness variation scores for both fiber types are comparative, earning scores of 2 or

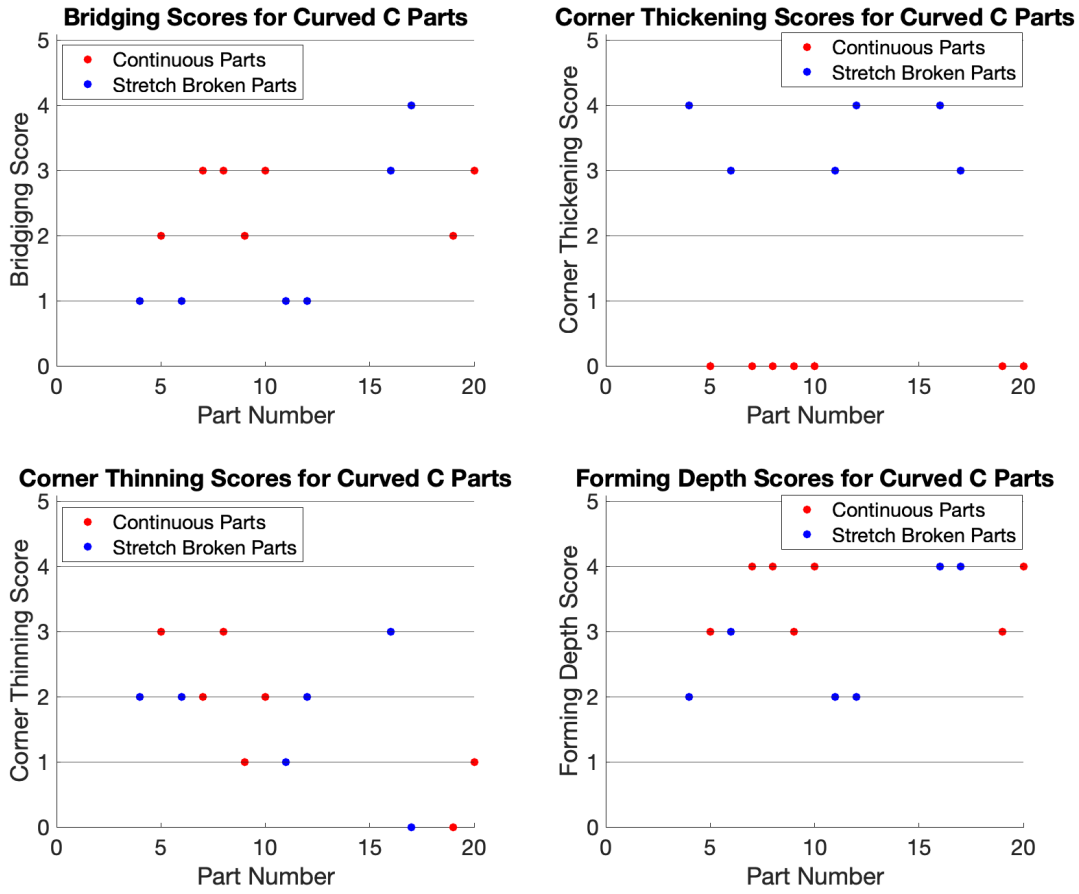


Figure 4.28: Metric Forming Scores for all Curved C-channel Trials: TOP LEFT - Bridging, TOP RIGHT - Corner Thickening, BOTTOM LEFT - Corner Thinning, BOTTOM RIGHT - Forming Depth

3 for all the Curved C-channel trials. The lower score of 2 is noticed to occur for both the previous trials presented that use intensifiers (continuous part MD010 and stretch broken part MD016). Slightly lower scores in thickness variation could be attributed to the use of an intensifier due to the forces applied by the intensifier on the material during the forming process.

Wrinkling scores tend to be higher for the continuous carbon fiber parts across all of the Curved C-channel tests. Since the stretch broken carbon fiber is thinner than the

continuous carbon fiber per ply, the final layup is thinner. This thinner layup has less compressive strength than the continuous carbon fiber layups, making it more susceptible to any compressive forces applied during the forming process. These forces cause the material to buckle and wrinkle in on itself. This provides a possible explanation for the lower wrinkling metric scores for stretch broken carbon fiber.

It is important to note that none of the scored Curved C-channel parts experience any splitting. An example of splitting for a Curved C-channel part that is not evaluated by the forming method is presented in Figure B.64 in Appendix B.

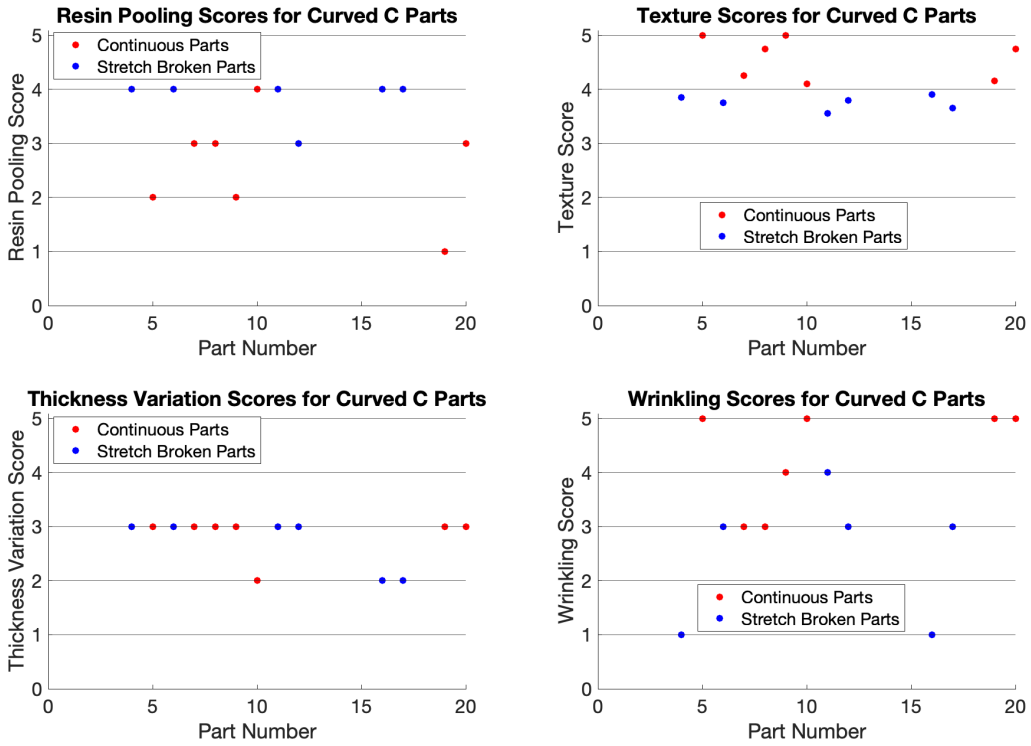


Figure 4.29: Metric Forming Scores for all Curved C-channel Trials: TOP LEFT - Resin Pooling, TOP RIGHT - Texture, BOTTOM LEFT - Thickness Variation, BOTTOM RIGHT - Wrinkling

Rounded Hat channel Results and Discussion

Continuous Carbon Fiber Results

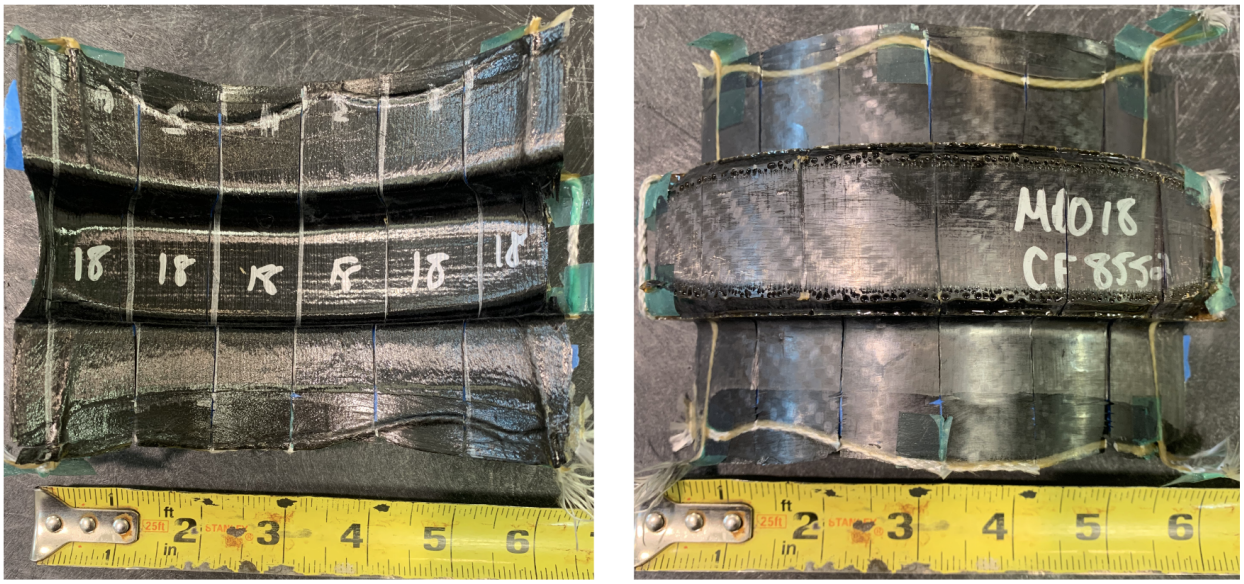


Figure 4.30: Continuous Carbon Fiber Rounded Hat channel Part MD018: LEFT - Top of Part, RIGHT - Bottom of Part

For the Rounded Hat channel continuous carbon fiber trial, Hexcel IM7/8552 prepreg was used (21; 22). This part, designated part MD018 seen in Figure 4.30, consists of four plies with a cross-ply layup of [0/90]s. The layup was cut in a rectangular shape with dimensions of 4 in [10.16 cm] by 6 in [15.24 cm]. The layup was applied ply by ply onto the Rounded Hat channel tool matching the curvature of the tool, but spanning the "gap" created by the hat cross-section. Breather strings were used on the edges of the laminate for edge breathing purposes. The cure cycle for this part involved a straight temperature ramp to 350°F [176°C] and dwelling for 120 minutes. Throughout the duration of the cure, pressures of 90 psi [620 KPa] were within the autoclave chamber. Figure 4.31 displays the corner thinning and corner thickening data for part MD018. For all measurement locations and radii, the part has an average corner thinning value of 87.70% of the average thickness

and an average corner thickening value of 140.31% of the average thickness. This earns part MD018 a corner thinning score of 2 and a corner thickening score of 0.

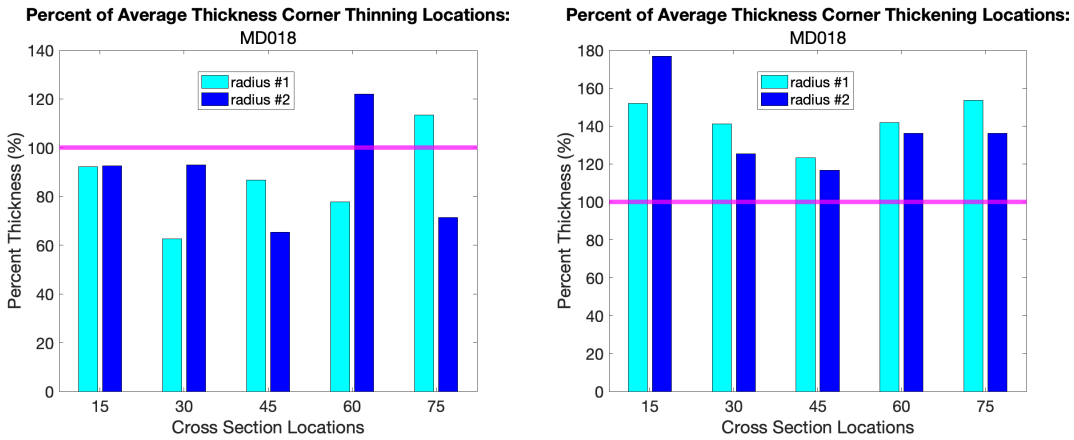


Figure 4.31: Continuous Carbon Fiber MD018 Results: LEFT - Corner Thinning (Average = 87.70%), RIGHT - Corner Thickening (Average = 140.31%)

Displayed in Figure 4.32 are the combined bridging and resin pooling data for part MD018. This part has an average bridging distance of $0.0631\,in$ $[0.1603\,cm]$ and a total resin pooling area of $0.00694\,in^2$ $[0.04477\,cm^2]$ averaged for all measurement locations and radii. This earns part MD018 a bridging score and resin pooling score of 3.

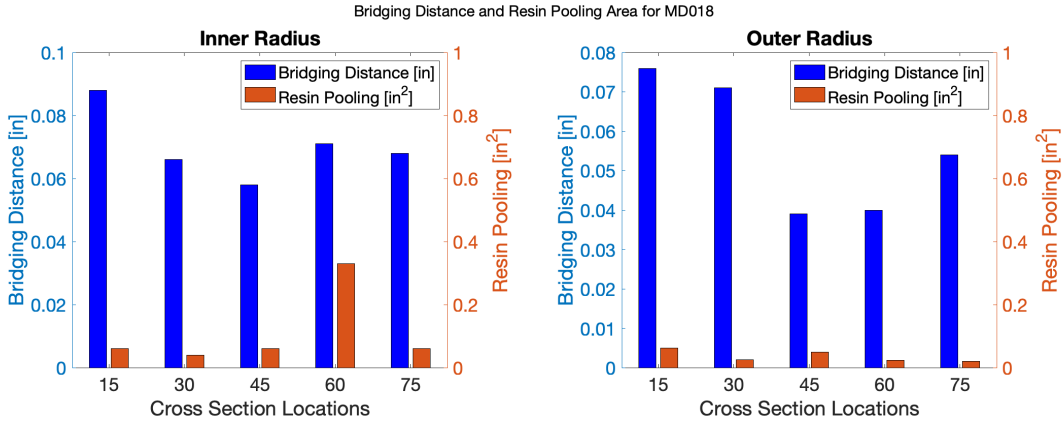


Figure 4.32: Continuous Carbon Fiber MD018 Results: Bridging (Average = $0.0631\,in$) and Resin Pooling (Total = $0.00694\,in^2$)

The thickness contour plots for continuous Rounded Hat channel part MD018 are presented in Figure 4.33. From the entire thickness measurement data set for this part the coefficient of variation is 0.1877. This value results in a thickness variation score of 3 for part MD018.

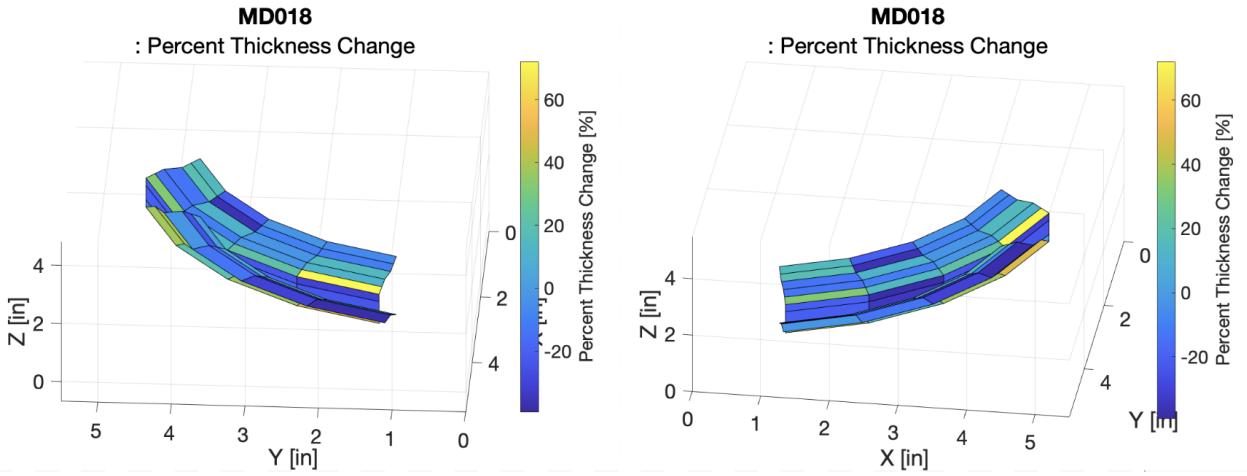


Figure 4.33: Continuous Carbon Fiber MD018 Results: Thickness Variation (Coefficient of Variation = 0.1877)

The forming depth data for Rounded Hat channel trial MD018 is displayed in Figure 4.34. For all measurement locations, the average forming depth is found to be 80.37%. This earns part MD018 a forming depth score of 3.

There is no wrinkling present on part MD018 in the non-critical region and the critical region. This earns Rounded Hat channel part MD018 a perfect score of 5 for wrinkling.

Table 4.10 presents the texture defect scores for part MD018. This part receives a perfect texture score of 5 as it presents no visual texture defects meaning that each individual texture metric receive scores of 5.

The combination of all the metric scores result in a final forming score of 3 for part MD018. The breakdown of the final score calculation as well as the additional defect scores are presented in Table 4.11.

Table 4.10: Continuous Carbon Fiber MD018: Texture Results

Metric	Weight	Ranking	Score
Hairiness	30%	5	-
Additional Resin Pooling	30%	5	-
Spaghettification	10%	5	-
Fractures/Shearing	15%	5	-
Pinholes	10%	5	-
Waves	5%	5	-
Total	100%	X	5

Table 4.11: Continuous Carbon Fiber MD018: Final Forming Score

Metric	Weight	Ranking	Score
Bridging	12.5%	3	-
Wrinkling	17.5%	5	-
Thickness Variation	15%	3	-
Forming Depth	12.5%	3	-
Corner Thinning	15%	2	-
Corner Thickening	10%	0	-
Resin Pooling	12.5%	3	-
Texture	5%	5	-
Total	100%	-	3

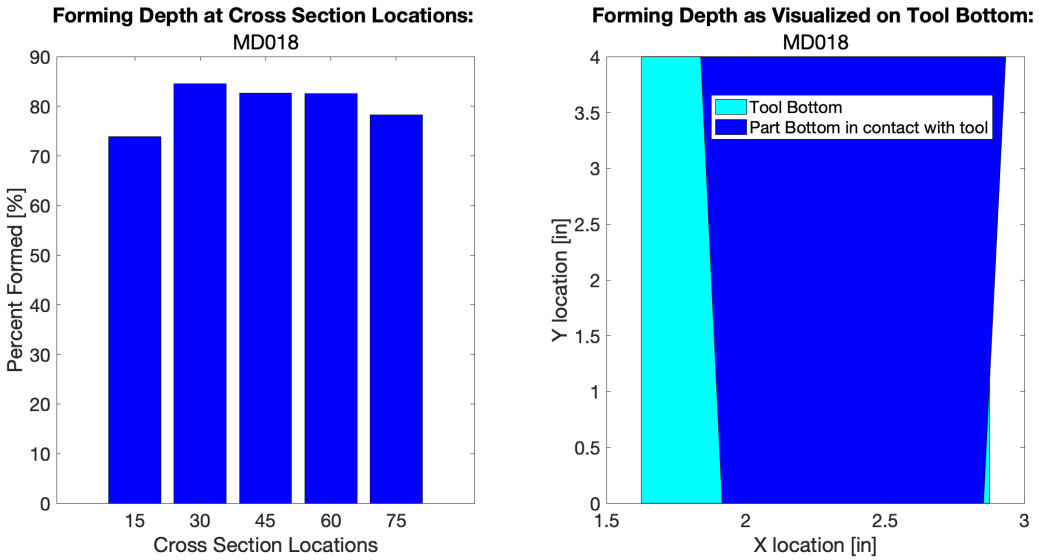


Figure 4.34: Continuous Carbon Fiber MD018 Results: Forming Depth (Average = 80.37%)

Stretch Broken Carbon Fiber Results

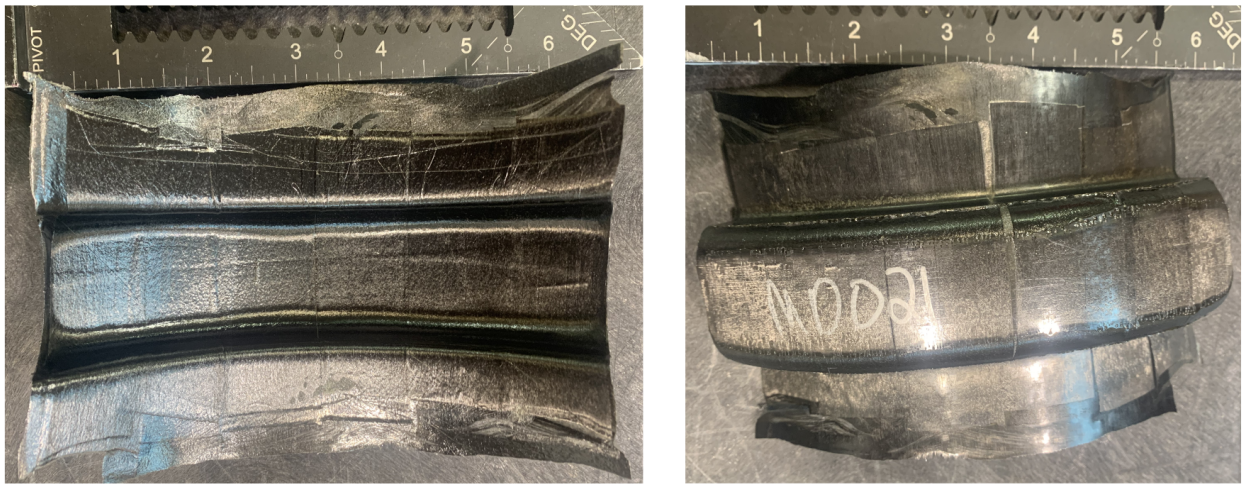


Figure 4.35: Stretch Broken Carbon Fiber Rounded Hat channel Part MD021: LEFT - Top of Part, RIGHT - Bottom of Part

For the Rounded Hat channel stretch broken carbon fiber trial, MSU SBCF/977-3 batch P0029 was the selected material, material data found in Appendix A (21; 23). The part, designated part MD021 seen in Figure 4.35, consists of three plies with a layup of [0/90/0].

The layup was cut in a rectangular shape with dimensions of $4in$ [$10.16cm$] by $6in$ [$15.24cm$]. The layup was applied to the Rounded Hat channel tool in a ply by ply manner that is curved to the tool geometry, but not molding into the hat cross-section curvatures. Breather strings were used on the edges of the laminate for edge breathing purposes. The cure cycle for this part started with a straight temperature ramp to 80°F [26°C] and dwelling for 30 minutes. Following this dwell, was a straight temperature ramp to 350°F [176°C] and a dwell for 6 hours. $90\,psi$ [$620\,KPa$] pressure was applied inside of the autoclave chamber for the entire run duration. The corner thinning and corner thickening data for this part can be seen in Figure 4.36. For all measurement locations and convex radii, the average corner thinning is 96.14% of the average thickness. For all measurement locations and concave radii, the average corner thickening is 150.93% of the average thickness. This earns stretch broken Rounded Hat channel part MD021 a corner thinning score of 3 and a corner thickening score of 0.

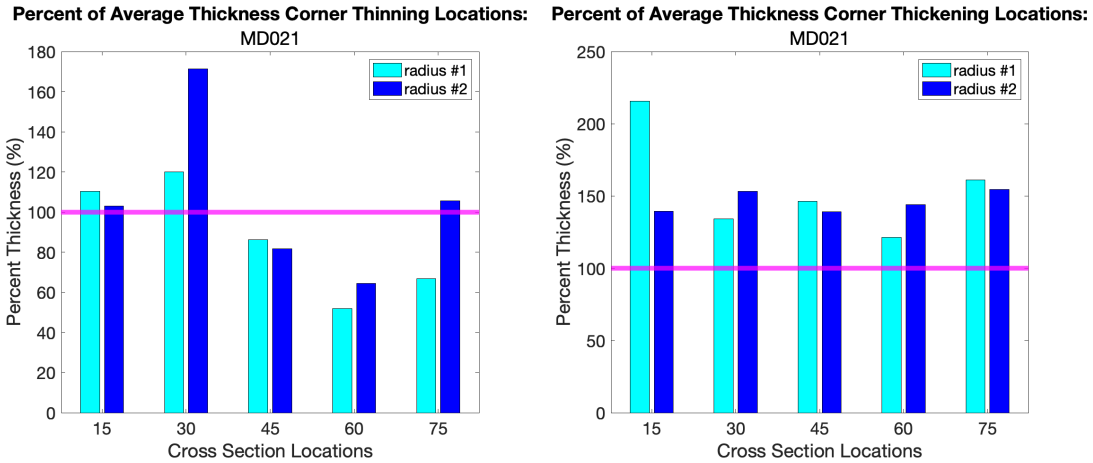


Figure 4.36: Stretch Broken Carbon Fiber MD021 Results: LEFT - Corner Thinning (Average = 96.14%), RIGHT - Corner Thickening (Average = 150.93%)

The combined bridging and resin pooling data for part MD021 is visualized in Figure 4.37. For all measurement locations and concave radii, this part has an average bridging distance of $0.0507\,in$ [$0.1288\,cm$] and a total resin pooling area of $0.00037\,in^2$ [$0.00239\,cm^2$].

These values result in a bridging score of 3 and a resin pooling score of 4 for stretch broken Rounded Hat channel part MD021.

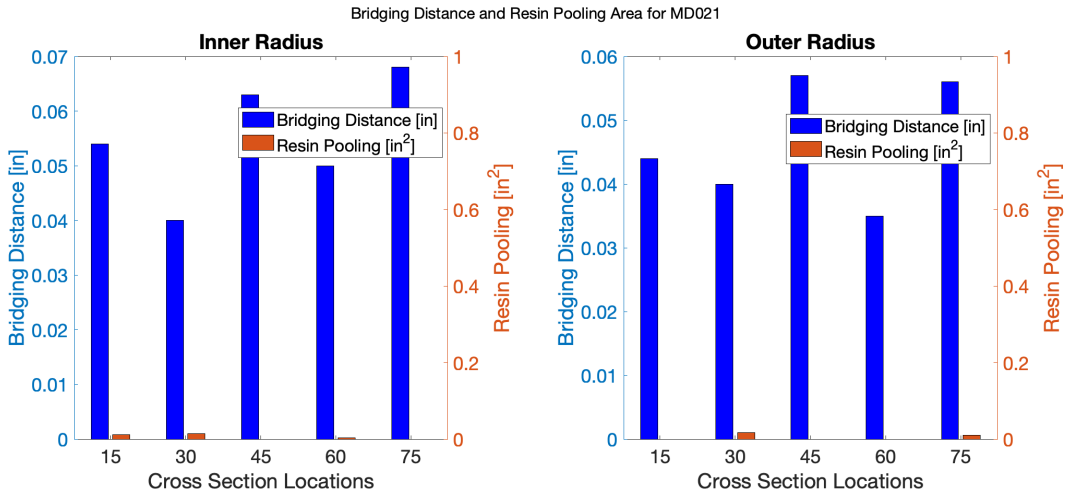


Figure 4.37: Stretch Broken Carbon Fiber MD021 Results: Bridging (Average = 0.0507 in) and Resin Pooling (Total = 0.00037 in^2)

Figure 4.38 presents the thickness contour plots for Rounded Hat channel part MD021. The coefficient of variation for all of the thickness measurements on the part is 0.2625 earning stretch broken part MD021 a thickness variation score of 2.

Figure 4.39 presents the forming depth data for part MD021. The average of all the measurements result in an average forming depth value of 83.18%. Stretch broken Rounded Hat channel part MD021 thus earns a forming depth score of 3.

Like the other Rounded Hat channel part, part MD021 also has no wrinkling present at any location on the part. This earns stretch broken part MD021 a perfect wrinkling score of 5.

The texture defect scores for part stretch broken part MD021 are seen in Table 4.12. This part receives a score of 5 for the hairiness, spaghettification, fractures/shearing, pinholes, and waves categories as these defects are not present on the part. This part does, however, have very minimal amounts of resin pooling at the outer edges of the part earning

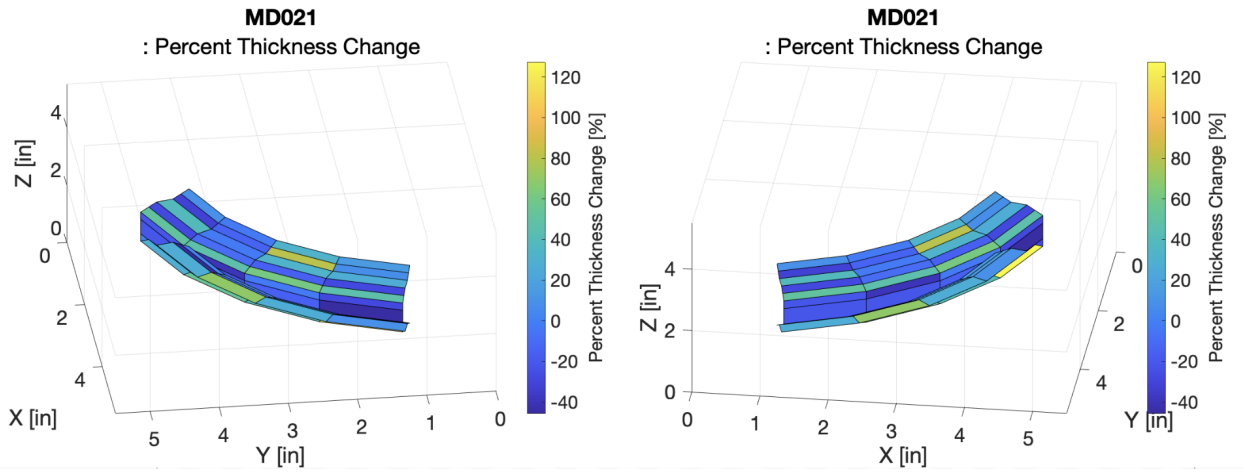


Figure 4.38: Stretch Broken Carbon Fiber MD021 Results: Thickness Variation (Coefficient of Variation = 0.2625)

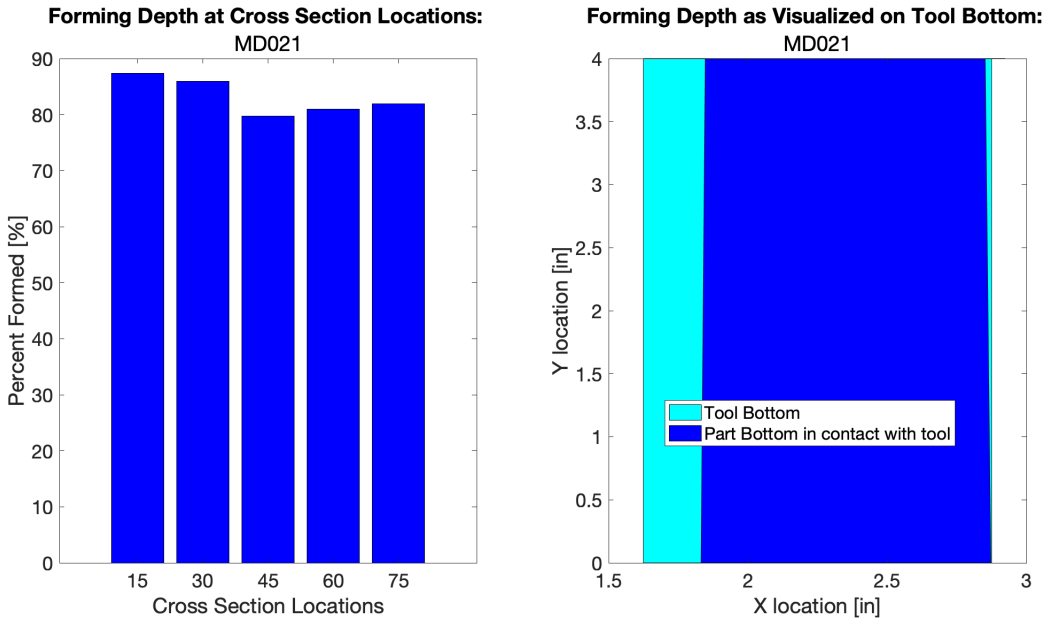


Figure 4.39: Stretch Broken Carbon Fiber MD021 Results: Forming Depth (Average = 83.18%)

a score of 4 for this defect. In total, the final texture score for stretch broken Rounded Hat channel part MD021 is 4.7.

The combined metric scores and final scores for part MD021 are tabulated in Table

Table 4.12: Stretch Broken Carbon Fiber MD021: Texture Results

Metric	Weight	Ranking	Score
Hairiness	30%	5	-
Additional Resin Pooling	30%	4	-
Spaghettification	10%	5	-
Fractures/Shearing	15%	5	-
Pinholes	10%	5	-
Waves	5%	5	-
Total	100%	X	4.7

4.13. The final forming score for the stretch broken Rounded Hat channel part is 3.14.

Table 4.13: Stretch Broken Carbon Fiber MD021: Final Forming Score

Metric	Weight	Ranking	Score
Bridging	12.5%	3	-
Wrinkling	17.5%	5	-
Thickness Variation	15%	2	-
Forming Depth	12.5%	3	-
Corner Thinning	15%	3	-
Corner Thickening	10%	0	-
Resin Pooling	12.5%	4	-
Texture	5%	4.7	-
Total	100%	-	3.14

Rounded Hat channel Discussion

A summary of the Rounded Hat channel trial results is seen in Table 4.14. Each trial experiences similar values for the different scoring metrics. The stretch broken carbon fiber, in this case, outperforms the continuous carbon fiber in the corner thinning and resin

Table 4.14: Summary of Rounded Hat channel Results

	MD018	**MD021**
Material	CF	SBCF
Plies	4	3
Intermediate Dwell	No	Yes
Intensifier	No	No
Layup Shape	Rectangle	Rectangle
Scores		
Bridging	3	3
Wrinkling	5	5
Thickness Variation	3	2
Forming Depth	3	3
Corner Thinning	2	3
Corner Thickening	0	0
Resin Pooling	3	4
Texture	5	4.7
Final Score	3	3.14

pooling categories. The corner thinning log rolling effect is present for each part, however the continuous carbon fiber does thin more. For the Rounded Hat channel trials, resin pooling scores seem to improve from the Curved C-channel trials for the continuous carbon fiber material.

Neither of the Rounded Hat channel parts have any wrinkling present, each earning a score of 5. This indicates that the part geometry plays a big factor in the performance of different metrics. The absence of wrinkling is mostly due to the geometric nature of the tool in that the required forces to form into the mold are entirely tensile.

Each part (MD018 and MD021) receive a bridging score and a forming depth score of 3. Seen in Figure 4.40 is the stretching versus slipping results for continuous part MD018. This part experiences large amounts of ply-ply slippage to help it form into the mold. Figure 4.41 displays the stretching versus slipping results for stretch broken part MD021. This part has far less ply-ply slippage, but still has an overall elongation to contribute to the bridging and forming depth scores. This implies the forming mechanism of stretching is present, attainable only for stretch broken carbon fiber.

The corner thickening scores for the Rounded Hat channel parts are both 0. In the Curved C-channel parts, stretch broken carbon fiber vastly outperforms continuous carbon fiber for the corner thickening metric. This is not the case for the Rounded Hat channel trials, alluding to mold design having an effect on corner thickening as well.

Sinusoidal C-channel Results and Discussion

Continuous Carbon Fiber Results

The Sinusoidal C-channel results presented below are from part MD022, and the part images are displayed in Figure 4.42. This part was constructed with continuous carbon fiber Hexcel IM7/8552 prepreg (21; 22). This part consists of 3 plies with a layup of [90/0/90]. As the tool for this part is a positive male mold, the plies were wrapped directly around the

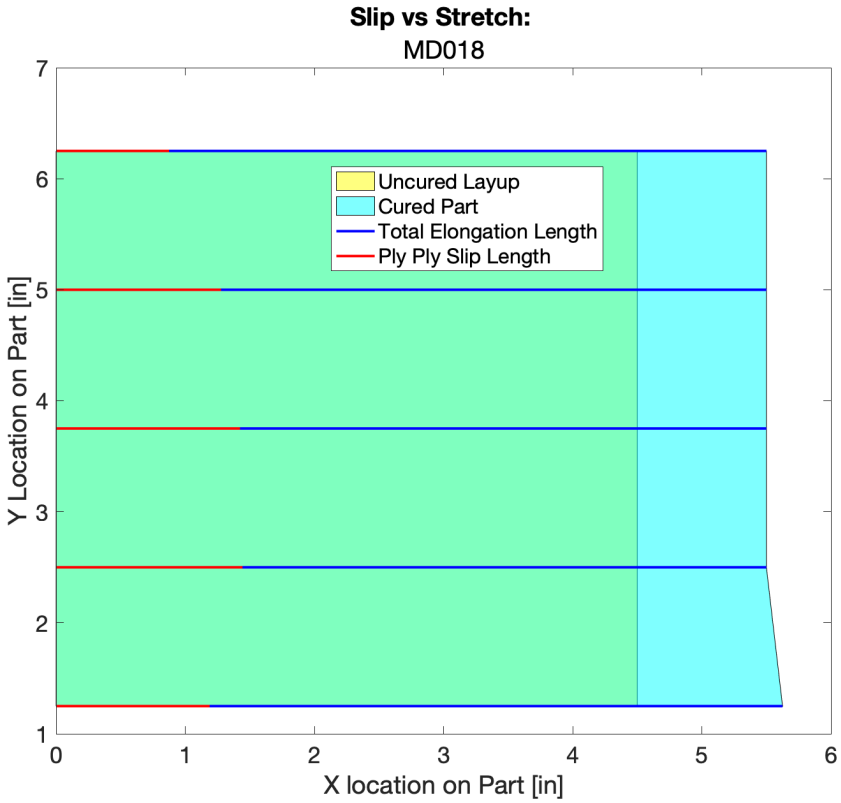


Figure 4.40: Continuous Carbon Fiber MD018 Results: Stretch vs Slip

mold. During the layup process, the plies were darted and cut to allow for easier wrapping around the mold. The cure cycle for this part involved a straight temperature ramp to 350°F [176°C] and dwelling for 120 minutes. Throughout the duration of the cure, 90 psi [620 KPa] pressure was applied within the autoclave chamber. Unfortunately, midway through the cure cycle vacuum was lost within the vacuum bag due to an autoclave error. The corner thinning and corner thickening results for this part can be seen in Figure 4.43. For all measurement locations and radii, Sinusoidal C-channel part MD022 has an average corner thinning value of 73.97% of the average thickness and an average corner thickening value of 168.58% of the average thickness. These values are both outside of the acceptable bounds for the metrics resulting in a score of 0 for both corner thinning and corner thickening.

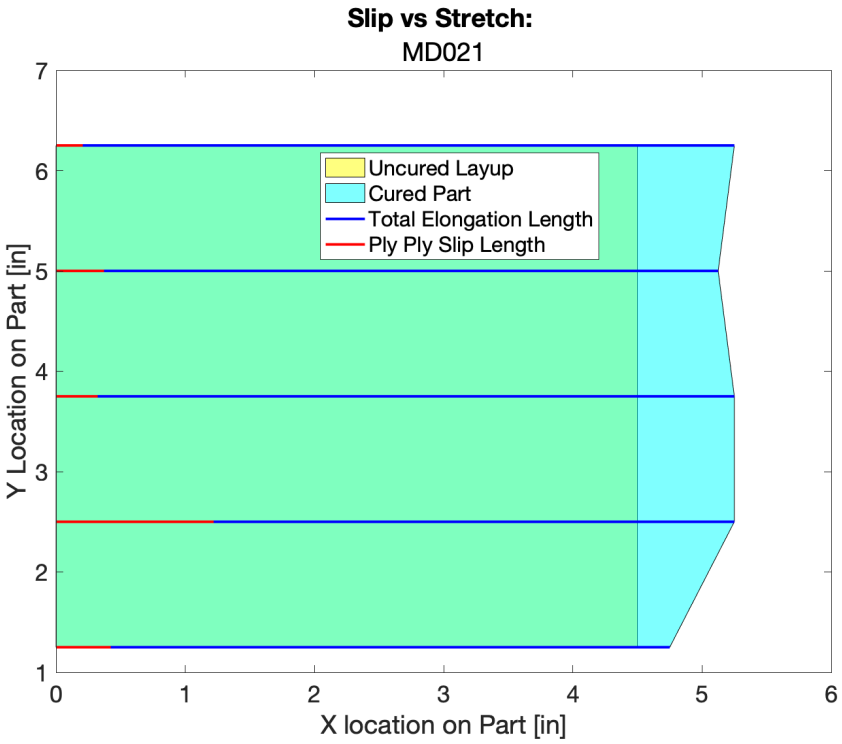


Figure 4.41: Stretch Broken Carbon Fiber MD021 Results: Stretch vs Slip

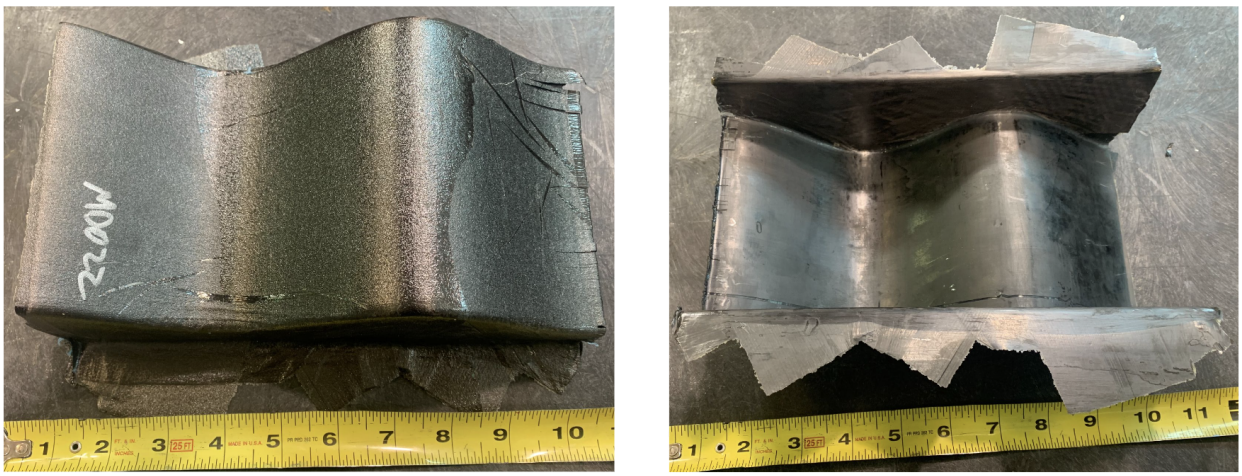


Figure 4.42: Continuous Carbon Fiber Sinusoidal C-channel Part MD022: LEFT - Top of Part, RIGHT - Bottom of Part

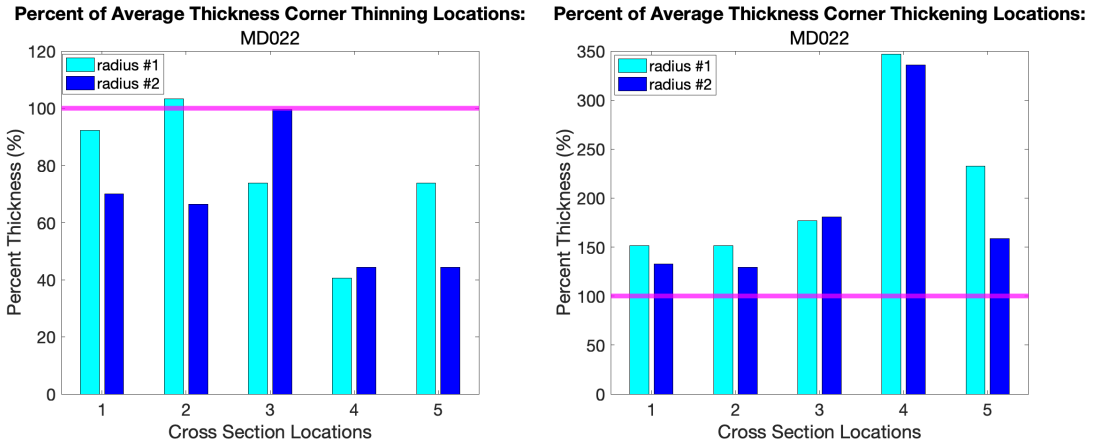


Figure 4.43: Continuous Carbon Fiber MD022 Results: LEFT - Corner Thinning (Average = 73.97%), RIGHT - Corner Thickening (Average = 168.58%)

After measuring part MD022 and processing the data, there is no bridging or resin pooling within the concave corners. This earns continuous Sinusoidal C-channel part MD022 scores of 5 for bridging and resin pooling.

Figure 4.44 displays the thickness contour plot for part MD022. Computing the coefficient of variation for all the thickness measurements from the part results in a value of 0.3932. This value earns continuous part MD022 a thickness variation score of 2.

The wrinkling data for part MD022 is displayed in Figure 4.45. Since the entire region of the part is deemed as a critical region, the total wrinkling amount and the total wrinkling within the critical region are equivalent. Both measurements receive a wrinkle area percent of 3.04%. This results in a final wrinkling score of 0 for Sinusoidal C-channel part MD022.

In Table 4.15 are the texture scoring results for continuous part MD022. For the hairiness, spaghettification, and pinholes defects, this part receives a score of 5 as these defects are not present on the part. The additional resin pooling category earns a score of 4 as there are minute amounts of resin pooling along the wrinkle edges of the part. There are fractures/shearing present within the critical regions of the part, resulting in a score of 0 for this defect. Also receiving a score of 0 is the waves category. Waves are observed around the

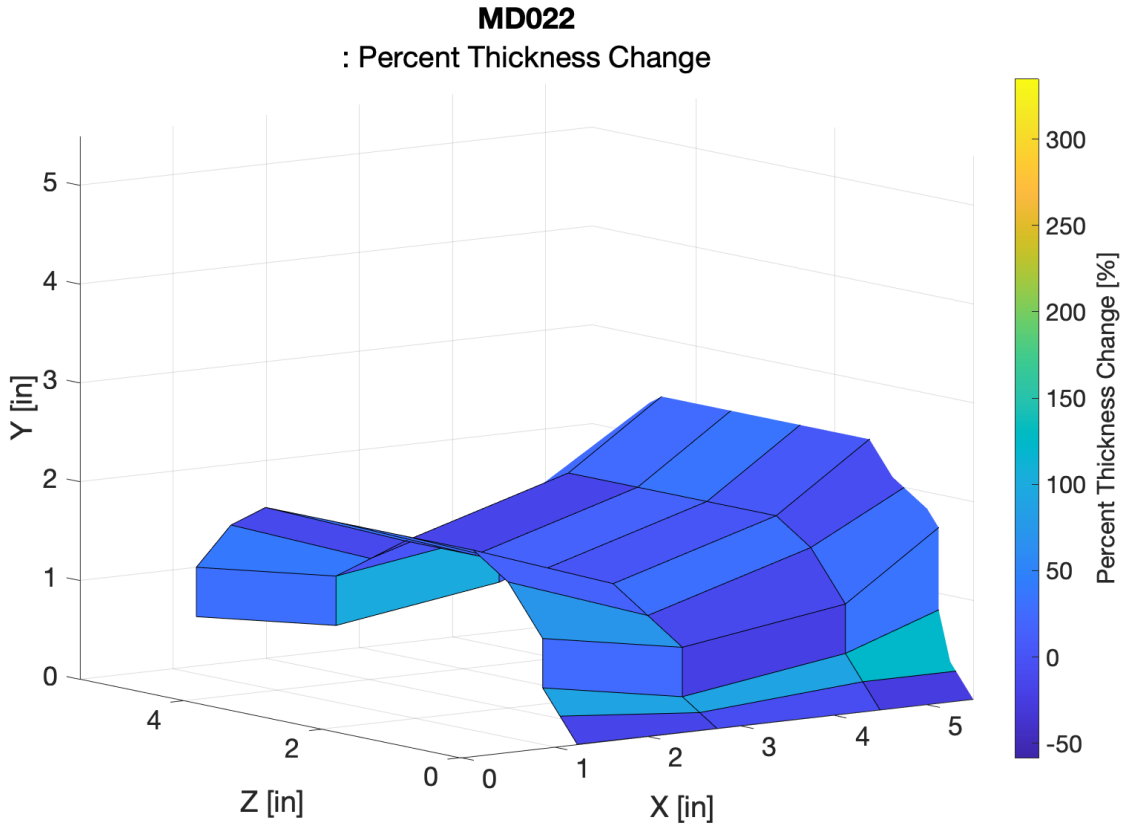


Figure 4.44: Continuous Carbon Fiber MD022 Results: Thickness Variation (Coefficient of Variation = 0.3932)

sinusoidal corners of the part. The combination of all these defect scores results in a final texture score of 3.7 for part MD022.

The final forming score and total metric score values are seen in Table 4.16 for Sinusoidal C-channel part MD022. As this part is molded using positive male tooling, the forming depth metric does not apply in this scenario. The forming depth metric weight is then consequently divided and split evenly between the remaining metrics. Compiling all the metric scores, continuous Sinusoidal C-channel part MD022 earns a final forming score of 2.

Table 4.15: Continuous Carbon Fiber MD022: Texture Results

Metric	Weight	Ranking	Score
Hairiness	30%	5	-
Additional Resin Pooling	30%	4	-
Spaghettification	10%	5	-
Fractures/Shearing	15%	0	-
Pinholes	10%	5	-
Waves	5%	0	-
Total	100%	X	3.7

Table 4.16: Continuous Carbon Fiber MD022: Final Forming Score

Metric	Weight	Ranking	Score
Bridging	14%	5	-
Wrinkling	19.25%	0	-
Thickness Variation	17%	2	-
Forming Depth	-%	-	-
Corner Thinning	17%	0	-
Corner Thickening	11.75%	0	-
Resin Pooling	14.25%	5	-
Texture	6.75%	3.7	-
Total	100%	-	2

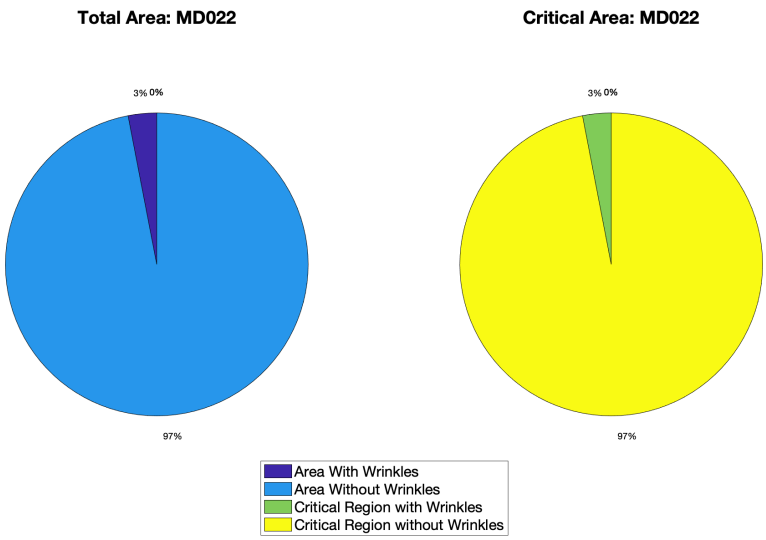


Figure 4.45: Continuous Carbon Fiber MD022 Results: Wrinkling (Total Wrinkling and Critical Region Wrinkling = 3.04%)

Sinusoidal C-channel Discussion

Unlike the other two mold types (Curved C-channel and Rounded Hat channel), the Sinusoidal C-channel mold type is entirely a positive mold that the carbon fiber must wrap around instead of drawing into. Due to the complex nature of the feature combined with the positive molding, wrinkling is very likely to occur as there are many areas in which the layup experiences compressive forces during the forming process. Figure 4.46 displays the stretching versus slipping results for Sinusoidal C-channel part MD022. The cyan region on the part shows that the material effectively shrunk in length in most of the locations which correlates with the wrinkling amounts seen on the part. The red lines prove that ply-ply slippage occurred during the forming process, which lengthens the laminate and results in higher wrinkling amounts.

This mold design, however, seems to allow for higher bridging scores as the material needs to wrap into the concave corners as opposed to drawing into the concave corners.

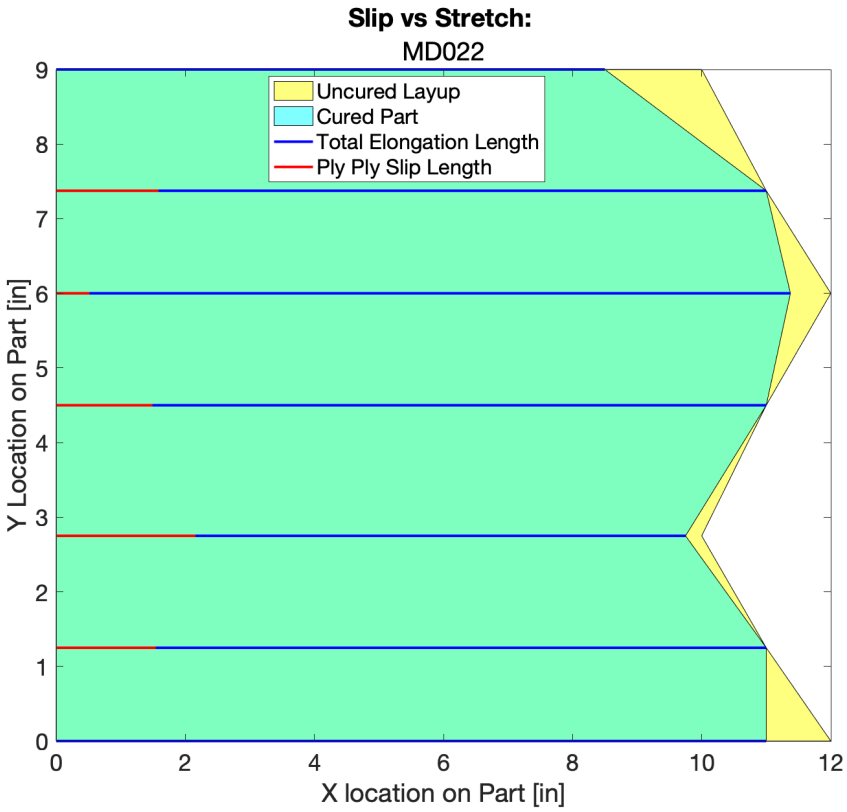


Figure 4.46: Continuous Carbon Fiber MD022 Results: Stretch vs Slip

This feature also helps prevent resin pooling within the concave corner regions since there remains no space for the resin to draw into as the material itself matches the concave corner geometry.

Mostly unchanged from the different part trials for continuous carbon fiber are the corner thickening and texture metrics. While the Sinusoidal C-channel in early trials seem to negate bridging and corner resin pooling, corner thickening still has a score of 0. Part MD022 does display nearly 70% thickening in the concave corner regions which is like continuous Curved C-channel part MD010. The texture defect score of 3.7 is predominately negatively impacted by the fractures/shearing defect and the waves defect. These defects seemingly appear randomly between part type and material but are likely indicators of the layup

method and demolding process. As this part is laid up around a sinusoidal curvature, waves are to be expected.

The corner thinning for this part is lower than the typical corner thinning score for all part types and materials, however it is not outside the bounds of results from the previous parts presented. As this mold type has similar convex corner features to the other molds as well as the test material choice of continuous carbon fiber, a low corner thinning score is unsurprising.

METHOD PERFORMANCE DISCUSSION

The method developed for the analysis of complex carbon fiber parts has consistently produced forming scores in the 1.5 to 3.5 range. As a score of 5 indicates a flawless part with no defects present, these resulting scores are representative of the material performance and manufacturing processes used during these trials. The span of the scores also indicate that the individual metric scoring tolerances are not too strict, allowing for a range of acceptable values that many of the trials scored within. The method also encapsulates a wide range of forming defects that vary between mold design as well as material type. This allows the user to understand how to improve mold design, the material manufacturing process, the layup method, and the cure cycle selection process.

The Curved C-channel trials are used to develop the method for evaluating forming. It is because of this, that the method applies perfectly to this mold type. The method has consistently produced results for all the various metrics and final forming scores for the Curved C-channel tests. These results are informative for how to improve the MSU SBCF material so that it effectively scores higher on the metrics. It also signifies the importance of how different layup practices and slight variations in cure cycle effect the final outcome of the part.

The Rounded Hat channel trials are used to test the method's application to similarly designed parts as the Curved C-channel. Both the Curved C-channel and the Rounded Hat channel have a C/Hat cross-section featuring concave and convex corner geometry. These tools both feature negative mold design for the material to draw into. The only difference between these mold designs is the axis of curvature with respect to the C/Hat cross-section. Due to the similarities between these mold designs, the method also applies flawlessly to the Rounded Hat channel trials. The method allows the users to compare slight differences in mold design to forming results of the part.

The Sinusoidal C-channel trials are used to test the method's application to more complex part designs. Through these trials, it is learned that not all metrics apply to all mold types. The forming depth metric, for example, does not apply to positive moldings, but does apply to negative moldings. For the purposes of using the method, it is very simple to remove a metric from the weighted matrix if it does not apply to the mold type. This implies that as other mold designs are introduced and tested, additional metrics could be added to the method for personalized forming evaluations. The Sinusoidal C-channel trials prove that the method is adaptable to different part geometries.

The original requirements for the method are that it must be primarily quantitative, repeatable, account for most carbon fiber forming defects, account for geometry discrepancies between the design and formed part, and be represented as an overall "Forming Score". This method is primarily quantitative and evaluates the qualitative aspect of texture defect in a numerical way. Repeatability for this method is defined as well documented, timely, and easily applied to multiple part geometries. This method is thoroughly documented both within this thesis and a shared folder within the program. The current method has room for improvement on measurement efficiency. The incorporation of a flatbed scanner greatly speeds up the process of data collection but could be further increased by introducing automation processes. This method is easily applied to multiple part geometries tested as it is adaptable, proven by the Sinusoidal C-channel trials. Though the current trials suggest that the method is repeatable, further analyses must be performed to accurately assess for repeatability. Overall, the method accounts for eight total carbon fiber defects with the texture metric accounting for six additional texture defects. However, the method does allow room for the addition of other metrics if the user so chooses. The method specifically accounts for geometry discrepancies between the design and the formed part by using the forming depth and bridging metrics. Additionally, as the original, ideal design for each geometric part type would receive a score of 5, any score the formed part achieves does

account for discrepancies from the ideal part. Finally, the method must be represented as an overall "Forming Score" which it has for every trial presented.

CONCLUSIONS

The forming evaluation method meets the initial goals set in the Introduction section. The method's adaptability allows for its application to future part geometries and mold designs. The method also allows for an overarching study of how different process variables and material choices directly impact the forming quality of a carbon fiber part. These process variables include the MSU SBCF manufacturing process, the layup specifics (ie: shape, orientation, and curvatures), the use of an intensifier, and the cure cycle parameters (*i.e.*: temperatures, pressures, and intermediate dwells). The method's ability to adequately account for the different defects further can provide supporting explanations for the process variable impacts. Finally, the stretch versus strain metric provides valuable insight into the forming mechanisms present, specifically stretching for MSU SBCF. Stretching for stretch broken carbon fiber is observed for many of the tests, but minimally. Using the method to study how to exploit certain forming mechanisms will be fundamental in establishing processing parameters that enable the advantages of stretch broken carbon fiber.

Preliminary use of this forming evaluation method generated a range of results for the different process variables, mold types, and materials. For the Curved C-channel mold specifically, stretch broken carbon fiber could be improved for the bridging, forming depth, corner thinning, and wrinkling metrics. However, material type is not the only factor affecting metric performance. The mold design also plays a large role in the metrics present. While stretch broken carbon fiber tends to wrinkle on the Curved C-channel mold, it exhibits no such wrinkling on the Rounded Hat channel mold. Continuous carbon fiber when formed into the Curved C-channel and Rounded Hat channel molds does not significantly wrinkle but achieved unacceptable levels of wrinkling for the Sinusoidal C-Channel mold type. Not only do geometric features affect metric performance; the use of a negative mold to draw into versus a positive mold to wrap over affects the amounts of certain defects. Mold design

also plays a part in the forming mechanisms present, and future designs can be adapted from the ones presented above to exploit the different mechanisms. Overall, the preliminary trials give indications as to where the stretch broken carbon fiber process as well as the mold designs can be improved.

FUTURE WORK RECOMMENDATIONS

There are many future work recommendations for the forming evaluation method. Firstly, would be to close the loop on the input versus output data. This method provides a system for tracking the quantity and location of defects for a given part. A rigid test matrix could be applied to test how certain processing parameters impact the presence of certain defects. These processing parameters, or input variables, could include: material type, layup orientation/pattern, layup size, layup shape, method of laying up the material, use of an intensifier, bagging procedure, positive or negative mold type, and cure cycle parameters. A test matrix could choose any combination of these input variables as a baseline. From there, the testing matrix should adjust one variable at a time with the forming evaluation method applied after curing to track the presence of defects for each adjusted variable. This would help generate a feedback loop for the impact of various input variables.

The second recommendation would be to include additional metrics. When viewing the scanned cross-sections of the various parts, voided areas can be seen. An example of one such voided region is presented in Figure 7.1. Voids are due to poor compaction between the carbon fiber plies. Figure 7.1 is unfocused in the magnified view, and increasing the scanning quality could allow for void content analyses similar to how Centea *et al.* performed with microscopy (28). Additional image analysis could be performed on the cross-sectional scans to either understand the total void content or at the very least the locations of voids within the material. A color picker tool could be used in image analysis to find locations and areas of similar voided regions to the example portrayed in Figure 7.1. Another option for void analysis is to measure the voided region similarly to how the resin pooling areas are measured. This option would be time consuming, but would also be simpler to implement. Void analysis was not chosen for this study due to the processing time required for microscope imaging and sample preparation. Additionally, many of the metrics either cause voids or are

caused by voids, therefore accounting for voidage in the ranking. The addition of the void analysis metric would allow for a more thorough analysis of forming quality as certain void percentages are cause for part rejection.

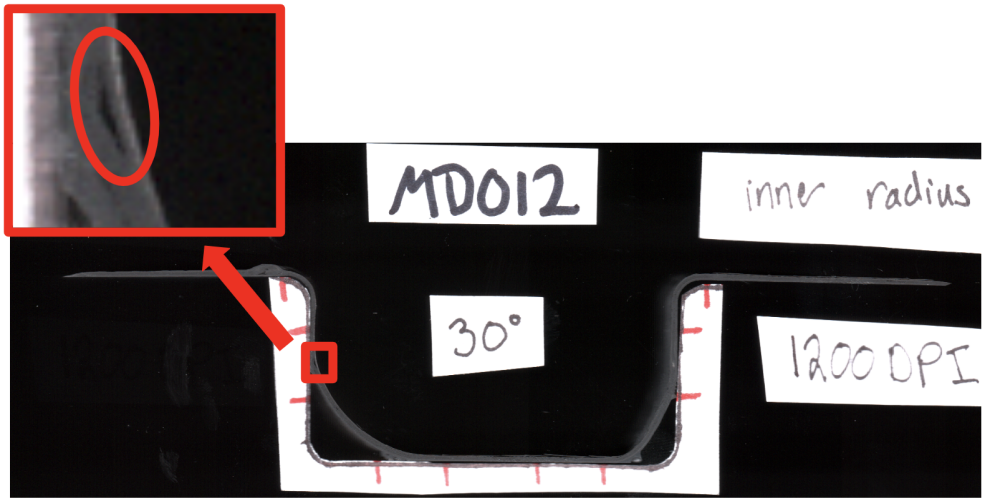


Figure 7.1: Void on Cross-Sectional Scan: Red boxed region shows zoomed in view of the area with a void detected on a cross-sectional scan of a stretch broken carbon fiber curved C-channel

Another metric to be considered is springback. Mujahid *et al.* and Beglinger each explored the amount of springback and how to decrease it with different forming processes (30; 33). Springback is observed with the naked eye during the Sinusoidal C-channel tests, but could also have been present with the Curved C-Channel and Rounded Hat channel trials. Evaluating this defect could provide another valuable metric of study when analyzing forming quality as springback results in deviations from the original geometric design of the part. A schematic for how to measure sprinback is presented in Figure 7.2. Figure 7.2 displays the before and after approximations of a carbon fiber part once it is removed from a mold. The blue arrows indicate where length measurements should be taken to determine the deviation from the model geometry. These measurements could simply be taken within the cross-sectional scans by using ImageJ and placing a line at the intended

locations. If springback is severe, it results in large variations from the original design which has consequences as the strengths of the part are no longer in the intended direction or location.

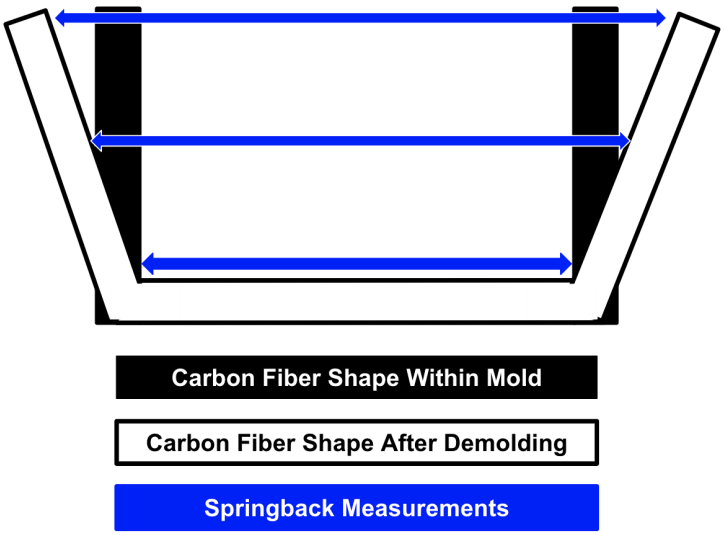


Figure 7.2: Springback Measurement Schematic: Black boxes shows carbon fiber laminate while still within the mold, White boxes show carbon fiber laminate after removing from the mold, Blue arrows indicate assigned length measurement locations

The next area for future work on the forming evaluation method is measurement and computation time. Automating the measurement process for some, if not all, of the metrics would greatly improve the efficiency and accuracy of this method. Developing an image analysis function within Matlab could generate all the measurements with little input from the user. Binary images scans could be used to generate a complete thickness profile across the part cross-section without relying on the user to place thickness lines. Color picker tools could be used to find regions of resin pooling and determine the area of such locations. Defects such as bridging, forming depth, and springback are more difficult to automate, but with some inputs from the user, MatLab could generate values for these defects as well. These measurements could also be accounted for by the use of a 3D scanner. This scan

could be directly compared to an ideal model of the part to compare for differences, which would account for the bridging, forming depth, and springback defects. The use of a 3D scanner could also determine thickness discrepancies between the model and the formed part if the scanning quality is high enough. Most 3D scanners allow the user to compare a scanned object to a model in computer-aided design software. The use of only a 3D scanner would improve the scanning time as it would take one scan as opposed to the current five scans. The recommendation, though, is to combine the use of MatLab automation and 3D scanning to result in more accurate and consistent measurements per multiple users. Intra-repeatability testing should take place for all current and future measurement systems to assure repeatability of the method for multiple users.

Another area for future work is to apply the method to other geometric part types. While the method does apply rather well to C-channel and C-channel adjacent geometries, the method could be applied to other geometric types. Some possible options for future cross-sections are presented in Figure 7.3. Certain metrics may not apply to all part types. For example, the bead cross-section metrics of bridging and forming depth are equivalent, so removing one of these would suffice for adjusting the metrics. Some parts may need new metrics applied such as the square tube cross-section which would require an angular version of the springback measurement to ensure the final shape is a square as a opposed to a rhombus. The method is designed to account for part geometries with more than two concave or convex radii, but it should be noted that cross-sections such as the I-beam could have four convex corners. The general rule for applying the method to various geometries is to remove metrics that do not apply and add those that do. By selecting only the metrics that correlate to the part type, a personalized forming evaluation can be applied.

Finally, future works needs to take place on the metric weight assignments. In order to refine the metric weights and ranks, complex parts, such as the curved C-channel, could be formed specifically to include certain defects. These parts with known defects could

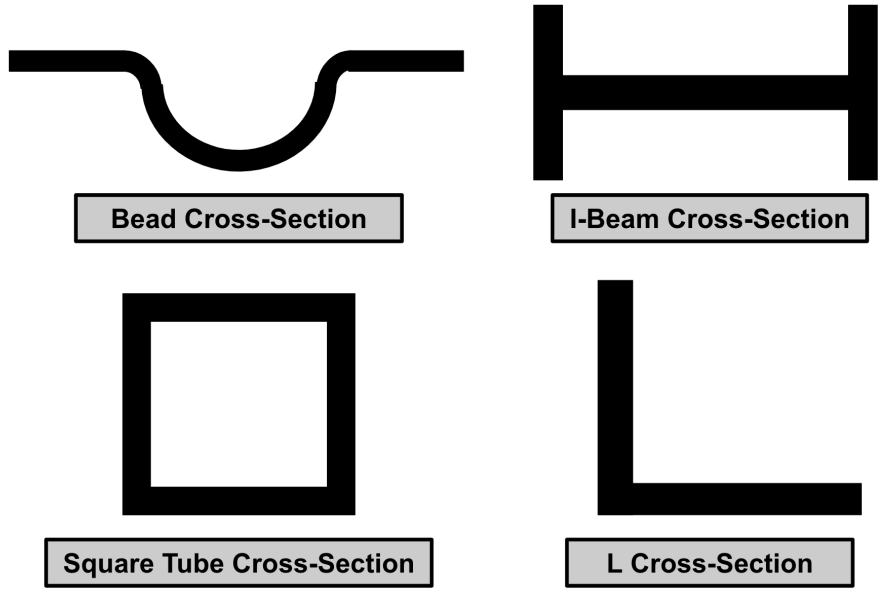


Figure 7.3: Other Cross-Sections for Consideration: TOP LEFT - Bead cross-section, TOP RIGHT - I-Beam cross-section, BOTTOM LEFT - Square Tube cross-section, BOTTOM RIGHT - L cross-section

be strength tested to determine how the presence and location of certain defects affect the overall performance of the part. The overall strength results could then be used to asses which defects have the highest impacts on performance and forming quality, and thus be assigned the highest weights. This strength testing as well as research on current acceptability criteria could allow for the rankings to be adjusted. Current acceptability criteria research could also allow for certain scores within the ranking schema to be assigned with acceptable or unacceptable levels of the defect.

REFERENCES CITED

[1] J. D. Anderson and M. L. Bowden, *Introduction to flight*. McGraw-Hill, 2022.

[2] H. JEX and F. CULICK, "Flight control dynamics of the 1903 wright flyer," *12th Atmospheric Flight Mechanics Conference*, 1985.

[3] E. J. Barbero, *Introduction to composite materials design*. CRC Press Taylor amp; Francis Group, 2018.

[4] W. D. Callister and D. G. Rethwisch, *Materials science and engineering: An introduction*. John Wiley and Sons Australia, Ltd, 2021.

[5] "Metal forming process: What are the basics?: Quest-tech." `https://questtech.ca/blog/basics-of-the-metal-forming-process/`, Sep 2021.

[6] D. F. Dreese, G. P. Dillon, D. B. Wess, editor = Rachau, Christopher L and Stiver, Donald HEditors, and K. L. Koudela, "Testing and analysis of stretch broken carbon fiber (sbcf) stiffened panels subjected to in-plane shear loading," *42nd ISTC*, Oct 2010.

[7] G. P. Dillon and D. H. Stiver, "Forming stretch broken carbon fiber composites into complex shapes," *SAMPE 2007*, June 2007.

[8] E. Booth, D. Cairns, and C. Ridgard, "Advances in the development of stretch broken carbon fiber for primary aircraft structure," *CAMX 2022*, 2022.

[9] G. Jacobsen and W. C. Schimpf, *Process Development and Characterization of Stretch Broken Carbon Fiber Materials*.

[10] J. Sun, M. Li, Y. Gu, D. Zhang, Y. Li, and Z. Zhang, "Interply friction of carbon fiber/epoxy prepreg stacks under different processing conditions," *Journal of Composite Materials*, vol. 48, no. 5, p. 515–526, 2013.

[11] T. Javin Nur, Z. White, B. Bossert, M. Egloff, C. A. Ryan, D. S. Bajwa, D. Cairns, and R. Amendola, "Novel experimental unit to evaluate inter-ply and tool-ply friction in carbon fiber reinforced polymer composites prepregs," *CAMX 2022*, 2022.

[12] D. J. Peery, *Aircraft structures*. E.P. Dutton, 2011.

[13] "Tight-tolerance multipurpose 6061 aluminum sheets and bars." `https://www.mcmaster.com/products/metals/shape~sheet-and-bar/tight-tolerance-multipurpose-6061-aluminum-sheets-and-bars/`.

[14] B. Dunbar, "The world's greatest piggyback ride." `https://www.nasa.gov/returntoflight/crew/ferryflight.html`.

[15] "Ltm 16b tooling prepreg technical data sheet." `https://www.solvay.com/en/product/ltm-16b`.

[16] "Intamsys i funmat ht i desktop 3d printer." https://www.intamsys.com/funmat-ht-3d-printer/, Sep 2022.

[17] "Technical data sheet: Carbonx™ cf-pla 3d printing filament." https://www.3dxtech.com/wp-content/uploads/2021/03/PLA_CF-TDS-v03.pdf.

[18] "Tc-1614 a/b epoxy penetrating sealing and coating resin system." https://bjbmaterials.com/pub/media/wysiwyg/pdfs/Epoxies/TC-1614.pdf, Sep 2020.

[19] Stratasys, *FDM for Composite Tooling 2.0 Design Guide*. stratasys, 2AD.

[20] K. Śledziewski and M. Górecki, "Finite element analysis of the stability of a sinusoidal web in steel and composite steel-concrete girders," *Materials*, vol. 13, no. 5, p. 1041, 2020.

[21] "Hextow im7 carbon fiber." https://www.hexcel.com/Resources/DataSheets/Carbon-Fiber, Feb 2023.

[22] "Product data - energy.ornl.gov." https://energy.ornl.gov/CFCrush/materials/uou/8552_eu.pdf.

[23] "Cycom® 977-3." https://www.solvay.com/en/product/cycom-977-3#product-documents.

[24] G. Fernlund, J. Griffith, R. Courdji, and A. Poursartip, "Experimental and numerical study of the effect of caul-sheets on corner thinning of composite laminates," *Composites Part A: Applied Science and Manufacturing*, vol. 33, no. 3, p. 411–426, 2002.

[25] J. Yanagimoto and K. Ikeuchi, "Sheet forming process of carbon fiber reinforced plastics for lightweight parts," *CIRP Annals*, vol. 61, no. 1, p. 247–250, 2012.

[26] W. Hoffman, "Scanning probe microscopy of carbon fiber surfaces," *Carbon*, vol. 30, no. 3, p. 315–331, 1992.

[27] T. Grankäll, P. Hallander, and M. Åkermo, "Vacuum-assisted hot-forming using tailored laminate temperature," *Applied Composite Materials*, vol. 28, no. 2, p. 247–269, 2021.

[28] Y. Ma, T. Centea, and S. R. Nutt, "Defect reduction strategies for the manufacture of contoured laminates using vacuum bag-only prepregs," *Polymer Composites*, vol. 38, no. 9, p. 2016–2025, 2015.

[29] A. Hosseini, M. Kashani, F. Sassani, A. Milani, and F. Ko, "Identifying the distinct shear wrinkling behavior of woven composite preforms under bias extension and picture frame tests," *Composite Structures*, vol. 185, p. 764–773, 2018.

[30] Y. Mujahid, N. Sallih, M. Mustapha, M. Z. Abdullah, and F. Mustapha, "Effects of processing parameters for vacuum-bagging-only method on shape conformation of laminated composites," *Processes*, vol. 8, no. 9, p. 1147, 2020.

[31] W. Jiang, Z. Huang, Y. Wang, B. Zheng, and H. Zhou, "Voids formation and their effects on mechanical properties in thermoformed carbon fiber fabric-reinforced composites," *Polymer Composites*, vol. 40, no. S2, 2018.

[32] M. McClain and J. Goering, "Dry forming of internal stiffeners using stretch broken carbon fiber preforms," *SAMPE 2007*, June 2007.

[33] J. Beglinger, *Forming of Advanced Composite Materials*. PhD thesis, 1998.

[34] "Loctite® frekote 770-nc™ technical data sheet." `http://tds.henkel.com/tds5/Studio/ShowPDF/?pid=FREKOTE%20770NC&format=MTR&subformat=REAC&language=EN&plant=WERCS`, Aug 2016.

[35] "Airtech flashbreaker 1 tape safety information sheet." `https://compositeenvisions.com/wp-content/uploads/2020/07/airtech-ps-tapes-sds-7_14_2020.pdf`, 2019.

[36] "High elongation fep perforated release film 60 - composite envisions." `https://compositeenvisions.com/product/high-elongation-fep-perforated-release-film-60/`, Apr 2023.

[37] "Vacuum breather / bleeder cloth 60 7oz - composite envisions." `https://compositeenvisions.com/product/vacuum-breather-bleeder-cloth-60-7oz/`, Apr 2023.

[38] "Stretchlon-850-cf-2in safety information sheet." `https://www.e-aircraftsupply.com/products/airtech--bagging-films/9402233/Stretchlon-850-CF-0002INX2INX160IN`, 2019.

[39] J.-L. Doumont, *Trees, maps, and theorems: Effective communication for rational minds*. Principiæ, 2014.

[40] "Max inscribed circles." `https://imagej.net/imagej-wiki-static/Max_Inscribed_Circles`, July 2016.

[41] N. Haleem and X. Wang, "Recent research and developments on yarn hairiness," *Textile Research Journal*, vol. 85, no. 2, p. 211–224, 2014.

[42] L. Fitzsimmons, *Carbon Fiber Defects [Powerpoint Presentation]*. 2022.

[43] D. Nold, D. Bajwa, D. Cairns, R. Amendola, C. Ryan, and C. Ridgard, "Tensile properties of stretch broken carbon fiber prepreg," *CAMX 2022*, 2022.

[44] B. Vidyashankar and A. Krishna Murty, "Analysis of laminates with ply drops," *Composites Science and Technology*, vol. 61, no. 5, p. 749–758, 2001.

APPENDICES

APPENDIX A

APPENDIX A: MATERIAL DATA SHEETS

MSU SBCF Prepreg Batches

Table A.1: Summary of MSU SBCF Prepreg Batches

Batch	Resin Type	Fiber Areal Weight (gsm)	Resin Content (%)	Water Pickup (%)
P0025	977-3	104	37	19.1
P0029	977-3	111.9	35	2.9
P0030	977-3	110.2	37.2	8.5
P0031	8552	110.8	35.7	4.4

Hexcel IM7 Fibers

HexTow® IM7 Carbon Fiber

HEXCEL®

Product Data Sheet

HexTow® IM7 carbon fiber is a continuous, high performance, intermediate modulus, PAN based fiber available in 12,000 (12K) filament count tows. This fiber has been surface treated and can be sized to improve its interlaminar shear properties, handling characteristics, and structural properties. It is suggested for use in weaving, prepregging, filament winding, braiding, and pultrusion.

The unique properties of HexTow® IM7 fiber, such as higher tensile strength and modulus, as well as good shear strength, allow structural designers to achieve both higher safety margins for both stiffness and strength critical applications.

IM7-G 12K (0.25%) carbon fiber has been qualified to NMS 818 Carbon Fiber Specification (NCAMP). This allows customers to call out an industry standard, aerospace grade carbon fiber without the need to write and maintain their own specification.

Typical Fiber Properties	U.S. Units	SI Units
Tensile Strength		
6K	800 ksi	5516 MPa
12K	825 ksi	5688 MPa
Tensile Modulus (Chord 6000-1000)	40.0 Msi	276 GPa
Ultimate Elongation at Failure		
6K	1.8%	1.8%
12K	1.8%	1.8%
Density	0.0643 lb/in^3	1.78 g/cm^3
Weight/Length		
6K	12.5 x 10^{-6} lb/in	0.223 g/m
12K	25.0 x 10^{-6} lb/in	0.446 g/m
Approximate Yield		
6K	6,674 ft/lb	4.48 m/g
12K	3,337 ft/lb	2.24 m/g
Tow Cross-Sectional Area		
6K	1.94 x 10^{-4} in^2	0.13 mm^2
12K	3.89 x 10^{-4} in^2	0.25 mm^2
Filament Diameter	0.203 mil	5.2 microns
Carbon Content	95.0%	95.0%
Twist	Never Twisted	Never Twisted

Typical HexPly 8552 Composite Properties (at Room Temperature)	U.S. Units	SI Units	Test Method
0º Tensile Strength	395 ksi	2,723 MPa	ASTM D3039
0º Tensile Modulus	23.8 Msi	164 GPa	
0º Tensile Strain	1.6%	1.6%	
0º Flexural Strength	270 ksi	1,862 MPa	ASTM D790
0º Flexural Modulus	22.0 Msi	152 GPa	
0º Short Beam Shear Strength	18.5 ks	128 MPa	ASTM D2344
0º Compressive Strength	245 ksi	1,689 MPa	ASTM Mod. D695
0º Compressive Modulus	21.7 Msi	150 GPa	
Open Hole Tensile Strength	62.1 ksi	428 MPa	ASTM D5766
Open Hole Compressive Strength	48.9 ksi	337 MPa	ASTM D6484
90º Tensile Strength	9.3 ksi	64.1 MPa	ASTM D3039
Fiber Volume	60%	60%	

Copyright © 2020 – Hexcel Corporation – All Rights Reserved.

Figure A.1: Hexcel IM7 Fiber Data Sheet Page 1



HexTow® IM7 carbon fiber

HEXCEL

Product Data Sheet

Yarn/Tow Characteristics	U.S. Units	SI Units
Specific Heat	0.21 Btu/lb-°F	0.21 cal/g-°C
Electrical Resistivity	4.9 x 10^{-5} ohm-ft	1.5 x 10^{-3} ohm-cm
Coefficient of Thermal Expansion	-0.36 ppm/°F	-0.64 ppm/°C
Thermal Conductivity	3.12 Btu/hr-ft-°F	5.40 W/m-°K

Carbon Fiber Certification
This carbon fiber is manufactured to Hexcel aerospace grade specification HS-CP-5000. A copy of this specification is available upon request. A Certification of Analysis will be provided with each shipment.

Available Sizing
Sizing compatible with various resin systems, based on application are available to improve handling characteristics and structural properties. Please see additional information on available Sizes on our website or contact our technical team for additional information.

Packaging
Standard packaging of HexTow® IM7 is as follows:

Filament Count	Sizing	Nominal Weight		Nominal Length	
		(lb)	(kg)	(ft)	(m)
6K	GP	5.0	2.3	33,330	10,160
12K	Unsized	4.0	1.8	13,330	4,060
	G, GP	8.0	3.6	26,670	8,130

Other package sizes may be available on request. The fiber is wound on a 3-inch ID by 11-inch long cardboard tube and overwrapped with plastic film.

Safety Information
Obtain, read, and understand the Safety Data Sheet (SDS) before use of this product.

For more information
Hexcel is a leading worldwide supplier of composite materials to aerospace and industrial markets. Our comprehensive range includes:

- HexTow® carbon fibers
- HexForce® reinforcements
- HiMax™ multiaxial reinforcements
- HexPly® prepregs
- HexMC®-i molding compounds
- HexFlow® RTM resins
- HexBond™ adhesives
- HexTool® tooling materials
- HexWeb® honeycombs
- Acousti-Cap® sound attenuating honeycomb
- Engineered core
- Engineered products
- Polyspeed® laminates & pultruded profiles
- HexAM® additive manufacturing

For US quotes, orders and product information call toll-free 1-866-556-2662. For other worldwide sales office telephone numbers and a full address list, please go to:

http://www.hexcel.com/contact

©2020 Hexcel Corporation *– All rights reserved. Hexcel Corporation and its subsidiaries ("Hexcel") believe that the technical data and other information provided herein was materially accurate as of the date this document was issued. Hexcel reserves the right to update, revise or modify such technical data and information at any time. Any performance values provided are considered representative but do not and should not constitute a substitute for your own testing of the suitability of our products for your particular purpose.* ***Hexcel makes no warranty or representation, express or implied, including but not limited to the implied warranties of merchantability and fitness for a particular purpose, and disclaims any liability arising out of or related to, the use of or reliance upon any of the technical data or information contained in this document.***

CTA 351 NV20

Figure A.2: Hexcel IM7 Fiber Data Sheet Page 2

Hexcel 8552 Resin

HexPly® 8552

mid-toughened, high strength, damage-resistant, structural epoxy matrix

HEXCEL®

Product Data Sheet

Description

HexPly® 8552 is an amine cured, toughened epoxy resin system supplied with unidirectional or woven carbon or glass fibers. HexPly® 8552 is recommended for structural applications requiring high strength, stiffness, and damage tolerance. HexPly® 8552 was developed as a low flow system to operate in environments of up to 250°F.

Features

- Service Temperature up to 250°F
- Impact Tolerant
- Low Flow

Applications

HexPly® 8552 is a versatile epoxy matrix system, typical uses include:

Commercial Aerospace	Space and Defense	Industrial
Primary Aircraft Structures	Aircraft Structures	Automotive
Secondary Aircraft Structures	Helicopters	Machinery
Engines	Missiles	Sports & Leisure
Nacelles	Space Launchers	Medical Equipment

Neat Resin Properties

Density	0.0470 lb/in^3
Tg dry - RDS 7700	392°F
Tg wet - RDS 7700	309°F
Tensile strength	17.5 ksi
Tensile modulus	0.677 msi
Tensile strain	1.7%
Fracture toughness, K_{1C}	1.475 ksi $\sqrt{}$ in
Strain energy release rate, G_{1C}	3.88 in-lb/in^2
Gel Time at 350°F	13 minutes

Copyright © 2020 – Hexcel Corporation – All Rights Reserved.

Figure A.3: Hexcel 8552 Resin Data Sheet Page 1

HexPly® 8552

mid-toughened, high strength, damage-resistant, structural epoxy matrix

HEXCEL

Product Data Sheet

Availability
HexPly® 8552 has variations and is available on a wide range of reinforcement types.

Resin Variations
8552: Standard version, toughened 350°F cure epoxy
8552ATL: Lower tack for automated tape layup
8552S: Solvated tower manufacture

Reinforcement Types	
Glass Fabrics	Aramid Fabric
Glass Tapes	Quartz Fabric
Carbon Fabrics	Polyester Fabric
Carbon Tapes	Ceramic Fabric
Carbon Towpreg	Metal Fabric
HexMC	

Typical Physical Properties

	Material Description	Carbon Tapes	Carbon Fabrics	Glass Tapes
Prepreg	% Resin Content	33-38	32-42	34-36
	% Flow	10-22	8-22	16-21
	% Volatiles	1.0 max	1.5 max	1.0 max
	Gel (min)	12-22	12-22	12-22

Copyright © 2020 – Hexcel Corporation – All Rights Reserved.

Figure A.4: Hexcel 8552 Resin Data Sheet Page 2



HexPly® 8552

mid-toughened, high strength, damage-resistant, structural epoxy matrix

HEXCEL

Product Data Sheet

Mechanical Properties

Property	Temp°F	Condition	AS4	IM7	A193-PW	A280-5H	SGP196-PW	SGP370-8H	S2GL
0° Tensile strength, ksi	-67	Dry	300	373	111	120	142	140	-
0° Tensile modulus, msi	-67	Dry	19.4	23.7	9.5	10.2	12.3	12.5	-
0° Tensile strength, ksi	77	Dry	310	395	120	127	158	147	251
0° Tensile modulus, msi	77	Dry	19.6	23.8	9.8	9.7	12.3	12.4	6.53
0° Tensile elongation, %	77	Dry	1.55	1.62	-	-	-	-	3.87
0° Tensile strength, ksi	195	Dry	293	**368***	116	131	-	-	-
0° Tensile modulus, msi	195	Dry	19.1	**23.7***	9.6	10	-	-	-
90° Tensile strength, ksi	-67	Dry	9.73	9.60	103	109	125	131	-
90° Tensile modulus, msi	-67	Dry	1.50	1.46	9.6	9.7	11.6	11.7	-
90° Tensile strength, ksi	77	Dry	9.27	9.3	115	116	137	139	-
90° Tensile modulus, msi	77	Dry	1.39	1.70	9.5	9.5	11.6	11.7	-
90° Tensile strength, ksi	200	Dry	-	-	111	112	**142***	**130***	-
90° Tensile modulus, msi	200	Dry	1.22	1.50	9.8	9.4	**11.5***	**11.5***	-
Major Poisson's Ratio, tension	77	Dry	0.302	0.316	-	-	-	-	-
± 45 Inplane shear	77	Dry	16.6	17.4	-	15.9	18.3	1436	-
± 45 Inplane shear	200	Dry	15.2	**15.4***	-	-	**15.5***	**13.1***	-
Major Poisson's Ratio, compression	77	Dry	0.335	0.356	-	-	-	-	-
0° Compression strength, ksi	-67	Dry	253	292	139	-	-	-	-
0° Compression modulus, msi	-67	Dry	18	20.5	8.7	-	-	-	-
0° Compression strength, ksi	77	Dry	222	245	128	134	-	-	217
0° Compression modulus, msi	77	Dry	18.6	21.7	8.7	9.3	-	-	6.6
0° Compression strength, ksi	195	Dry	184	215	110	109	-	-	-
0° Compression modulus, msi	195	Dry	17.7	23.5	8.8	9.7	-	-	-
0° Compression strength, ksi	160	Wet	203	-	102	-	-	-	-
0° Compression modulus, msi	160	Wet	17.0	-	8.6	-	-	-	-
0° Compression strength, ksi	195	Wet	184	**173 ♦**	85	**74**	-	-	-
0° Compression modulus, msi	195	Wet	18.1	**20.7 ♦**	-	**9.9**	-	-	-
Fill compression strength, ksi	-67	Dry	51.4	55.3	127	150	124	132	-
Fill compression modulus, msi	-67	Dry	1.56	1.53	8.7	9.2	-	-	-
Fill compression strength, ksi	77	Dry	38.9	44.2	127	129	116	121	-
Fill compression modulus, msi	77	Dry	1.43	1.82	9	9.1	10.4	10.5	-
Fill compression strength, ksi	195	Dry	-	-	114	-	**103***	**96***	-
Fill compression modulus, msi	195	Dry	-	-	8.9	-	**10.6***	**10.5***	-
Fill compression strength, ksi	77	Wet	-	34.2	116	-	95	94	-
Fill compression strength, ksi	160	Wet	-	**24.6****	101	-	**81****	**88****	-
Fill compression strength, ksi	195	Wet	**19.7 ♦**	19 ♦	87	-	**87***	-	-
Compression after impact, ksi									
after 500 in-in-lb/in impact	77	Dry	50	-	-	-	-	-	-
after 1,500 in-in-lb/in impact	77	Dry	32	34	-	-	-	-	-
after 2,000 in-in-lb/in impact	77	Dry	28	-	-	-	-	-	-
after 2,500 in-in-lb/in impact	77	Dry	27	-	-	-	-	-	-

Bold - 200° **Bold* - 220°** **Bold** - 180°** **Bold ♦ - 250°**

Copyright © 2020 – Hexcel Corporation – All Rights Reserved.

Figure A.5: Hexcel 8552 Resin Data Sheet Page 3

HexPly® 8552

mid-toughened, high strength, damage-resistant, structural epoxy matrix

HEXCEL

Product Data Sheet

Mechanical Properties

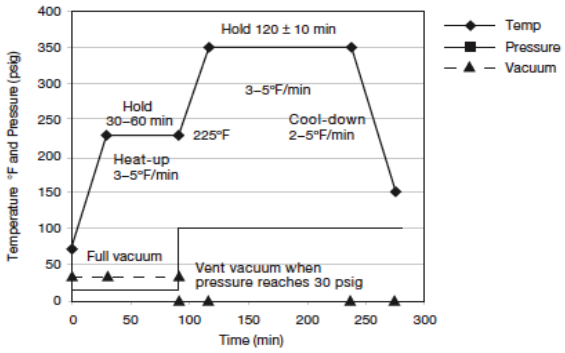
Property	Temp°F	Condition	AS4	IM7	A193-PW	A280-5H	SGP196-PW	SGP370-8H	S2GL
0° Short beam shear, ksi	-67	Dry	23.8	21	14.6	-	-	-	-
0° Short beam shear, ksi	77	Dry	18.5	19.9	12.2	11.4	12.7	13	14.1
0° Short beam shear, ksi	195	Dry	**14.7 ♦**	**13.6***	10.2	10	**10***	**10.8***	-
0° Short beam shear, ksi	77	Wet	16.9	16.7	10.9	10	11.6	12.1	-
0° Short beam shear, ksi	160	Wet	12.2	**11.6****	10.4	-	**8.8****	**9.1****	-
0° Short beam shear, ksi	195	Wet	**8.25 ♦**	**8.25 ♦**	8.5	-	-	-	-
Fill short beam shear, ksi	-67	Dry	-	-	10.8	13.7	-	-	-
Fill short beam shear, ksi	77	Dry	-	-	11.8	11.7	-	-	-
Fill short beam shear, ksi	195	Dry	-	-	10.2	-	-	-	-
Fill short beam shear, ksi	77	Wet	-	-	11.4	-	-	-	-
Fill short beam shear, ksi	195	Wet	-	-	8.5	-	-	-	-
0° Flexural strength, ksi	77	Dry	274	270	-	150	165	164	233
0° Flexural modulus, msi	77	Dry	18.4	22	-	8.5	11.1	10.8	6.38
Quasi-Isotropic 25/50/25									
Tensile strength, ksi	77	Dry	107	104	-	-	-	-	-
OHT strength, ksi	77	Dry	63.5	62.1	-	51	56.7	58.3	-
OHC strength, ksi	77	Dry	47.8	48.9	-	53.7	52.1	49.2	-
CAI strength, ksi	77	Dry	34.6	31	-	40.8	42.5	40	-
CBI strength, ksi	77	Dry	91.2	-	-	76.3	-	-	-

Bold - 200° **Bold* - 220°** **Bold** - 180°** **Bold ♦ - 250°**

Cure Cycle

Autoclave

1. Apply full vacuum and 15 psig pressure.
2. Heat at 3–5°F/minute to 225°F.



Cure Procedure

3. Hold at 225°F for 30–60 minutes.
4. Raise pressure to 85–100 psig;
5. Vent vacuum when pressure reaches 30 psig.
6. Hold at 350°F for 120 ± 10 minutes.
7. Cool at 2–5°F to 150°F and vent pressure.

Note: Alternative cure cycles available upon request.

Copyright © 2020 – Hexcel Corporation – All Rights Reserved.

Figure A.6: Hexcel 8552 Resin Data Sheet Page 4

APPENDIX B

APPENDIX B: ADDITIONAL COMPLEX PART TRIAL RESULTS

Additional Curved C Channel Results

Table B.1: Summary of Curved C Channel Results

Part	Fiber	Resin	Batch	Plies	Layup Shape	Intensifier	Inter-mediate Dwell	Final Dwell	Cure Pressure
MD005	CF	8552	N/A	8	Square	No	-	350F - 2 hrs	90 psi
MD006	SBCF	977-3	P0025	8	Square	Yes	80F-0.5 hrs	350F-6 hrs	90 psi
MD007	CF	8552	N/A	8	Square	No	-	350F-2 hrs	90 psi
MD008	CF	8552	N/A	8	Square	Yes	-	350F-2 hrs	90 psi
MD009	CF	8552	N/A	8	Square	No	-	350F-2 hrs	90 psi
MD011	SBCF	977-3	P0029	8	1/4 Circ	Yes	80F-0.5 hrs	350F-6 hrs	90 psi
MD012	SBCF	977-3	P0029	8	1/4 Circ	Yes	80F-0.5 hrs	350F-6 hrs	90 psi
MD017	SBCF	8552	P0030	8	1/4 Circ	Yes	-	350F-2 hrs	90 psi
MD020	CF	8552	N/A	8	Square	No	-	350F-2 hrs	90 psi

Part MD005

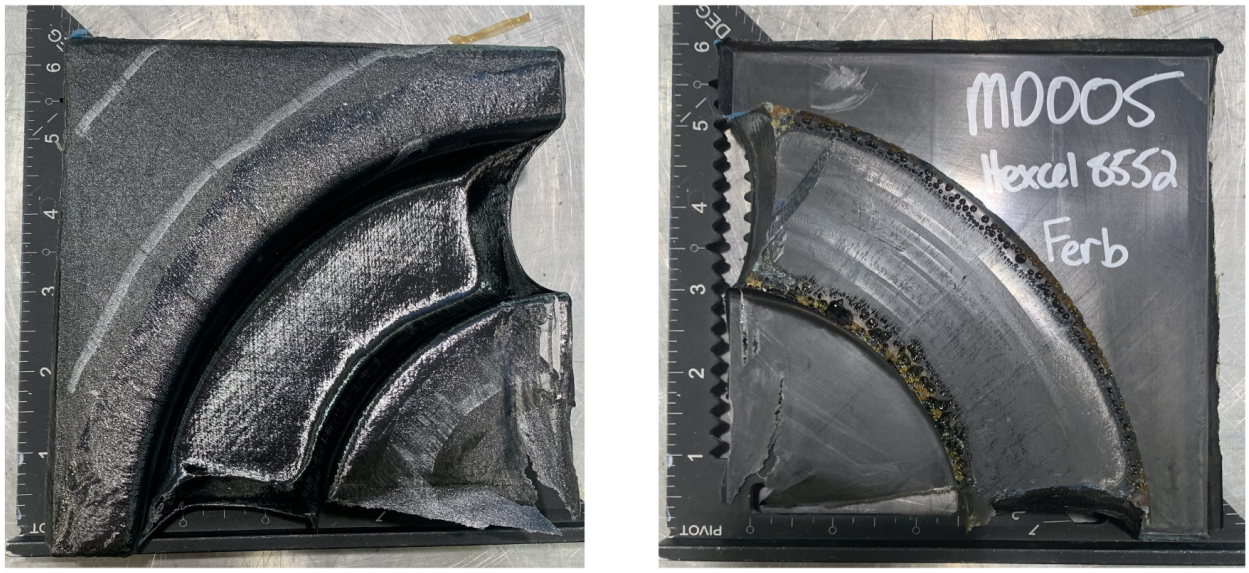


Figure B.1: Continuous Carbon Fiber Curved C Channel Part MD005: Left - Top of Part, Right - Bottom of Part

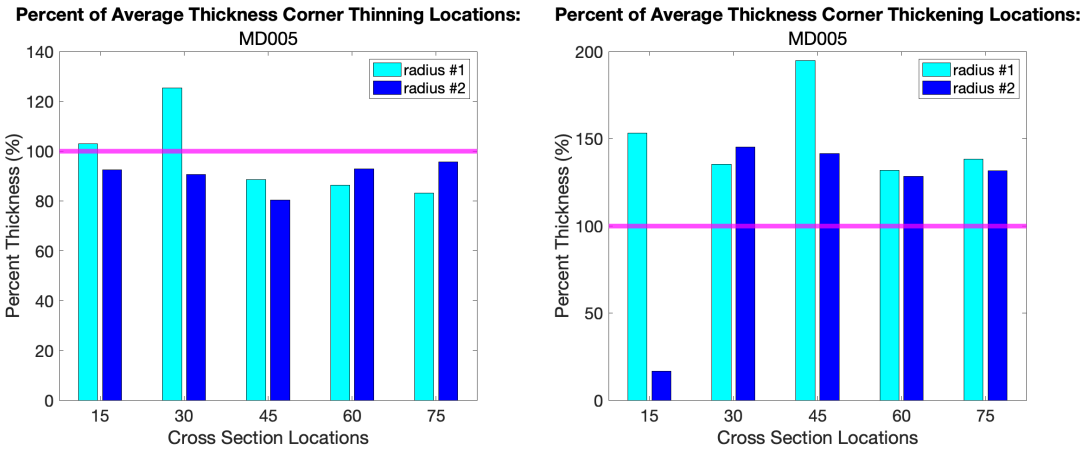


Figure B.2: Continuous Carbon Fiber MD005 Results: Left - Corner Thinning (Average = 93.82%), Right - Corner Thickening (Average = 131.62%)

Table B.2: Continuous Carbon Fiber MD005: Texture Results

Metric	Weight	Ranking	Score
Hairiness	30%	5	-
Additional Resin Pooling	30%	5	-
Spaghettification	10%	5	-
Fractures/Shearing	15%	5	-
Pinholes	10%	5	-
Waves	5%	5	-
Total	100%	X	5

Table B.3: Continuous Carbon Fiber MD005: Final Forming Score

Metric	Weight	Ranking	Score
Bridging	12.5%	2	-
Wrinkling	17.5%	5	-
Thickness Variation	15%	3	-
Forming Depth	12.5%	3	-
Corner Thinning	15%	3	-
Corner Thickening	10%	0	-
Resin Pooling	12.5%	2	-
Texture	5%	5	-
Total	100%	-	2.9

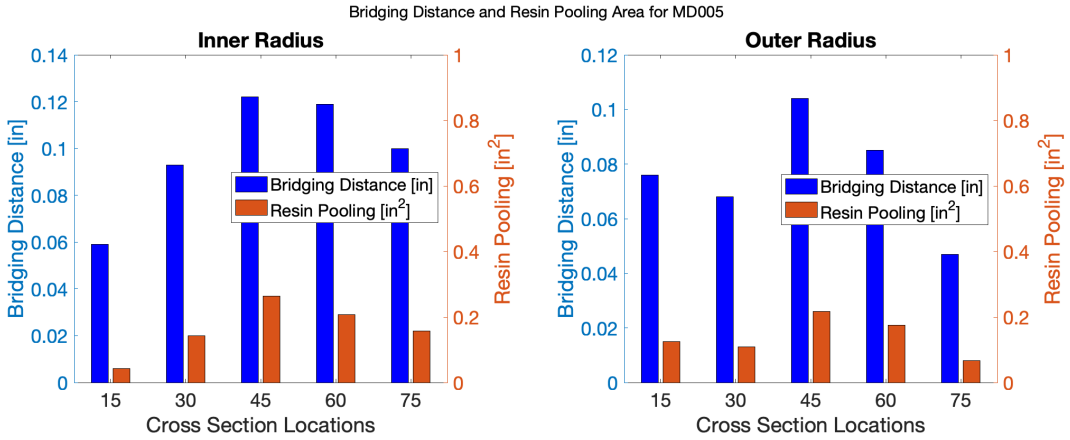


Figure B.3: Continuous Carbon Fiber MD005 Results: Bridging (Average = 0.0873 in) and Resin Pooling (Total = $0.0197 in^2$)

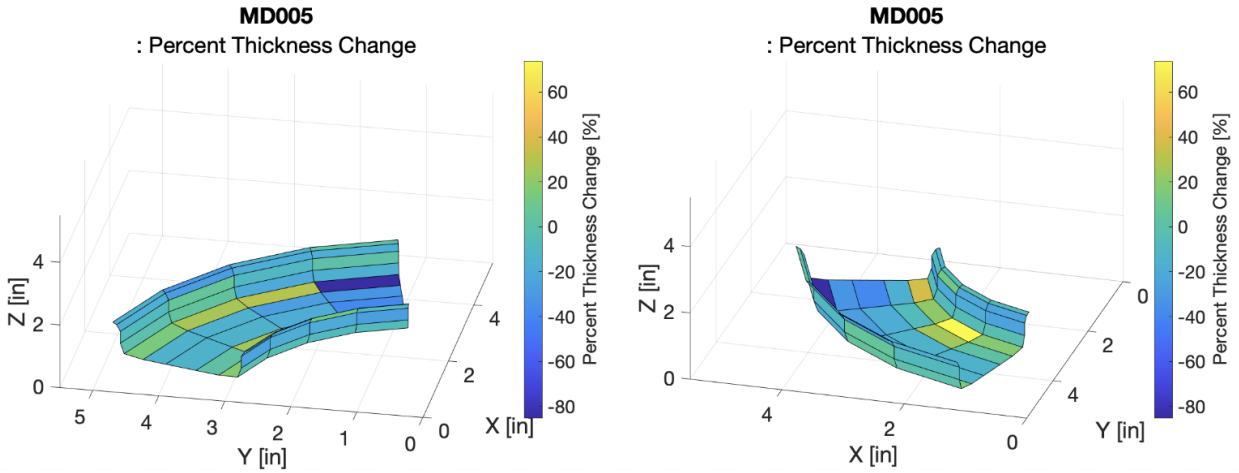


Figure B.4: Continuous Carbon Fiber MD005 Results: Thickness Variation, Left - "Radius #1" Orientation, Right - "Radius #2" Orientation (Coefficient of Variation = 0.1332)

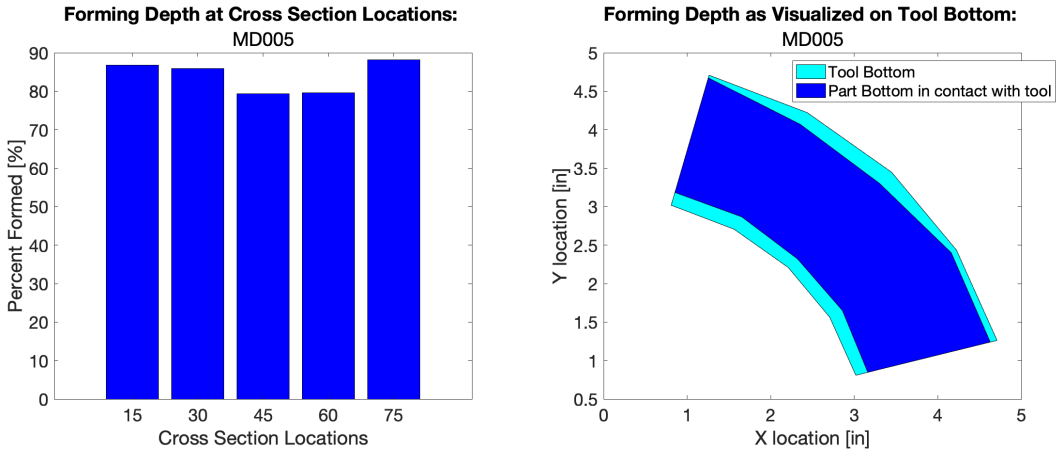


Figure B.5: Continuous Carbon Fiber MD005 Results: Forming Depth (Average = 83.93%)

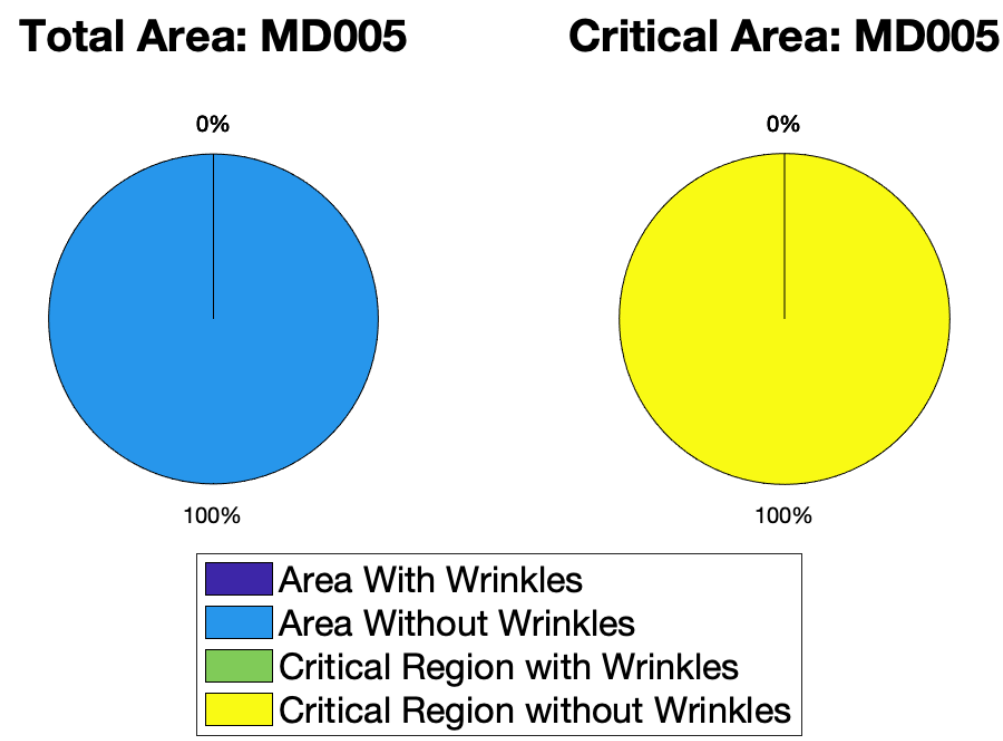


Figure B.6: Continuous Carbon Fiber MD005 Results: Wrinkling (Total Wrinkling = 0%, Critical Region Wrinkling = 0%)

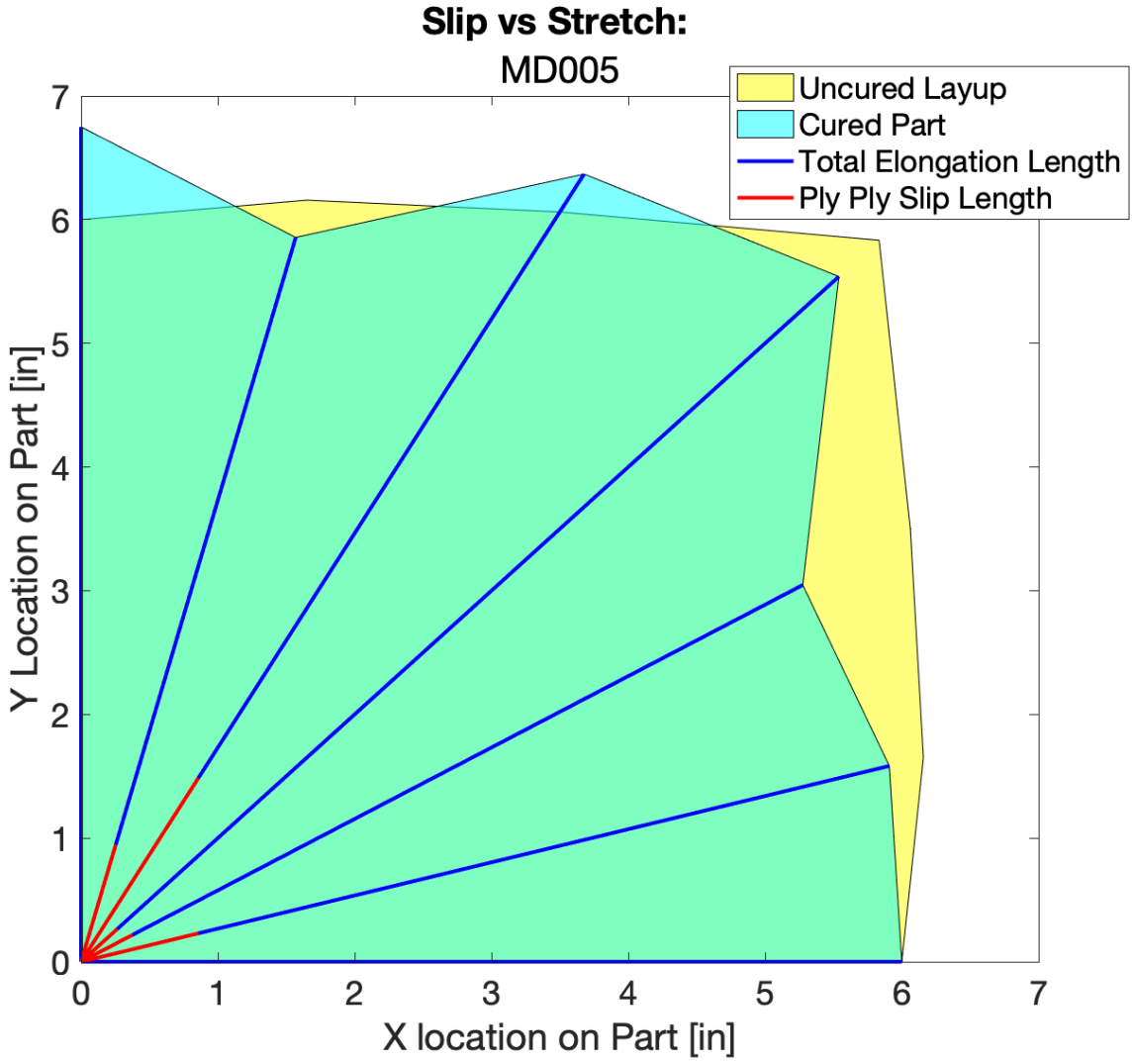


Figure B.7: Continuous Carbon Fiber MD005 Results: Stretching versus Slipping

Part MD006

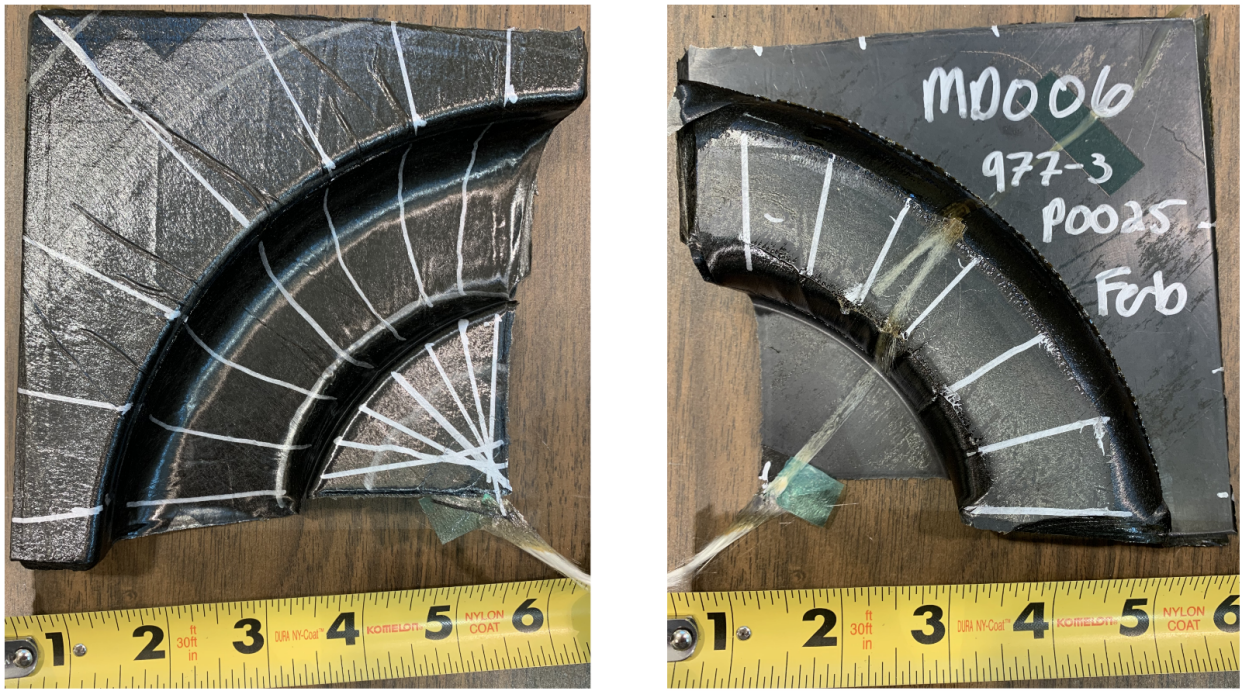


Figure B.8: Stretch Broken Carbon Fiber Curved C Channel Part MD006: Left - Top of Part, Right - Bottom of Part

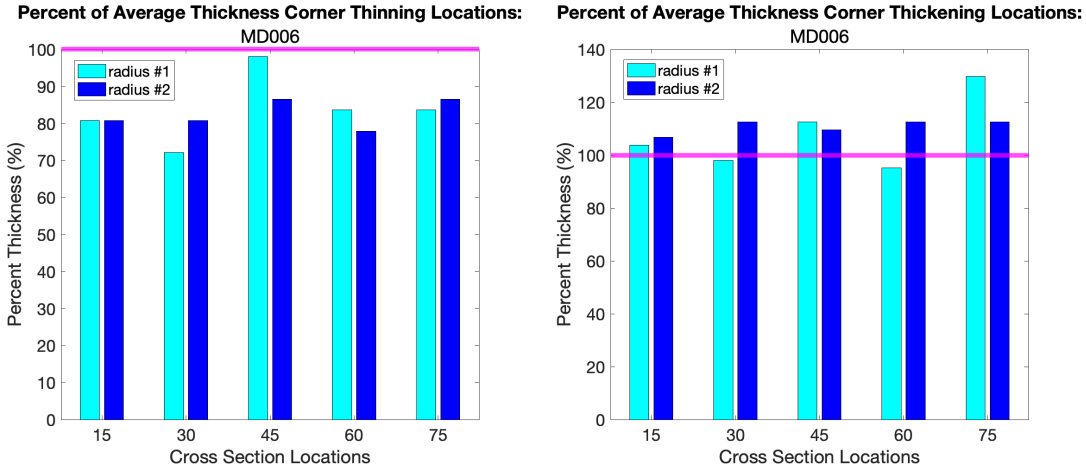


Figure B.9: Stretch Broken Carbon Fiber MD006 Results: Left - Corner Thinning (Average = 83.05%), Right - Corner Thickening (Average = 109.28%)

Table B.4: Stretch Broken Carbon Fiber MD006: Texture Results

Metric	Weight	Ranking	Score
Hairiness	30%	5	-
Additional Resin Pooling	30%	5	-
Spaghettification	10%	5	-
Fractures/Shearing	15%	0	-
Pinholes	10%	0	-
Waves	5%	5	-
Total	100%	X	3.75

Table B.5: Stretch Broken Carbon Fiber MD006: Final Forming Score

Metric	Weight	Ranking	Score
Bridging	12.5%	1	-
Wrinkling	17.5%	3	-
Thickness Variation	15%	3	-
Forming Depth	12.5%	3	-
Corner Thinning	15%	2	-
Corner Thickening	10%	3	-
Resin Pooling	12.5%	4	-
Texture	5%	3.75	-
Total	100%	-	2.76

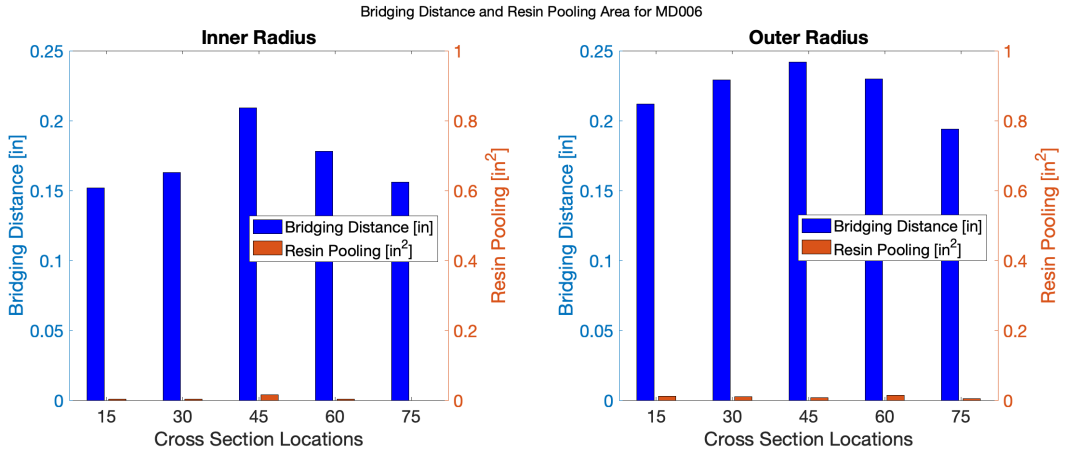


Figure B.10: Stretch Broken Carbon Fiber MD006 Results: Bridging (Average = 0.1965 in) and Resin Pooling (Total = $0.0019 in^2$)

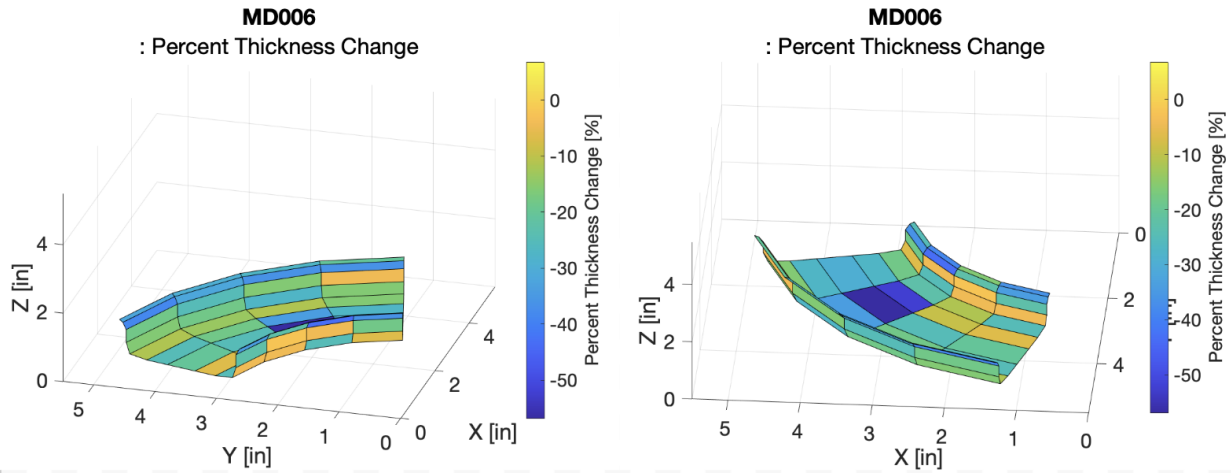


Figure B.11: Stretch Broken Carbon Fiber MD006 Results: Thickness Variation, Left - "Radius #1" Orientation, Right - "Radius #2" Orientation (Coefficient of Variation = 0.1570)

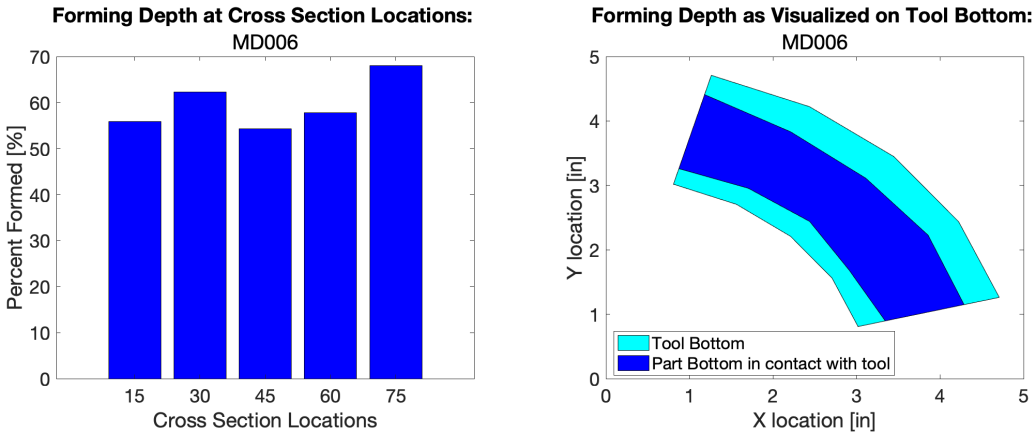


Figure B.12: Stretch Broken Carbon Fiber MD006 Results: Forming Depth (Average = 59.65%)

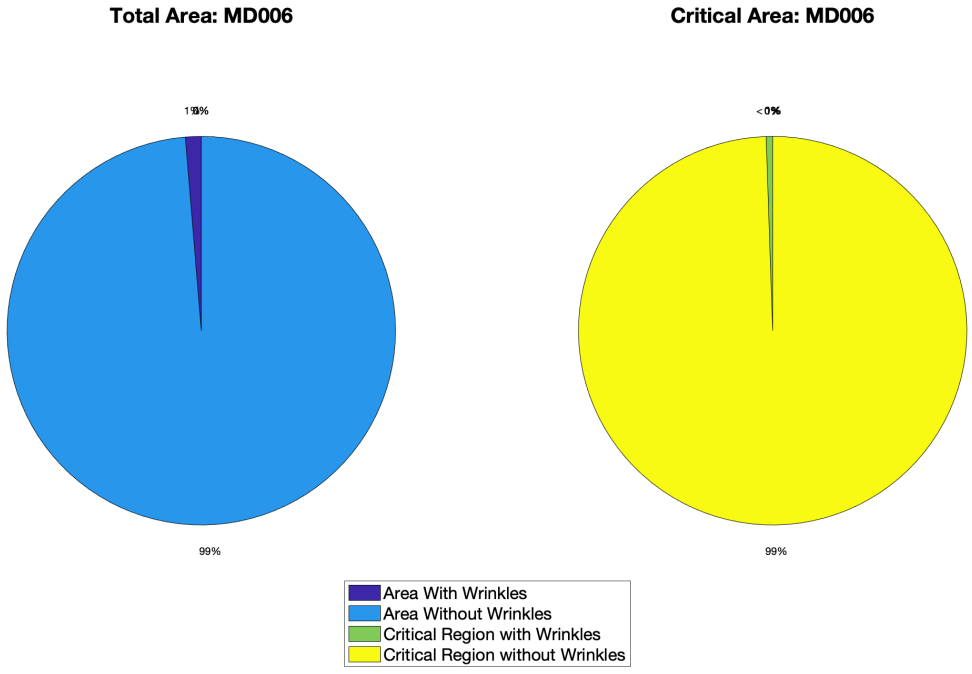


Figure B.13: Stretch Broken Carbon Fiber MD006 Results: Wrinkling (Total Wrinkling = 1.31%, Critical Region Wrinkling = 0.54%)

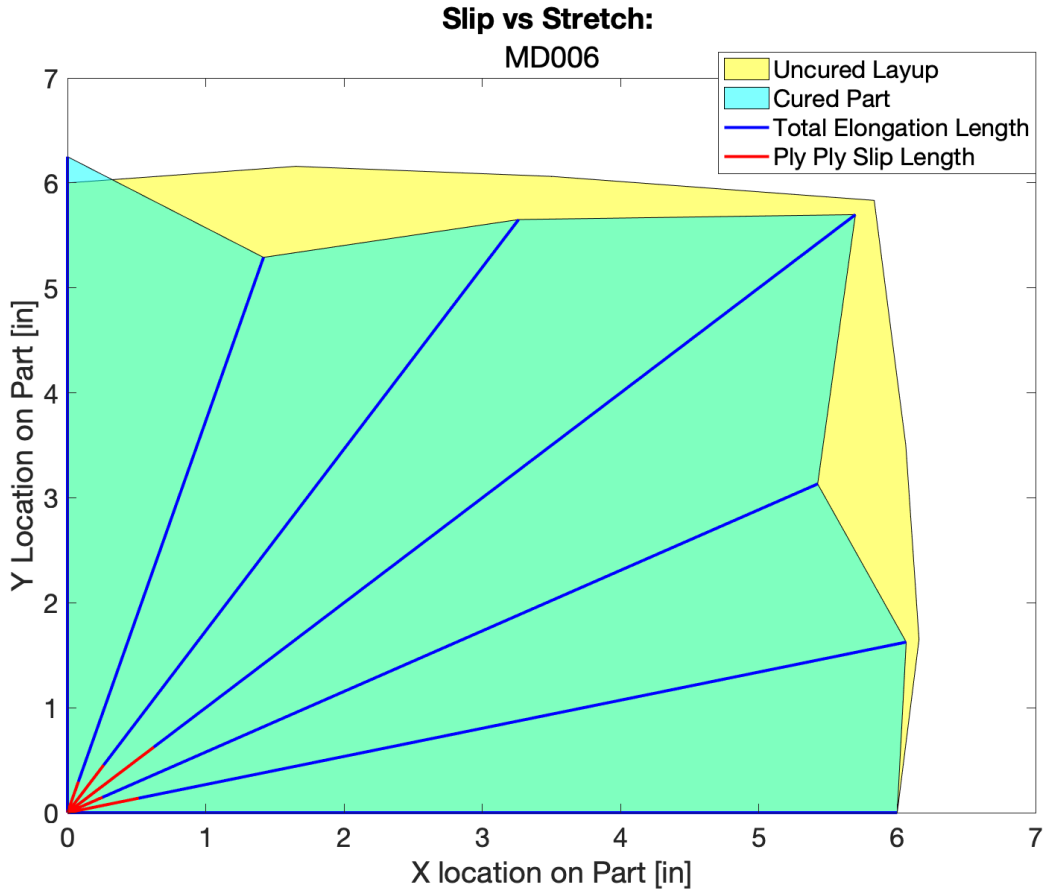


Figure B.14: Stretch Broken Carbon Fiber MD006 Results: Stretching versus Slipping

Part MD007

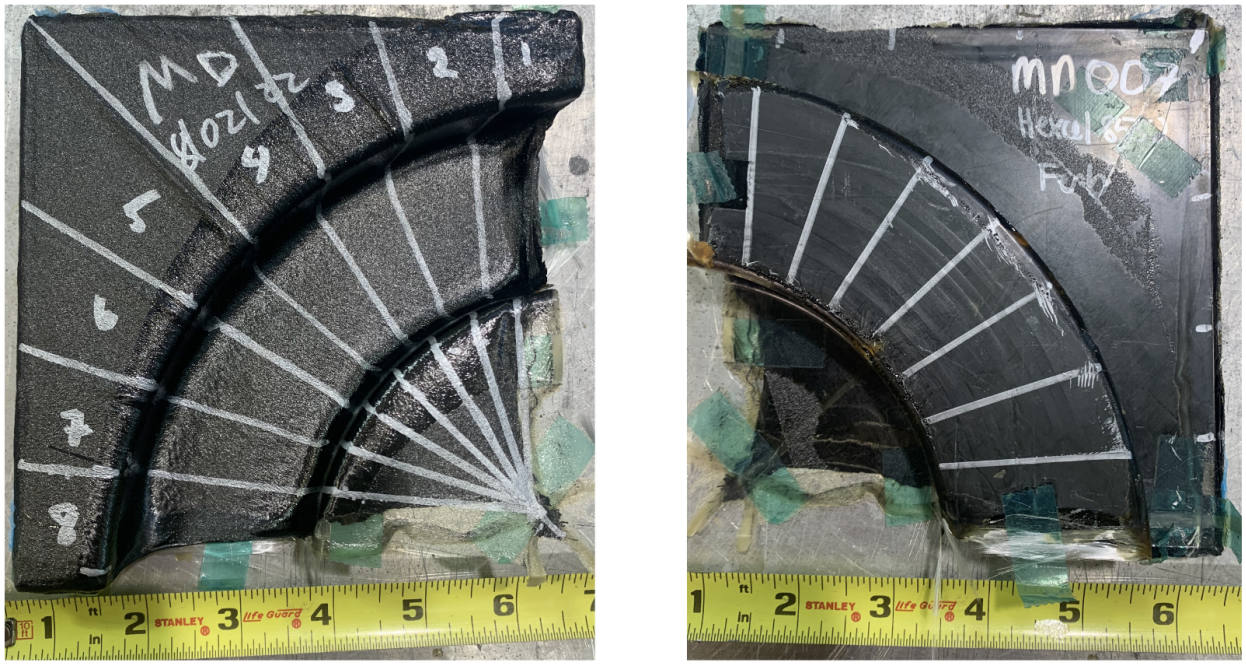


Figure B.15: Continuous Carbon Fiber Curved C Channel Part MD007: Left - Top of Part, Right - Bottom of Part

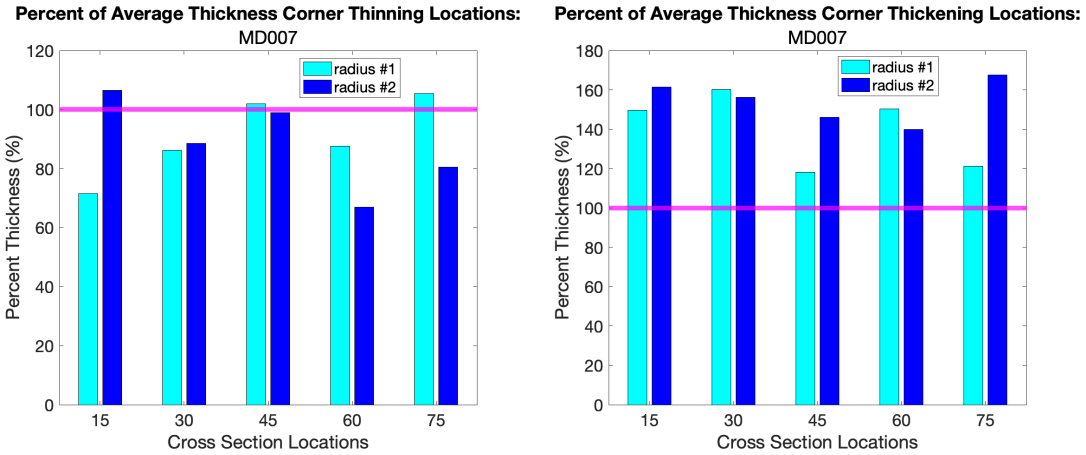


Figure B.16: Continuous Carbon Fiber MD007 Results: Left - Corner Thinning (Average = 89.39%), Right - Corner Thickening (Average = 147.11%)

Table B.6: Continuous Carbon Fiber MD007: Texture Results

Metric	Weight	Ranking	Score
Hairiness	30%	5	-
Additional Resin Pooling	30%	5	-
Spaghettification	10%	5	-
Fractures/Shearing	15%	0	-
Pinholes	10%	5	-
Waves	5%	5	-
Total	100%	X	4.25

Table B.7: Continuous Carbon Fiber MD007: Final Forming Score

Metric	Weight	Ranking	Score
Bridging	12.5%	3	-
Wrinkling	17.5%	3	-
Thickness Variation	15%	3	-
Forming Depth	12.5%	4	-
Corner Thinning	15%	2	-
Corner Thickening	10%	0	-
Resin Pooling	12.5%	3	-
Texture	5%	4.25	-
Total	100%	-	2.74

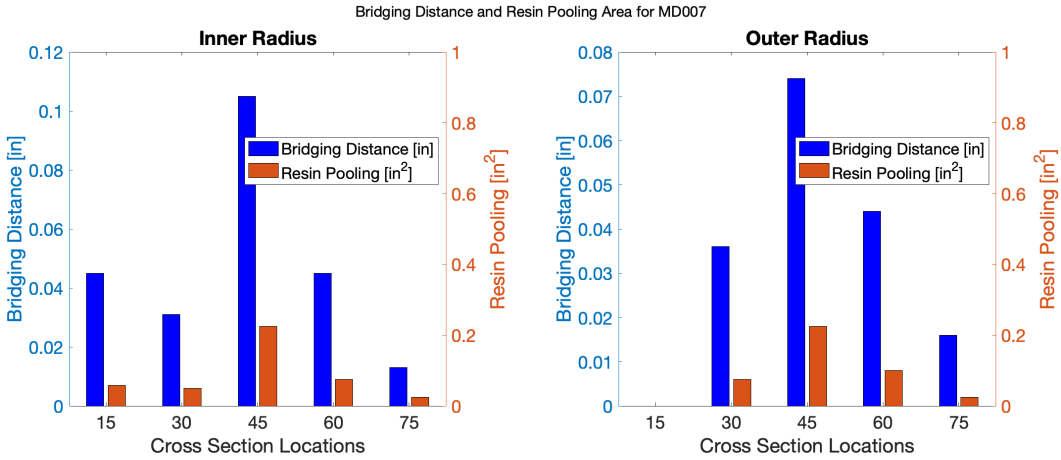


Figure B.17: Continuous Carbon Fiber MD007 Results: Bridging (Average = 0.0409 in) and Resin Pooling (Total = $0.0086 in^2$)

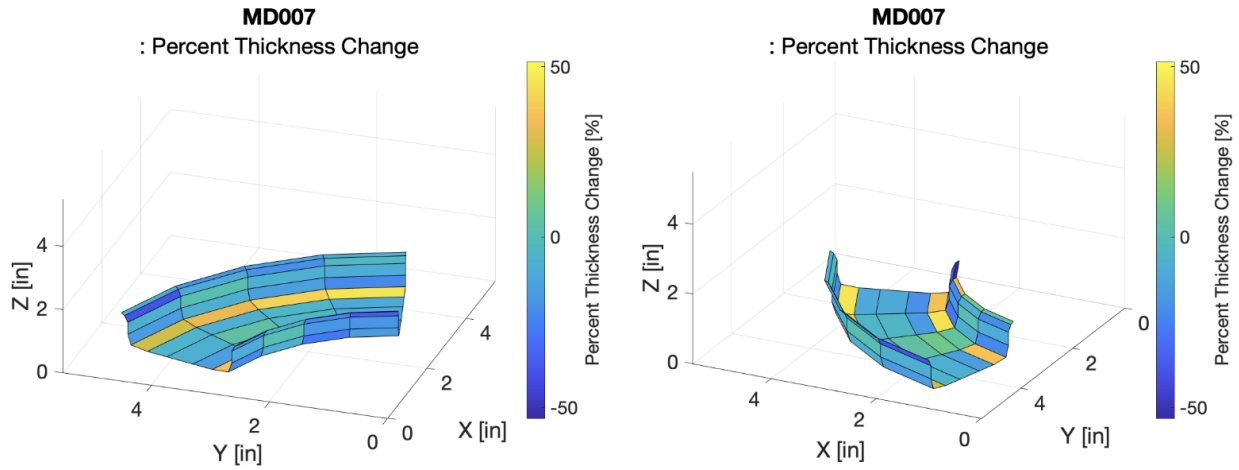


Figure B.18: Continuous Carbon Fiber MD007 Results: Thickness Variation, Left - "Radius #1" Orientation, Right - "Radius #2" Orientation (Coefficient of Variation = 0.1494)

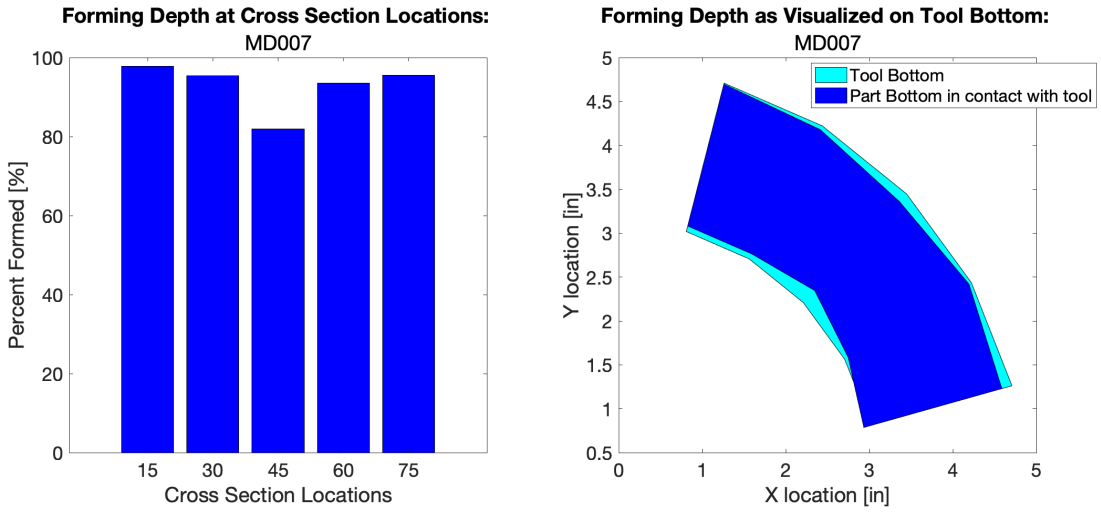


Figure B.19: Continuous Carbon Fiber MD007 Results: Forming Depth (Average = 92.86%)

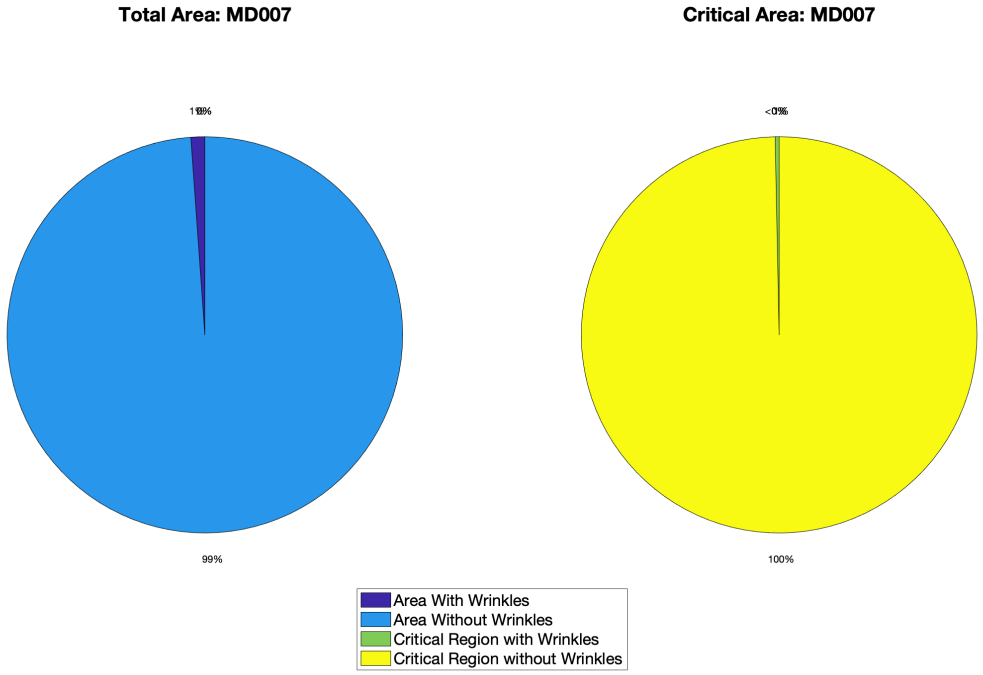


Figure B.20: Continuous Carbon Fiber MD007 Results: Wrinkling (Total Wrinkling = 1.13%, Critical Region Wrinkling = 0.32%)

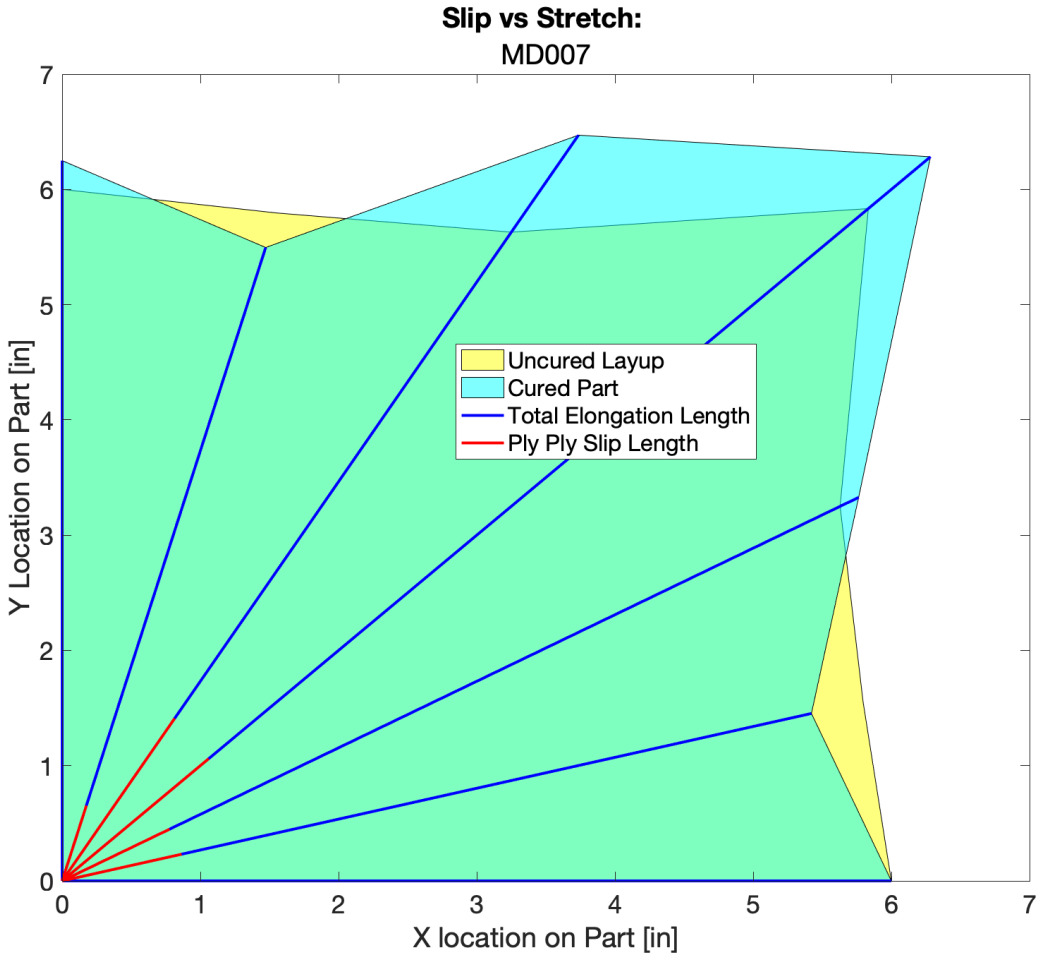


Figure B.21: Continuous Carbon Fiber MD007 Results: Stretching versus Slipping

Part MD008

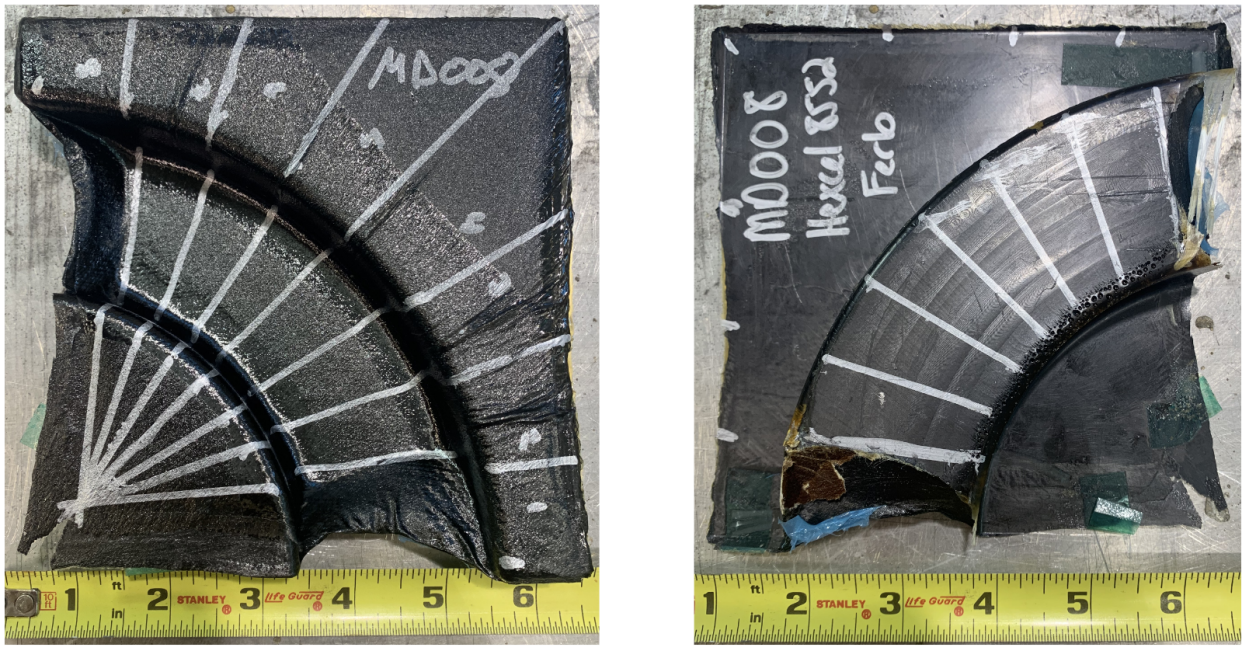


Figure B.22: Continuous Carbon Fiber Curved C Channel Part MD008: Left - Top of Part, Right - Bottom of Part

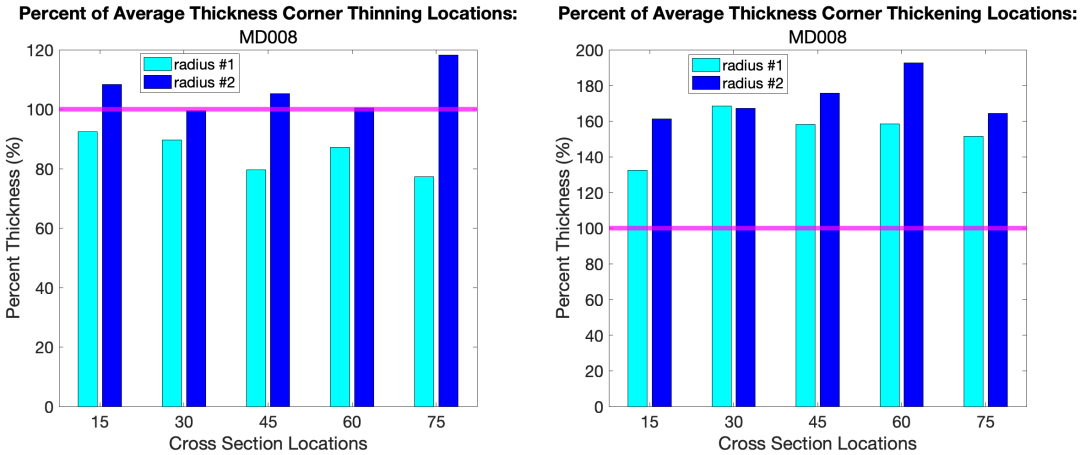


Figure B.23: Continuous Carbon Fiber MD008 Results: Left - Corner Thinning (Average = 95.80%), Right - Corner Thickening (Average = 162.98%)

Table B.8: Continuous Carbon Fiber MD008: Texture Results

Metric	Weight	Ranking	Score
Hairiness	30%	5	-
Additional Resin Pooling	30%	5	-
Spaghettification	10%	5	-
Fractures/Shearing	15%	5	-
Pinholes	10%	5	-
Waves	5%	0	-
Total	100%	X	4.75

Table B.9: Continuous Carbon Fiber MD008: Final Forming Score

Metric	Weight	Ranking	Score
Bridging	12.5%	3	-
Wrinkling	17.5%	3	-
Thickness Variation	15%	3	-
Forming Depth	12.5%	4	-
Corner Thinning	15%	3	-
Corner Thickening	10%	0	-
Resin Pooling	12.5%	3	-
Texture	5%	4.75	-
Total	100%	-	2.91

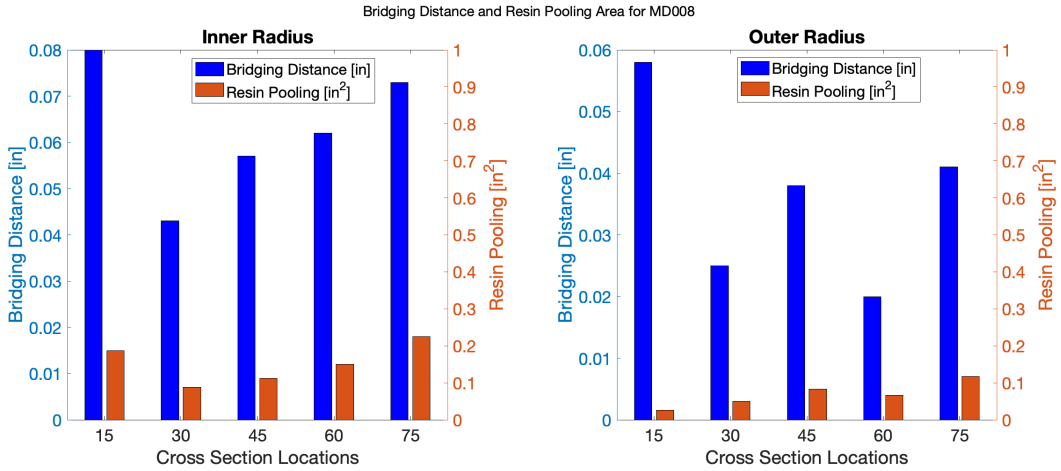


Figure B.24: Continuous Carbon Fiber MD008 Results: Bridging (Average = 0.0497 in) and Resin Pooling (Total = $0.0082 in^2$)

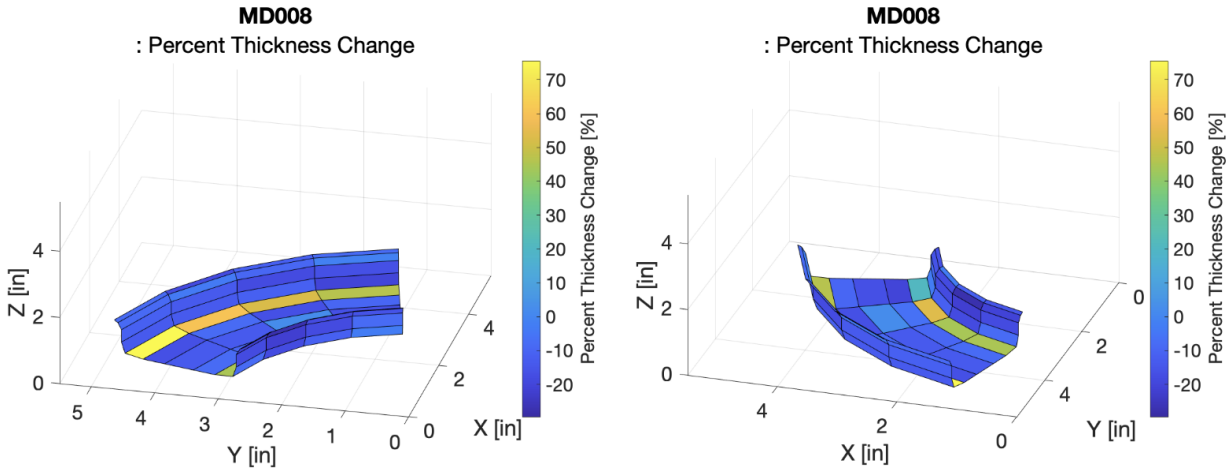


Figure B.25: Continuous Carbon Fiber MD008 Results: Thickness Variation, Left - "Radius #1" Orientation, Right - "Radius #2" Orientation (Coefficient of Variation = 0.1568)

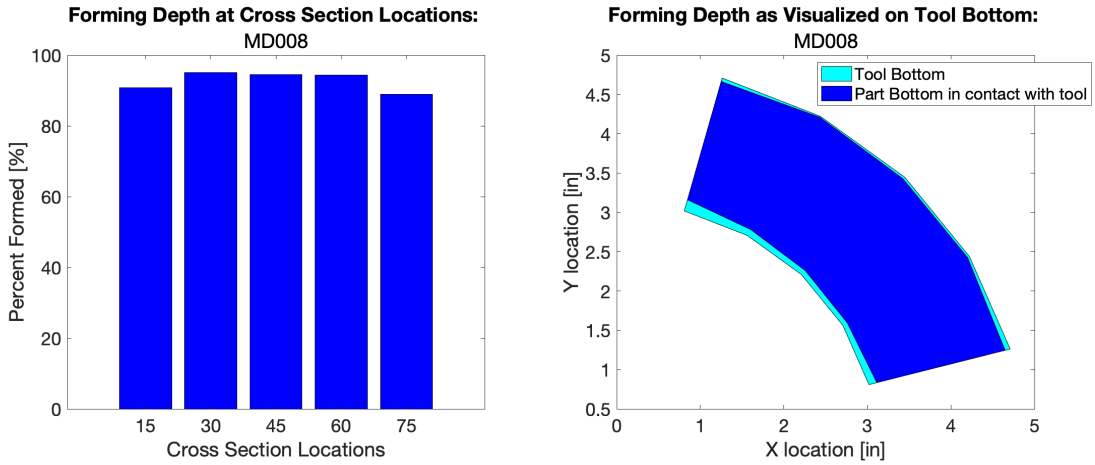


Figure B.26: Continuous Carbon Fiber MD008 Results: Forming Depth (Average = 92.73%)

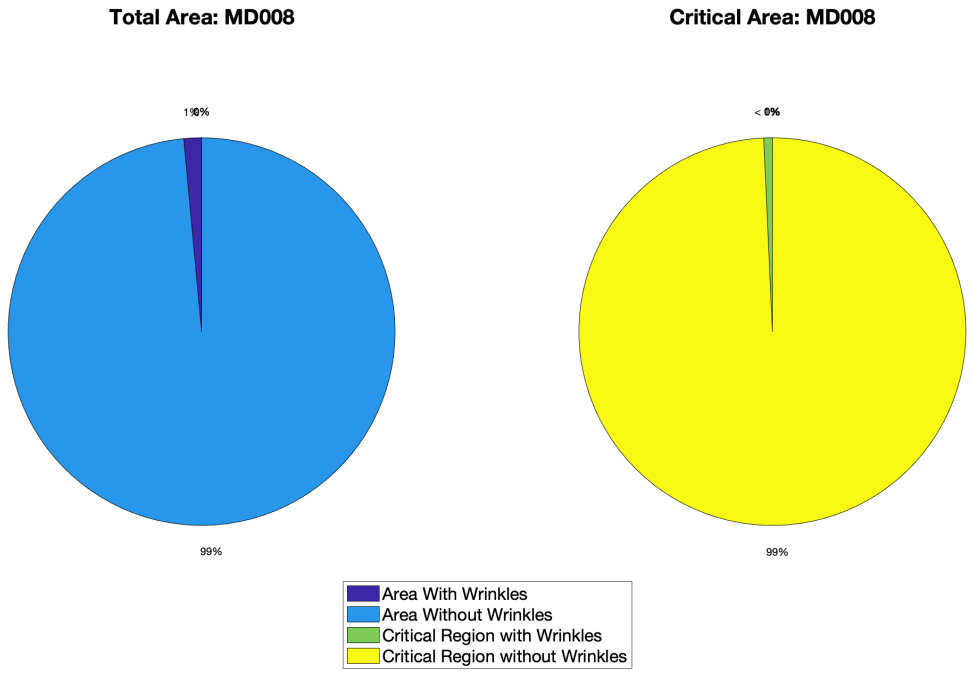


Figure B.27: Continuous Carbon Fiber MD008 Results: Wrinkling (Total Wrinkling = 1.48%, Critical Region Wrinkling = 0.72%)

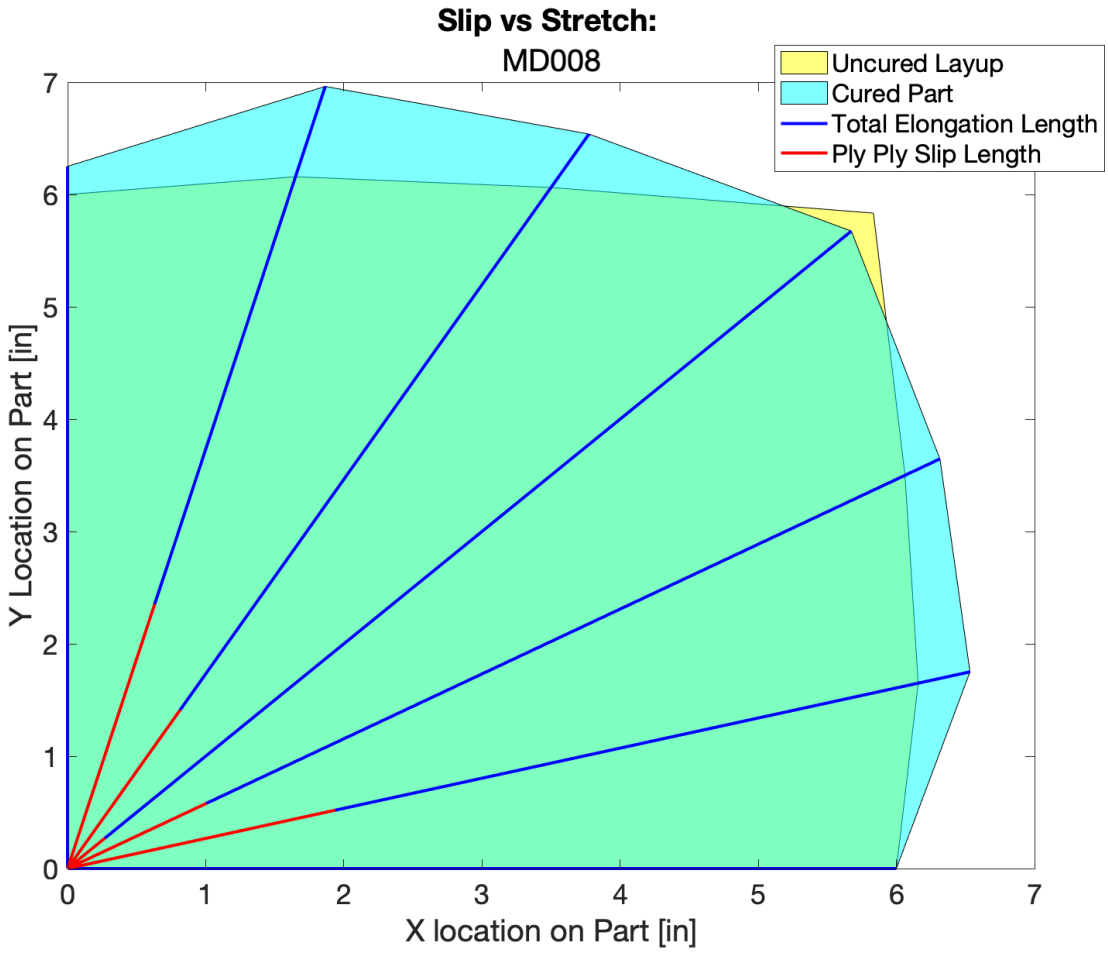


Figure B.28: Continuous Carbon Fiber MD008 Results: Stretching versus Slipping

Part MD009

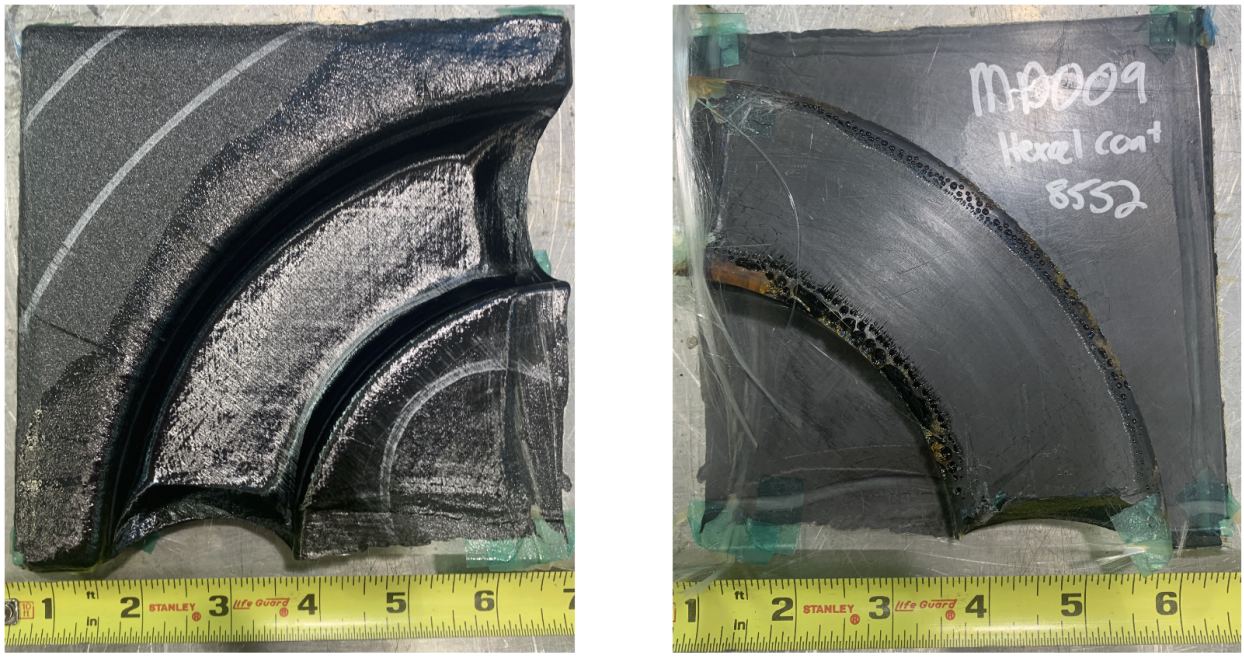


Figure B.29: Continuous Carbon Fiber Curved C Channel Part MD009: Left - Top of Part, Right - Bottom of Part

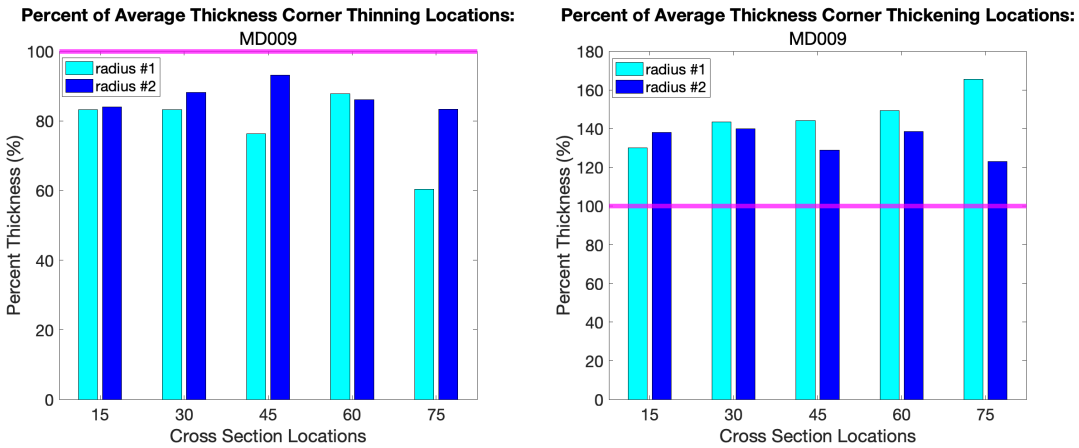


Figure B.30: Continuous Carbon Fiber MD009 Results: Left - Corner Thinning (Average = 82.58%), Right - Corner Thickening (Average = 140.12%)

Table B.10: Continuous Carbon Fiber MD009: Texture Results

Metric	Weight	Ranking	Score
Hairiness	30%	5	-
Additional Resin Pooling	30%	5	-
Spaghettification	10%	5	-
Fractures/Shearing	15%	5	-
Pinholes	10%	5	-
Waves	5%	5	-
Total	100%	X	5

Table B.11: Continuous Carbon Fiber MD009: Final Forming Score

Metric	Weight	Ranking	Score
Bridging	12.5%	2	-
Wrinkling	17.5%	4	-
Thickness Variation	15%	3	-
Forming Depth	12.5%	3	-
Corner Thinning	15%	1	-
Corner Thickening	10%	0	-
Resin Pooling	12.5%	2	-
Texture	5%	5	-
Total	100%	-	2.43

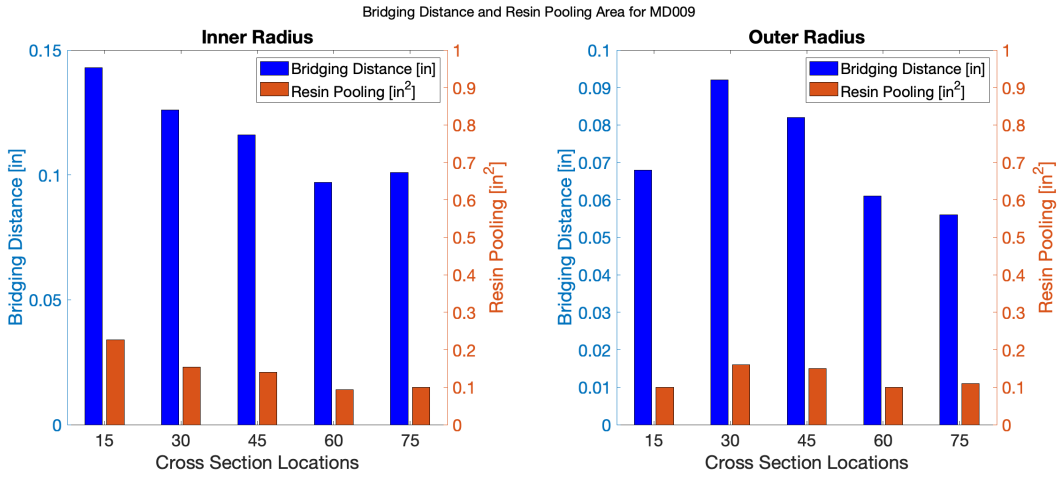


Figure B.31: Continuous Carbon Fiber MD009 Results: Bridging (Average = 0.0942 in) and Resin Pooling (Total = $0.0169 in^2$)

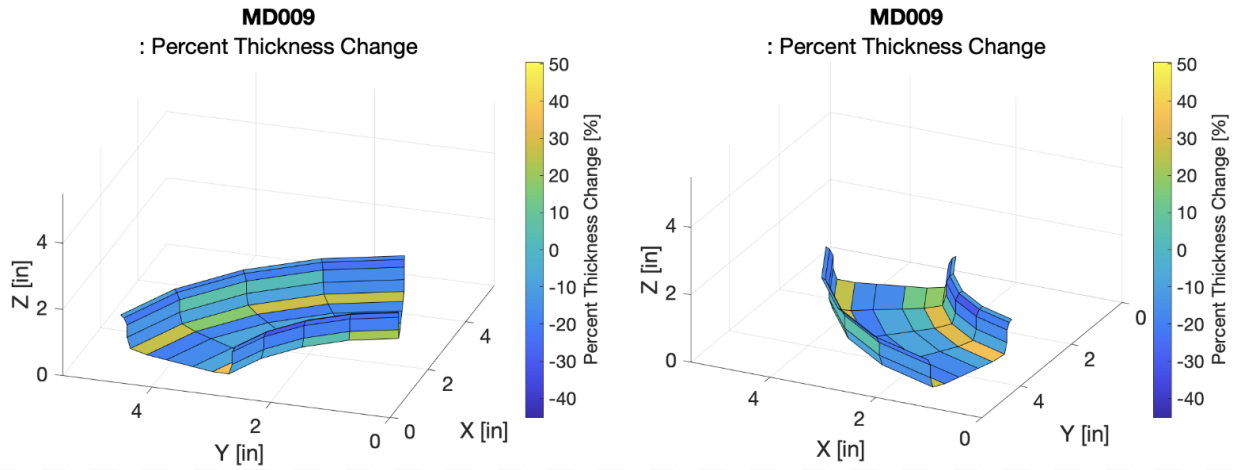


Figure B.32: Continuous Carbon Fiber MD009 Results: Thickness Variation, Left - "Radius #1" Orientation, Right - "Radius #2" Orientation (Coefficient of Variation = 0.1126)

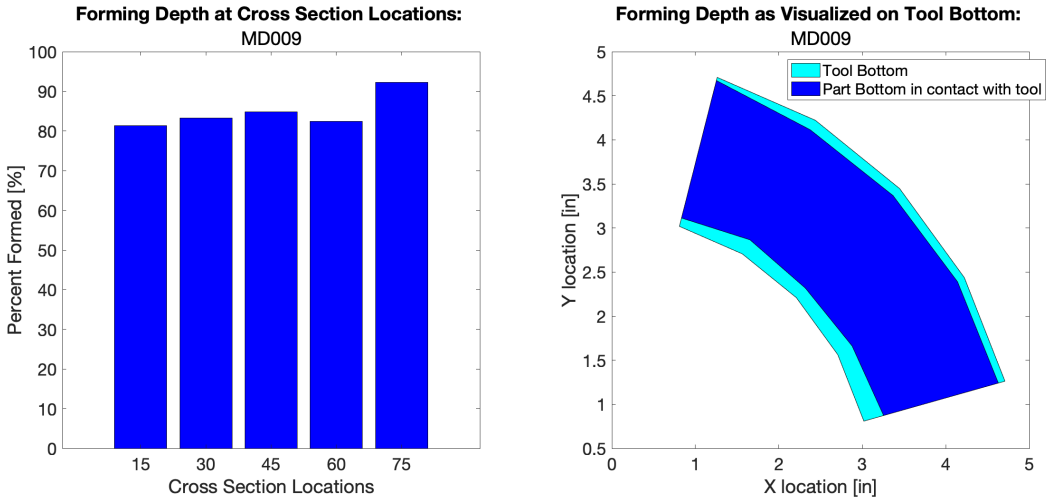


Figure B.33: Continuous Carbon Fiber MD009 Results: Forming Depth (Average = 84.83)

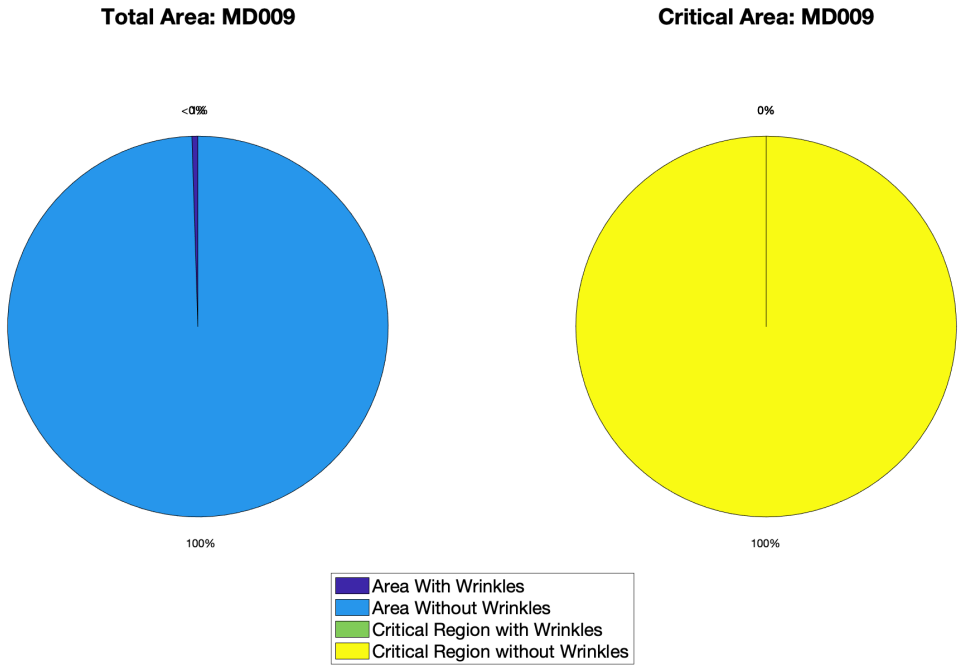


Figure B.34: Continuous Carbon Fiber MD009 Results: Wrinkling (Total Wrinkling = 0.50%, Critical Region Wrinkling = 0%)

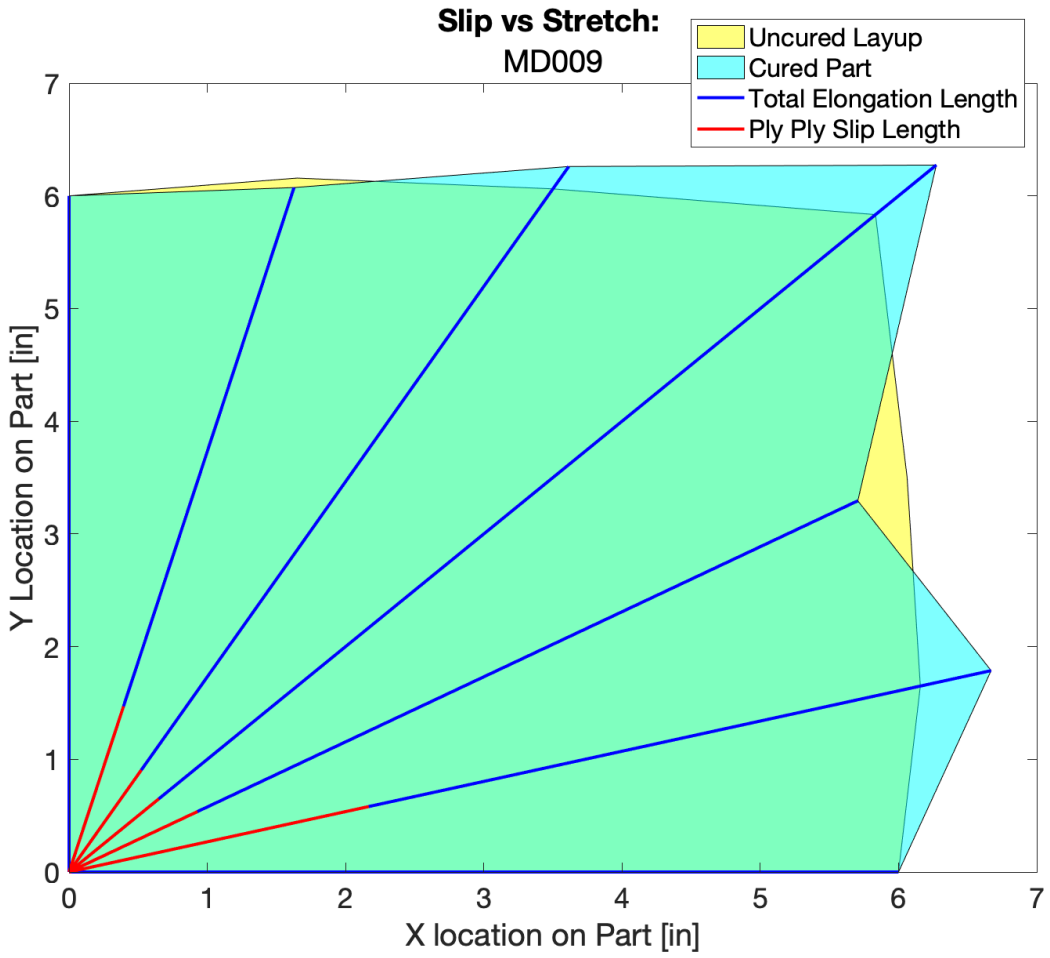


Figure B.35: Continuous Carbon Fiber MD009 Results: Stretching versus Slipping

Part MD011

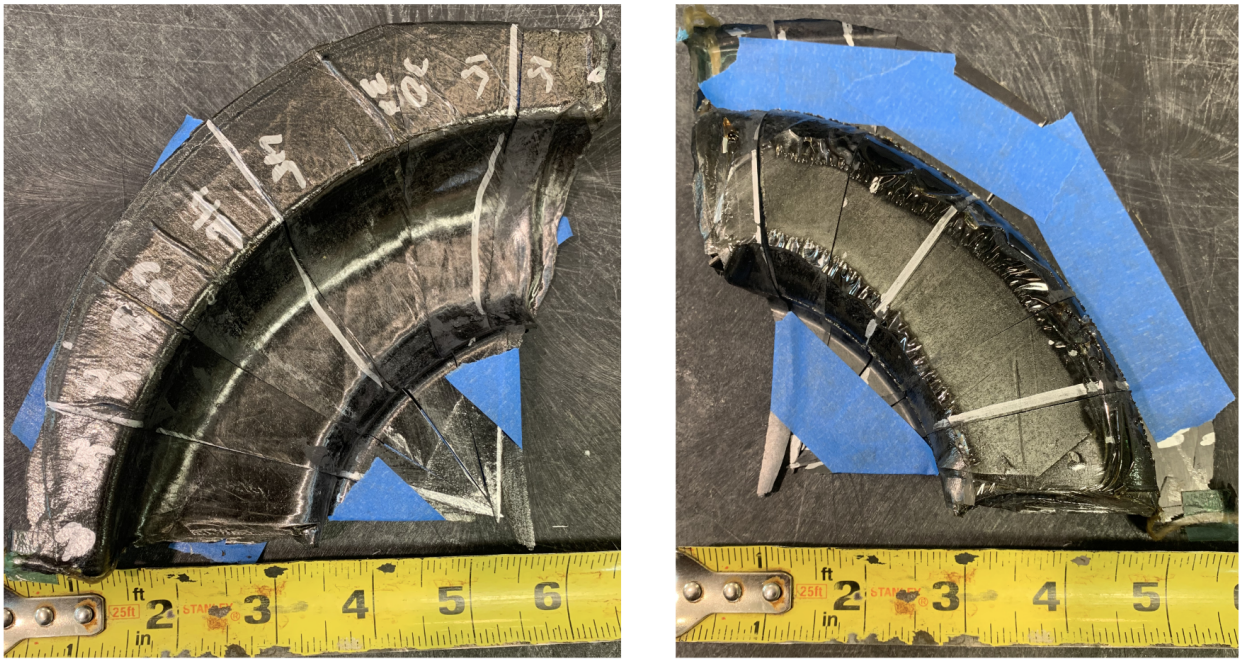


Figure B.36: Stretch Broken Carbon Fiber Curved C Channel Part MD011: Left - Top of Part, Right - Bottom of Part

Table B.12: Stretch Broken Carbon Fiber MD011: Texture Results

Metric	Weight	Ranking	Score
Hairiness	30%	3	-
Additional Resin Pooling	30%	3	-
Spaghettification	10%	5	-
Fractures/Shearing	15%	5	-
Pinholes	10%	5	-
Waves	5%	0	-
Total	100%	X	3.55

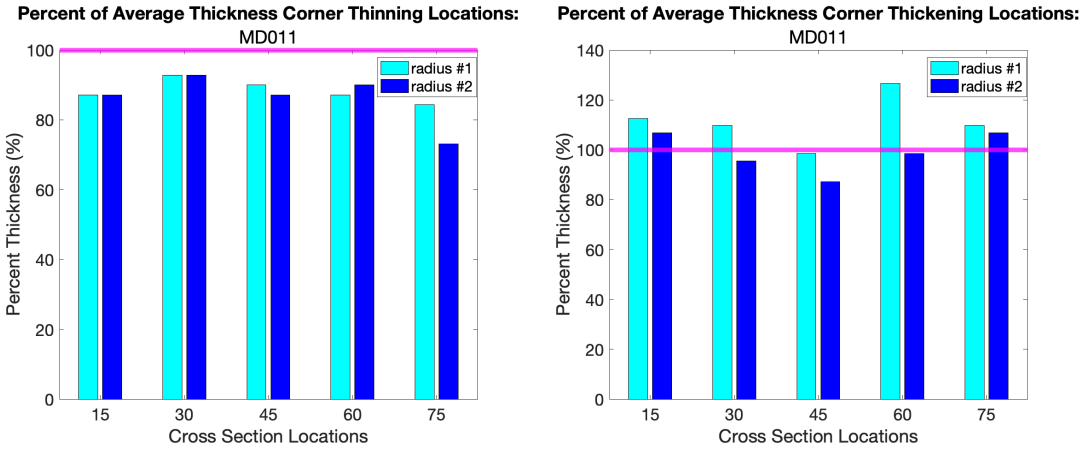


Figure B.37: Stretch Broken Carbon Fiber MD011 Results: Left - Corner Thinning (Average = 87.18%), Right - Corner Thickening (Average = 105.17%)

Table B.13: Stretch Broken Carbon Fiber MD011: Final Forming Score

Metric	Weight	Ranking	Score
Bridging	12.5%	1	-
Wrinkling	17.5%	4	-
Thickness Variation	15%	3	-
Forming Depth	12.5%	2	-
Corner Thinning	15%	1	-
Corner Thickening	10%	3	-
Resin Pooling	12.5%	4	-
Texture	5%	3.55	-
Total	100%	-	2.65

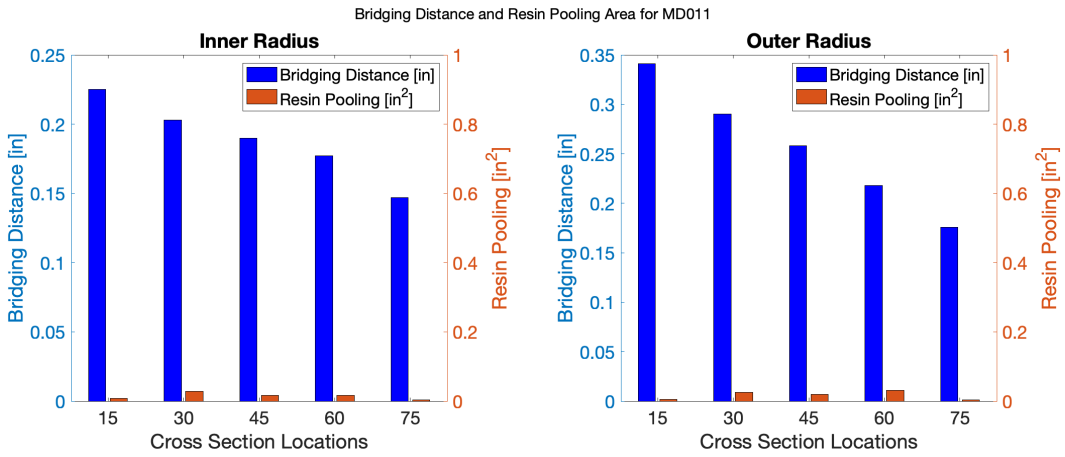


Figure B.38: Stretch Broken Carbon Fiber MD011 Results: Bridging (Average = 0.2225 in) and Resin Pooling (Total = $0.0048 in^2$)

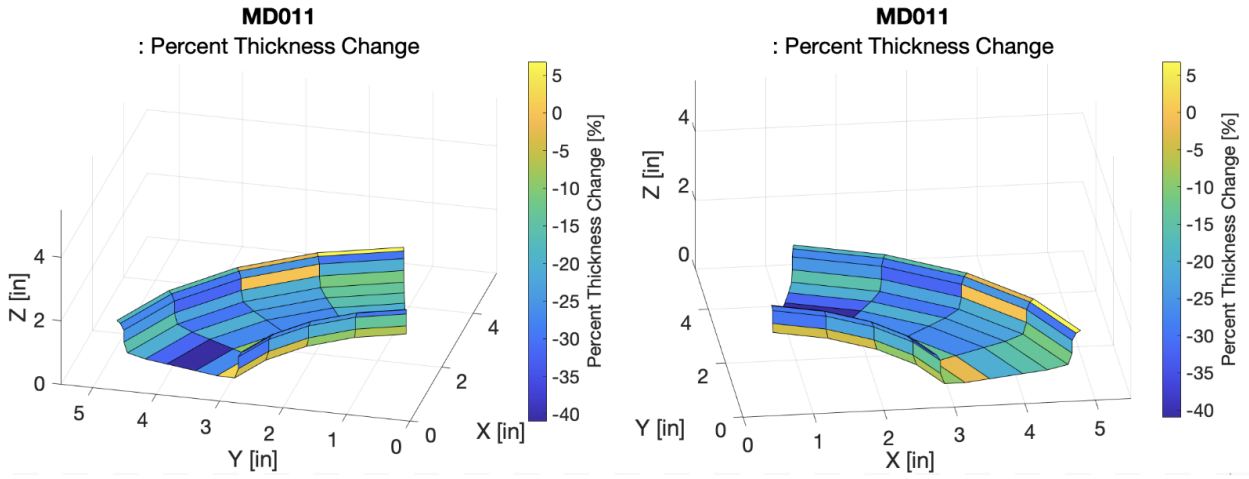


Figure B.39: Stretch Broken Carbon Fiber MD011 Results: Thickness Variation, Left - "Radius #1" Orientation, Right - "Radius #2" Orientation (Coefficient of Variation = 0.1245)

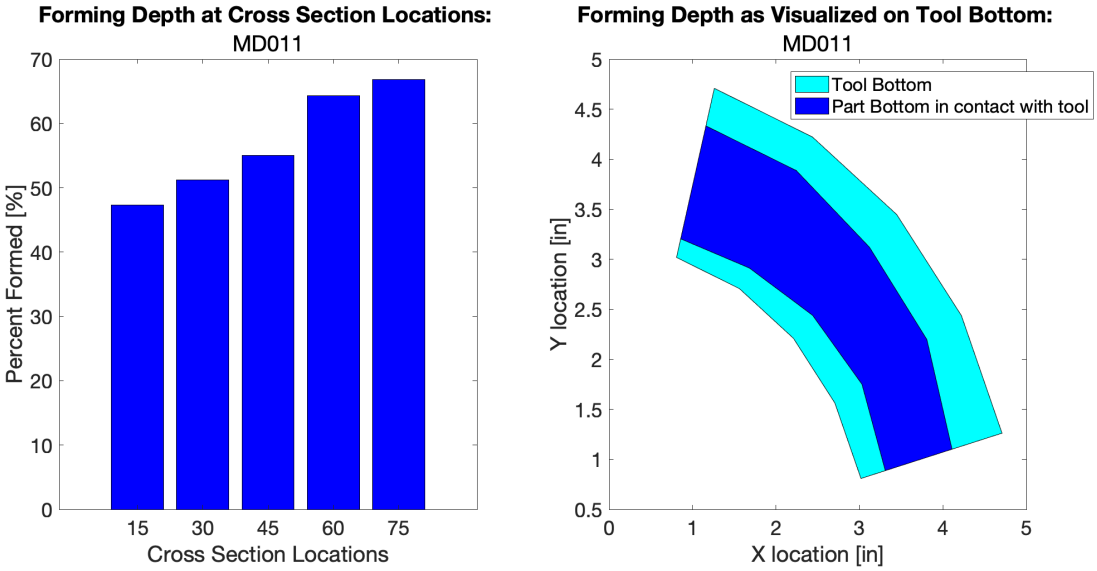


Figure B.40: Stretch Broken Carbon Fiber MD011 Results: Forming Depth (Average = 56.94%)

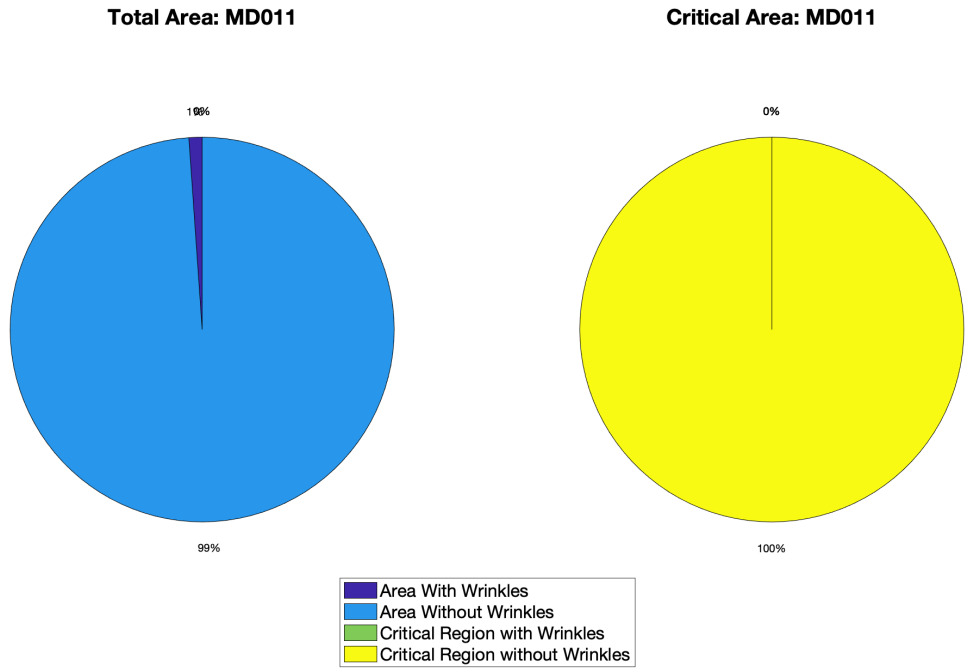


Figure B.41: Stretch Broken Carbon Fiber MD011 Results: Wrinkling (Total Wrinkling = 1.11%, Critical Region Wrinkling = 0%)

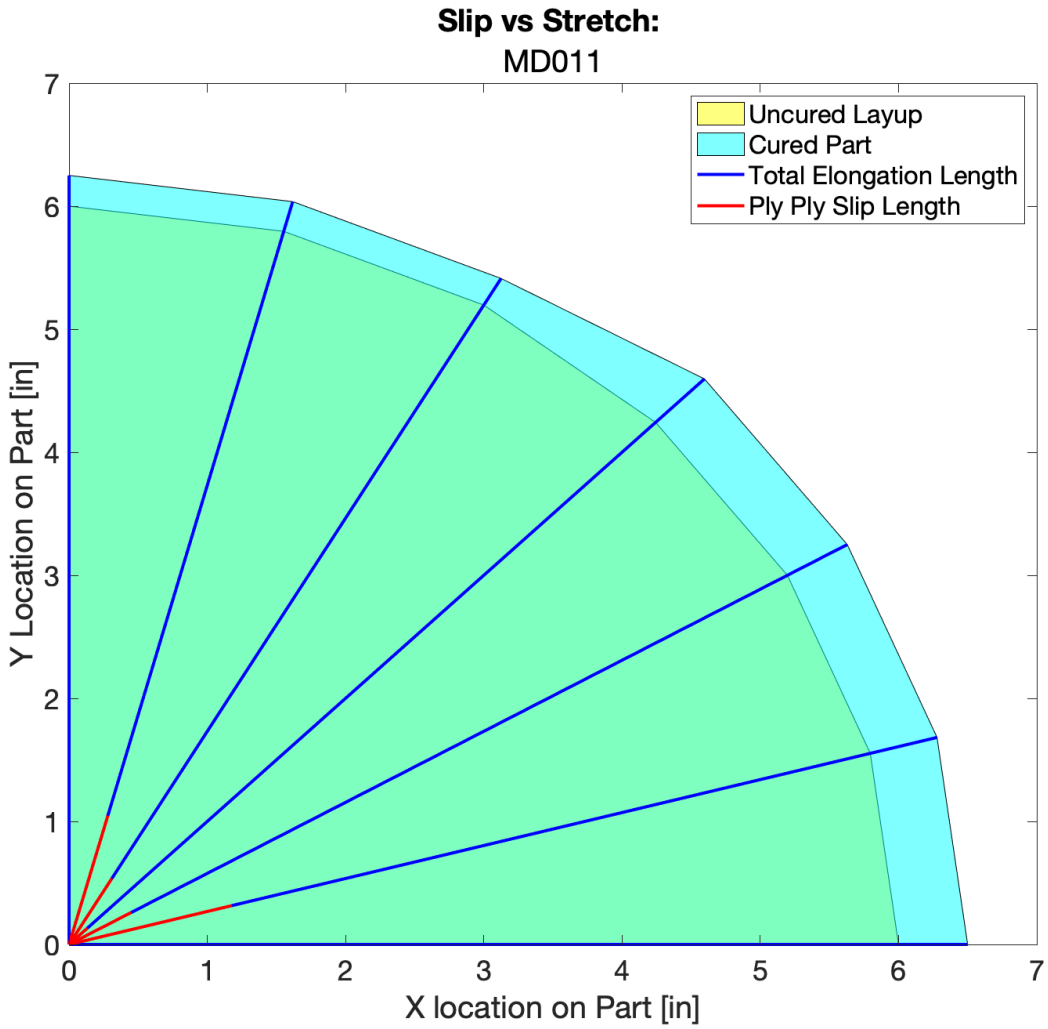


Figure B.42: Stretch Broken Carbon Fiber MD011 Results: Stretching versus Slipping

Part MD012

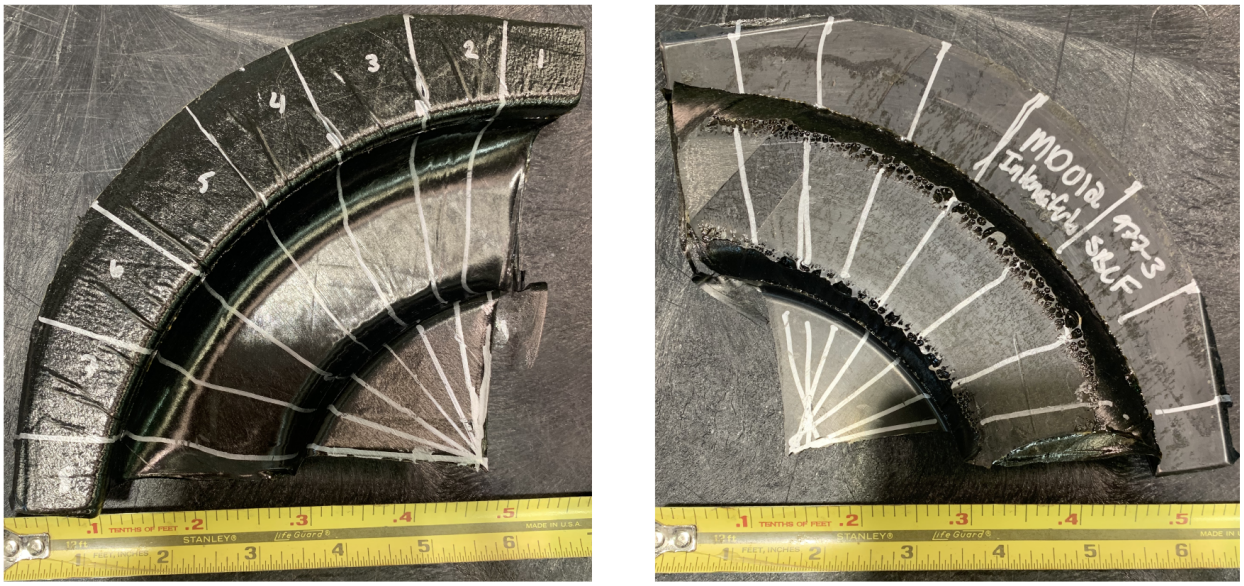


Figure B.43: Stretch Broken Carbon Fiber Curved C Channel Part MD012: Left - Top of Part, Right - Bottom of Part

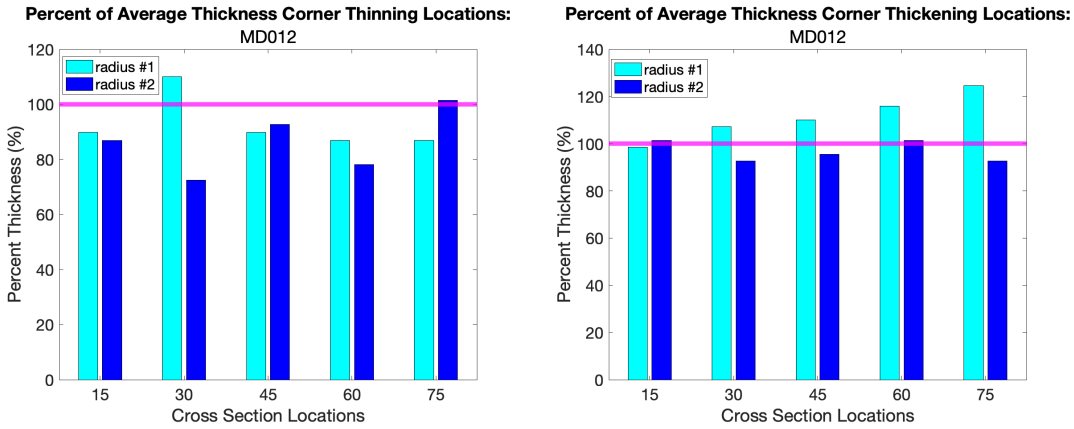


Figure B.44: Stretch Broken Carbon Fiber MD012 Results: Left - Corner Thinning (Average = 89.51%), Right - Corner Thickening (Average = 104.00%)

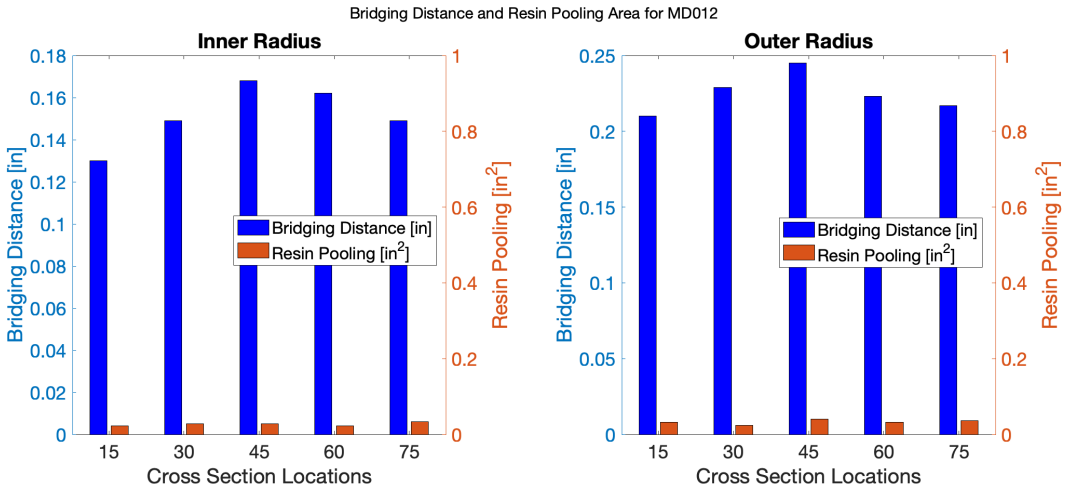


Figure B.45: Stretch Broken Carbon Fiber MD012 Results: Bridging (Average = 0.1882 in) and Resin Pooling (Total = $0.0065in^2$)

Table B.14: Stretch Broken Carbon Fiber MD012: Texture Results

Metric	Weight	Ranking	Score
Hairiness	30%	3	-
Additional Resin Pooling	30%	3	-
Spaghettification	10%	5	-
Fractures/Shearing	15%	5	-
Pinholes	10%	5	-
Waves	5%	5	-
Total	100%	X	3.8

Table B.15: Stretch Broken Carbon Fiber MD012: Final Forming Score

Metric	Weight	Ranking	Score
Bridging	12.5%	1	-
Wrinkling	17.5%	3	-
Thickness Variation	15%	3	-
Forming Depth	12.5%	2	-
Corner Thinning	15%	2	-
Corner Thickening	10%	4	-
Resin Pooling	12.5%	3	-
Texture	5%	3.8	-
Total	100%	-	2.62

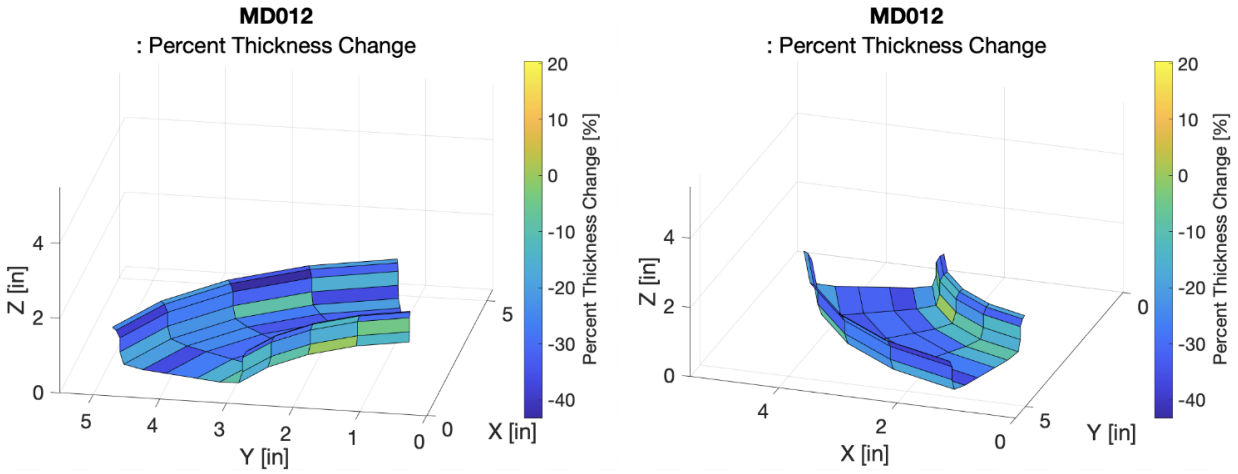


Figure B.46: Stretch Broken Carbon Fiber MD012 Results: Thickness Variation, Left - "Radius #1" Orientation, Right - "Radius #2" Orientation (Coefficient of Variation = 0.1511)

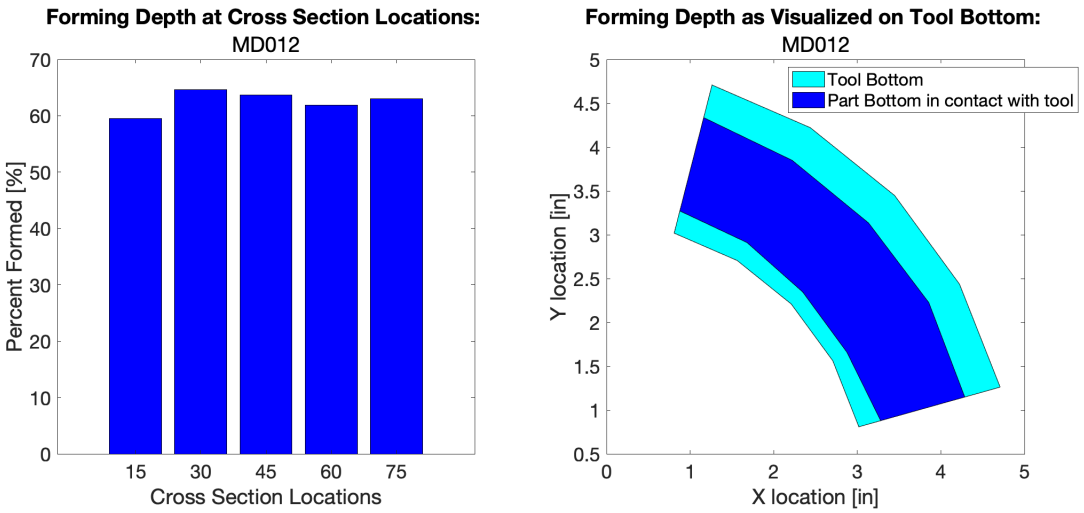


Figure B.47: Stretch Broken Carbon Fiber MD012 Results: Forming Depth (Average = 62.56%)

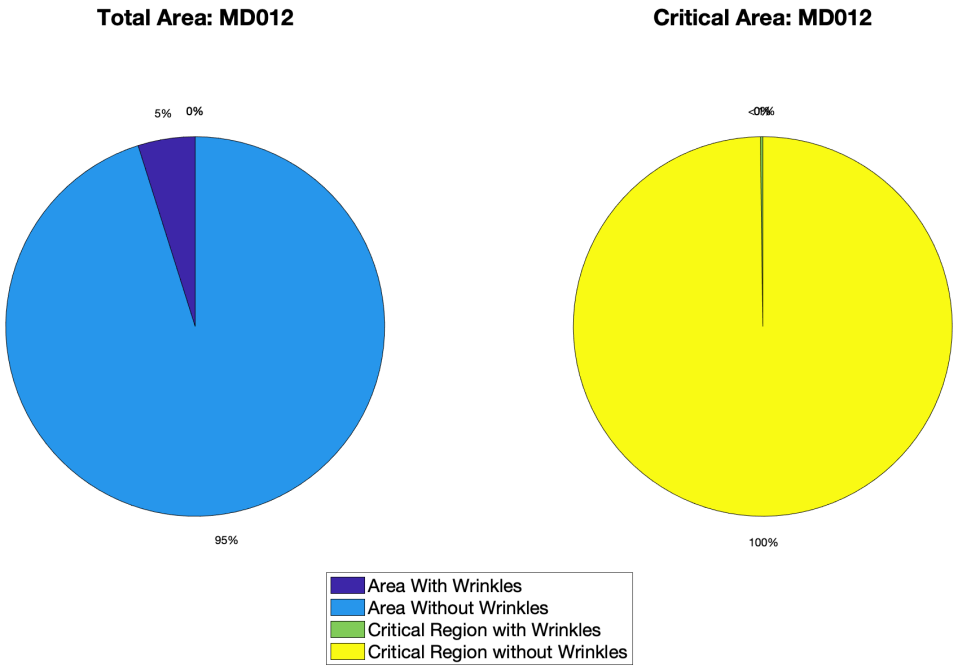


Figure B.48: Stretch Broken Carbon Fiber MD012 Results: Wrinkling (Total Wrinkling = 4.88%, Critical Region Wrinkling = 0.20%)

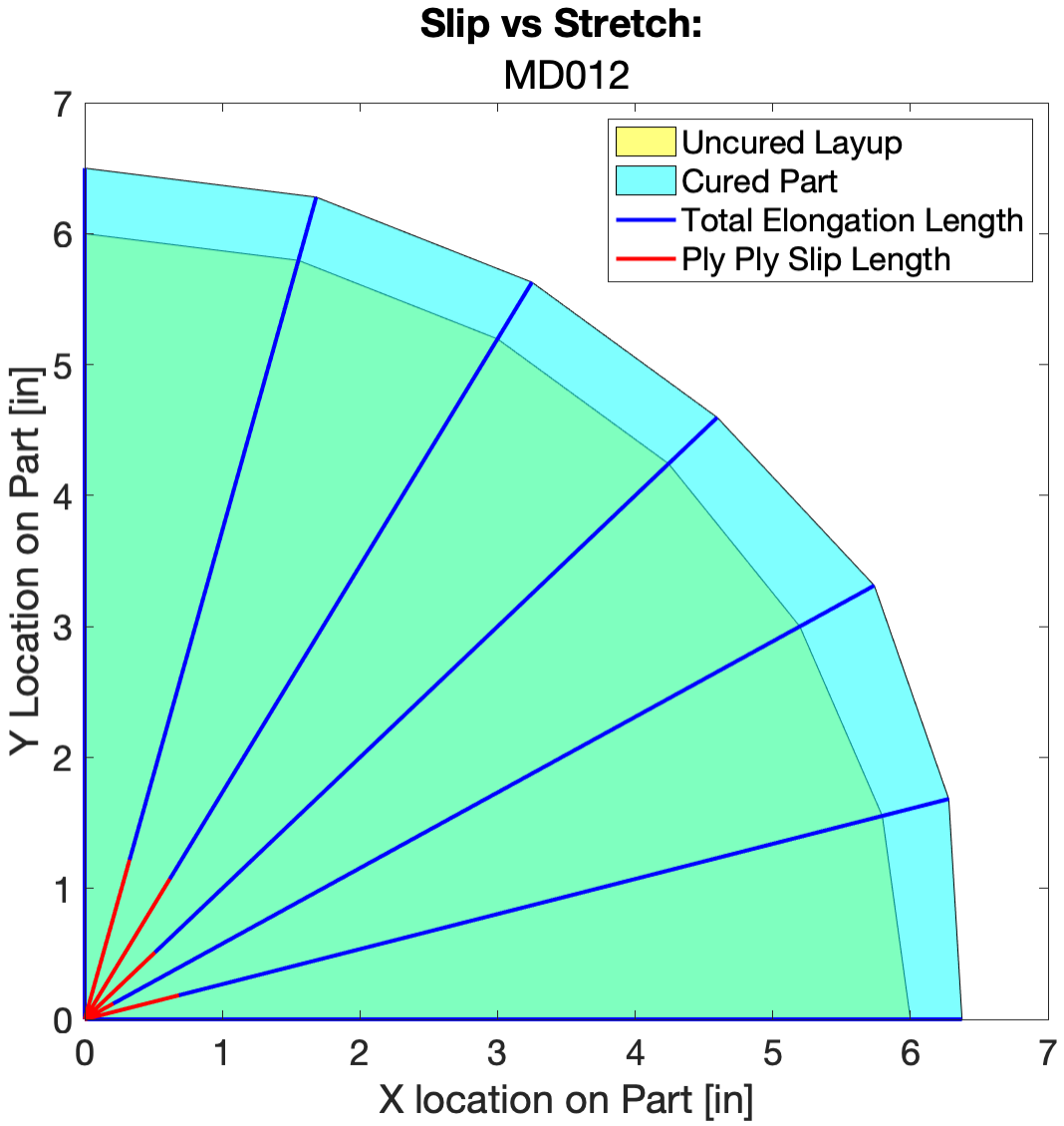


Figure B.49: Stretch Broken Carbon Fiber MD012 Results: Stretching versus Slipping

Part MD017

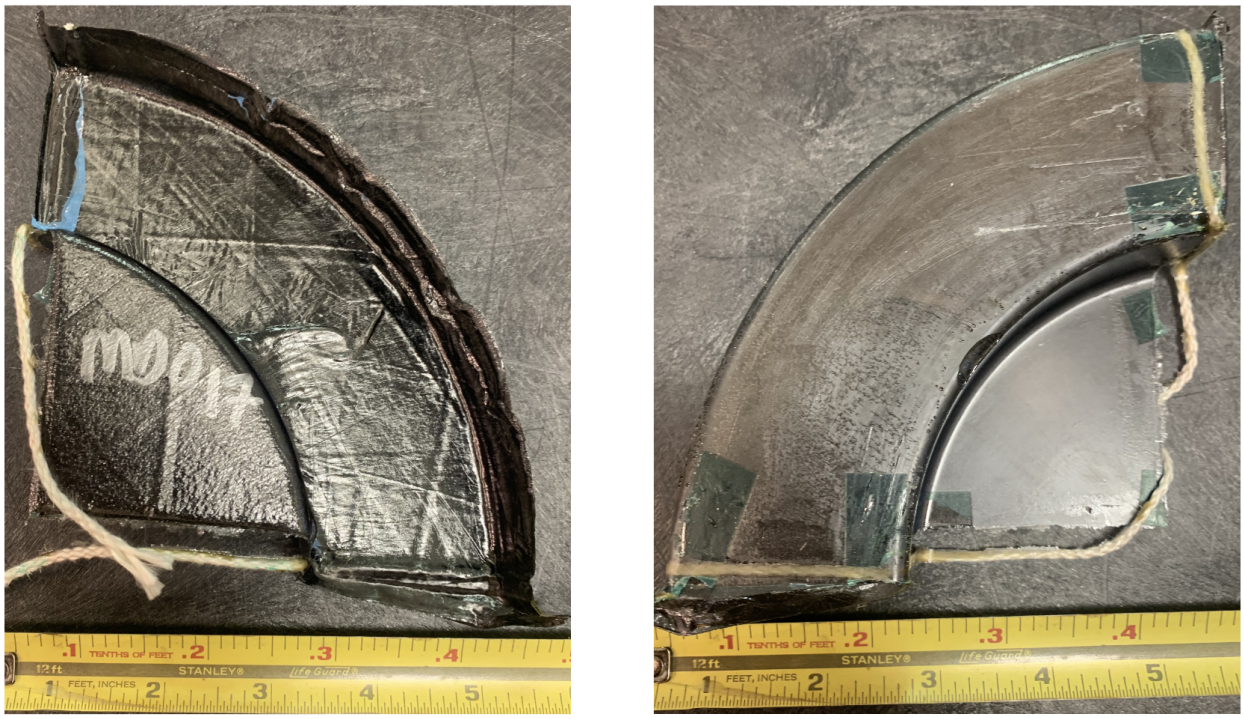


Figure B.50: Stretch Broken Carbon Fiber Curved C Channel Part MD017: Left - Top of Part, Right - Bottom of Part

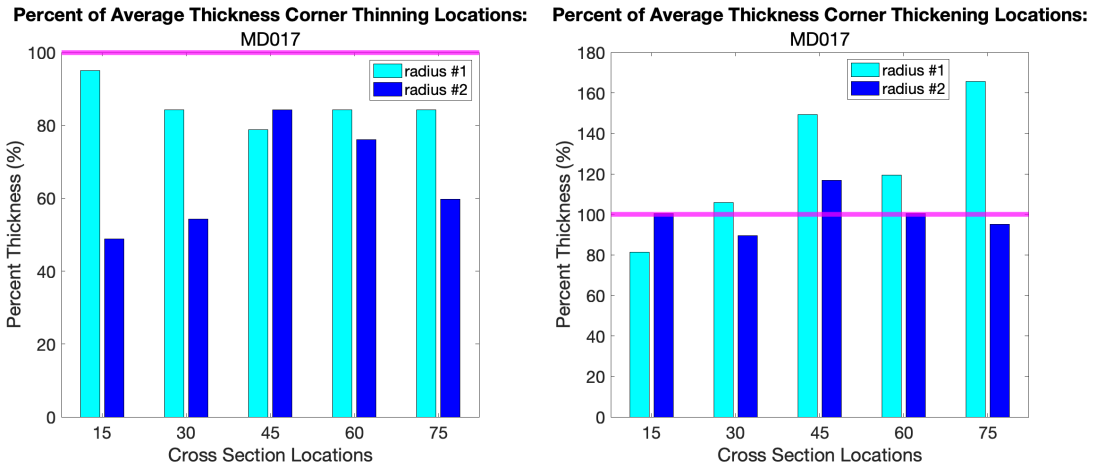


Figure B.51: Stretch Broken Carbon Fiber MD017 Results: Left - Corner Thinning (Average = 75.64%), Right - Corner Thickening (Average = 113.46%)

Table B.16: Stretch Broken Carbon Fiber MD017: Texture Results

Metric	Weight	Ranking	Score
Hairiness	30%	5	-
Additional Resin Pooling	30%	3	-
Spaghettification	10%	5	-
Fractures/Shearing	15%	0	-
Pinholes	10%	5	-
Waves	5%	5	-
Total	100%	X	3.65

Table B.17: Stretch Broken Carbon Fiber MD017: Final Forming Score

Metric	Weight	Ranking	Score
Bridging	12.5%	4	-
Wrinkling	17.5%	3	-
Thickness Variation	15%	2	-
Forming Depth	12.5%	4	-
Corner Thinning	15%	0	-
Corner Thickening	10%	3	-
Resin Pooling	12.5%	4	-
Texture	5%	3.65	-
Total	100%	-	2.81

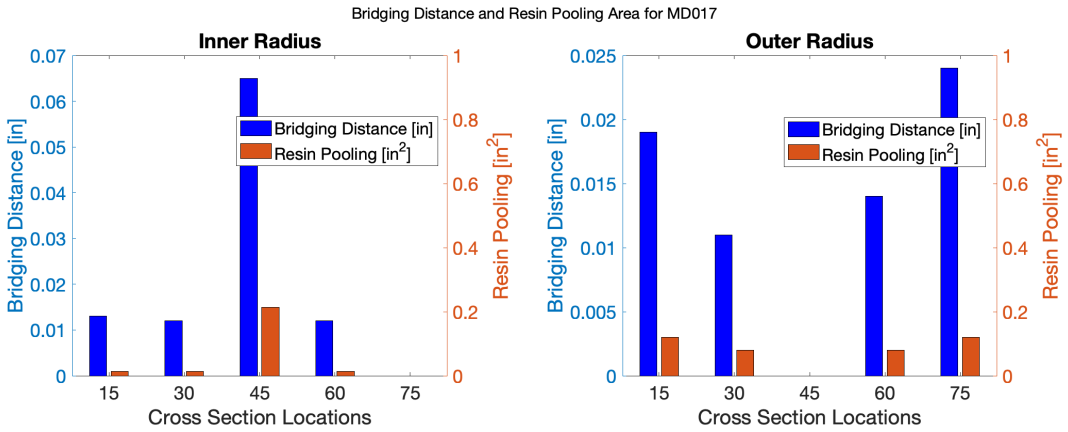


Figure B.52: Stretch Broken Carbon Fiber MD017 Results: Bridging (Average = 0.0170 in) and Resin Pooling (Total = $0.0028 in^2$)

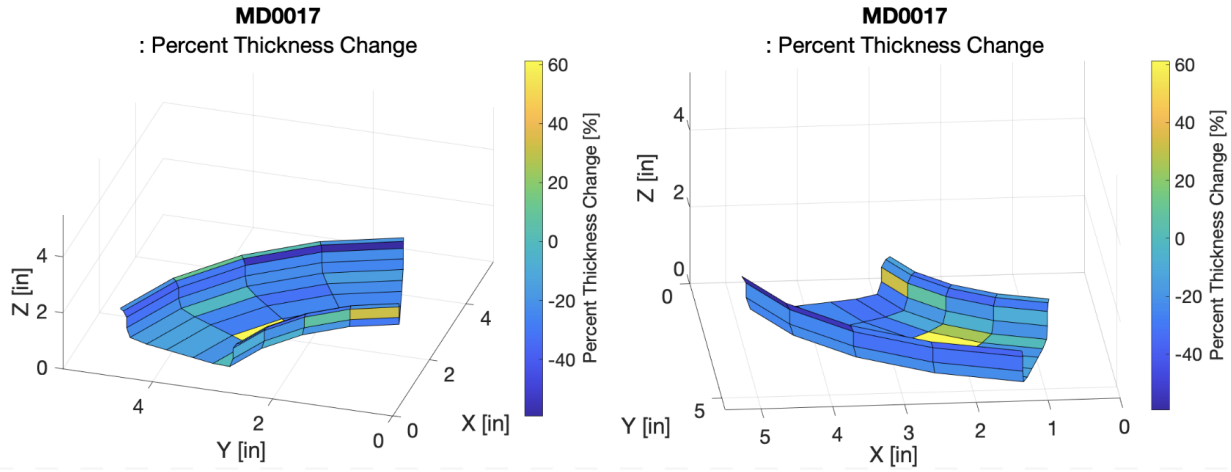


Figure B.53: Stretch Broken Carbon Fiber MD017 Results: Thickness Variation, Left - "Radius #1" Orientation, Right - "Radius #2" Orientation (Coefficient of Variation = 0.2089)

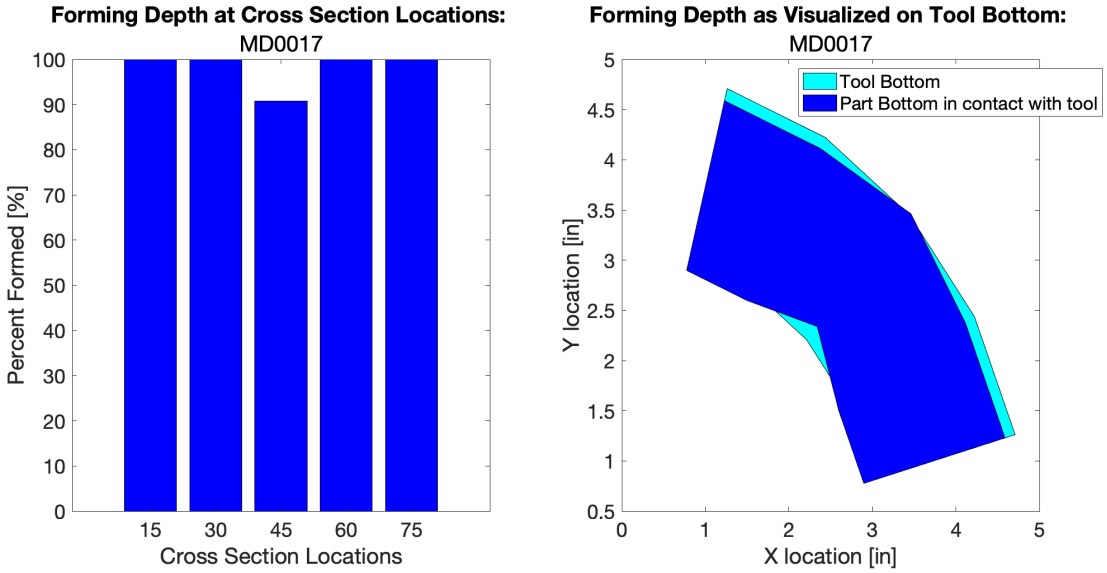


Figure B.54: Stretch Broken Carbon Fiber MD017 Results: Forming Depth (Average = 98.15%)

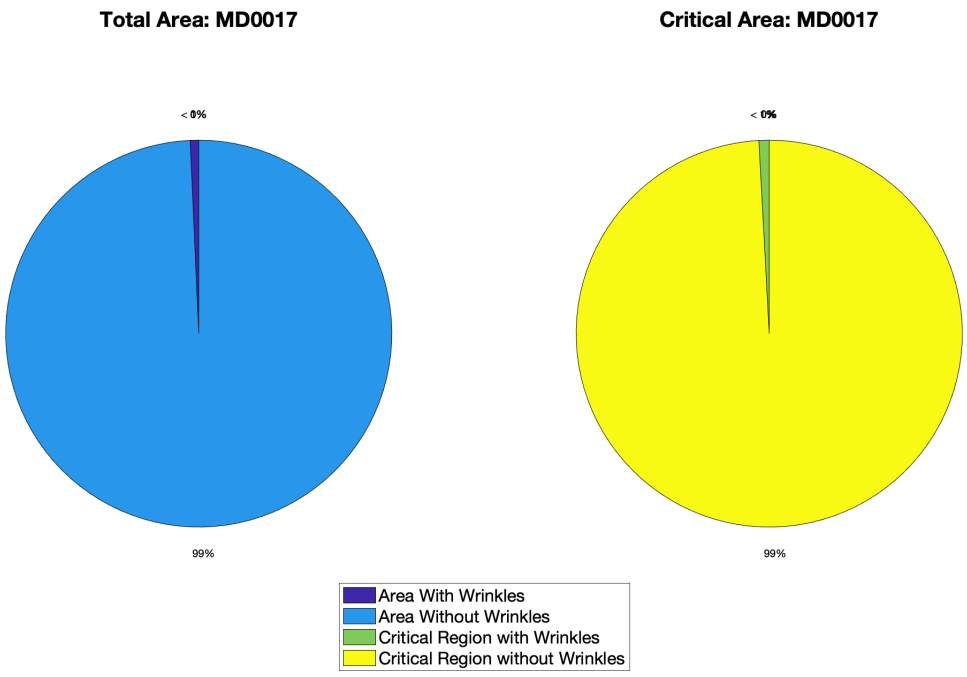


Figure B.55: Stretch Broken Carbon Fiber MD017 Results: Wrinkling (Total Wrinkling = 0.71%, Critical Region Wrinkling = 0.86%)

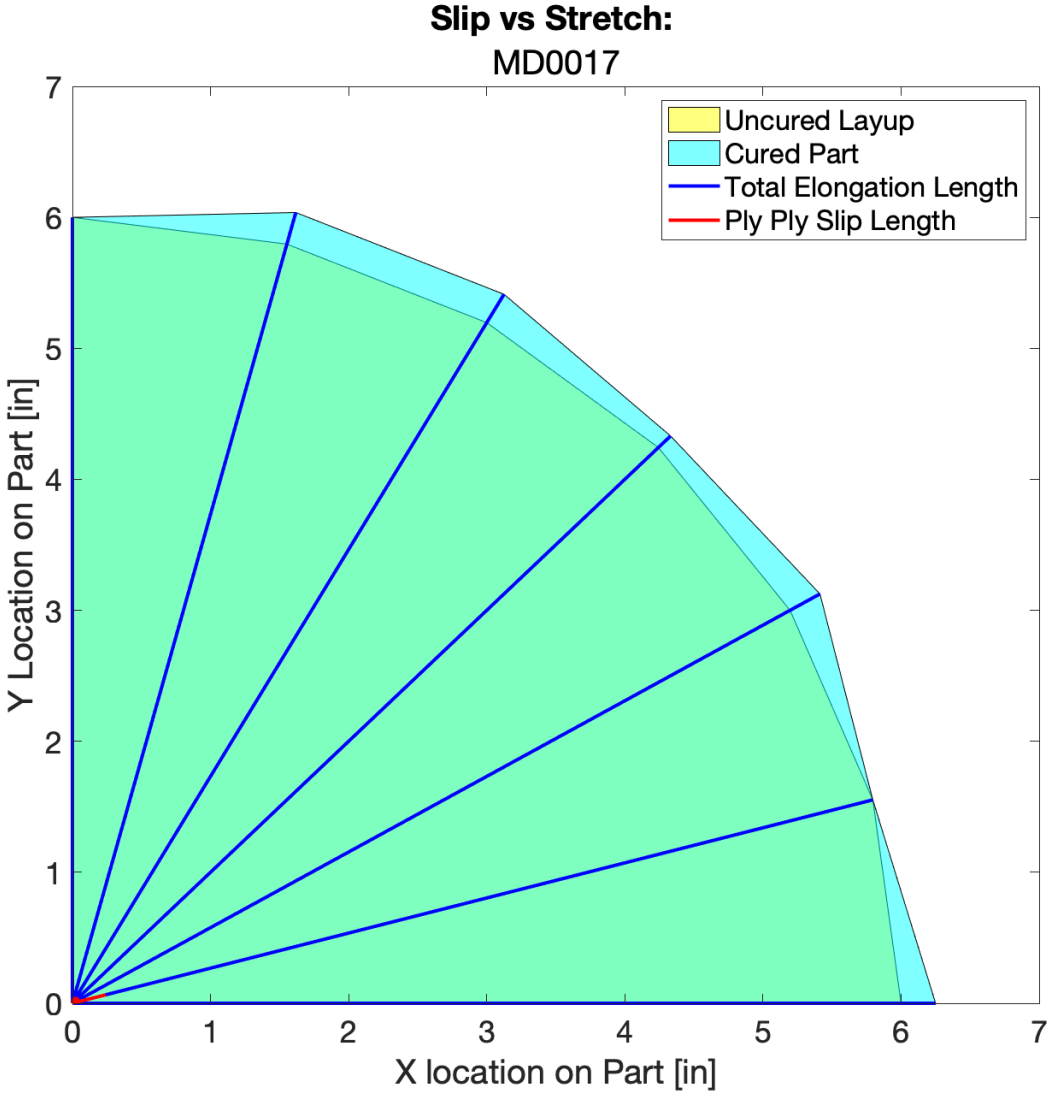


Figure B.56: Stretch Broken Carbon Fiber MD017 Results: Stretching versus Slipping

Part MD020



Figure B.57: Continuous Carbon Fiber Curved C Channel Part MD020: Left - Top of Part, Right - Bottom of Part

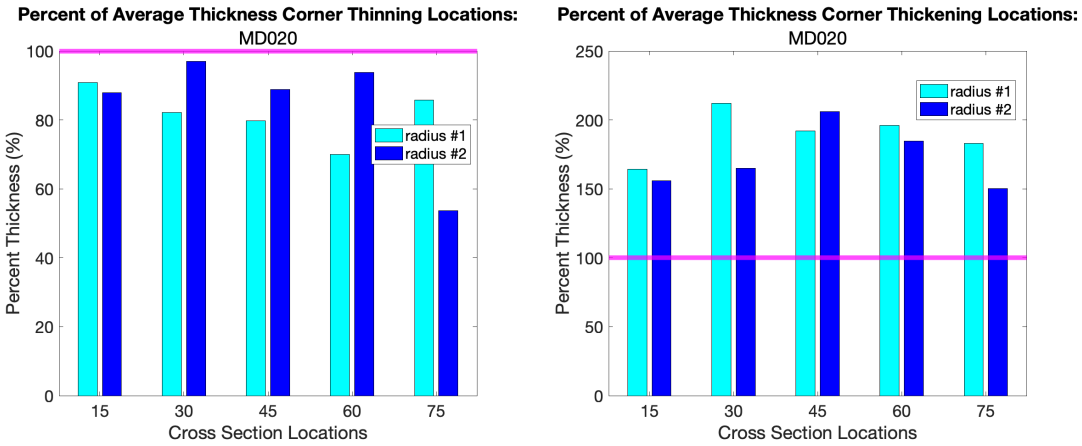


Figure B.58: Continuous Carbon Fiber MD020 Results: Left - Corner Thinning (Average = 82.97%), Right - Corner Thickening (Average = 180.94%)

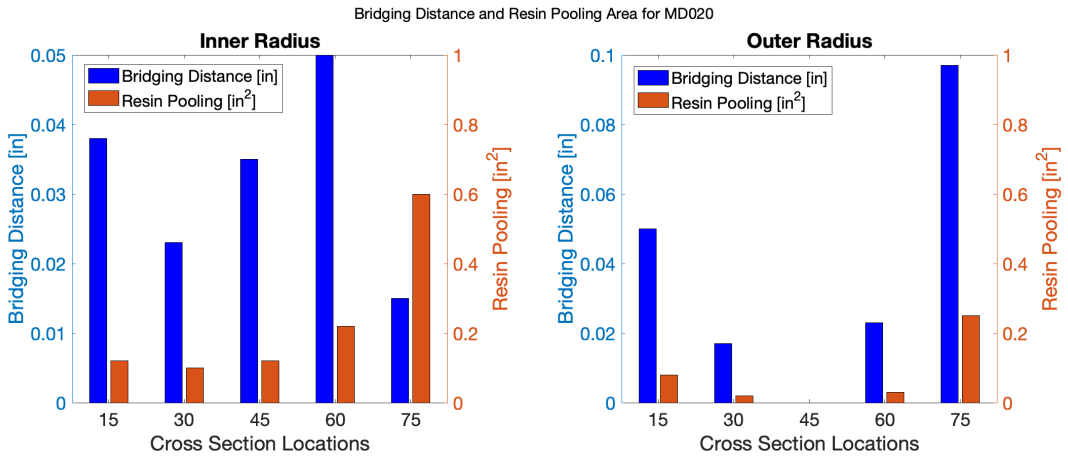


Figure B.59: Continuous Carbon Fiber MD020 Results: Bridging (Average = 0.0348 in) and Resin Pooling (Total = $0.0096 in^2$)

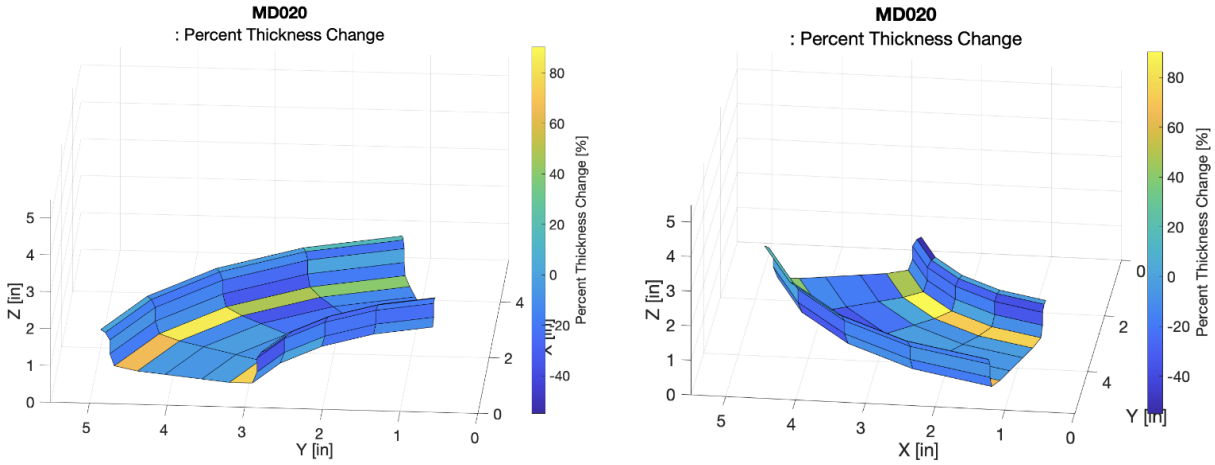


Figure B.60: Continuous Carbon Fiber MD020 Results: Thickness Variation, Left - "Radius #1" Orientation, Right - "Radius #2" Orientation (Coefficient of Variation = 0.1770)

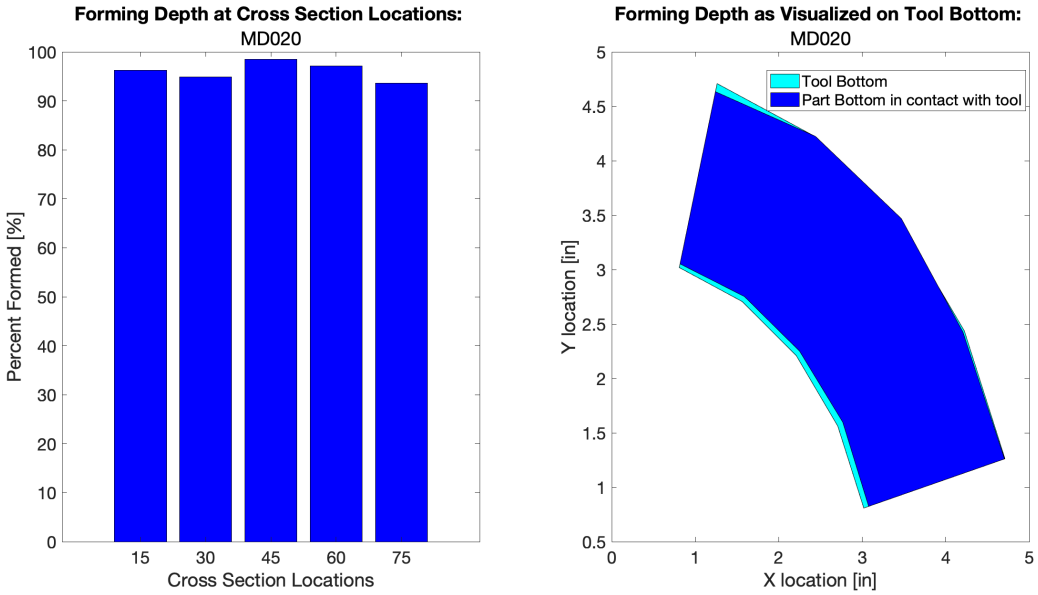


Figure B.61: Continuous Carbon Fiber MD020 Results: Forming Depth (Average = 96.06%)

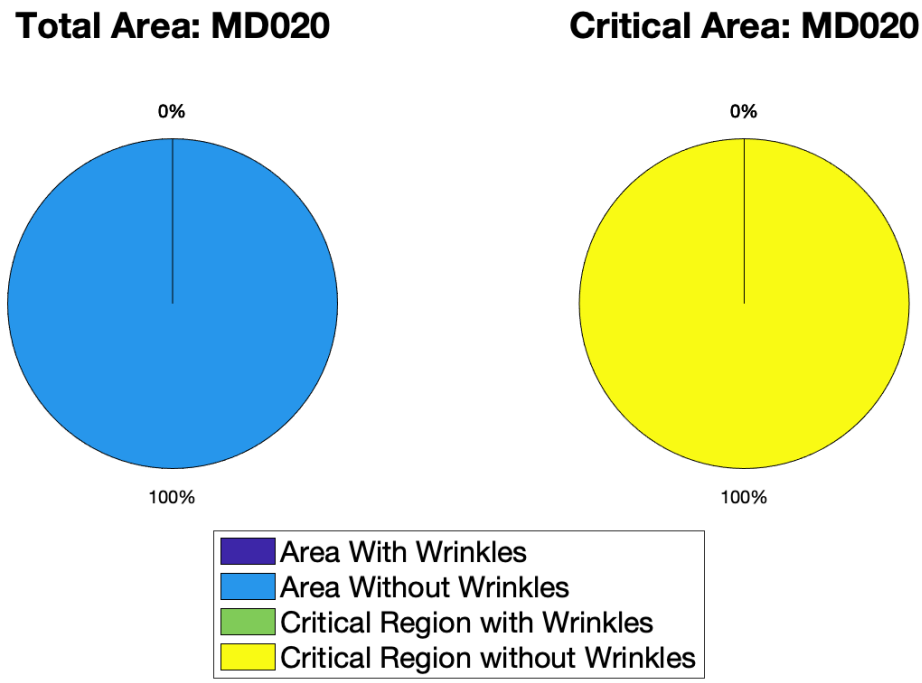


Figure B.62: Continuous Carbon Fiber MD020 Results: Wrinkling (Total Wrinkling = 0%, Critical Region Wrinkling = 0%)

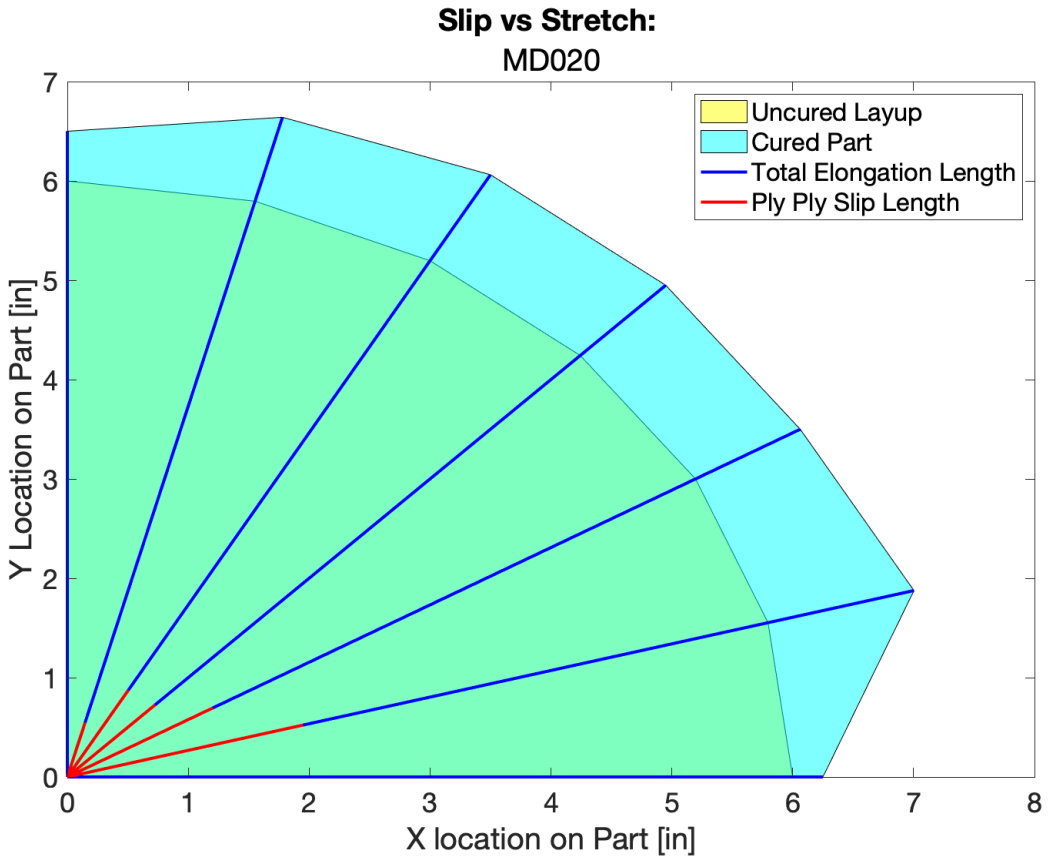


Figure B.63: Continuous Carbon Fiber MD020 Results: Stretching versus Slipping

Table B.18: Continuous Carbon Fiber MD020: Texture Results

Metric	Weight	Ranking	Score
Hairiness	30%	5	-
Additional Resin Pooling	30%	5	-
Spaghettification	10%	5	-
Fractures/Shearing	15%	5	-
Pinholes	10%	5	-
Waves	5%	0	-
Total	100%	X	4.75

Table B.19: Continuous Carbon Fiber MD020: Final Forming Score

Metric	Weight	Ranking	Score
Bridging	12.5%	3	-
Wrinkling	17.5%	5	-
Thickness Variation	15%	3	-
Forming Depth	12.5%	4	-
Corner Thinning	15%	1	-
Corner Thickening	10%	0	-
Resin Pooling	12.5%	3	-
Texture	5%	4.75	-
Total	100%	-	2.96

Unscored Curved C Channel Trial

Part MD002



Figure B.64: Stretch Broken Carbon Fiber Curved C Channel Part MD020: Left - Top of Part, Right - Bottom of Part

Additional Sinusoidal C Channel Results

Table B.20: Summary of Sinusoidal C Channel Results

Part	Fiber	Resin	Batch	Plies	Layup Shape	Intensifier	Intermediate Dwell	Final Dwell	Cure Pressure
MD023	CF	8552	N/A	8	Unwrap	No	-	350F - 2 hrs	90 psi

Part MD023

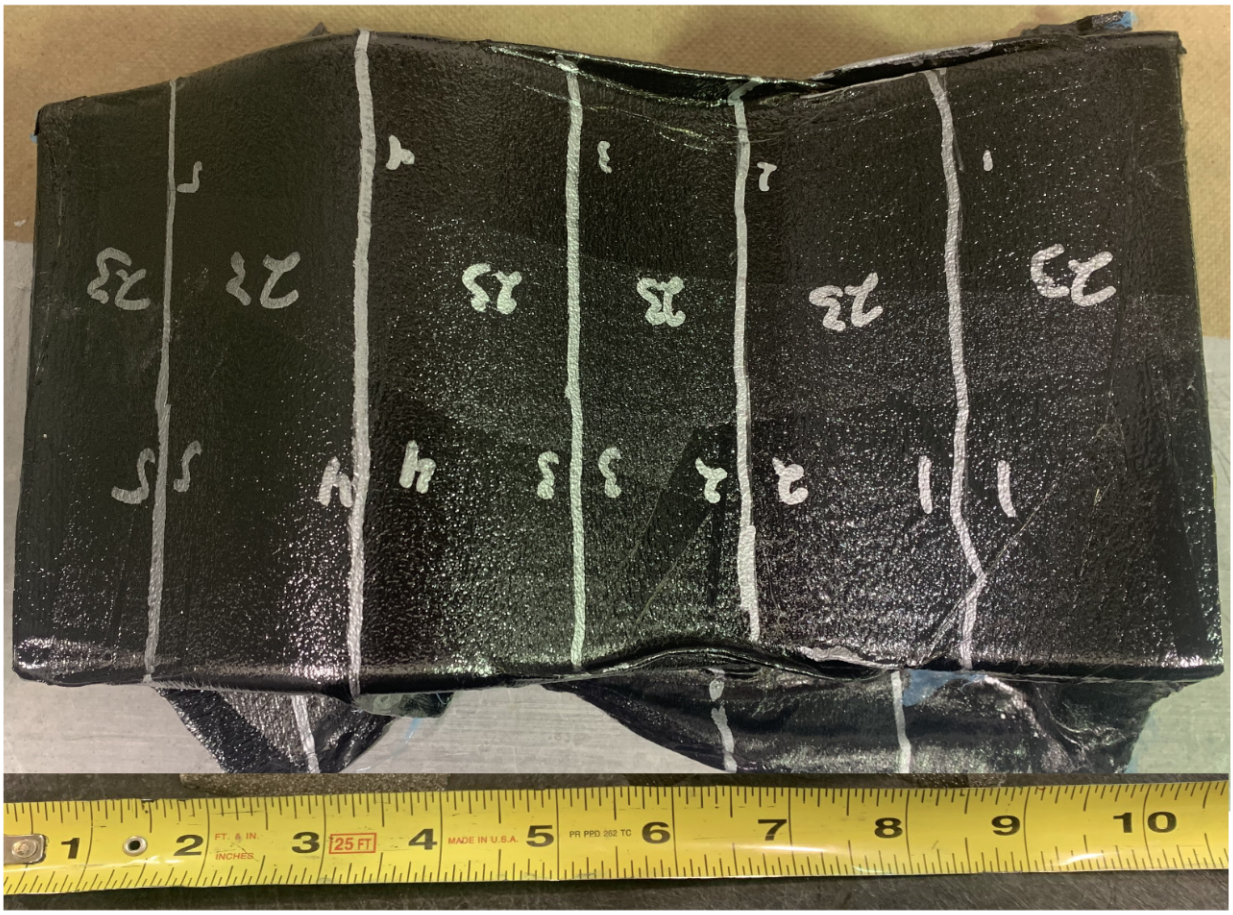


Figure B.65: Continuous Carbon Fiber Curved C Channel Part MD023

Table B.21: Continuous Carbon Fiber MD023: Texture Results

Metric	Weight	Ranking	Score
Hairiness	30%	5	-
Additional Resin Pooling	30%	1	-
Spaghettification	10%	5	-
Fractures/Shearing	15%	0	-
Pinholes	10%	5	-
Waves	5%	5	-
Total	100%	X	3.05

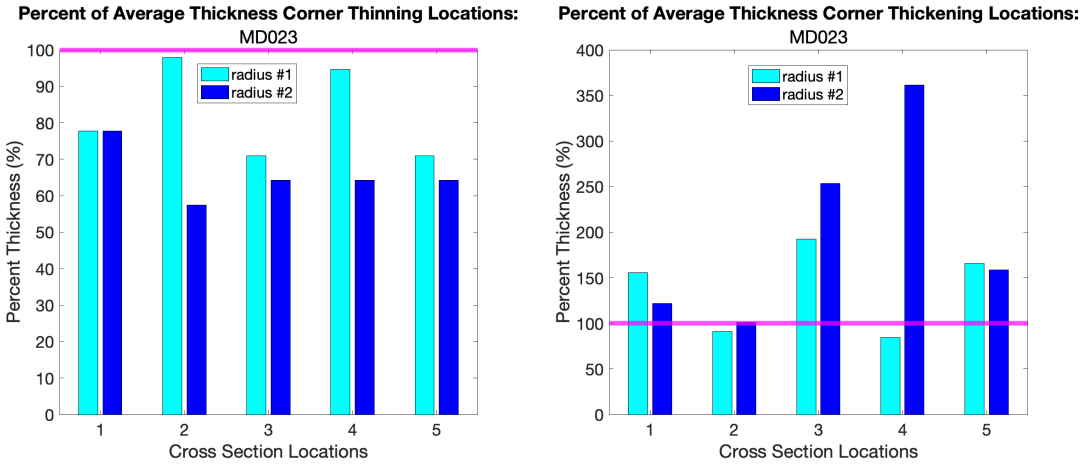


Figure B.66: Continuous Carbon Fiber MD023 Results: Left - Corner Thinning (Average = 73.99%), Right - Corner Thickening (Average = 168.58%)

Table B.22: Continuous Carbon Fiber MD023: Final Forming Score

Metric	Weight	Ranking	Score
Bridging	14%	5	-
Wrinkling	19.25%	0	-
Thickness Variation	17%	2	-
Forming Depth	-	-	-
Corner Thinning	17%	0	-
Corner Thickening	11.75%	0	-
Resin Pooling	14.25%	5	-
Texture	6.75%	3.05	-
Total	100%	-	1.96

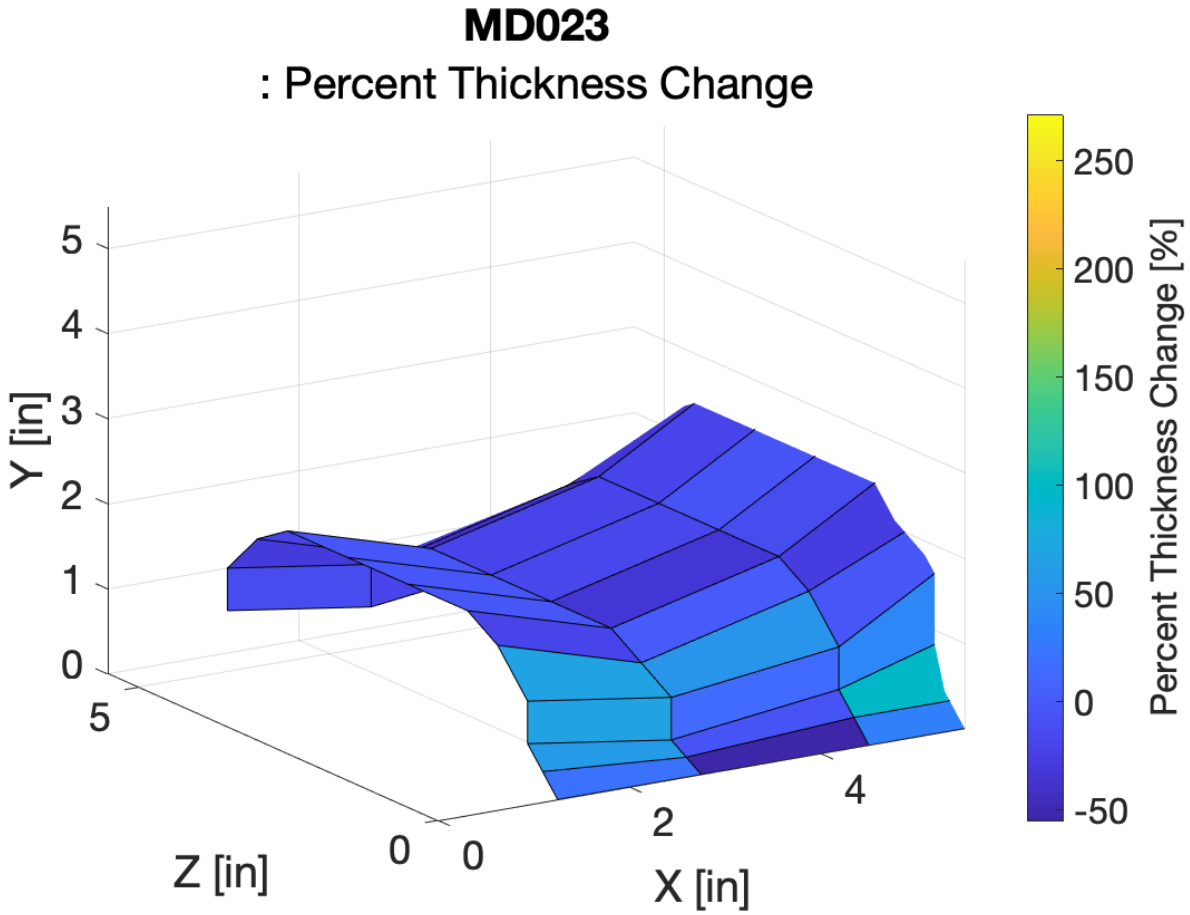


Figure B.67: Continuous Carbon Fiber MD023 Results: Thickness Variation (Coefficient of Variation = 0.3263)

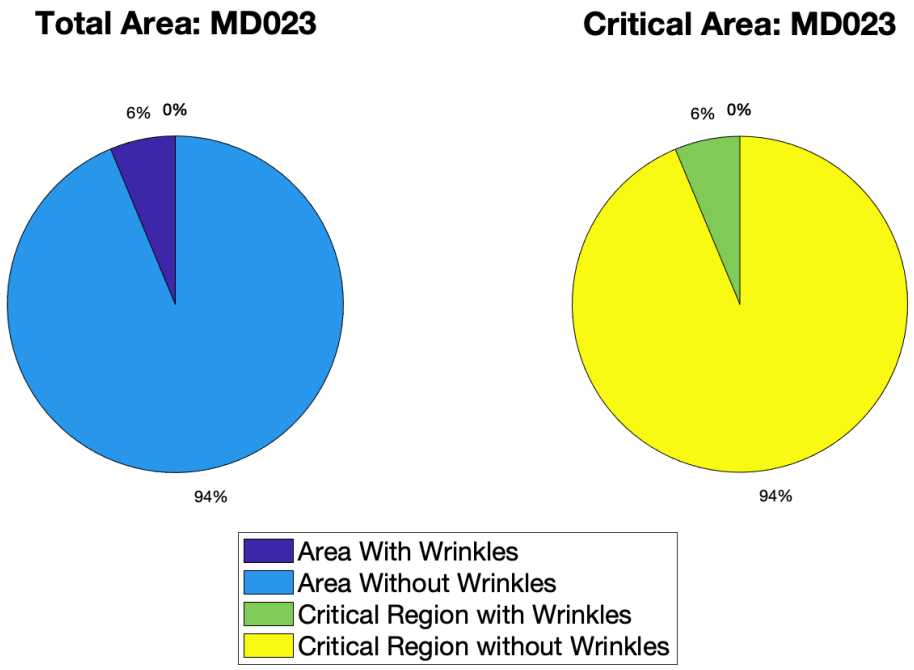


Figure B.68: Continuous Carbon Fiber MD023 Results: Wrinkling (Total Wrinkling = 6.29%, Critical Region Wrinkling = 6.29%)

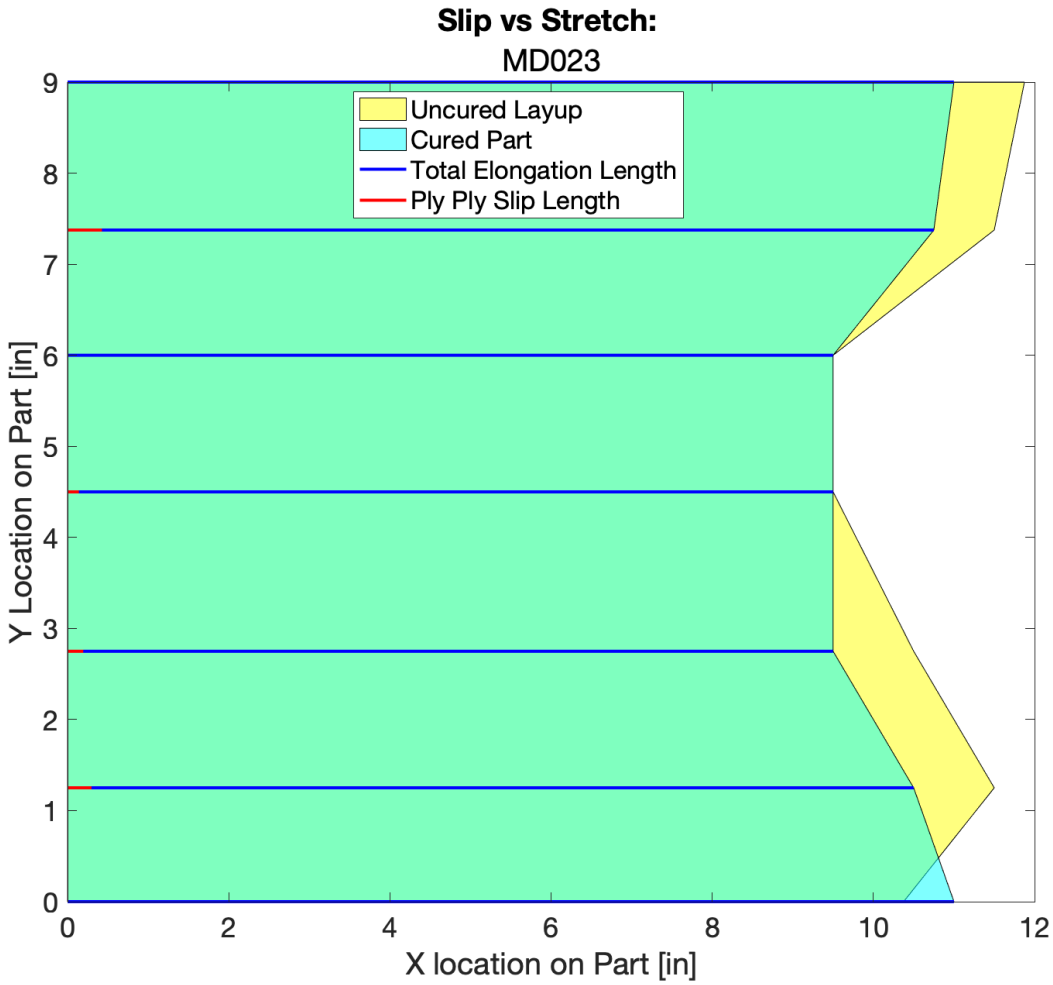


Figure B.69: Continuous Carbon Fiber MD023 Results: Stretching versus Slipping

APPENDIX C

APPENDIX C: MATLAB CODE

Curved C Channel Code

Main Curved C Channel Script

```
%% Main Code for Ferb Data Processing
clear all
clc

%% Change these variables based on the part

name  =             'MDXXX'      % Name of the part
file  =       'MDXXX.xlsx';      % Part xcel file
t_i   =            0.0576;       % Original thickness of uncured layup [
    in]
mat   =                ''       % Material- 'SBCF' or 'CF'
res   =                ''       % Resin type - '8552' or '977-3'
type  =            'Ferb'       % Part type, Ferb for this file
layup =                ''       % layup of the part

% Notes about the layup
lay_notes = 'Flat on tool, edge breathing, quarter circle layup shape'
% Notes about the cure cycle
cure_notes = 'Cure Cycle B (8552)'



rad_t =            0.125;       % radius size of the tool [in]
r_w   =                3;       % the radial distance to the wall for
    which d
                                % is measured from

%% Extracting Variables from Excel Sheet

% calling extraction function
[theta, bridg_dat, wrink_dat, thick_dat, L_t, L_p, d, thin_dat,...
    thicken_dat, resin_dat, L_uncured, L_cured, L_pp, r_thick, r_thin,
        r_thicken,...
    z_thick, z_thin, z_thicken] = ferb_data_extract(file);


% creating a theta variable to account for edges
theta_large = [0;theta;90];


%% Calling Calculation Functions
```

```
% Bridging Calculation
av_bridg = bridging(theta,bridg_dat,name);

% Thickness Calculation
[coeff_var, av_thick] = thickness_analysis_polar(r_thick,theta,z_thick,
    thick_dat,name,t_i);

% Corner Thickening Calculation
[cornerthick_av,thicken] = cornerthick(theta,thicken_dat,av_thick,name)
    ;

% Corner Thinning Calculation
[cornerthin_av,thin] = cornerthin(theta,thin_dat,av_thick,name);
a = size(thin);
lab = [];
for i = 1:a(2)
    lab = [lab;strcat('radius #',string(i))];
end
figure()
subplot(1,2,1)
b=bar(theta,thin,'g','b');
% setting the colors of the individual bars
b(1).FaceColor = [0 1 1];
b(2).FaceColor = [0 0 1];
title('Percent of Average Thickness Corner Thinning Locations:',name)
xlabel('Cross Section Locations')
ylabel('Percent Thickness (%)')
legend(lab)
set(gca,'Fontsize',18)

subplot(1,2,2)
b = bar(theta,thicken);
% setting the colors of the individual bars
b(1).FaceColor = [0 1 1];
b(2).FaceColor = [0 0 1];
title('Percent of Average Thickness Corner Thickening Locations:',name)
xlabel('Cross Section Locations')
ylabel('Percent Thickness (%)')
legend(lab)
set(gca,'Fontsize',18)


% Resin Pooling Calculation
res_tot = resinpool(theta,resin_dat,name);
```

```
% Stretch vs Slip Calculation
strain = stretchslip(theta_large',L_uncured',L_cured',L_pp',name);

%% Wrinkle Calculation
a = wrinkle_analysis(wrink_dat,name);


% Thickness including corner thinning/thickening
r_t = [r_thin(1),r_thicken(1),r_thicken(2),r_thin(2)];
z_t = [z_thin,z_thicken];
thick_t(:,:,1) = thin_dat;
thick_t(:,:,2) = thicken_dat;
[coeff_var, av_thick] = thickness_polar_withthinthick(transpose(r_thick
    ),transpose(theta),transpose(z_thick),thick_dat,name,t_i,r_t, z_t,
    thick_t);

% bridging to resin pooling comparison
bridgpool(resin_dat,bridg_dat,theta,name)

% Forming Depth Calculation
form_av = form_depth_polar(L_t',L_p',d',r_thick',theta',name,r_w,rad_t)
    ;
```

Curved C Channel Data Extraction Function

```
function [theta, bridg_dat, wrink_dat, thick_dat, L_t, L_p, d, thin_dat
    ,...
     thicken_dat, resin_dat, L_uncured, L_cured, L_pp, r_thick, r_thin,
        r_thicken,...
     z_thick, z_thin, z_thicken] = ferb_data_extract(file)

% This function extracts the data from the part forming data
    spreadsheets,
% specifically the ferb style mold. There are additional extraction
% functions for different part models. If you wish to create new ones
    for
% the parts specified, keep in mind the variables you wish to extract
    and
% the required size for each one

% NOTE: THE FERB DATA SHEET MUST BE DOWNLOADED AND SAVED AS AN XLSX
    FILE.
%       MAKE SURE TO DELETE ANY BLANK ROWS OR COLUMNS PLACED BEFORE THE
```

```
%       START OF THE DATA TABLE OR ELSE THE VARIABLES WILL EXTRACT WITH
    THE
%       WRONG DATA

% Output : theta          - The section labels and measurement locations
    in
%                           degrees for the Ferb tests. Should be
%                           [15,30,45,60,75]
%          bridg_dat      - The bridging data for the inner and outer
    radii
%                           of the part. The rows correspond with the
    theta
%                           locations and the columns correspond with
    radii 1
%                           and radii 2. This data is represented in
    inches
%                           from the desired radius
%          wrink_dat      - The wrinkle data is an array of two values.
    The
%                           first value is the wrinkle percentage for the
%                           entire part where the second value is the
%                           percentage of wrinkles within the critical
    area
%          thick_dat      - The thickness data for the entire part
    excluding
%                           the corner thinning and corner thickening
    data.
%                           The rows correspond to the theta measurement
%                           locations and the columns correspong to the
%                           number of measurement locations for each
    cross
%                           section. Measured in inches
%          L_t            - The length across the negative bottom of the
    mold
%                           not including radii. Should be a singular
    value
%                           measured in inches, but could also be an
    array of
%                           values corresponding to the cross section
%                           locations. For ferb this is 1.75
%          L_p            - The contact length of where the part touches
    the
%                           mold for each cross section. This is an array
%                           with the same length as theta. Measured in
    inches
```

```
%           d               - The distance from the first radii wall to the
%                             start of the L_p measurements. This is
    measured
%                             in inches and is an array with the same
    length as
%                             theta
%           thin_dat        - The corner thinning data for the part. The
    rows
%                             correspond to the theta cross section
    locations
%                             and the columns correspond to the nuumber of
%                             convex radii. Measured in inches
%           thicken_dat     - The corner thickening data for the part. The
    rows
%                             correspond to the theta cross section
    locations
%                             and the columns correspond to the nuumber of
%                             concave radii. Measured in inches
%           resin_dat       - The resin pooling data for the part. The rows
%                             correspond to the theta cross section
    locations
%                             and the columns correspond to the nuumber of
%                             concave radii. Measured in inches squared
%           L_uncured       - The length vector of the uncured layup of
    carbon
%                             fiber. The rows correspond to each theta
    cross
%                             sectional length and the values are the
    distance
%                             along the cross sectional path in inches
%           L_cured         - The length vector of the cured carbon fiber
    part.
%                             The rows correspond to each theta cross
    sectional
%                             length and the values are the distance along
    the
%                             cross sectional path in inches
%           L_pp            - The ply ply slip length, rows correspond to
%                             measurement locations. Length is measured in
%                             inches
%           r_thick         - The r location vector of where each thickness
%                             measurement is taken per cross section.
    Should be
%                             the same length as the columns of thick_dat.
%                             Measured in inches from the origin of the
```

```
    tool C
%                           channel radius.
%           r_thin          - The r location vector of where each corner
%                           thinning measurement is taken per cross
    section.
%                           The values correspond to the position of each
%                           convex tooling curvature. Measured in inches
%           r_thicken       - The r location vector of where each corner
%                           thickening measurement is taken per cross
%                           section. The values correspond to the
    position of
%                           each concave tooling curvature. Measured in
%                           inches
%           z_thick         - The z location vector of where each thickness
%                           measurement is taken per cross section.
    Should be
%                           the same length as the r_thick array.
    Measured in
%                           inches.
%           z_thin          - The z location value of where the corner
    thinning
%                           measurements are taken corresponding to the
%                           position of the convex radii. Measured in
    inches.
%           z_thicken       - The z location value of where the corner
%                           thickening measurements are taken
    corresponding
%                           to the position of the concave radii.
    Measured in
%                           inches.

% Inputs : file - the data sheet excel file containing all the part
    data
%                   for the ferb complex shape


% Written by Madison Dube for Thesis on Forming Analysis of Complex
    Carbon
% Fiber Parts for the MSU Stretch Broken Carbon Fiber Research Group


%% Reading in the data

% Reading the data in from the excel file
[num,txt,raw] = xlsread(file);
```

```
% assigning the variables to different cells from the xcel file
theta = [15;30;45;60;75];
bridg_dat = num(2:6,1:2);
wrink_dat = num(9,5:6);
thick_dat = num(2:6,7:16);
L_t = num(2:6,17);
L_p = num(2:6,18);
d = num(2:6,19);
thin_dat = num(2:6,21:22);
thicken_dat = num(2:6,23:24);
resin_dat = num(2:6,25:26);
L_uncured = num(1:7,27);
L_cured = num(1:7,28);
L_pp = num(2:6,29);
r_thick = num(1:10,30);
r_thin = num(1:2,31);
r_thicken = num(1:2,32);
z_thick = num(1:10,33);
z_thin = num(1,34);
z_thicken = num(1,35);



end
```

Rounded Hat Channel Code

Main Rounded Hat Channel Script

```
%% Main Code for Perry Data Processing
clear all
clc

%% Change these variables based on the part

name   =              'MDXXX'     % Name of the part
file   =         'MDXXX.xlsx';    % Part xcel file
t_i    =                    ;     % Original thickness of uncured layup
   [in]
mat    =                   ''     % Material- 'SBCF' or 'CF'
res    =                   ''     % Resin type - '8552' or '977-3'
type   =                   ''     % Part type, Ferb for this file
layup  =                   ''    % layup of the part
```

```
% Notes about the layup
lay_notes = ''
% Notes about the cure cycle
cure_notes = ''



rad_t =                     ;     % radius size of the tool [in]
r_w   =                     ;     % the radial distance to the wall for
    which d
                                  % is measured from

%% Extracting Variables from Excel Sheet

% calling extraction function
[sect, bridg_dat, wrink_dat, thick_dat, L_t, L_p, d, thin_dat,...
    thicken_dat, resin_dat, L_uncured, L_cured, L_pp, r_thick, r_thin,
        r_thicken,...
    z_thick, z_thin, z_thicken] = perry_data_extract(file);


% creating a theta variable to account for edges


%% Calling Calculation Functions

% Bridging Calculation
av_bridg = bridging(sect,bridg_dat,name);

% Thickness Calculation
[coeff_var, av_thick] = thickness_analysis_polar(r_thick,sect,z_thick,
    thick_dat,name,t_i);

% Corner Thickening Calculation
[cornerthick_av,thicken] = cornerthick(sect,thicken_dat,av_thick,name);

% Corner Thinning Calculation
[cornerthin_av,thin] = cornerthin(sect,thin_dat,av_thick,name);


a = size(thin);
lab = [];
for i = 1:a(2)
    lab = [lab;strcat('radius #',string(i))];
```

```
end
figure()
subplot(1,2,1)
b=bar(sect,thin,'g','b');
% setting the colors of the individual bars
b(1).FaceColor = [0 1 1];
b(2).FaceColor = [0 0 1];
title('Percent of Average Thickness Corner Thinning Locations:',name)
xlabel('Cross Section Locations')
ylabel('Percent Thickness (%)')
legend(lab)
set(gca,'Fontsize',18)

subplot(1,2,2)
b = bar(sect,thicken);
% setting the colors of the individual bars
b(1).FaceColor = [0 1 1];
b(2).FaceColor = [0 0 1];
title('Percent of Average Thickness Corner Thickening Locations:',name)
xlabel('Cross Section Locations')
ylabel('Percent Thickness (%)')
legend(lab)
set(gca,'Fontsize',18)

% Resin Pooling Calculation
res_tot = resinpool(sect,resin_dat,name);


% Stretch vs Slip Calculation
strain = stretchslipperry(sect',L_uncured',L_cured',L_pp',name);

%% Wrinkle Calculation
wrink_dat = [0,0];
a = wrinkle_analysis(wrink_dat,name);


% Thickness including corner thinning/thickening
r_t = [r_thin,r_thicken];
z_t = [z_thin(1),z_thicken(1),z_thicken(2),z_thin(2)];
thick_t(:,:,1) = thin_dat;
thick_t(:,:,2) = thicken_dat;
[coeff_var, av_thick] = thickness_polar_withthinthickperry(transpose(
    r_thick),transpose(sect),transpose(z_thick),thick_dat,name,t_i,r_t,
    z_t,thick_t);
```

```
% bridging to resin pooling comparison
bridgpool(resin_dat,bridg_dat,sect,name)

% Forming Depth Calculation
form_av = form_depth_perry(L_t',L_p',d',r_thick',sect',name,r_w,rad_t);
```

Rounded Hat Channel Data Extraction Function

```
function [sect, bridg_dat, wrink_dat, thick_dat, L_t, L_p, d, thin_dat
    ,...
    thicken_dat, resin_dat, L_uncured, L_cured, L_pp, r_thick, r_thin,
       r_thicken,...
    z_thick, z_thin, z_thicken] = perry_data_extract(file)

% This function extracts the data from the part forming data
    spreadsheets,
% specifically the ferb style mold. There are additional extraction
% functions for different part models. If you wish to create new ones
    for
% the parts specified, keep in mind the variables you wish to extract
    and
% the required size for each one

% NOTE: THE FERB DATA SHEET MUST BE DOWNLOADED AND SAVED AS AN XLSX
    FILE.
%       MAKE SURE TO DELETE ANY BLANK ROWS OR COLUMNS PLACED BEFORE THE
%       START OF THE DATA TABLE OR ELSE THE VARIABLES WILL EXTRACT WITH
     THE
%       WRONG DATA

% Output : sect          - The section labels and measurement locations
    in
%                          for the Perry tests
%          bridg_dat     - The bridging data for the inner and outer
    radii
%                          of the part. The rows correspond with the
    theta
%                          locations and the columns correspond with
    radii 1
%                          and radii 2. This data is represented in
    inches
%                          from the desired radius
%          wrink_dat     - The wrinkle data is an array of two values.
    The
%                          first value is the wrinkle percentage for the
```

```
%                           entire part where the second value is the
%                           percentage of wrinkles within the critical
    area
%           thick_dat     - The thickness data for the entire part
    excluding
%                           the corner thinning and corner thickening
    data.
%                           The rows correspond to the theta measurement
%                           locations and the columns correspong to the
%                           number of measurement locations for each
    cross
%                           section. Measured in inches
%           L_t           - The length across the negative bottom of the
    mold
%                           not including radii. Should be a singular
    value
%                           measured in inches, but could also be an
    array of
%                           values corresponding to the cross section
%                           locations. For ferb this is 1.75
%           L_p           - The contact length of where the part touches
    the
%                           mold for each cross section. This is an array
%                           with the same length as theta. Measured in
    inches
%           d             - The distance from the first radii wall to the
%                           start of the L_p measurements. This is
    measured
%                           in inches and is an array with the same
    length as
%                           theta
%           thin_dat      - The corner thinning data for the part. The
    rows
%                           correspond to the theta cross section
    locations
%                           and the columns correspond to the nuumber of
%                           convex radii. Measured in inches
%           thicken_dat   - The corner thickening data for the part. The
    rows
%                           correspond to the theta cross section
    locations
%                           and the columns correspond to the nuumber of
%                           concave radii. Measured in inches
%           resin_dat     - The resin pooling data for the part. The rows
%                           correspond to the theta cross section
```

```
    locations
%                           and the columns correspond to the nuumber of
%                           concave radii. Measured in inches squared
%           L_uncured     - The length vector of the uncured layup of
    carbon
%                           fiber. The rows correspond to each theta
    cross
%                           sectional length and the values are the
    distance
%                           along the cross sectional path in inches
%           L_cured       - The length vector of the cured carbon fiber
    part.
%                           The rows correspond to each theta cross
    sectional
%                           length and the values are the distance along
    the
%                           cross sectional path in inches
%           L_pp          - The ply ply slip length, rows correspond to
%                           measurement locations. Length is measured in
%                           inches
%           r_thick       - The r location vector of where each thickness
%                           measurement is taken per cross section.
    Should be
%                           the same length as the columns of thick_dat.
%                           Measured in inches from the origin of the
    tool C
%                           channel radius.
%           r_thin        - The r location vector of where each corner
%                           thinning measurement is taken per cross
    section.
%                           The values correspond to the position of each
%                           convex tooling curvature. Measured in inches
%           r_thicken     - The r location vector of where each corner
%                           thickening measurement is taken per cross
%                           section. The values correspond to the
    position of
%                           each concave tooling curvature. Measured in
%                           inches
%           z_thick       - The z location vector of where each thickness
%                           measurement is taken per cross section.
    Should be
%                           the same length as the r_thick array.
    Measured in
%                           inches.
%           z_thin        - The z location value of where the corner
```

```
    thinning
%                           measurements are taken corresponding to the
%                           position of the convex radii. Measured in
    inches.
%           z_thicken     - The z location value of where the corner
%                           thickening measurements are taken
    corresponding
%                           to the position of the concave radii.
    Measured in
%                           inches.

% Inputs : file - the data sheet excel file containing all the part
    data
%                   for the ferb complex shape


% Written by Madison Dube for Thesis on Forming Analysis of Complex
    Carbon
% Fiber Parts for the MSU Stretch Broken Carbon Fiber Research Group


%% Reading in the data

% Reading the data in from the excel file
[num,txt,raw] = xlsread(file);


% assigning the variables to different cells from the xcel file
sect = [15;30;45;60;75];
bridg_dat = num(1:5,1:2);
wrink_dat = num(9,5:6);
thick_dat = num(1:5,7:16);
L_t = num(1:5,17);
L_p = num(1:5,18);
d = num(1:5,19);
thin_dat = num(1:5,20:21);
thicken_dat = num(1:5,22:23);
resin_dat = num(1:5,24:25);
L_uncured = num(1:5,26);
L_cured = num(1:5,27);
L_pp = num(1:5,28);
r_thick = num(1:10,29);
r_thin = num(1,30);
r_thicken = num(1,31);
z_thick = num(1:10,32);
```

```
z_thin = num(1:2,33);
z_thicken = num(1:2,34);



end
```

Sinusoidal C Channel Code

Main Sinusoidal C Channel Script

```
%% Main Code for Jeremy Data Processing
clear all
clc

%% Change these variables based on the part

name =              'MDXXX'     % Name of the part
file =              'MDXXX';    % Part xcel file
t_i  =                    ;    % Original thickness of uncured layup [in
   ]
mat  =                   ''     % Material- 'SBCF' or 'CF'
res  =                   ''     % Resin type - '8552' or '977-3'
type =            'Jeremy'      % Part type, Ferb for this file
layup =                  ''     % layup of the part

% Notes about the layup
lay_notes = ''
% Notes about the cure cycle
cure_notes = ''



rad_t =              0.25;      % radius size of the tool [in]
r_w   =                 3;      % the radial distance to the wall for
   which d
                                 % is measured from

%% Extracting Variables from Excel Sheet

% calling extraction function
[section, xloc, bridg_dat, wrink_dat, thick_dat, thin_dat, ...
    thicken_dat, resin_dat, L_uncured, L_cured, L_pp, y_thick135, ...
    y_thick2, y_thick4, y_corn135, y_corn2, y_corn4, z_thick, z_thin
       ,...
```

```
    z_thicken] = jeremy_data_extract(file);


%% Calling Calculation Functions


% Bridging Calculation
av_bridg = bridging(section,bridg_dat,name);


% Thickness Calculation
[coeff_var,av_thick] = avthickjeremy(thick_dat);


% Corner Thickening Calculation
[cornerthick_av,thicken] = cornerthick(section,thicken_dat,av_thick,
    name);


% Corner Thinning Calculation
[cornerthin_av,thin] = cornerthin(section,thin_dat,av_thick,name);
a = size(thin);
lab = [];
for i = 1:a(2)
    lab = [lab;strcat('radius #',string(i))];
end
figure()
subplot(1,2,1)
b=bar(section,thin,'g','b');
% setting the colors of the individual bars
b(1).FaceColor = [0 1 1];
b(2).FaceColor = [0 0 1];
title('Percent of Average Thickness Corner Thinning Locations:',name)
xlabel('Cross Section Locations')
ylabel('Percent Thickness (%)')
legend(lab)
set(gca,'Fontsize',18)

subplot(1,2,2)
b = bar(section,thicken);
% setting the colors of the individual bars
b(1).FaceColor = [0 1 1];
b(2).FaceColor = [0 0 1];
title('Percent of Average Thickness Corner Thickening Locations:',name)
```

```
xlabel('Cross Section Locations')
ylabel('Percent Thickness (%)')
legend(lab)
set(gca,'Fontsize',18)

% Resin Pooling Calculation
res_tot = resinpool(section,resin_dat,name);


% Stretch vs Slip Calculation
strain = stretchslipcartesian(xloc','L_uncured','L_cured','L_pp', name);


%% Wrinkle Calculation
a = wrinkle_analysis(wrink_dat,name);


% Thickness including corner thinning/thickening
thickness_analysis_thinthickjeremy(av_thick,thick_dat,thicken_dat,...
    thin_dat,xloc,y_corn135,y_corn2,y_corn4,y_thick135,y_thick2,...
    y_thick4,z_thick,z_thicken,z_thin,t_i,name)


% bridging to resin pooling comparison
bridgpool(resin_dat,bridg_dat,section,name)
```

Sinusoidal C Channel Data Extraction Function

```
function [section, xloc, bridg_dat, wrink_dat, thick_dat, thin_dat, ...
    thicken_dat, resin_dat, L_uncured, L_cured, L_pp, y_thick135, ...
    y_thick2, y_thick4, y_corn135, y_corn2, y_corn4, z_thick, z_thin
        ,...
    z_thicken] = jeremy_data_extract(file)

% This function extracts the data from the part forming data
    spreadsheets,
% specifically the jeremy style mold. There are additional extraction
% functions for different part models. If you wish to create new ones
    for
% the parts specified, keep in mind the variables you wish to extract
    and
% the required size for each one
```

```
% NOTE: THE JEREMY DATA SHEET MUST BE DOWNLOADED AND SAVED AS AN XLSX
    FILE.
%       MAKE SURE TO DELETE ANY BLANK ROWS OR COLUMNS PLACED BEFORE THE
%       START OF THE DATA TABLE. CURRENTLY DOES NOT INCLUDE FORMING
    DEPTH
%       AS THE MOLD WHEN THIS CODE WAS WRITTEN IS A MALE MOLD

% Output : section      - The section labels and measurement locations
    in
%                         degrees for the Jeremy tests. Should be
%                         [1,2,3,4,5]
%          xloc         - The x locations of all the sections in inches
%          bridg_dat    - The bridging data for the inner and outer
    radii
%                         of the part. The rows correspond with the
    theta
%                         locations and the columns correspond with
    radius 1
%                         and radius 2. This data is represented in
    inches
%                         from the desired radius
%          wrink_dat    - The wrinkle data is an array of two values.
    The
%                         first value is the wrinkle percentage for the
%                         entire part where the second value is the
%                         percentage of wrinkles within the critical
    area
%          thick_dat    - The thickness data for the entire part
    excluding
%                         the corner thinning and corner thickening
    data.
%                         The rows correspond to the theta measurement
%                         locations and the columns correspong to the
%                         number of measurement locations for each
    cross
%                         section. Measured in inches
%          thin_dat     - The corner thinning data for the part. The
    rows
%                         correspond to the theta cross section
    locations
%                         and the columns correspond to the nuumber of
%                         convex radii. Measured in inches
%          thicken_dat  - The corner thickening data for the part. The
    rows
%                         correspond to the theta cross section
```

```
locations
%                          and the columns correspond to the nuumber of
%                          concave radii. Measured in inches
%          resin_dat     - The resin pooling data for the part. The rows
%                          correspond to the theta cross section
locations
%                          and the columns correspond to the nuumber of
%                          concave radii. Measured in inches squared
%          L_uncured     - The length vector of the uncured layup of
carbon
%                          fiber. The rows correspond to each theta
cross
%                          sectional length and the values are the
distance
%                          along the cross sectional path in inches
%          L_cured       - The length vector of the cured carbon fiber
part.
%                          The rows correspond to each theta cross
sectional
%                          length and the values are the distance along
the
%                          cross sectional path in inches
%          L_pp          - The ply ply slip length, rows correspond to
%                          measurement locations. Length is measured in
%                          inches
%          y_thick135    - The y location vector of the thickness
%                          measurements in inches for sections 1, 3, and
 5
%          y_thick2      - The y location vector of the thickness
%                          measurements in inches for section 2
%          y_thick4      - The y location vector of the thickness
%                          measurements in inches for section 4
%          y_corn135     - The y location vector of the corner thinning
and
%                          corner thickening locations for sections 1,
3,
%                          and 5
%          y_corn2       - The y location vector of the corner thinning
and
%                          corner thickening locations for section 2
%          y_corn4       - The y location vector of the corner thinning
and
%                          corner thickening locations for section 4
%          z_thick       - The z location vector for the thickness
%                          measurements of all the sections in inches
```

```
%           z_thin        - The z location vector for the corner thinning
%                           locations of all the sections in inches
%           z_thicken     - The z location vector for the corner
    thickening
%                           locations of all the sections in inches


% Inputs : file - the data sheet excel file containing all the part
    data
%                   for the jeremy complex shape



% Written by Madison Dube for Thesis on Forming Analysis of Complex
    Carbon
% Fiber Parts for the MSU Stretch Broken Carbon Fiber Research Group

%% Reading in the Data

% Reading in the data from the excel file
[num,txt,raw] = xlsread(file);


% assigning the variables to different cells from the xcel file
section     =                  [1;2;3;4;5];
xloc        = [0;1.25;2.75;4.5;6;7.375;9];
bridg_dat   =                num(2:6,1:2);
wrink_dat   =                  num(9,5:6);
thick_dat   =               num(2:6,7:16);
thin_dat    =              num(2:6,21:22);
thicken_dat =              num(2:6,23:24);
resin_dat   =              num(2:6,25:26);
L_uncured   =                 num(1:7,27);
L_cured     =                 num(1:7,28);
L_pp        =                 num(1:7,29);
y_thick135  =               num(1:10,30);
y_thick2    =               num(1:10,31);
y_thick4    =               num(1:10,32);
y_corn135   =                 num(1:2,33);
y_corn2     =                 num(1:2,34);
y_corn4     =                 num(1:2,35);
z_thick     =               num(1:10,36);
z_thin      =                 num(1:2,37);
z_thicken   =                 num(1:2,38);
```

```
end
```

Sinusoidal C Thickness Analysis Function

```
function [] = ...
    thickness_analysis_thinthickjeremy(av_thick,thick_dat,thicken_dat
        ,...
    thin_dat,xloc,y_corn135,y_corn2,y_corn4,y_thick135,y_thick2,...
    y_thick4,z_thick,z_thicken,z_thin,t_i,name)


x = xloc(2:6);
z = [z_thick(1),z_thicken(1),(z_thick(2:3))',z_thin(1),(z_thick(4:7))
    ',...
    z_thin(2),(z_thick(8:9))',z_thicken(2),z_thick(10)];

Y(1,:)= [y_thick135(1),y_corn135(2),(y_thick135(2:3))',y_corn135(1),...
    (y_thick135(4:7))',y_corn135(1),(y_thick135(8:9))',y_corn135(2),...
    y_thick135(10)];
Y(2,:)= [y_thick2(1),y_corn2(2),(y_thick2(2:3))',y_corn2(1),...
    (y_thick2(4:7))',y_corn2(1),(y_thick2(8:9))',y_corn2(2),...
    y_thick2(10)];
Y(3,:)= [y_thick135(1),y_corn135(2),(y_thick135(2:3))',y_corn135(1),...
    (y_thick135(4:7))',y_corn135(1),(y_thick135(8:9))',y_corn135(2),...
    y_thick135(10)];
Y(4,:)= [y_thick4(1),y_corn4(2),(y_thick4(2:3))',y_corn4(1),...
    (y_thick4(4:7))',y_corn4(1),(y_thick4(8:9))',y_corn4(2),...
    y_thick4(10)];
Y(5,:)= [y_thick135(1),y_corn135(2),(y_thick135(2:3))',y_corn135(1),...
    (y_thick135(4:7))',y_corn135(1),(y_thick135(8:9))',y_corn135(2),...
    y_thick135(10)];


[Z,X] = meshgrid(z,x);

a = size(Y);

% Combining the thickness data
thick_combo = [thick_dat(:,1),thicken_dat(:,1),thick_dat(:,2:3),
   thin_dat(:,1),thick_dat(:,4:6),thin_dat(:,2),thick_dat(:,7:8),
   thicken_dat(:,2),thick_dat(:,9:10)];


%% Contour Plot Creation
```

```
% Generating colormap based on thickness data analyzed as percent
    thinning
C = ones(a(1),a(2)).*((thick_combo./t_i.*100)-100);


% Plotting the data
figure()
% creating surface plot
surf(X, Z, Y,C);
% setting fontsize
set(gca,'Fontsize',18)
% setting x, y, and z limits
xlim([0,5.5])
ylim([0,5.5])
zlim([0,5.5])
% adding the colorbar
colorbar
% adding the colorbar label
b = colorbar;
b.Label.String = 'Percent␣Thickness␣Change␣[%]';
% labeling axes and including title
xlabel("X [in]")
ylabel("Z [in]")
zlabel("Y [in]")
title(name,": Percent Thickness Change")

clear a
end
```

Cartesian Coordinate Designed Functions

Stretching vs Slipping Function

```
function [strain] = stretchslipcartesian(xloc,L_uncured,L_cured,L_pp,
    name)
% This function analyzes the stretch vs slip data for complex carbon
    fiber
% parts

% Output : strain      - The stretch vs slip ratio calculated with a
    strain
%                        formula
%          figure()    - A plot of the original lengths of the uncured
    layup
```

```
%                          when compared to the new lengths after the cure
%
% Inputs : theta      - the theta array of the measurement locations,
    note
%                          that for the curved c channel, lines 0 and 90
    are
%                          included
%          L_uncured  - the array of the uncured length measurements at
    each
%                          cross section location
%          L_cured    - the array of the cured length measurements at
    each
%                          cross section location
%          L_pp       - ply ply slip length, array the length of the
%                          sections in inches
%          name       - the name of the part as a string. ex: 'MDXXX'

% Written by Madison Dube for Thesis on Forming Analysis of Complex
    Carbon
% Fiber Parts for the MSU Stretch Broken Carbon Fiber Research Group

%% Plotting the uncured data
figure()

x = [0,L_uncured,0];
y = [xloc(1),xloc,xloc(end)];
fill(x,y,'yellow','FaceAlpha',0.5)
hold on
clear x


%% Plotting the cured data

% plotting the filled cured data area
x = [0,L_cured,0];

fill(x,y,'cyan','FaceAlpha',0.5)
hold on
clear x y
set(gca,'Fontsize',18)


% plotting the cured data lines
for i = 1:length(xloc)
    x = [0,L_cured(i)];
```

```
    y = [xloc(i),xloc(i)];
    plot(x,y,'bl','LineWidth',2,'DisplayName','')

end

% plotting the ply ply data lines
for i = 1:length(L_pp)
    x = [0,L_pp(i)];
    y = [xloc(i),xloc(i)];
    plot(x,y,'r','LineWidth',2,'DisplayName','')

end


% Adding headers to the graph
legend({'Uncured Layup','Cured Part','Total Elongation Length','','','',
    '','','','','','Ply Ply Slip Length'})
xlabel('X location on Part [in]')
ylabel('Y Location on Part [in]')
title('Slip vs Stretch: ',name)

strain = (L_cured-L_uncured)./L_uncured;
end
```

Thickness Variation Function

```
function [coeff_var, av_thick] = thickness_analysis_cartesian(x,y,z,
    thick,name,t_i)
% This function analyzes the thickness of carbon fiber complex parts in
% cartesian coordinates

% Output : coeff_var - the coefficient of variation of the thickness
    data
%          figure()  - the 3D contour plot of the thinning and
    thickening
%                      of the part based on geometric locations
%          av_thick  - the average thickness of the data

% Inputs : x      - the x location vector of the measurement locations
    in
%                   inches
%          y      - the y location vector of the measurement locations
    in
%                   inches
```

```
%           z      - the height location vector of the measurement
    locations
%                    in inches (must be the same length as x)
%           thick  - the (m,n) tensor of thickness data corresponding to
    the
%                    x, y, and z measurement locations in inches (must be
     the
%                    size of y by x)
%           name   - a string of the part name example: 'MD003'
%           t_i    - the initial thickness of the uncured laminate in
    inches

% Written by Madison Dube for Thesis on Forming Analysis of Complex
    Carbon
% Fiber Parts for the MSU Stretch Broken Carbon Fiber Research Group


%% Contour Plot Creation

% Creating a mesh based on the x and y locations
[X, Y] = meshgrid(x,y);


% Writing Z matrix to correspond with mesh size
for i = 1:length(y)
    Z(i,:) = z;
end

% Determining the size of Z for the colormap
a = size(Z);


% Generating colormap based on thickness data analyzed as percent
    thinning
C = ones(a(1),a(2)).*((thick./t_i.*100)-100);


% Plotting the data
figure()
% creating surface plot
surf(X, Y, Z, C);
% setting fontsize
set(gca,'Fontsize',18)
% setting x, y, and z limits
xlim([0,5.5])
```

```
ylim([0,5.5])
zlim([0,5.5])
% adding the colorbar
colorbar
% adding the colorbar label
b = colorbar;
b.Label.String = 'Percent Thickness Change [%]';
% labeling axes and including title
xlabel("X [in]")
ylabel("Y [in]")
zlabel("Z [in]")
title(name,": Percent Thickness Change")


clear a

%% Coefficient of Variation Calculation

a = size(thick);
thick_c = [];
for i = 1:a(1)
    thick_c = [thick_c,thick(i,:)];
end

n = length(thick_c);
x_bar = sum(thick_c)/n;

coeff_var = (1/x_bar) * sqrt(sum((thick_c - x_bar).^2)/(n-1));


%% Average Thickness

av_thick = x_bar;

end
```

Forming Depth Function

```
function [form_av] = form_depth_perry(L_t,L_p,d,r,theta,name,r_w,rad_t,
    z)
% This function analyzes the forming depth data for complex carbon
    fiber
% parts

% Output : form_av    - The average forming depth percent of the entire
```

```
%                       parts section measurements.
%          figure()   - The first plot in the figure is a bar graph of
   the
%                       forming depth percentages based on each cross
%                       section location. The second plot is an area
%                       representation of the total area of the bottom
   of
%                       the tool when compared to the contact area
   between
%                       the carbon fiber and the tool surface
%
% Inputs : L_t - the distance across the drawn in area of the tool, not
%                including the radii on either side in inches. For the
   Ferb
%                parts, this distance is 1.25 in.
%          L_p - the array of forming depth measurements at the various
%                cross section locations. This is the distance across
   the
%                bottom where the part touches the tool in inches.
%            d - the distance over from the wall of the first radii
   where
%                the part first starts touching the bottom of the mold.
%                This is an array the same length as L_p in inches.
%            r - the r location vector for all measurement locations (
   can
%                use the same one from the thickness data). Measured in
%                inches
%        theta - the theta location vector for all measurement
   locations
%                (can use the same one from the thickness data).
   Measured
%                in degrees.
%         name - the name of the part as a string. ex: 'MDXXX'
%          r_w - The radial distance of the wall value for where d is
%                measured from. Singular value in inches
%        rad_t - The radii measurements of the tool, specifically the
%                concave corners
%            z - The z location vector for the measurements


% Written by Madison Dube for Thesis on Forming Analysis of Complex
   Carbon
% Fiber Parts for the MSU Stretch Broken Carbon Fiber Research Group
```

```
%% Forming Depth by location bar graph


% Calculating the percent formed for each location
form_percent = L_p./L_t.*100;

% Calculating the forming depth average of all the data
form_av = sum(form_percent)./length(form_percent);

disp('The average forming depth percent for the entire part is:')
form_av


% Plotting the data on a bar graph
figure()
subplot(1,2,1)
bar(theta,form_percent,'blue')
title('Forming Depth at Cross Section Locations: ',name)
xlabel('Cross Section Locations')
ylabel('Percent Formed [%]')
set(gca,'Fontsize',18)


%% Plotting the shapes of the contact area


% Calculating radii values
R1 = ones(1,length(theta)).*(r_w+rad_t);
R2 = ones(1,length(theta)).*(r(9)-rad_t);


% Plotting the tool area
subplot(1,2,2)
fill([r_w,r_w,r_w+L_t(1),r_w+L_t(1)],[0,4,4,0],'cyan')
hold on


% Data adjustments for forming depth data radii
X = [d+r_w,d+r_w+L_p];
Y = [0,4*ones(1,length(X)-2),0];


% Plotting the part area
fill(X,Y,'blue')
```

```
title('Forming Depth as Visualized on Tool Bottom: ',name)
xlabel('X location [in]')
ylabel('Y location [in]')
legend('Tool Bottom', 'Part Bottom in contact with tool')
set(gca,'Fontsize',18)
hold off
end
```

Polar Coordinate Designed Functions

Stretching vs Slipping Function

```
function [strain] = stretchslip(theta,L_uncured,L_cured,L_pp, name)
% This function analyzes the stretch vs slip data for complex carbon
    fiber
% parts

% Output : strain      - The stretch vs slip ratio calculated with a
    strain
%                        formula
%          figure()    - A plot of the original lengths of the uncured
    layup
%                        when compared to the new lengths after the cure
%
% Inputs : theta       - the theta array of the measurement locations,
    note
%                        that for the curved c channel, lines 0 and 90
    are
%                        included
%          L_uncured   - the array of the uncured length measurements at
    each
%                        cross section location
%          L_cured     - the array of the cured length measurements at
    each
%                        cross section location
%          L_pp        - ply ply slip length, array the length of the
%                        sections in inches
%          name        - the name of the part as a string. ex: 'MDXXX'

% Written by Madison Dube for Thesis on Forming Analysis of Complex
    Carbon
% Fiber Parts for the MSU Stretch Broken Carbon Fiber Research Group

%% Plotting the uncured data
figure()
```

```
x = [0.*cosd(theta),L_uncured.*cosd(theta)];
y = [0.*sind(theta),L_uncured.*sind(theta)];
fill(x,y,'yellow','FaceAlpha',0.5)
hold on
clear x y


%% Plotting the cured data

% plotting the filled cured data area
x = [0.*cosd(theta),L_cured.*cosd(theta)];
y = [0.*sind(theta),L_cured.*sind(theta)];
fill(x,y,'cyan','FaceAlpha',0.5)
hold on
clear x y
set(gca,'Fontsize',18)


% plotting the cured data lines
for i = 1:length(theta)
    x = [0.*cosd(theta(i)),L_cured(i).*cosd(theta(i))];
    y = [0.*sind(theta(i)),L_cured(i).*sind(theta(i))];
    plot(x,y,'bl','LineWidth',2,'DisplayName','')

end

% plotting the ply ply data lines
for i = 1:length(L_pp)
    x = [0.*cosd(theta(i)),L_pp(i).*cosd(theta(i+1))];
    y = [0.*sind(theta(i)),L_pp(i).*sind(theta(i+1))];
    plot(x,y,'r','LineWidth',2,'DisplayName','')

end


% Adding headers to the graph
legend({'Uncured Layup','Cured Part','Total Elongation Length','','','',
    '','','','','','Ply Ply Slip Length'})
xlabel('X location on Part [in]')
ylabel('Y Location on Part [in]')
title('Slip vs Stretch: ',name)

strain = (L_cured-L_uncured)./L_uncured;
end
```

Thickness Variation Function

```
function [coeff_var, av_thick] = thickness_polar_withthinthick(r,theta,
    z,thick,name,t_i,r_t, z_t,thick_t)
% This function analyzes the thickness of carbon fiber complex parts in
% polar coordinates

% NOTE: THIS ONLY WORKS FOR 10 MEASUREMENT LOCATIONS PER CROSS SECTION
%       WHERE THE CORNER THINNING DATA IS AFTER LOCATIONS 1 AND 9 AND
    THE
%       CORNER THICKENING DATA IS AFTER LOCATIONS 3 AND 7. LINES 43-52
    DEAL
%       WITH ORGANIZING THE THICKNESS DATA BY ORDER OF LOCATION. IF YOU
%       WANT TO MAKE THIS WORK FOR A DIFFERENT NUMBER OF MEASUREMENTS,
    YOU
%       HAVE TO CHANGE HOW R, THICK_COMBO, AND Z ARE CALCULATED HERE.

% Output : coeff_var - the coefficient of variation of the thickness
    data
%          figure()  - the 3D contour plot of the thinning and
    thickening
%                      of the part based on geometric locations
%          av_thick  - the average thickness of the data

% Inputs : r      - the r location vector of the measurement locations
    in
%                   inches (1 by 10)
%          theta - the theta location vector of the measurement
    locations
%                   in degrees (1 by however many)
%          z      - the height location vector of the measurement
    locations
%                   in inches (1 by 10)
%          thick - the (m,n) tensor of thickness data corresponding to
    the
%                   r, theta, and z measurement locations in inches (
    must be
%                   the size of theta by r)
%          name  - a string of the part name example: 'MD003'
%          t_i   - the initial thickness of the uncured laminate in
    inches
%          r_t   - the r location vector of the corner locations for
    corner
%                   thinning and thickening data should be a 1 by 4
%          z_t   - the z location vector of the corner locations for
    corner
```

```
%                   thinning and thickening data z_t = [height of corner
%                   thinning locations, height of corner thickening
%                   locations]
%         thick_t - the corner thinning and thickness data (m,n,p)
    matrix
%                   where thick_t(:,:,1) corresponds to the thinning
    data
%                   and thick_t(:,:,2) corresponds to the thickness data
    .
%                   The first two dimensions correspond to the size of
    theta
%                   by r_t

% Written by Madison Dube for Thesis on Forming Analysis of Complex
    Carbon
% Fiber Parts for the MSU Stretch Broken Carbon Fiber Research Group


%% Combining thickness, corner thinning, and corner thickening data

% Combining the r data
r = [r(1),r_t(1),r(2:3),r_t(2),r(4:7),r_t(3),r(8:9),r_t(4),r(10)];

% Combining the thickness data
thick_combo = [thick(:,1),thick_t(:,1,1),thick(:,2:3),thick_t(:,1,2),
    thick(:,4:6),thick_t(:,2,2),thick(:,7:8),thick_t(:,2,1),thick
    (:,9:10)];

% Writing Z matrix to correspond with mesh size
for i = 1:length(theta)
    Z(i,:) = [z(1),z_t(1),z(2:3),z_t(2),z(4:7),z_t(2),z(8:9),z_t(1),z
        (10)];
end

% Determining the size of Z for the colormap
a = size(Z);

% Creating a mesh based on the r and theta locations
[R, THETA] = meshgrid(r,theta);


%% Contour Plot Creation

% Generating colormap based on thickness data analyzed as percent
    thinning
```

```
C = ones(a(1),a(2)).*((thick_combo./t_i.*100)-100);


% Plotting the data
figure()
% creating surface plot
surf(R.*cosd(THETA), R.*sind(THETA), Z,C);
% setting fontsize
set(gca,'Fontsize',18)
% setting x, y, and z limits
xlim([0,5.5])
ylim([0,5.5])
zlim([0,5.5])
% adding the colorbar
colorbar
% adding the colorbar label
b = colorbar;
b.Label.String = 'Percent Thickness Change [%]';
% labeling axes and including title
xlabel("X [in]")
ylabel("Y [in]")
zlabel("Z [in]")
title(name,": Percent Thickness Change")

clear a

%% Coefficient of Variation Calculation

a = size(thick);
thick_c = [];
for i = 1:a(1)
    thick_c = [thick_c,thick(i,:)];
end

n = length(thick_c);
x_bar = sum(thick_c)/n;

coeff_var = (1/x_bar) * sqrt(sum((thick_c - x_bar).^2)/(n-1));

disp('The Coefficient of Variation is:')
coeff_var

%% Average Thickness

av_thick = x_bar;
```

```
disp('The Average Thickness of the Part in inches is:')
av_thick

end
```

Forming Depth Function

```
function [form_av] = form_depth_polar(L_t,L_p,d,r,theta,name,r_w,rad_t)
% This function analyzes the forming depth data for complex carbon
    fiber
% parts

% Output : form_av     - The average forming depth percent of the entire
%                        parts section measurements.
%          figure()    - The first plot in the figure is a bar graph of
    the
%                        forming depth percentages based on each cross
%                        section location. The second plot is an area
%                        representation of the total area of the bottom
    of
%                        the tool when compared to the contact area
    between
%                        the carbon fiber and the tool surface
%
% Inputs : L_t - the distance across the drawn in area of the tool, not
%                including the radii on either side in inches. For the
    Ferb
%                parts, this distance is 1.75 in.
%          L_p - the array of forming depth measurements at the various
%                cross section locations. This is the distance across
    the
%                bottom where the part touches the tool in inches.
%           d  - the distance over from the wall of the first radii
    where
%                the part first starts touching the bottom of the mold.
%                This is an array the same length as L_p in inches.
%           r  - the r location vector for all measurement locations (
    can
%                use the same one from the thickness data). Measured in
%                inches
%        theta - the theta location vector for all measurement
    locations
%                (can use the same one from the thickness data).
    Measured
```

```
%                 in degrees.
%          name - the name of the part as a string. ex: 'MDXXX'
%           r_w - The radial distance of the wall value for where d is
%                 measured from. Singular value in inches
%         rad_t - The radii measurements of the tool, specifically the
%                 concave corners


% Written by Madison Dube for Thesis on Forming Analysis of Complex
    Carbon
% Fiber Parts for the MSU Stretch Broken Carbon Fiber Research Group



%% Forming Depth by location bar graph


% Calculating the percent formed for each location
form_percent = L_p./L_t.*100;

% Calculating the forming depth average of all the data
form_av = sum(form_percent)./length(form_percent);

disp('The average forming depth percent for the entire part is:')
form_av


% Plotting the data on a bar graph
figure()
subplot(1,2,1)
bar(theta,form_percent,'blue')
title('Forming Depth at Cross Section Locations: ',name)
xlabel('Cross Section Locations')
ylabel('Percent Formed [%]')
set(gca,'Fontsize',18)


%% Plotting the shapes of the contact area


% Calculating radii values
R1 = ones(1,length(theta)).*(r_w+rad_t);
R2 = ones(1,length(theta)).*(r(9)-rad_t);
```

```
% Plotting the tool area
subplot(1,2,2)
fill([flip(R2.*cosd(theta)),R1.*cosd(theta)],[flip(R2.*sind(theta)),R1
    .*sind(theta)],'cyan')
hold on


% Data adjustments for forming depth data radii
R3 = d+r_w;
R4 = R3+L_p;


% Plotting the part area
fill([flip(R4.*cosd(theta)),R3.*cosd(theta)],[flip(R4.*sind(theta)),R3
    .*sind(theta)],'blue')
title('Forming Depth as Visualized on Tool Bottom: ',name)
xlabel('X location [in]')
ylabel('Y location [in]')
legend('Tool Bottom', 'Part Bottom in contact with tool')
set(gca,'Fontsize',18)
hold off
end
```

Additional Functions

Wrinkling Function

```
function [a] = wrinkle_analysis(wrink_data,name)
% This function plots the wrinkling data for complex carbon fiber parts

% Output : a           - percentage of wrinkles to the total area
%          figure()    - two pie charts showing the percentage of
    wrinkles
%                        compared to the total area and another with the
%                        percentage of wrinkles within the critical
    region
%                        compared to wrinkles not in the critical region
%
% Inputs : wrink_data - a 1 by 2 array where wrink_data(1) = total
    wrinkle
%                        percentage and wrink_data(2) = percentage of
%                        wrinkles within the critical area
%          name        - string with the name of the part or the part
    number
%                        but it MUST be a string. Example - "MDXXX"
```

```
%
% Written by Madison Dube for Thesis on Forming Analysis of Complex
    Carbon
% Fiber Parts for the MSU Stretch Broken Carbon Fiber Research Group


%% Wrinkle Data Analysis and Representation


% wrinkle percentage
a = wrink_data(1);

% wrinkle percentage in critical area
b = wrink_data(2);

% assigning pie chart values
x = [a,100-a,0,0];
y = [0,0,b,100-b];

% making labels
lab_a = ['Total Area: ', name];
lab_b = ['Critical Area: ', name];

% Plotting the data
figure()
labels = {'Area With Wrinkles','Area Without Wrinkles','Critical Region
    with Wrinkles','Critical Region without Wrinkles'};
t = tiledlayout(1,2);


% Create pie charts
set(gca,'Fontsize',18)
ax1 = nexttile;
pie(ax1,x)
set(gca,'Fontsize',18)
t = title(lab_a, 'Units', 'normalized', 'Position', [0.5, 1.15, 0]); %
    Set Title with correct Position
set(gca,'Fontsize',18)


ax2 = nexttile;
set(gca,'Fontsize',18)
pie(ax2,y)
set(gca,'Fontsize',18)
t = title(lab_b, 'Units', 'normalized', 'Position', [0.5, 1.15, 0]); %
```

```
    Set Title with correct Position
set(gca,'Fontsize',18)


% Create legend
lgd = legend(labels);
set(gca,'Fontsize',18)
lgd.Layout.Tile = 'south';


end
```

Resin Pooling Function

```
function [res_tot] = resinpool(section,resin_dat,name)
% This function analyzes the resin pooling data based of complex cabon
% fiber parts

% Output : figure()  - the bar graph of the resin pooling data
    represented
%                      at each measurement location


% Inputs : section   -  section numbers or degrees saved as an array
%          resin_dat -  matrix of the resin pooling data where the
    columns
%                       correspond to the radii "number" or which radii
     the
%                       measurements are taken at. The rows correspond
    to
%                       which section the measurements were taken at,
    such
%                       as the degree sections for the curved c
    channels
%          name       -  a string of the part name example: 'MD003'


% Written by Madison Dube for Thesis on Forming Analysis of Complex
    Carbon
% Fiber Parts for the MSU Stretch Broken Carbon Fiber Research Group


%% Plotting the data

% generating the legend strings based on the number of radii
```

```
a = size(resin_dat);
lab = [];
for i = 1:a(2)
    lab = [lab;strcat('radius #',string(i))];
end



% plotting

figure()

b = bar(section,resin_dat);
% setting the colors of the individual bars
b(1).FaceColor = [0 0 1];
b(2).FaceColor = [0 1 1];
title('Area of Resin Pooling at Various Locations: ',name)
xlabel('Cross Section Locations')
ylabel('Area of Resin Pooling [in^2]')
legend(lab)
set(gca,'Fontsize',18)



% if there are more corners in your part, you will need to add a sum()
   for
% every corner here to calculate the total
res_tot = sum(sum(resin_dat));

disp('The total resin pooling for all of the cross sections is:')
res_tot
end
```

Corner Thinning Function

```
function [cornerthin_av,y] = cornerthin(section,thin_dat,av_thick,name)
% This function analyzes the corner thinning data based on the
   thickness
% analysis of complex cabon fiber parts

% Output : cornerthin_av- the average value of percent of average
   thickness
%          figure()  - the bar graph of the thinning data represented
   at
%                      each measurement location
```

```
% Inputs : section  -  section numbers or degrees saved as an array
%          thin_dat -  matrix of the thinning data where the columns
%                      correspond to the radii "number" or which radii
   the
%                      measurements are taken at. The rows correspond
   to
%                      which section the measurements were taken at,
   such
%                      as the degree sections for the curved c channels
%          av_thick -  the average thickness value calculated in the
%                      thickness analysis code
%          name     -  a string of the part name example: 'MD003'


% Written by Madison Dube for Thesis on Forming Analysis of Complex
   Carbon
% Fiber Parts for the MSU Stretch Broken Carbon Fiber Research Group


%% Calculations


% Calculating the percent of the average thickness for each location
y = thin_dat./av_thick .* 100;


% generating the legend strings based on the number of radii
a = size(y);
lab = [];
for i = 1:a(2)
    lab = [lab;strcat('radius #',string(i))];
end


%% Plotting the Data


figure()
b=bar(section,y,'g','b');
% setting the colors of the individual bars
b(1).FaceColor = [0 1 1];
b(2).FaceColor = [0 0 1];
title('Percent of Average Thickness Corner Thinning Locations:',name)
```

```
xlabel('Cross Section Locations')
ylabel('Percent Thickness (%)')
legend(lab)
set(gca,'Fontsize',18)

%% Average

cornthin_tot = [];
for i = 1:length(y(1,:))
    cornthin_tot = [cornthin_tot;y(:,i)];
end
cornerthin_av = sum(cornthin_tot)/length(cornthin_tot);


disp('The average Corner Thinning for All Radii is:')

cornerthin_av
end
```

Corner Thickening Function

```
function [cornerthick_av,y] = cornerthick(section,thicken_dat,av_thick,
    name)
% This function analyzes the corner thickening data based on the
    thickness
% analysis of complex cabon fiber parts

% Output : cornerthick_av  - the values of percent of average thickness
%          figure()        - the bar graph of the thickening data
    represented at
%                            each measurement location


% Inputs : section     -  section numbers or degrees saved as an array
%          thicken_dat -  matrix of the thickening data where the
    columns
%                         correspond to the radii "number" or which radii
    the
%                         measurements are taken at. The rows correspond
    to
%                         which section the measurements were taken at,
    such
%                         as the degree sections for the curved c channels
%          av_thick -  the average thickness value calculated in the
%                      thickness analysis code
```

```
%           name      -  a string of the part name example: 'MD003'


% Written by Madison Dube for Thesis on Forming Analysis of Complex
    Carbon
% Fiber Parts for the MSU Stretch Broken Carbon Fiber Research Group


%% Calculations


% Calculating the percent of the average thickness for each location
y = thicken_dat./av_thick .* 100;


% generating the legend strings based on the number of radii
a = size(y);
lab = [];
for i = 1:a(2)
    lab = [lab;strcat('radius #',string(i))];
end


%% Plotting the Data

figure()
b = bar(section,y);
% setting the colors of the individual bars
b(1).FaceColor = [0 1 1];
b(2).FaceColor = [0 0 1];
title('Percent of Average Thickness Corner Thickening Locations:',name)
xlabel('Cross Section Locations')
ylabel('Percent Thickness (%)')
legend(lab)
set(gca,'Fontsize',18)



%% average

cornthick_tot = [];
for i = 1:length(y(1,:))
    cornthick_tot = [cornthick_tot;y(:,i)];
end
```

```
cornerthick_av = sum(cornthick_tot)/length(cornthick_tot);

disp('The Average Corner Thickening for all Radii is:')
cornerthick_av
end
```

Bridging and Resin Pooling Comparison Function

```
function [] = bridgpool(resin_dat,bridg_dat,section,name)
% This function compares the bridging data to the resin pooling data

% Output : figure()  - the bar graph of the resin pooling and bridgin
    data
%                      represented at each measurement location


% Inputs : section   -  section numbers or degrees saved as an array
%          bridg_dat -  matrix of the bridgin data where the columns
%                       correspond to the radii "number" or which radii
     the
%                       measurements are taken at. The rows correspond
    to
%                       which section the measurements were taken at,
    such
%                       as the degree sections for the curved c
    channels
%          resin_dat -  matrix of the resin pooling data where the
    columns
%                       correspond to the radii "number" or which radii
     the
%                       measurements are taken at. The rows correspond
    to
%                       which section the measurements were taken at,
    such
%                       as the degree sections for the curved c
    channels
%          name      -  a string of the part name example: 'MD003'


% Written by Madison Dube for Thesis on Forming Analysis of Complex
    Carbon
% Fiber Parts for the MSU Stretch Broken Carbon Fiber Research Group


a = size(bridg_dat);
```

```
lab = [];
for i = 1:a(2)
    lab = [lab;strcat('radius #',string(i))];
end

% plotting
figure()
subplot(1,2,1)
yyaxis left
b = bar(section,[bridg_dat(:,1),resin_dat(:,1)]);
b(1).FaceColor = [0 0 1];
b(2).FaceColor = [0 1 1];
ylabel('Bridging Distance [in]')
yyaxis right
ylabel('Resin Pooling [in^2]')
title('Inner Radius')
xlabel('Cross Section Locations')
legend('Bridging Distance [in]','Resin Pooling [in^2]')
set(gca,'Fontsize',18)

subplot(1,2,2)
yyaxis left
c = bar(section,[bridg_dat(:,2),resin_dat(:,2)]);
c(1).FaceColor = [0 0 1];
c(2).FaceColor = [0 1 1];
ylabel('Bridging Distance [in]')
yyaxis right
ylabel('Resin Pooling [in^2]')
title('Outer Radius')
xlabel('Cross Section Locations')


legend('Bridging Distance [in]','Resin Pooling [in^2]')
set(gca,'Fontsize',18)


sgtitle(['Bridging Distance and Resin Pooling Area for ', name])
set(gca,'Fontsize',18)
end
```

Bridging Function

```
function [av_bridg] = bridging(section,bridg_dat,name)
% This function analyzes the bridging data based of complex cabon fiber
```

```
% parts

% Output : figure()  - the bar graph of the bridgin data represented
%                      at each measurement location
%          av_bridg  - the average bridging distance for all radii and
%                      cross sections


% Inputs : section   -  section numbers or degrees saved as an array
%          bridg_dat -  matrix of the bridging data where the columns
%                       correspond to the radii "number" or which radii
    the
%                       measurements are taken at. The rows correspond
   to
%                       which section the measurements were taken at,
   such
%                       as the degree sections for the curved c
   channels
%          name       -  a string of the part name example: 'MD003'


% Written by Madison Dube for Thesis on Forming Analysis of Complex
   Carbon
% Fiber Parts for the MSU Stretch Broken Carbon Fiber Research Group


%% Plotting the data

% generating the legend strings based on the number of radii
a = size(bridg_dat);
lab = [];
for i = 1:a(2)
    lab = [lab;strcat('radius #',string(i))];
end

% plotting
figure()
b = bar(section,bridg_dat);
b(1).FaceColor = [0 0 1];
b(2).FaceColor = [0 1 1];
title('Bridging Distance at Various Locations: ',name)
xlabel('Cross Section Locations')
ylabel('Bridging Distance [in]')
legend(lab)
set(gca,'Fontsize',18)
```

```
%% Calculating Average Brigding

bridg_tot = [];
for i = 1:length(bridg_dat(1,:))
    bridg_tot = [bridg_tot;bridg_dat(:,i)];
end
av_bridg = sum(bridg_tot)/length(bridg_tot);

disp('The␣Average␣Briding␣Value␣for␣all␣Radii␣is:')
av_bridg
end
```